International Atomic Energy Agency

INDC(NDS)-107/G+Special

INDC INTERNATIONAL NUCLEAR DATA COMMITTEE

PROCEEDINGS OF THE CONSULTANTS' MEETING ON DELAYED NEUTRON PROPERTIES, VIENNA, 26-30 MARCH 1979

August 1979

IAEA NUCLEAR DATA SECTION, WAGRAMERSTRASSE 5, A-1400 VIENNA

INDC(NDS)-107/G+Special

PROCEEDINGS OF THE CONSULTANTS' MEETING ON DELAYED NEUTRON PROPERTIES, VIENNA, 26-30 MARCH 1979

August 1979

FOREWORD

The Consultants' Meeting on Delayed Neutron Properties was convened by the IAEA Nuclear Data Section at IAEA Headquarters in Vienna, Austria, from 26 - 30 March 1979, following a recommendation by the International Nuclear Data Committee (INDC). The meeting was attended by 13 scientists from 7 member states.

The main objectives of the meeting were to review the current requirements for delayed neutron data with special emphasis on energy applications, to review the status of delayed neutron data and try to resolve the existing discrepancies in experimental data, and to formulate specific recommendations for necessary future work and its coordination.

These proceedings contain the papers presented and discussed at the meeting as well as the report on the final conclusions and recommendations of the meeting related to the following subjects:

- Requirements for delayed neutron data (for reactor design, power reactor operation, critical experiment operation and interpretation, reactor dynamics and safety);
- Delayed neutron yields;
- Delayed neutron branching ratios;
- Delayed neutron energy spectra (including equilibrium and near-equilibrium spectra, decay-group spectra, separated precursor spectra and theoretical spectra).

As a result a number of new measurements, compilations and evaluations were recommended in areas where no or only few data exist or where existing data are discrepant.

CONTENTS

REQUIREMENTS OF DELAYED NEUTRON DATA FOR THE DESIGN, OPERATION, DYNAMICS AND SAFETY OF FAST BREEDER AND THERMAL POWER REACTORS

Ph. HAMMER

- INTRODUCTION -

1. Delayed neutron characteristics play an important role in various reactor applications through the direct part they have in the kinetic response of a reactor /1/.

These Delayed Neutron Data include for each fissile isotope :

- the absolute delayed neutron yield $a(e)$;
- the group half lives and yields corresponding to the Keepin 6 group scheme usually adopted for the delayed neutron calculations /2/ $\lambda_i(e)$, $a_i(e)$;
- the delayed neutron spectra $\chi_d(e)$;
- eventually, the delayed neutron precursors for specific applications (fuel failure detection)

. At the design level, the Delayed Neutron Constants (D.N.C.) are used to determine the integral delayed neutron parameters which characterize globally the reactor from the kinetic point of view : the effective delayed neutron fractio βeff, the effective delayed neutron decay constant λeff and the "in hour" value. These parameters, which are issued from neutronic calculations are used for the dynamic and safety studies.

. For the reactor operation, the D.N.C. are needed either for the control rod calibration (inverse kinetics methods, or for the direct measurement of the core reactivity level (Reactimeter). In both cases, the D.N.C. are used as input data which must be sufficiently reliable and accurate to provide significant measured results.

. For the fuel failure detection, the characteristics of the delayed neutron precursors must be known : delayed neutron emission probabilities (Pn) and fission yields.

. From the dynamics and safety points of view, the D.N.C. are directly used to describe the transient neutronic phenomena issuing from reactivity changes which may result from any perturbation (in the cooling system for example).

2. It must be noted that for power reactors, the accuracy requirements concerning the D.N.C. vary strongly with the purpose of their use. Obviously in the design situation, a rough estimate of the integral delayed neutron data is quite sufficient (≃ ± 10%), and therefore the D.N.C. used have not to be accurately known. The situation is quite the same for the dynamics and safety studies, where many physical processes involved : temperature evolutions, coolant behaviour, reactivity feed back, are not completely known and cannot be well represented. In this case, the uncertainties corresponding to the neutronic parameters are smaller than the other ones, and in particular no special requirement is presently made for the D.N.C.

For the reactor operation, a better accuracy is required for the β_{eff} and λ_{eff} parameters (≃ 5%) in order to obtain significant reactivity measurements using the calibrated control rods. Such measurements, if they are sufficiently accurate, may give informations on several core parameters as the internal breeding gain, or the power and temperature coefficients.

For fuel failure detection problems, the order of magnitude requested by designers on the delayed neutron precursor characteristics is ≃ 20% (periods, Pn) for the precursors having a period greater than one second /3/.

3. In fact, the most constraining requirements concerning the accuracies on D.N.C. do not come from power reactor applications but from critical experiments.

In this case, βeff is used as a conversion factor between experimental results and calculated ones. As far as reactivity is concerned, i.e. mainly for the following measurements :

- *control rod antireactivity /4/ ;*
- *sample reactivity worths /5/ ;*
- *sodium void effects /6/, Doppler effect...*

In order to obtain a significant calculation to experiment comparison between the experimental results, originally expressed with the βeff unit, and the calculated ones directly available in ΔK/K, one has to use a value of βeff with an uncertainty as low as possible. This implies to have a reliable and accurate set of D.N.C.

It must be noted that in some cases the problem of accuracy of βeff can be avoided by choosing other units to express the reactivities under study :

- *for the control rod antireactivities, the critical balance technique /7/ lead to compare calculated and measured critical radius variations instead of ΔK/K values ;*
- *for the sample reactivity worths, the values are mostly expressed with respect to a 235 U sample effect considered as a reference /8/.*

4. At the last IAEA Panel devoted to Fission Product nuclear data (BOLOGNE 1973) /9/, several conclusions concerning the D.N.C. were drawn : they are briefly recalled here before discussing the present target accuracies for the D.N.C.

a) Absolute total delayed neutron yields :

The situation is considered satisfactory for all fissile nuclides from the reactor design and operation point of view.

Nethertheless, the 238 U and 239 Pu yields corresponding to the "fast" fission have to be improved to meet the ± 5% accuracy.

b) Composite half life groups :

The use of 6 groups seems to satisfy pratical requirements. The data for the group half lives and yields given for thermal and fast fission show only small differences which are probably not significant when considering various fast reactor spectra.

c) Delayed neutron precursors :

For most pratical purposes, the chemical and isotopic identity of delayed neutron sources is unimportant except when chemical processes may be of interest.

d) Energy spectra :

The neutron energy spectrum per delayed neutrons as one group is available but no complete time dependant spectra.

Since, this panel a quite important work has been performed to improve the D.N.C. /10/ new evaluations of the delayed neutron absolute yields /11/ and /12/, integral experiments performed to check the available data /13/, new evaluations of the delayed neutron spectra /14/.

In this paper, one attemps to define the target accuracies for the D.N.C. (i.e. absolute delayed neutron yields, decay constants, delayed neutron spectra) from the design point of view and to compare these requirements to the present situation resulting from all these recent improvements.

In section I, the relation betwenn the D.N.C. and the reactor integral delayed neutron parameters are recalled and discussed, and the target accuracies are defined for the D.N.C.

In section II, the present situation of the D.N.C. is compared to these requirements.

Some further improvements are suggested , on the basis of the analysis of integral experiments performed at the SNEAK critical assembly /13/.

I - RELATIONS BETWEEN THE DELAYED NEUTRON INTEGRAL PARAMETERS βeff, λeff AND THE DIFFERENTIAL DATA -

I-1/ Determination of the reactor delayed neutron parameters :

The integral parameters characterizing the delayed neutrons in a reactor : effective delayed neutron fraction, mean decay - constant, are deduced from the individual delayed neutron data corresponding to each fissile isotope present in the core by neutronic calculations which take into account the flux and the importance distributions throughout the reactor : $\phi(E,r)$, $\phi^*(E,r)$.

The delayed neutron data used are :

- *the absolute yield a(e) of delayed neutrons emitted by each fissile isotope "e" ;*
  Sometimes instead of this absolute yield a(e), one considers the natural proportion β(e) of delayed neutrons to prompt neutrons, for one fission : $\beta(e) = \frac{a(e)}{\bar{\nu}}$. *But it must be noted that if a(e) can be considered as pratically constant between ≃ 0.1 MeV and 4 MeV /10, 11, 12/ this is not the case for β(e). Nethertheless numerical tests have shown that the use of β(e) instead of a(e) for the determination of the effective delayed neutron fraction leads to a variation < 1% of the βeff values.*

- *The repartition of the delayed neutron yield a(e) in six groups with different decay constants* $\lambda_i(e)$. *This repartition is the one adopted by Keepin /15/, which has in fact no physical basis /10/, but provides with six exponentials a good fit of the real decay curve for the precursors . This repartition is quite widely used in the design calculations.*

- *The energy distribution of the delayed neutron emitted by each fissile isotope :* $\chi_i^d(e,E)$. *This spectrum does not seem to depend strongly of the fissile isotope but is more related to the precursor family.*
  An approximation generally used in design multigroup calculations consists in assuming that : $\chi_i^d(E) = \delta(E-E_i')$. *where* E_i' *is the energy level for delayed neutron emitted in group i. As an example the following table gives the approximation done in the CARNAVAL system used at CEA for fast breeder neutronic calculations :*

Delayed neutron group	Decay constant (235 U) sec.	Energy range (KeV) for delayed neutrons
1	55	$183 < E < 302$
2	22	$498 < E < 821$
3	6	$498 < E < 821$
4	2.2	$498 < E < 821$
5	0.5	$302 < E < 498$
6	0.2	$498 < E < 821$

In a reactor including k regions, the effective fraction of delayed neutrons emitted by the fissile isotope "e" in the group "i", is given by :

$$\tilde{\beta}_i(k,e) = \frac{a_i(e)}{INF} \sum_k N_{(e,k)} \int_{V_K} \vec{dr} \int_o^\infty dE' \; \phi(E',r) \chi_i^d(E') \int_o^\infty dE \sigma_f(e,E,k) \phi(E,r) \qquad (1)$$

$$\text{where} \quad INF = \sum_k \int_{V_K} \vec{dr} \int dE' \; \phi^*(E',r) \bar{\chi}(E') \int_o^\infty dE \; \Sigma_f(E,r) \phi(E,s)$$

For each fissile isotope "e", the effective fraction is given by :

$$\tilde{\beta}(e) = \sum_k \sum_i \tilde{\beta}_i(e,k)$$

For each group "i", the effective fraction is given by :

$$\tilde{\beta}_i = \sum_k \sum_e \tilde{\beta}_i(c,k)$$

For each reactor region "k", the effective fractio is given by :

$$\overset{\gamma}{\beta}(k) = \sum_{e}\sum_{i}\overset{\gamma}{\beta}_{i}(e,k)$$

The total effective fractionof delayed neutronsis :

$$\overset{\gamma}{\beta}eff = \sum_{e}\overset{\gamma}{\beta}_{(e)} = \sum_{i}\overset{\gamma}{\beta}_{(i)} = \sum_{k}\overset{\gamma}{\beta}_{(k)}$$

From equation (1), it appears that the accuracy on βeff depends upon the uncertainties on the following parameters :

- $a(e)$;
- $\chi_d(e)$;
- the spatial calculations of $\phi(E,r)$ and $\phi^*(E,r)$
- $\sigma(e)$ and $\nu\sigma_f(e)$

I-2/ Delayed neutron parameters for fast breeders :

a) Effective delayed neutron fractio per element :

The following table presents the delayed neutron fractions corresponding to the various fissile elements for a typical fast power plant of the SUPER-PHENIX size (beginning of cycle situation) :

Isotope	$\beta_i^*(e).10^{-5}$	$\overset{\gamma}{\beta}_i(e).10^{-5}$	$\frac{\overset{\gamma}{\beta}_i(e)}{\beta eff}$ %
235 U	673	12.4	3.4
238 U	1585	165	46.2
239 Pu	214	149	41.7
240 Pu	277	10.6	3.0
241 Pu	533	19.9	5.6
242 Pu	483	0.3	0.1

* Values deduced from the Tomlinson data /16/.

The two major contributions to βeff are due to 238 U and 239 Pu (≃ 42 %). The other isotopes : 235 U, 240 Pu, 241 Pu, have much lower contributions (≃ 4 %) and the 242 Pu has a negligible effect on βeff.

The main requirements will therefore concern the 238 U and 239 Pu total absolute yields, loss restrictive accuracies being needed for 235 U, 240 Pu, 241 Pu yields.

b) Effective delayed neutron fractio per reactor zone :

For each reactor zone, the effective delayed neutron fraction is determined by using flux and importance distributions $\phi(r,E)$, $\phi^*(r,E)$, which are calculated with the diffusion approximation. The following table presents the contributions of the different core zones for a 1200 MWe power plant :

Region "k"	$\tilde{\beta}(k).10^{-5}$	$\frac{\tilde{\beta}(k)}{\beta eff}$ %
Core inner zone	227.1	64
Core outer zone	121	34
Radial blanket	3.1	1
Axial blankets	5.7	2

If the diffusion approximation is appropriate for the core zones, it may lead to important Calculation to Experiment deviations on the spatial flux distribution in the blankets. But, this deviation will have no significant influence on the βeff determination due to the small contribution of the blankets (3%) to the total delayed neutron fraction.

c) Group decay constants λ_i and mean decay constant λ_{eff} :

The group decay constant λ_i are deduced from the individual data $\lambda_i(e)$ per isotope either by combination of $\lambda_i(e)$ /11/ :

$$\lambda_i = \frac{\sum_e \lambda_i(e)\ \overset{\gamma}{\beta}_i(e)}{\sum_e \overset{\gamma}{\beta}_i(e)} \qquad (1)$$

or combination of $1/\lambda_i(e)$ /11/ :

$$\frac{1}{\lambda_i} = \frac{\sum_e \frac{\overset{\gamma}{\beta}_i(e)}{\lambda_i(e)}}{\sum \overset{\gamma}{\beta}_i(e)} \qquad (2)$$

It must be noted that due to the very close values of $\lambda_i(e)$ for the various fissile isotopes /11/, these different procedures for calculating λ_i and λ do not lead to very different results (differences lower that 2%).

Typical group values λ_i for a fast breeder of 1200 MWe are given as an example here under : one can observe how they are close to the group constant given for each fissile isotope in Table I :

Group	1	2	3	4	5	6
$\bar{\lambda}_i$ sec^{-1}	0.0129	0.0313	0.1346	0.3442	1.3764	3.7425

The corresponding mean decay constant is :

$$\bar{\lambda} = 0.0883\ sec^{-1}$$

I-3/ Delayed neutron parameters for light water reactors

For light water reactors, the fuel composition variation during the cycle is quite important : the 235 U enrichment decreases by ≃ 1% and the 239 Pu content increases by ≃ 1%. Therefore, the effective delayed neutron fraction varies significantly (by ≃ 30%) during the life of the reactor. As an example the following table gives the delayed neutron fractions for a 900 MWe power plant :

Isotope	$\beta_i^*(e)$	Beginning of life		End of life	
		$\gamma\beta_i(e)$	$\frac{\gamma\beta_i(e)}{\gamma\beta eff}$ %	$\gamma\beta_i(e)$	$\frac{\gamma\beta_i(e)}{\gamma\beta eff}$ %
235 U	641	597	85.4	307.7	61.8
238 U	1480	102	14.6	112.1	22.5
239 Pu	204	/	/	78.5	15.7

* Value deduced from the Keepin data.

One notes that for thermal power reactors it is necessary to know with an equivalent accuracy the 235 U, 238 U, and 239 Pu data.

I-4/ Target accuracies on D.N.C. deduced from the power reactor and critical experiment requirements :

. Absolute delayed neutron yields :

The accuracies asked for the absolute delayed neutron yields are deduced from the global accuracy which is required for βeff and which takes into account :

- *the necessity of a low uncertainty for reactor physics applications (≃ ± 3 %) ;*
- *the requirements of designers for both fast and thermal power plants (≃ ± 5 %).*

Therefore, the present required accuracy on βeff is ± 3% (1σ).

In the determination of βeff (cf. Section I-1/), one can assume that there are presently the following uncertainties coming from to the various terms involved in equation (1) :

- $\phi(E,r)\phi$, $\phi(r,E)$: ± 2 %
- $\sigma_f(e)$, $\nu\sigma_f(e)$: ± 1.5 %
- $\chi_i^d(E)$: ± 0.5 %

(An error on the delayed neutron spectrum has no significant influence on the βeff value : see here after § II-2/).

Assuming that these uncertainties are independant., to achieve the target accuracy on βeff one has to determine the absolute yields with a ± 1.5% error margin for the major fissile isotopes (235 U, 238 U, 239 Pu).

For a fast breeder, if the major fissile isotope yields are determined with a ± 1.5% uncertainty, one has to know the Plutonium higher isotope data with an uncertainty of ± 7% to achieve the target accuracy on βeff.

The following table summarizes the target accuracies for the absolute delayed neutron yields of the main fissile isotopes present in fast breeders or thermal power reactors :

235 U	238 U	239 Pu	240 Pu	241 Pu	242 Pu	241 Am
±1.5 %	±1.5 %	±1.5 %	± 7 %	± 7 %	±20 %	±20 %

. *Decay constants, λ_i and yield repartition $a_i(e)$:*

The six groups delayed neutron scheme and the corresponding decay constants evaluated by Keepin /15/, are adopted in the most recent D.N.C. evaluations : in particular, Tomlinson /16/, Tuttle /11/, Cox /12/.

One has to note that the group decay constants λ_i do not depend very much either upon the fissile isotope e, as shown in Table I or upon the energy of the fission (fast or thermal, cf. /16/).

The following table gives mean values of λ_i for all the main isotopes (U and Pu), and compares the dispersion associated to these mean values with the uncertainties applied to the individual values $\lambda_i(e)$ and given in /11/ :

Delayed Neutron Group	Mean Value λ_i for all U and Pu	Dispersion	Error
1	0.0129	± 1.3%	≃± 3%
2	0.0309	± 3.3%	≃± 3%
3	0.130	± 6.7%	≃± 8%
4	0.337	± 4.9%	≃± 6%
5	1.405	± 8.1%	≃± 10%
6	3.710	± 8.9%	≃± 15%

One notes that the differences between $\lambda_i(e)$ corresponding to one group and various isotopes are not really significant due to the error margins.

The present accuracies given on the λ_i seem sufficient for the kinetic calculations.

As to the yield repartition $a_i(e)$ for each isotope, the values have been determined by Keepin /15/ with uncertainties which do not depend much of the isotope but rather of the group i. The mean value of these uncertainties are given hereafter :

Delayed neutron group	1	2	3	4	5	6
Mean uncertainty on a_i (%)	± 15	2.5	20	7	12	20

The present uncertainties on $a_i(e)$ seem acceptable for the reactor applications. In particular βeff is not sensitive to the $a_i(e)$ modification /17/.

. *Delayed neutron spectra* :

Presently, most of the design calculations for fast breeders or for thermal reactors uses a very rough representation of the delayed neutron spectra. A typical assumption is to admit that in each group of the Keepin scheme, the delayed neutron are emitted at the same mean energy. The mean energies used may be those of Hughes et al., or of Burgy et al., or Batchelor and Hyder. But one has to note that the discrepancies between these three mean energy evaluations have in fact no real consequence on the multigroup calculations. This is shown for fast breeders in the following table where the French CARNAVAL 25 groups scheme is compared to the mean energies of delayed neutrons given by various authors /16/.

Delayed Neutron Group	CARNAVAL SCHEME (KeV)	Hughes et al. (KeV)	Burgy et al (KeV)	Batchelor and Hyder (KeV)
1	183 - 302	250 ± 60	300 ± 60	250 ± 20
2	498 - 821	560 ± 60	670 ± 60	460 ± 10
3	498 - 821	430 ± 60	650 ±100	405 ± 20
4	302 - 498	620 ± 60	910 ± 90	450 ± 20
5	498 - 821	420 ± 60	400 ± 70	/

In typical design calculations for hight water reactors, 2 or 4 groups only are used and therefore the delayed spectra have no influence on the integral results.

For fast reactors an improvement of the calculational method implies to have the delayed neutron spectra for the 6 groups with an accuracy of ≃± 20%. This improvement seems necessary for the βeff calculations performed for critical experiments in order to reduce the uncertainty on this parameter. Presently, the influence of assumption made on the delayed neutron spectra may reach 0.5 to 1% in some cases /18/.

The efforts suggested concern the accuracy on the spectrum components : ±20% (which is not yet reached in the lower part of the spectrum : E < 0.5 MeV /14, 16/) and the evaluation of spectra for the 5^{th} and 6^{th} delayed neutron groups.

With an accuracy of 20%, it must be noted that the differences between the spectra evaluated for one delayed neutron group, but corresponding to different fissile isotopes are not significant /14/ and therefore, it does not seem necessary to define a set of six spectra per fissile isotope.

II - COMPARISON OF THE PRESENT AVAILABLE D.N.C. TO THE REQUIREMENTS -

II-1/ Analysis of the available evaluations of the absolute yields :

To perform the reactor calculations involving the D.N.C., several sets of recommended yields are available.

The oldest one given by Keepin /15/ is still widely used as well for the thermal power reactor as for the breeder ones.

More recent evaluations have been proposed by Tomlinson /16/, Cox /12/ and Tuttle /11/.

a) Values for fast breeders calculations :

The following table gives the various recommended yields and the dispersion (1σ) between the values proposed for each isotope :

.../...

	Keepin 1965	Tomlinson 1972	Tuttle 1975	Cox 1974	Dispersion
U 5	0.0165 ± 4.5 %	0.0165 ± 1.8 %	0.01697 ± 1.2 %	0.01668 ± 4.2 %	± 1.3%
U 8	0.0412 ± 6.1 %	0.0440 ± 4.8 %	0.04508 ± 1.3 %	0.0460 ± 5.4 %	± 4.7%
Pu9	0.0063 ± 7.1 %	0.0064 ± 3.1 %	0.00655 ± 1.8 %	0.00645 ± 6.2 %	± 1.6%
Pu40	0.0088 ±10.2 %	0.0088 ±10 %	0.0096 ±11.5 %	0.0090 ±10 %	± 4.2%
Pu41	0.0154 ±14.3%	0.159 ±10.0 %	0.160 ±10 %	0.0157 ± 9.6 %	± 1.7%
Pu42	/	0.016 ±31.2 %	0.0228 ±11 %	/	±24.8%
Th2	0.0496 ± 6.0 %	0.0520 ± 7.7 %	0.0545 ± 2.1 %	0.0527 ± 7.6 %	± 4 %
U233	0.0070 ± 8.6 %	0.0069 ± 2.9 %	0.00698 ± 1.9 %	0.0740 ± 5.4 %	± 3.2%

- The 235 U values are quite in agreement and the dispersion is lower than the maximum uncertainty (± 1.5%) accepted to achieve the target accuracy of ± 3% on βeff.

- The 239 Pu results are in good agreement, the dispersion has the maximum value compatible with the accuracy required for βeff.

- The 238 U values have a dispersion significantly higher than the limit uncertainty which is researched (± 1.5%).

- For the Pu higher isotopes 240 Pu and 241 Pu, one has to note that there are good agreements between the different evaluations, but the results given have high experimental uncertainties.

- *For 242 Pu, the important discrepancy between the two available results should be reduced.*

b) Values for thermal reactors :

The following table give the recommended values for thermal fission according to various evaluations :

	Keepin 1965	Tomlinson 1972	Tuttle 1975	Dispersion 1σ
U 233	0.0066 ± 6.8 %	0.0069 ± 2.9 %	0.00664 ± 2.8 %	± 2.4 %
U 235	0.0158 ± 4.7 %	0.0165 ± 1.8 %	0.01654 ± 2.5 %	± 2.6 %
Pu 239	0.0061 ± 7.4 %	0.0064 ± 3.1 %	0.00624 ± 3.9 %	± 2.4 %

For the thermal values, for each isotope, the dispersion between the various evaluations is higher than the target accuracy (± 1.5%) previously quoted for the absolute yields.

c) Analysis of integral measurements :

In order to test the various evaluations of the absolute yields, integral measurements of βeff have been performed on the critical facility SNEAK at KARLSRUHE and reported in detail in /13/. The cores on which the βeff measurements are performed are successively loaded with Uranium and PuO_2-UO_2, and their compositions are given in /13/.

The analysis performed at CADARACHE with the 25 groups CARNAVAL III cross-section set and various sets of absolute delayed neutron yields show the same tendancies as the ones previously given by Fischer in /13/.

However, a systematic discrepancy of 2% between the Calculation to Experiment deviations presented in /13/ and the ones given hereafter can be attributed to the differences existing between the two cross-section sets used. This discrepancy is not significant with the experimental uncertainties.

The two following tables present the experimental results (issued from /13/), and the calculated ones, and the Calculation to Experiment deviations corresponding to the various sets of delayed neutron yields :

Core	Fuel/Diluant	βeff Experiment	βeff Keepin	Tomlinson	Tuttle combined	Tuttle "fast"
9C1	U/Na	758 ± 3.5%	704	712.6	734.6	740.6
9C2	PuO_2-UO_2/Na	422 ± 5 %	368.1	381.7	392.1	395.1
7A	PuO_2-UO_2/C	395 ± 3 %	363.3	377.2	386.1	389.1
7B	PuO_2-UO_2/UO_2	429 ± 3 %	398.8	407.4	417.1	419.9

$\frac{E - C}{C}$ % ↘	Keepin	Tomlinson	Tuttle combined
9C1	7.7 ± 3.5	6.4 ± 3.5	3.2 ± 3.5
9C2	14.6 ± 5	10.6 ± 5	7.6 ± 5
7A	8.7 ± 3	4.7 ± 3	2.3 ± 3
7B	10.1 ± 3	5.3 ± 3	2.8 ± 3

/COMMENTS/

. *Uranium core : 9C1 :*

The βeff values are significantly underestimated by the Keepin and Tomlinson sets : this is due mainly to the 235 U data according to the following sensitivity coefficients of βeff :

$\frac{\delta\beta}{\beta} / \frac{\delta_{a5}}{a5}$	0.8
$\frac{\delta\beta}{\beta} / \frac{\delta_{a8}}{a8}$	0.2

The Tuttle yields provide a calculated value of βeff which is in good agreement with the experimental result within the error margin.

A more refined analysis of the available yields would be necessary to determine if it is still necessary to increase slightly (by 1 to 2%) the a5, a8 values recommended by Tuttle :

- *for 235 U , an increase by 2% of the Tuttle recommended yield would amount to give more weight to values as those obtained by Masters (1969) or Clifford (1972) quoted in /11/ ;*
- *for 238 U , there are some values significantly higher than the one recommended by Tuttle (cf. /11/ and /12/), but it must be noted that the βeff measured in 9C1 is not very sensitive to the 238 data : an increase by 2% of the a8 leads only to an increase of ≃ 0.5% of βeff.*

. *Plutonium cores : 9C2, 7A, 7B :*

The following table gives the βeff sensitivity coefficients for the three Pu fuelled cores (the 235 U, 240 Pu contributions can be neglected for these cores) :

	9C2	7A	7B
$\frac{\delta\beta}{\beta} / \frac{\delta_{a9}}{a9}$	0.56	0.57	0.49
$\frac{\delta\beta}{\beta} / \frac{\delta_{a8}}{a8}$	0.43	0.43	0.51

The Keepin and Tomlinson sets provide underestimated values of βeff for the three cores, and these underestimations can be attributed both to the 238 U and 239 Pu data, according to the sensitivity coefficients given hereabove.

The Tuttle yields give calculated βeff which are in good agreement -within the errors bars- whith the measurements for the SNEAK 7A and 7B cores, but a underestimated value of βeff for SNEAK 9C2.

Therefore, it should be examined if the 239 Pu recommended yields have not to be slightly increased : this corresponds to accept the tendancy given by Cox /12/.

Increasing a9 by ≃2% (a9 = 0.669 instead of a9 = 0.655) leads to increase βeff by ≃ 1% for the cores under study. This would lead to a mean value of the Calculation to Experiment deviation which remains within the error bars.

A significant global comparison of the various sets of absolute delayed neutron data yields is presented in the following table where are given the βeff calculated for a fast reactor of the PHENIX size (250 MWe) :

	Keepin set	Tomlinson set	Tuttle set	* Tuttle yields except Pu9 a9 = 0.00669
βeff 10^{-5}	311.5	346.5	357.9	361.5

* Set which is presently recommended for the delayed neutron calculations for fast breeders at CEA.

II-2/ Delayed neutron spectra

The delayed neutron spectra are obviously of higher importance for fast breeders than for thermal reactors, as far as the calculations of the integral delayed neutron parameters are concerned.

Nevertheless, as it has been said before, these delayed neutron spectra are not systematically used in the reactor calculations. Moreover, several analysis show that the βeff determination is not very sensitivite to delayed neutron spectra, provided one respects the mean values of the energy levels corresponding to the delayed neutron emissions.

For example in /18/, it is show that the replacement of a delayed neutron spectrum by the assumption of only one energy group modifies βeff by less than 0.5%. The same observation has been made for the SNEAK cores studied hereabove.

The same conclusion appears in /17/ where the sentivity coefficients of βeff to the delayed neutron spectra in the PEC reactor are less than 0.5% for the 235 U , 239 Pu , 238 U isotopes, and in /14/ where various delayed neutron spectra are tested.

Several data sets are presently available : the Batchelor and Hyder data /19/ and more recently the Fieg spectra /20/, which are in rather good agreement with the precedent ones, and the Shalev and Cuttler spectra /21/.

The Fieg measurements as will as Shalev and Cuttler ones concern delayed neutron spectra per isotope 235 U, 238 U, 239 Pu and per delayed neutron group.

These data are presently sufficient for the design calculations of fast or thermal power reactors.

Nevertheless some improvements are ncessary in view of :
- *calculations corresponding to dynamics studies /14/ ;*
- *accurate determination of βeff for critical assemblies.*

These improvements concern :
- *completeness of the six group spectra (in most cases group 5 and 6 spectra are not determined /11, 12/ ;*
- *the energy range (measurements should go into ≈ 100 KeV) ;*
- *informations on the spectra corresponding to 240 Pu and 241 Pu for the fast breeders.*

The aim of these improvements is to provide spectra known with an accuracy of ≈ 20% which could be used: -either to provide "realistic" mean spectra for the six delayed neutron groups, which are independant of the isotope, for design calculations ;

-or to allow refin calculations in which the spectra used depend on the delayed neutron group and the fissile isotope (critical assemblies).

II-3/ Keepin group scheme : decay constants and relative yields :

The Keepin 6 group scheme is widely used for power reactor applications : this scheme has been adopted by recent evaluations : Tuttle /11/, Cox /12/, Saphier et al. /14/, Tomlinson /16/, which confirm that this scheme is well suited to the delayed neutron decay problems.

There is presently no real incentive to modify this scheme from the reactor designers or from the reactor physicists.

As said before the accuracies on λ_i and a_i seem presently acceptable for all reactor applications.

- CONCLUSION -

During the last years, an quite important work has been performed on the D.N.C.. In parallel, the requirements for reactor applications have become more precise and more constraining :

a) in view of power reactor operation ;

b) in order to improve the reactor physics analysis performed on the critical experiments.

Taking into account the power reactor and the critical facility requirements concerning the D.N.C., one aims to determine βeff with a ± 3% (1σ) uncertainty.

Such a target accuracy leads to uncertainties on the absolute delayed neutron yields much smaller than the ones suggested at the last FPND panel held in BOLOGNA (1973).

In order to achieve this aim, supplementary efforts are needed to improve the D.N.C. :

- The total absolute yields should be known with a ± 1.5% (1σ) accuracy for the major fissile isotopes : 235 U 238 U - 239 Pu, and with a ± 7% accuracy for 240 Pu - 241 Pu.

- Taking into account the present situation of evaluated sets for absolute delayed neutron yields, an affort should be done to have more consistent evaluated results, especially for 238 U and 239 Pu (fast reactors), 235 U (thermal reactor) to reach the ± 1.5% accuracy : the present dispersion between the various evaluated results is significantly higher than the maximum uncertainty required for the evaluated results.

- Moreover, the opportunity of a slight readjustment of the absolute yields for 238 U and 239 Pu should be examined if one takes into the integral experiment results. In the light of these experiments, one observes that the Tuttle evaluation /11/ provides the best absolute yields presently available.

- The independancy of the absolute yields with respect to energy between 1 KeV and 4 MeV seems to be clearly established /11, 12/. However, complementary informations would be necessary between 4 and 14 MeV for the fast breeders, especially for media with relatively hard spectrum (fissile zones of heterogeneous cores).

- The delayed neutron spectra presently known should be improved especially in the lower energy range (E < 400 KeV) with a target accuracy of ≃ ± 20%. If the spectra associated to different fissile isotopes are not different within the error margins, an evaluation of neutron spectra per isotope appears unuseful for power reactor calculations. In this case, the major effort will concern the delayed neutron spectra per group of the Keepin scheme.

- The Keepin scheme and the associated decay constants λ_i and relative abundances $a_i(e)$ seem presently well fitted to the reactor applications and no real incentive appears to modify the scheme at this moment.

-oOo-

- BIBLIOGRAPHY -

/1/ - J.C. TYROR, R.I. VAUGHAN -
"An Introduction to the Neutrons Kinetics of Nuclear Power Reactors"
PERGAMON PRESS (1970)

/2/ - G.R. KEEPIN -
"Physics of Nuclear Kinetics"
ADDISON WESLEY PUBLISHING COMPANY (1965)

/3/ - C. DEVILLERS -
"Importance of Fission Product Nuclear Data for Engineering Design and Operation of Reactors"
PROCEEDINGS OF A PANEL ON FISSION PRODUCT NUCLEAR DATA (I.A.E.A.) - BOLOGNE - 26/30 November 1973.

/4/ - S.G. CARPENTER -
"Measurements of Control Rod Worths Using ZPPR"
REUNION DE SPECIALISTES SUR LES TECHNIQUES DE MESURES DE BARRES DE COMMANDE (OCDE/NEACRP) - CEN/CADARACHE 21/22 Avril 1976

/5/ - J.M. STEVENSON and H. YOSHIDA -
"A Review of the Central and Distributed Perturbation Experiments in the MOZART Programme"
INTERNATIONAL SYMPOSIUM ON PHYSICS OF FAST REACTORS TOKYO, October 1973

/6/ - E.A. FISHER, F. HELM -
"Recent Improvements in the Prediction of Reactivity Coefficients Relevant to LMFBR Accident Analysis"
CHICAGO CONFERENCE (1976)

/7/ - P. HAMMER et al. -
"Control Rod Studies in the CEA Fast Reactor Physics programme"
ANS CONFERENCE ON ADVANCED REACTORS : PHYSICS, DESIGN AND ECONOMICS - ATLANTA - September 1974

/8/ - J. BOUCHARD -
"Etude neutronique de milieux multiplicateurs à neutrons rapides sur l'assemblage critique thermique-rapide ERMINE"
RAPPORT CEA-R-4246 (1971)

/9/ -
"Fission Product Nuclear Data"
PROCEEDINGS OF A PANEL ON FISSION PRODUCT NUCLEAR DATA (IAEA) - BOLOGNE - 26/30 November 1973

/10/ - G. RUDSTAM -
"Status of Delayed Neutron Data"
PETTEN CONFERENCE (1977).

/11/ - R.J. TUTTLE -
"Delayed Neutron Data for Reactor Physics Analysis"
NUCLEAR SCIENCE AND ENGINEERING, 56, 37-71 (1975)

/12/ - S. COX -
"Delayed Neutron Data - Review and Evaluation"
ARGONNE NATIONAL LABORATORY (A.N.L.) NDM-5 (1974)

/13/ - E.A. FISHER -
"Integral Measurements of the Effective Delayed Neutron Fractions in the Fast Critical Assembly SNEAK"
NUCLEAR SCIENCE AND ENGINEERING, 62, 105-116 (1977)

/14/ - D. SAPHIER et al. -
"Evaluated Delayed Neutron Spectra and their Importance in Reactor Calculations"
NUCLEAR SCIENCE AND ENGINEERING, 62, 660-694 (1977)

/15/ - G.R. KEEPIN et al -
PHYSICAL REVIEW, 107 - 1044 (1957)

/16/ - L. TOMLINSON -
"Delayed Neutron From Fission"
AERE-R-6993 (1972)

/17/ - A. D'ANGELO -
"Sensitivity Study of the Effective Fraction of Delayed Neutrons βeff to Basic Data Uncertainties for the TAPIRO and PEC Fast Reactors"
ENERGIA NUCLEARE - Vol. 23, N°12 - Décember 1976

/18/ - L. MOBERG and J. KOCKUM -
"Measurement of the Effective Delayed Neutron Fraction in Three Differents Cores of the Fast Assembly FRO"
NUCLEAR SCIENCE AND ENGINEERING, 52, 343-349 (1973)

/19/ - R. BATCHELOR and H. HYDER -
JOURNAL OF NUCLEAR ENERGY, 3, 7 (1956)

/20/ - G. FIEG -
JOURNAL OF NUCLEAR ENERGY, 26, 585 (1972)

/21/ - S. SHALEV and J.M. KUTTLER -
NUCLEAR SCIENCE AND ENGINEERING, 51, 52 (1973)

TABLE I

DECAY CONSTANT $\lambda_i(e)$ PER DELAYED NEUTRON GROUP AND FISSILE ELEMENT ($\lambda_i(e)$ sec^{-1})

Isotope \ Group i	1	2	3	4	5	6
U - 235	0.0127	0.0317	0.115	0.311	1.4	3.87
U - 238	0.0132	0.0321	0.139	0.358	1.41	4.02
Pu- 239	0.0129	0.0311	0.134	0.331	1.26	3.21
Pu- 240	0.0129	0.0313	0.135	0.333	1.36	4.04
Pu- 241	0.0128	0.0299	0.124	0.352	1.61	3.47
* Pu- 242	0.0129	0.0295	0.131	0.338	1.39	3.65

DELAYED-NEUTRON YIELDS IN NUCLEAR FISSION*

by

R. J. Tuttle

Energy Systems Group
Rockwell International Corporation

Abstract

Measurements of delayed-neutron yields from nuclear fission induced by neutrons, charged particles, and photons are reviewed and used to derive a recommended set of yields for neutron-induced fission. The energy dependence of neutron-induced yields is examined in detail.

INTRODUCTION

Emission of delayed neutrons following nuclear fission is a rare event constituting at most a few delayed neutrons per hundred prompt neutrons. Yet, this uncommon phenomenon is extremely significant in the control of nuclear reactors and in the interpretation of reactor experiments, and warrants the development of precise and accurate data. The fission process in nuclear reactors is induced by neutrons of a wide range of energy. However, other fission processes can contribute additional information to assist in developing a more complete set of data.

This review summarizes the current status of delayed-neutron yield measurements for various forms of nuclear fission, and concentrates on the development of a recommended data-set for neutron-induced fission. These recommendations are based largely on yield values for fission of five nuclides, induced by neutrons with energies ranging from thermal to 15 MeV. This continues and extends the evaluation presented previously (1).

---

* Revised May 1979

NEW DATA AND REVISIONS

Since the previous evaluation, some data has been more formally published, or has otherwise been revised by the researchers. One set of measurements with greatly improved precision has been reported. In addition, some results noted in that evaluation, but not adjusted nor included in the analysis, are more completely treated here.

Notea, 1969 (Ref. 2)

Yield measurements were made for thermal fission of U-233, U-235, and Pu-239, and for 14-MeV fission of Th-232 and U-238, all relative to thermal fission of U-235.

The reported values were adjusted to account for neutrons of the shortest half-life group, using the fractional yield data of Keepin (3) for thermal fission, and of Herrmann (4) for 14-MeV fission. The adjusted values were converted to interrelated ratios for use in the evaluation.

Kull, et al., 1970 (Ref. 5)

Samples of U-235 and U-238 were irradiated by bremsstrahlung with endpoint energies of 8 and 10 MeV. Group yields were determined using the group half-lives reported by Nikotin and Petrzhak (6). Total yields were not determined.

Brown, et al., 1971 (Ref. 7)

Yields from fission of Pa-231, Th-232, and U-238 at 14.8 MeV were reported.

These were adjusted for the loss of the two shortest half-life delayed neutron groups, using the fractional yield data of Herrmann (4). The application of this correction to Pa-231 is very uncertain; an uncertainty of ±20% was assumed for this correction.

Clifford, 1972 (Ref. 8)

Yield measurements were made with U-235 and U-238 fissioned by neutrons in the reflector of VIPER.

As the work described under Besant, et al., below, progressed, improvements in the calibrations and data analysis were developed, and McTaggart (9) suggested that the uncertainty previously reported for U-235 should be increased from 0.0008 to 0.0015 and for U-238, from 0.0025 to 0.0050. Following completion of the new measurements, McTaggart (10) recommended disregarding entirely the values previously reported. These values have been omitted from this evaluation.

Chulick and Reeder, 1971 (Ref. 11)

A cyclotron was used as a source of τ-(He-3) and α-particles in the energy range of 20-34 MeV to cause fissions in bismuth, thorium, and uranium (presumably natural U). The targets were mounted within a neutron counter consisting of a parafin moderator and four BF3 or two He-3 neutron detectors. Targets were repetitively irradiated and counted with timing sequences selected to allow analysis of different half-life precursor groups.

These experiments measured the cross section for production of delayed neutrons. With measured and estimated fission cross sections, the delayed neutron yields were derived.

Interpretation of these results and comparison with delayed neutron yields at low excitation energies (induced by 0-4 MeV neutrons, photons, and spontaneous) is difficult because of the high excitation energy (15-40 MeV) and the consequent fissioning of many different nuclides after evaporation of various numbers of neutrons.

Caldwell and Dowdy, 1975 (Ref. 12)

In an extension of the measurements described previously by Caldwell, et al., (13), samples of Th-232, U-233, U-234, U-235, U-236, U-238, Np-237, and Pu-239 were irradiated with bremsstrahlung produced by an electron linear accelerator. The bremsstrahlung end point was varied from 8 to 13 MeV.

Neutrons were counted by an arrangement of 53 He-3 detectors in a polythene cube. Delayed neutron counts were recorded between linac pulses, after the prompt neutron flux following a fission had decayed.

The fission rate was derived by analysis of the prompt neutron counting data. The earlier results have been superseded by the data in this reference.

Miyao, et al., 1975 (Ref. 14, 15)

Additional measurements with Th-232 (ThO2) and U-238 (U3O8) fissioned by bremsstrahlung pulses from a betatron using the method previously developed by Moscati and Goldemberg (16) have been described. The end-point energy in these measurements extended from 13 to 38 MeV.

These measurements concentrated on the variation of group yields with bremsstrahlung energy. Little variation was found at 30, 20, 30, and 38 MeV for U-238, or at 15 and 20 MeV for Th-232. Comparison of total yield at 20 Mev with that at 13 or 15 MeV showed a slight increase at the higher energy, 7% for Th-232 and 9% for U-238, contrary to an expected decrease due to the increase in second-chance fission.

Lukens and Bramblett, 1976 (Ref. 17)

Samples of highly enriched (93.13-93.28% U-235) U308, U02, and UC2 were irradiated in a thermal flux. Delayed neutrons were counted for 50 sec, after a 30-sec irradiation and 30-sec delay, by pneumatically transferring the sample to a multiple BF3 detector counting system.

It was found that the U02 samples exhibited delayed neutron yields that were greater than those of the U308 by 3.1, 4.1, and 5.0% for different sample types. The uncertainty in these differences is about ±1.2%. The U02 and UC2 samples showed essentially identical delayed neutron yields.

While these measurements do not provide information of use in developing the evaluated data set, the implications are significant and will be discussed later.

Besant, et al., 1977 (Ref. 18)

Samples of U-235, U-238, and Pu-239 were irradiated in the copper reflector of VIPER, in the same manner as developed by Clifford (8). VIPER was used to produce neutron pulses with a full width at half maximum of 400 μs having a spectrum similar to a fast breeder reactor. This spectrum is somewhat softer than those previously used, in GODIVA (3), ZEPHYR (19), and EBR (20). Following irradiation, each sample was transferred to a neutron counter in less than 35 ms.

The neutron counter consisted of two separate detectors, one a Li-6 zinc sulphide scintillator and the other a B-10 glass disc. Delayed neutrons emitted by the transferred sample were thermalized in a polyethylene cylinder surrounding the sample position. The scintillators were placed adjacent to the polyethylene but were shielded from direct gamma radiation from the sample by lead.

The performance of these detectors was well characterized in terms of energy and spatial sensitivity, dead time, and counting efficiency.

The fissions in each sample were measured by determining the La-140 activity produced in a thin foil during the irradiation. This was done by counting the 1596-keV gamma-ray from La-140 using a Ge(Li) detector, after sufficient delay that all La-140 activity was produced as daughter activity from Ba-140. The yield of this gamma ray was correlated with the number of fissions by use of calibrated fission chambers for each nuclide.

Different size samples and different pulsed irradiation conditions were used. The results were combined and analyzed with a complex least-squares fitting routine. Alternate analytical methods were used as checks of the results. Corrections of from 3.8% to 7.6% were made, using Keepin's group abundance and decay constant data, to account for delayed neutrons emitted prior to the start of counting. This delay was occasioned by high count rates requiring large dead time corrections.

In addition to the absolute delayed neutron yields for the three nuclides, these measurements have also determined the group abundances and decay constants. These were compared with Keepin's values and the comparison shows occasional differences outside of the estimated uncertainties. Comparative calculations were made of the period-reactivity relationship using the two sets of parameters and showed differences of less than 3.5% in the reactivity values.

The absolute yield values were modified by the authors to account for the lower delayed neutron yield above about 5 MeV, as shown by Krick and Evans (21).

The effect of an isotropic neutron emission from the Am-Li neutron source used for the neutron detector calibration has been calculated to change the calibration factor by 1.4% (22). The delayed neutron yields have been increased by 1.4% for this evaluation.

No adjustments have been made for this evaluation.

Schrack 1978 (Ref. 23)

Measurements were performed specifically to investigate the chemical dependence reported by Lukens and Bramblett, for UO2 and U3O8. Gamma-ray measurements were inconclusive. Fission rate measurements, using a split fission chamber, showed no significant difference in fission rate for the two forms, compared to the estimated overall uncertainty in the measurements (± 0.2%). Delayed-neutron measurements were performed using identical masses of U-235 as UO2 and U3O8 (from the same standard material) sealed in quartz ampoules. Samples were irradiated in a reactor thermal column and then counted for delayed-neutron activity with an irradiation/delay/count cycle of 100 sec/100 sec/100 sec, to emphasize the longer lived groups. The ratio of UO2/U3O8 delayed neutrons was found to be 0.9914 ±0.012 for seven pairs of samples in two separate experiments.

While these measurements support the assumption that delayed-neutron yields are independent of chemical form, the significance of the effect demands further investigation.

Synetos and Williams, 1979 (Ref. 24)

Samples of uranium metal foil enriched to 95.54% U-235 were irradiated in a thermal column of the University of London Reactor (CONSORT II) and pneumatically transferred to a delayed neutron detector, following a 10-min. irradiation. The delayed neutron detector consisted of a water tank containing two BF_3 counters placed near the sample location in the center of the tank. Fissions in the sample were determined by counting a gamma-ray from the decay of La-140, produced from the 12.8-day half-life Ba-140.

The neutron detector was calibrated by use of an Am-Li neutron source, relying on the similarity of that spectrum and delayed neutron spectra and on comparative efficiency calculations using different spectra to assure minimal error in the calibration due to spectral effects. The fission-rate measurement was calibrated by use of a fission counter to determine the absolute fission rate at the irradiation location along with a foil for determination of the associated La-140 production.

The transit time of the sample to the detector was 0.38 sec, and so most of the delayed neutrons in Group 6 (0.23 sec half-life) were not detected. Time-dependent delayed neutron count data were analyzed into five groups, resulting in group parameters similar in value to the corresponding Keepin parameters. The Keepin six-group parameters were used with total delayed neutron count data to determine the yield.

No adjustments have been made for this evaluation.

A complete summary of reported measurements, updated from the earlier evaluation, is presented in Table I. Measured values for the five most significant nuclides and the results of various calculations are shown in Figures 1-5.

TABLE I

DELAYED NEUTRON YIELD MEASUREMENTS

Reference	Energy (MeV)	Yield		Adjustment Basis
		Reported	Adjusted	
^{209}Bi		Charged - Particle Fission		
Chulick & Reeder, 1971	29.1 33.7	0.0009 ± .0001mb 0.0172 ± .0024mb		Two shortest-lived groups missed, delayed neutron production cross section reported.
^{231}Pa		Neutron Fission		
Brown et al, 1971	14.8	0.0060 ± 25%	0.0080 ± .0026	Increased 34% for Groups 5 and 6.
^{232}Th		Neutron Fission		
Sun et al., 1950	14.0 max	0.08 ± 0.03	0.08 ± 0.03	No adjustment. Used in limited ratios.
Brunson et al., 1955	3.0	$3.09 \times Y_f$ ^{235}U ± 17%	0.0568 ± 0.0145	Added 7.8% for 6 groups. Probable error converted to standard deviation. Interrelated ratios.
Rose & Smith, 1957 also reported as	3.0	0.038 ± 0.008 $2.21 \pm 0.27 \times Y_f$ ^{235}U	0.0375 ± 0.0090	Absolute, added 4.3% for 6 groups; relative, added 1.8% for 6 groups. Probable error converted to standard deviation. Interrelated ratios. Omitted.
Keepin et al., 1957	3.5	0.0496 ± 0.0020	0.0505 ± 0.0052	Probable error converted to standard deviation. Systematic errors not reduced. Spectrum effect corrected.

TABLE I

DELAYED NEUTRON YIELD MEASUREMENTS

Reference	Energy (MeV)	Yield		Adjustment Basis
		Reported	Adjusted	
Maksyutenko, 1959	2.4	$3.4 \pm 0.28 \times Y_t$ ^{235}U	0.0571 ± 0.0051	Interrelated ratios.
	3.3	$3.18 \pm 0.26 \times Y_t$ ^{235}U	0.0534 ± 0.0048	Interrelated ratios.
	15.0	$5.11 \pm 0.38 \times U_t$ ^{235}U	0.0835 ± 0.0069	Evaluated yield for ^{235}U. Used in limited ratios.
McGarry et al., 1960	14.0	0.058 ± 0.014	0.058 ± 0.014	No adjustment. Used in limited ratios.
Shpakov et al., 1961	14.5	0.075 ± 0.007	0.0782 ± 0.0075	Added 4.3% for 6 groups. Used in limited ratios.
Herrmann, 1966	14.0	0.019 ± 0.005	0.0218 ± 0.0030	Evaluated yield for ^{235}U. Error reduced from 2x standard deviation.
Masters et al., 1969	3.1	$1.94 \pm 0.11 Y_{15}$ ^{232}Th	0.0566 ± 0.0042	As reported by Evans et al. and interrelated ratios.
	14.9	0.030 ± 0.002	0.030 ± 0.002	
Keepin, 1969	14.1	$1.19^a \pm 0.14$	0.0311 ± 0.0037	Divide by $\sigma_f = 0.366$ b, recalibration of neutron source.
	14.9	$1.23^a \pm 0.11$	0.0287 ± 0.0026	Divide by $\sigma_f = 0.410$ b, recalibration of neutron source.
Notea, 1969	14.0	$0.77 \pm 0.30 \times Y_t$ ^{235}U	0.0170 ± 0.0072	Added 1.8% for 6 groups. Interrelated ratios.
Benedict, 1970	14.0	0.0191 ± 0.0065	0.0209 ± 0.0042	Error reduced from 2x standard deviation. Interrelated ratios.

[a] Delayed neutrons per atom/100 incident neutrons.

TABLE I

DELAYED NEUTRON YIELD MEASUREMENTS

Reference	Energy (MeV)	Yield		Adjustment Basis
		Reported	Adjusted	
Cox & Dowling Whiting, 1970	1.3 - 1.6	0.0505	0.0525 ± 0.0040	Added 1.8% for 6 groups. Interrelated ratios.
Brown et al., 1971	14.8	0.0269 ± 15%	0.0286 ± 0.0048	Increased 34% for Groups 5 and 6. Adjusted to σ_f = 0.404.
^{232}Th		Photofission		
Moscati & Goldemberg, 1962	12, 20	0.0285 ± 0.008	0.0285 ± 0.008	No adjustment.
Nikotin & Petrzhak, 1966	15	0.038 ± 0.006	0.038 ± 0.006	No adjustment.
Caldwell et al., 1973	8 - 12	0.0280 ± 0.0012	0.0280 ± 0.0012	No adjustment.
Caldwell & Dowdy, 1974	8 - 13	0.0280 ± 0.0028	0.0280 ± 0.0028	No adjustment.
^{232}Th		Charged Particle Fission		
Chulick & Reeder, 1971	τ21.7	0.022 ± .004	0.022 ± .004	No adjustment.
	τ23.3	0.021 ± .003	0.021 ± .003	
	τ28.9	0.013 ± .002	0.013 ± .002	
	τ33.8	0.0044 ± .0009	0.0044 ± .0009	
	σ19.9	0.053 ± .010	0.053 ± .010	
	α28.9	0.018 ± .002	0.018 ± .002	
^{233}U		Neutron Fission		
Brunson et al., 1955	0.0	$0.39 \times Y_f \left(\frac{^{235}U}{^{235}U}\right)$	± 7.5% 0.00629 ± 0.00073	Reduce 6.4% for 6 groups. Probable error converted to standard deviation. Interrelated ratios.
	0.27	$0.414 \times Y_f \left(\frac{^{235}U}{^{235}U}\right)$	± 7.5% 0.00652 ± 0.00075	

TABLE I

DELAYED NEUTRON YIELD MEASUREMENTS

Reference	Energy (MeV)	Yield		Adjustment Basis
		Reported	Adjusted	
Rose & Smith, 1957 also reported as	1.0	0.0074 ± 0.0006 $0.429 \pm 0.026 \times Y_f$ ^{235}U	0.00737 ± 0.00080	Absolute, added 2.3% for 6 groups; relative, reduced 0.3% for 6 groups. Probable error converted to standard deviation. Interrelated ratios.
Keepin et al., 1957	0.0 1.45	0.0066 ± 0.0003 0.0070 ± 0.0004	0.0066 ± 0.0007 0.00729 ± 0.00081	Probable error converted to standard deviation. Systematic errors not reduced. Fast fission spectrum effect corrected.
McGarry et al., 1960	14.0	0.0142 ± 0.0042	0.0142 ± 0.0042	No adjustment. Used in limited ratios
Masters et al., 1969	3.1 14.9	$1.79 \pm 0.10 \times Y_{15}$ ^{233}U 0.0041 ± 0.0003	0.00751 ± 0.00061 0.0041 ± 0.0003	Evaluated yield, Y_{15} ^{233}U, and as reported by Evans et al.
Keepin, 1969	14.1	$1.09^a \pm 0.10$	0.00439 ± 0.00041	Divide by $\sigma_f = 2.374$ b, recalibration of neutron source.
	14.9	$1.09^a \pm 0.11$	0.00433 ± 0.00044	Divide by $\sigma_f = 2.406$ b, recalibration of neutron source.
Notea, 1969	0.0	$0.345 \pm 0.086 \times Y_t$ ^{235}U	0.0082 ± 0.0026	Reduced 0.3% for 6 groups. Interrelated ratios.
Conant & Palmedo, 1970	0.0	$\beta = 0.0027 \pm 0.0001$	0.00674 ± 0.00042	Multiply by $\bar{\upsilon} = 2.498$, adjusted uncertainty.
Krick & Evans, 1970	0.1 - 1.8	0.0075 ± 0.0006	0.0075 ± 0.0006	As reported by Evans et al.

[a] Delayed neutrons per atom/100 incident neutrons.

DELAYED NEUTRON YIELD MEASUREMENTS

Reference	Energy (MeV)	Yield		Adjustment Basis
		Reported	Adjusted	
^{233}U		Photofission		
Caldwell & Dowdy, 1974	8 - 13	0.00553 ± 0.00044	0.00553 ± 0.00044	No adjustment
^{234}U		Photofission		
Caldwell & Dowdy, 1974	8 - 13	0.0094 ± 0.00094	0.00094 ± 0.00094	No adjustment
^{235}U		Neutron Fission		
Snell et al., 1947	0.0	β = 0.010 ± 0.002	0.0176 ± 0.0054	Corrected for ^{238}U fissions. Probable error converted to standard deviation. Multiply by $\bar{\nu}$ = 2.4229.
Hughes, et al., 1948	0.0	β = 0.00755 ± 0.00050	0.0183 ± 0.0026	Multiply by $\bar{\nu}$ = 2.4229. Probable error converted to standard deviation. Increased energy correction uncertaint
Brunson et al., 1955	0.0 0.29	1.017 x Y_f (^{235}U) + 11% (reference)	0.0175 ± 0.0028 0.0172 ± 0.0023	Probable error converted to standard deviation. Interrelated ratios.
Rose & Smith, 1957	1.0	0.0174 ± 0.0014	0.0174 ± 0.0019	Absolute, added 3% for 6 groups. Probable error converted to standard deviation. Interrelated ratios.
Keepin et al., 1957	0.0 1.45	0.0158 ± 0.0005 0.0165 ± 0.0005	0.0158 ± 0.0016 0.01675 ± 0.0017	Probable error converted to standard deviation. Systematic errors not reduced. Fast fission spectrum effec corrected.

DELAYED NEUTRON YIELD MEASUREMENTS

Reference	Energy (MeV)	Yield		Adjustment Basis
		Reported	Adjusted	
Maksyutenko, 1959	0.0	(reference)	0.0173 ± 0.0012	Interrelated ratios.
	2.4	$1.03 \pm 0.04 \times Y_t$ ^{235}U	0.0178 ± 0.0012	Interrelated ratios.
	3.3	$0.99 \pm 0.04 \times Y_t$ ^{235}U	0.0171 ± 0.0012	Interrelated ratios.
	15.0	$1.86 \pm 0.06 \times Y_t$ ^{235}U	0.0304 ± 0.0015	Evaluated yield for ^{235}U. Used in limited ratios.
McGarry et al., 1960	14.0	0.022 ± 0.005	0.022 ± 0.005	No adjustment. Used in limited ratios
Herrmann, 1966	0.0	(reference)	0.0221 ± 0.0031	Interrelated ratios.
Masters et al., 1969	3.1	$1.89 \pm 0.11 \times Y_{15}$ ^{235}U	0.0173 ± 0.0012	Evaluated yield, Y_{15} ^{235}U, and as reported by Evans et al.
Keepin, 1969	14.1	2.12[a] ± 0.17	0.0094 ± 0.0008	Divide by σ_f = 2.164 b, recalibration of neutron source.
	14.9	2.14[a] ± 0.17	0.0092 ± 0.0007	Divide by σ_f = 2.226 b, recalibration of neutron source.
Notea, 1969	0.0	(reference)	0.0254 ± 0.0081	Interrelated ratios.
Benedict, 1979	0.0	(reference)	0.0217 ± 0.0039	Interrelated ratios.
Cox & Dowling Whiting, 1970	0.25 - 1.50	(reference)	0.0170 ± 0.0011	Interrelated ratios.
Conant & Palmedo, 1970	0.0	β = 0.0065 ± 0.0003	0.0157 ± 0.0010	Multiply by $\bar{\upsilon}$ = 2.4188, adjusted uncertainty.
Krick & Evans, 1970	0.1 - 1.8	0.0163 ± 0.0013	0.0163 ± 0.0013	As reported by Evans et al.
Clifford, 1972	0.63	0.0174 ± 0.0015		Omitted.

[a]Delayed neutrons per atom/100 incident neutrons.

TABLE I

DELAYED NEUTRON YIELD MEASUREMENTS

Reference	Energy (MeV)	Yield		Adjustment Basis
		Reported	Adjusted	
Cox, 1974	0.96	0.01650 ± 0.00100	0.01650 ± 0.00100	No adjustment.
	1.97	0.01657 ± 0.00100	0.01657 ± 0.00100	
	2.98	0.01696 ± 0.00100	0.01696 ± 0.00100	
	3.98	0.01666 ± 0.00100	0.01666 ± 0.00100	
Besant et al., 1977	0.63	0.0164 ± .0006	0.0166 ± .0006	Revised by Williams for anisotropic calibration source.
Synetos and Williams, 1979	0	0.0156 ± 0.0010	0.0156 ± 0.0010	As reported for 6 groups.
^{235}U		Photofission		
Nikotin & Petrzhak, 1966	15	0.0096 ± 0.0013	0.0096 ± 0.0013	No adjustment.
Caldwell et al., 1973	8 - 12	0.0102 ± 0.0004	0.0102 ± 0.0004	No adjustment.
Caldwell & Dowdy, 1974	8 - 13	0.0102 ± 0.0008	0.0102 ± 0.0008	No adjustment.
^{236}U		Photofission		
Caldwell & Dowdy, 1974	8 - 13	0.0160 ± 0.0013	0.0160 ± 0.0013	No adjustment.
^{238}U		Neutron Fission		
Sun et al., 1950	14.0 max	0.08 ± 0.03	0.08 ± 0.03	No adjustment. Used in limited ratios
Brunson et al., 1955	2.7	$2.23 \times Y_f$ ^{235}U ± 7.5%	0.0463 ± 0.0071	Added 21% for 6 groups. Probable error converted to standard deviation. Interrelated ratios.

TABLE I

DELAYED NEUTRON YIELD MEASUREMENTS

Reference	Energy (MeV)	Yield		Adjustment Basis
		Reported	Adjusted	
Rose & Smith, 1957	3.0	0.037 ± 0.004 $2.20 \pm 0.15 x Y_f$ ^{235}U	0.0386 ± 0.0052	Absolute, added 7.5% for 6 groups; relative, added 5.3% for 6 groups. Probable error converted to standard deviation. Interrelated ratios.
Keepin et al., 1957	3.01	0.0412 ± 0.0017	0.0421 ± 0.0043	Probable error converted to standard deviation. Systematic errors not reduced. Spectrum effect corrected.
	0.0	(Reference)	0.0173 ± 0.0012	Interrelated ratios.
Maksyutenko, 1959	2.4	$2.58 \pm 0.14 x Y_t$ ^{235}U	0.0426 ± 0.0027	Interrelated ratios.
	3.3	$2.45 \pm 0.17 x Y_t$ ^{235}U	0.0404 ± 0.0031	Interrelated ratios.
	15.0	$4.60 \pm 0.28 x Y_t$ ^{235}U	0.0752 ± 0.0053	Evaluated yield for ^{235}U. Used in limited ratios.
McGarry et al., 1960	14.0	0.066 ± 0.017	0.066 ± 0.017	No adjustment. Used in limited ratios.
Herrmann, 1966	14.0	0.022 ± 0.003	0.0282 ± 0.0040	Error reduced from 2x standard deviation. Interrelated ratios.
Bucko, 1966	14.7	$1.6 x Y_t$ $^{235}U \pm 10\%$	0.0261 ± 0.0028	Evaluated yield for ^{235}U.
Masters et al., 1969	3.1	$1.71 \pm 0.10 x Y_{15}$ ^{235}U	0.0474 ± 0.0032	As reported by Evans et al. and interrelated ratios.
	14.9	0.0283 ± 0.0013	0.0283 ± 0.0013	
Keepin, 1969	14.1	$3.27^a \pm 0.27$	0.0280 ± 0.0024	Divide by $\sigma_f = 1.154$ b, recalibration of neutron source and fission counter.
	14.9	$3.32^a \pm 0.27$	0.0262 ± 0.0022	Divide by $\sigma_f = 1.250$ b, recalibration of neutron source and fission counter.
Notea, 1969	14.0	$0.96 \pm 0.29 x Y_t$ ^{235}U	0.0209 ± 0.0074	Added 5.3% for 6 groups. Interrelated ratios.
Benedict, 1970	14.0	0.0228 ± 0.0082	0.0277 ± 0.0058	Error reduced from 2x standard deviation. Interrelated ratios.

TABLE I

DELAYED NEUTRON YIELD MEASUREMENTS

Reference	Energy (MeV)	Yield		Adjustment Basis
		Reported	Adjusted	
Krick & Evans, 1970	1.8 - 7.0	Energy-dependent yield normalized to Masters, 1969		Ratio of evaluated yield for ^{238}U to Masters, 1969.
Cox & Dowling Whiting, 1970	0.9 - 2.4	0.0406	0.0436 ± 0.0028	Interrelated ratios.
Brown et al., 1971	14.8	0.0182 ± 15%	0.0230 ± .0039	Increased 34% for Groups 5 and 6. Adjusted to σ_f = 1.240.
Clifford, 1972	2.77	0.0492 ± 0.0050		Omitted.
Cox, 1974	1.97	0.04390 ± 0.00260	0.04390 ± 0.00260	No adjustment.
	2.98	0.04347 ± 0.00260	0.04347 ± 0.00260	
	3.98	0.04288 ± 0.00260	0.04288 ± 0.00260	
Besant et al., 1977	2.77	0.0439 ± .0017	0.0445 ± .0017	Revised by Williams for anisotropic calibration source.
^{238}U		Photofission		
Moscati & Goldemberg, 1962	12, 20	0.036 ± 0.008	0.036 ± 0.008	No adjustment.
Nikotin & Petrzhak, 1966	15	0.031 ± 0.004	0.031 ± 0.004	No adjustment.
Caldwell et al., 1973	8 - 12	0.0291 ± 0.0009	0.0291 ± 0.0009	No adjustment.
Caldwell & Dowdy, 1974	8 - 13	0.0291 ± 0.0020	0.0291 ± 0.0020	No adjustment.

TABLE I

DELAYED NEUTRON YIELD MEASUREMENTS

Reference	Energy (MeV)	Yield		Adjustment Basis
		Reported	Adjusted	
^{238}U		Charged - Particle Fission		
Chulick & Reeder, 1971	τ21.4	0.012 ± .002	0.012 ± .002	No adjustment.
	τ23.3	0.013 ± .002	0.013 ± .002	
	τ28.7	0.016 ± .003	0.016 ± .003	
	τ33.8	0.007 ± .001	0.007 ± .001	
	α19.8	0.030 ± .003	0.030 ± .003	No adjustment.
	α24.5	0.0086 ± .0007	0.0086 ± .0007	
	α28.6	0.014 ± .002	0.014 ± .002	
^{237}Np		Photofission		
Caldwell & Dowdy, 1974	8 - 13	0.0047 ± 0.0004	0.0047 ± 0.0004	No adjustment.
^{239}Pu		Neutron Fission		
Wilson, 1947	0.0	$0.46 \times Y_t\ (^{235}U)$	0.0076	Evaluated yield for ^{235}U. Omitted.
de Hoffmann & Feld, 1947	0.0	$\beta^{49}/\beta^{25} = 0.47 \pm 0.07$	0.0090 ± 0.0015	Multiply by ratio of $\bar{\upsilon}(1.189)$. Reduce b 1.9% for 6 groups. Increase uncertainty for $\upsilon\sigma_f$, evaluated yield for ^{235}U. Omitted.
Brunson, et al., 1955	0.0	$0.36 \times Y_f\ (^{235}U) \pm 7.5\%$	0.00604 ± 0.00068	Reduced by 1.9% for 6 groups. Interrelated ratios.
	0.42	$0.405 \times Y_f\ (^{235}U) \pm 7.5\%$	0.00692 ± 0.00082	Also reduced by 2% for ^{240}Pu delayed neutrons. Interrelated ratios.

TABLE I

DELAYED NEUTRON YIELD MEASUREMENTS

Reference	Energy (MeV)	Yield		Adjustment Basis
		Reported	Adjusted	
Rose & Smith, 1957 also reported as:	1.0	0.0070 ± 0.0006 0.406 ± 0.024xY_f ^{235}U	0.00721 ± 0.00082	Absolute, added 3.5% for 6 groups; relative, added 0.9% for 6 groups. Probable error converted to standard deviation. Interrelated ratios.
Keepin et al., 1957	0.0 1.59	0.0061 ± 0.0003 0.0063 ± 0.0003	0.0061 ± 0.0007 0.0064 ± 0.0007	Probable error converted to standard deviation. Systematic errors not reduced. Fast-fission spectrum effect corrected.
Shpakov et al., 1961	14.5	0.0130 ± 0.0015	0.0135 ± 0.0016	Added 3.5% for 6 groups. Used in limited ratios.
Masters et al., 1969	3.1 14.9	1.60 ± 0.09xY_{15} ^{239}Pu 0.0041 ± 0.0002	0.00664 ± 0.00047 0.0041 ± 0.0002	Evaluated yield, Y_{15} ^{239}Pu, and as reported by Evans et al.
Keepin, 1969	14.1	1.13[a] ± 0.10	0.00424 ± 0.00038	Divide by σ_f = 2.5478 b, recalibration of neutron source.
	14.9	1.20[a] ± 0.11	0.00439 ± 0.00041	Divide by σ_f = 2.6142 b, recalibration of neutron source.
Notea, 1969	0.0	0.31 ± 0.12xY_t ^{235}u	0.0076 ± 0.0032	Added 0.9% for 6 groups. Interrelated ratios.
Conant & Palmedo, 1970	0.0	β = 0.0023 ± 0.0003	0.00661 ± 0.00078	Multiply by $\bar{\upsilon}$ = 2.8733, adjusted uncertainty.
Krick & Evans, 1970	0.0 - 1.8	0.0062 ± 0.0005	0.0062 ± 0.0005	As reported by Evans et al.
Cox, 1974	0.96 1.97 2.98 3.98	0.00674 ± 0.00043 0.00669 ± 0.00043 0.00640 ± 0.00043 0.00663 ± 0.00043	0.00674 ± 0.00043 0.00669 ± 0.00043 0.00640 ± 0.00043 0.00663 ± 0.00043	No adjustment.
Besant et al., 1977	0.74	0.00598 ± .00022	0.00606 ± 0.00022	Revised by Williams for anisotropic calibration source.

[a]Delayed neutrons per atom/100 incident neutrons.

TABLE I

DELAYED NEUTRON YIELD MEASUREMENTS

Reference	Energy (MeV)	Yield		Adjustment Basis
		Reported	Adjusted	
^{239}Pu		Photofission		
Nikotin & Petrzhak, 1966	15	0.0036 ± 0.0006	0.0036 ± 0.0006	No adjustment.
Caldwell et al., 1973	10.2 - 12	0.00372 ± 0.00013	0.00372 ± 0.00013	No adjustment.
Caldwell & Dowdy, 1974	10.2 - 13	0.0037 ± 0.0004	0.0037 ± 0.0004	No adjustment.
^{240}Pu		Neutron Fission		
Keepin et al., 1957	2.13	0.0088 ± 0.0006	0.0092 ± 0.0011 -	Probable error converted to standard deviation. Ratio of Keepin values to evaluated values. Spectrum effect corrected.
Keepin, 1969	14.1	1.49[a] ± 0.13	0.00631 ± 0.00056	Divide by σ_f = 2.2566 b, recalibration of neutron source.
	14.9	1.42[a] ± 0.12	0.00597 ± 0.00051	Divide by σ_f = 2.275 b, recalibration of neutron source.
^{241}Pu		Neutron Fission		
Cox, 1961	0.0	0.0154 ± 0.0015	0.0162 ± 0.0016	Revised by Cox and evaluated yield for ^{235}U.
Keepin, 1969	14.1	2.06[a] ± 0.19	0.00762 ± 0.00071	Divide by σ_f = 2.5852 b, recalibration of neutron source.
	14.9	1.99[a] ± 0.18	0.00732 ± 0.00067	Divide by σ_f = 2.5996 b, recalibration of neutron source.

[a] Delayed neutrons per atom/100 incident neutrons.

TABLE I

DELAYED NEUTRON YIELD MEASUREMENTS

Reference	Energy (MeV)	Yield		Adjustment Basis
		Reported	Adjusted	
^{242}Pu		Neutron Fission		
Krick & Evans, 1970	0.7 - 1.3	0.015 ± 0.005	0.015 ± 0.005	As reported by Evans et al.
^{252}Cf		Spontaneous Fission		
Cox et al., 1958	(0)	0.0086 ± 0.0010	0.0086 ± 0.0010	No adjustment.

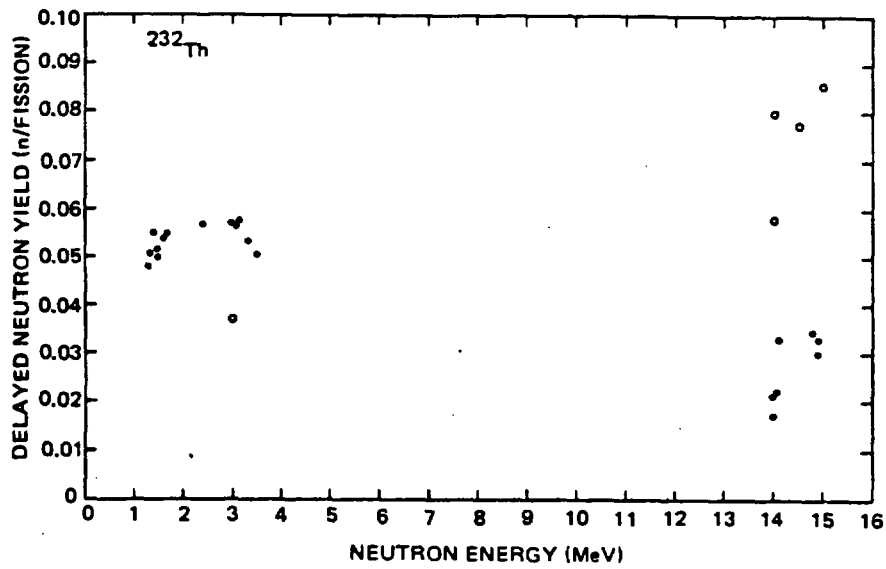

Figure 1. Delayed-Neutron Yield Measurements for Th-232
(Open symbols have been omitted from the evaluation)

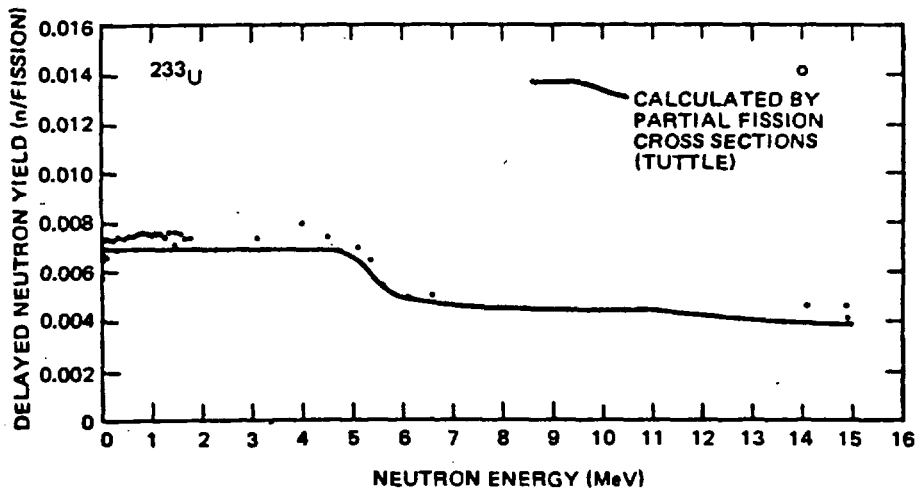

Figure 2. Delayed-Neutron Yield Measurements and Calculations for U-233
(Open symbols have been omitted from the evaluation)

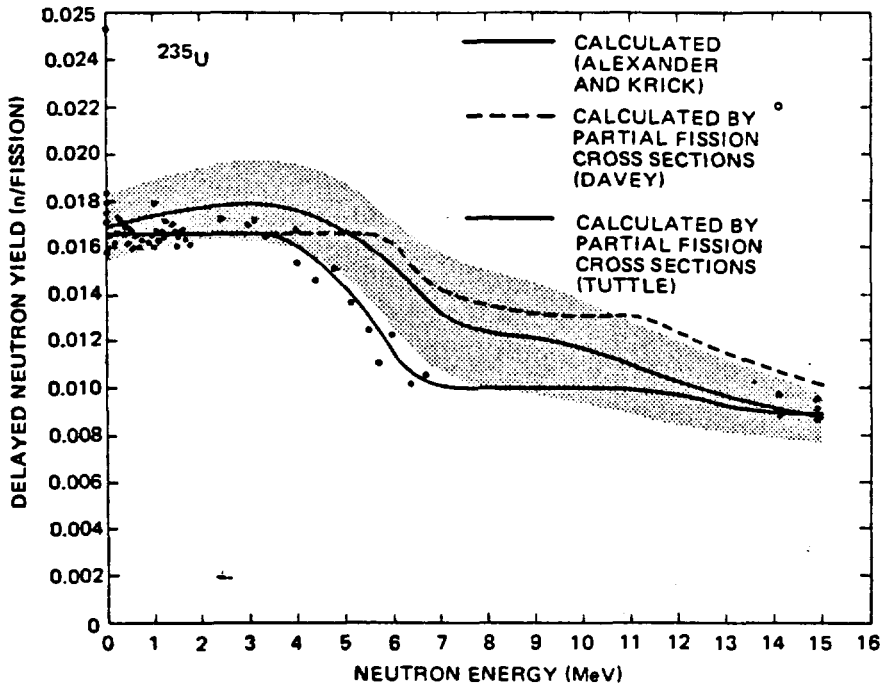

Figure 3. Delayed-Neutron Yield Measurements and Calculations for U-235
(Open symbols have been omitted from the evaluation)

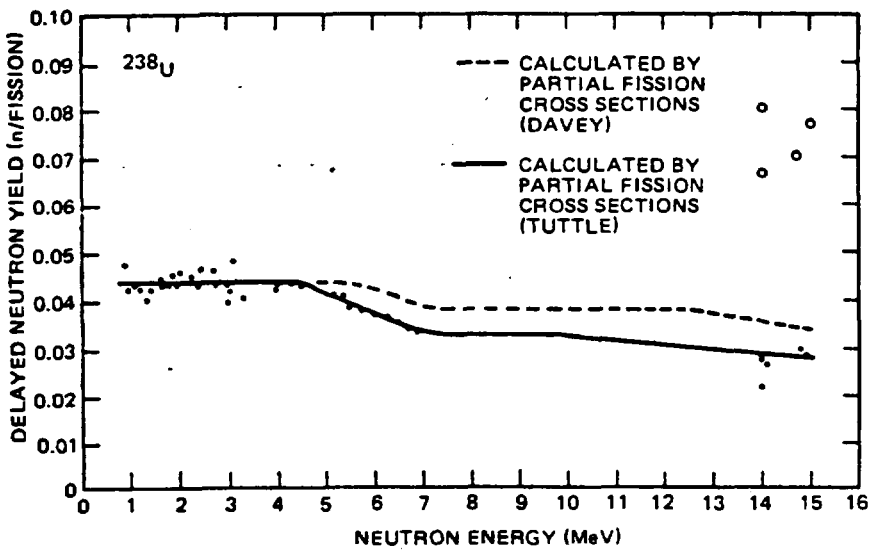

Figure 4. Delayed-Neutron Yield Measurements and Calculations for U-238
(Open symbols have been omitted from the evaluation)

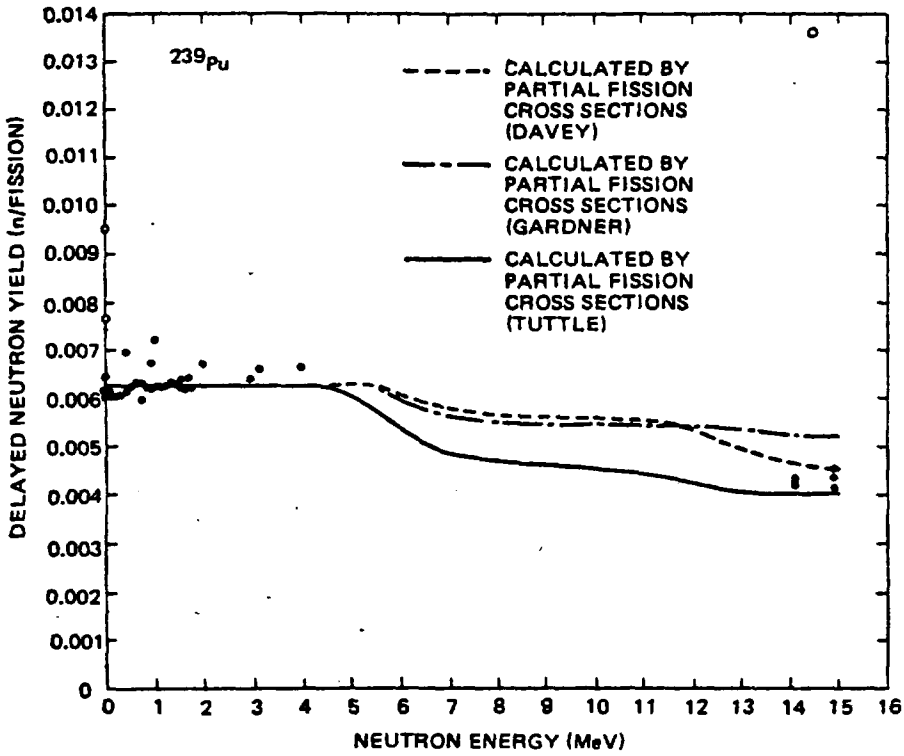

Figure 5. Delayed-Neutron Yield Measurements and Calculations for Pu-239
(Open symbols have been omitted from the evaluation)

INTERPRETATIONS

The energy dependence of delayed neutron yields is currently not well defined. The recommended values at 14-15 MeV result from rejection of the absolute values of all measurements made prior to 1966, for no objective reasons other than disagreement with predictions and the post-1966 measurements. The yields in the low energy range have been assumed to be constant with energy, and this is moderately well supported by the experimental data, although a detailed calculation shows an increase from 0 to 3 MeV, that is also suggested by the measured values.

This calculation, by Alexander and Krick (25), uses the fission yields and neutron emission probabilities of 47 identified delayed-neutron precursors.

The delayed neutron yield calculated in this manner for U-235 shows an increase of about 6% from 0 to 3 MeV neutron energy. While the evaluated yields produced by separate processing of the thermal- and fast-fission measurements for U-235 do not support this variation, it should be noted that only four measurements (Besant, Keepin, Rose, and Brunson), provide 40% of the weight in determining the fast-fission yield. These four measurements may all involve spectrum-dependent corrections. Unfortunately, it is likely that the results of these corrections will be consistent with whichever energy dependence is chosen for calculating them.

Keepin's values for fast and thermal fission show increases in the yield in the fast spectrum relative to that in the thermal spectrum, amounting to 3.3% for Pu-239, 4.4% for U-235, and 6.1% for U-233, using unadjusted values.

The data of Krick and Evans, produced by use of monoenergetic neutrons from 0.05 to 1.75 MeV, have been fit, by the least squares method, to a linear relation:

$$Y(E) = Yo + \frac{\Delta Y}{\Delta E} E$$

This shows the following values and uncertainties for $\Delta Y/\Delta E$:

U-233	$(+14.7 \pm 3.9) \times 10^{-5}$ d.n./MeV
U-235	$(+9.2 \pm 15.8) \times 10^{-5}$ d.n./MeV
Pu-239	$(+12.6 \pm 3.4) \times 10^{-5}$ d.n./MeV

This analysis demonstrates an increase in yield from 0.05 to 1.75 MeV for U-233 and Pu-239, but not for U-235.

The measurements by Masters, et al., (26), used the same fission counters and Pu-238-Li neutron source as were later used by Krick and Evans. Therefore, the major systematic errors should be the same for these two sets of data. Comparison of the zero-energy intercept values

obtained from the linear least-squares fits to the Krick and Evans data with the yields measured at 3.1 MeV by Masters shows the following values for $\Delta Y/\Delta E$:

	Yo	Y(3.1)	$\Delta Y/\Delta E$
U-233	0.007359	0.007400	$(1.3 \pm 13.3) \times 10^{-5}$
U-235	0.01629	0.01720	$(29.4 \pm 34.1) \times 10^{-5}$
Pu-239	0.006106	0.006600	$(15.9 \pm 12.6) \times 10^{-5}$

The value observed for U-235 is essentially identical to that derived for a linear increase from 0 to 3 MeV in the Alexander and Krick calculations.

The values measured by Keepin show a similar effect between thermal and fast-spectrum fission (adjusted for the flux spectrum to a plateau value, assumed valid at 3 MeV). The values for $\Delta Y/\Delta E$ are:

U-233	$(15.3 \pm 24.4) \times 10^{-5}$
U-235	$(31.7 \pm 47.6) \times 10^{-5}$
Pu-239	$(10.0 \pm 22.9) \times 10^{-5}$

While individually these values do not show any increase in yield with energy, taken together they support a definite increase between 0 and 3 MeV.

Attempts to represent the delayed-neutron yield as a sum of yields from the different compound nuclei, formed in different proportions in first-chance, second-chance, and third-chance fission reactions as a consequence of pre-fission neutron emission, have not been completely successful. These attempts, shown here and in the previous evaluation, rely on the use of partial fission cross sections and yields for low-excitation fission of each compound nucleus.

Since this is a very mechanistic model – above the second-chance threshold, there are two compound nuclei fissioning and the resultant yield should reflect this, and similarly for third-chance fission – the discrepancy is not easy to explain. Either the representations of the partial cross sections are considerably inadequate, or the yield values reported by Krick and Evans are too low in energy (by ~1 MeV) and too low in yield (by 10%). Comparison of the yield curve calculated by Alexander and Krick for U-235 with that using the partial cross sections derived graphically by Davey (27) shows more agreement between the calculations than with the measured values. Similarly, relatively little difference is shown between the yield curve using the partial cross sections calculated for Pu-239 by Gardner (28) and those graphically derived by Davey.

As shown previously (1), the measured yield values can be reproduced by the partial cross section method, but only by accepting severe competition between fission modes: second-chance fission becomes dominant with

increasing energy, only to be replaced by third-chance fission as that becomes energetically possible. In addition, the threshold energies needed for this agreement seem low.

The competition between different fission modes can reflect relatively small differences in the fission barrier height. For example, calculations by Moller and Nix (29) show differences of only about 3.8 MeV between asymmetric fission (which is highly probable) and symmetric fission (which is relatively improbable). This small difference in barrier height produces a factor of 600:1 between the two modes of fission.

The difficulties with this model may arise from a different relative population of the two different spin states formed in the fissioning nucleus, when it is formed directly by neutron capture or excitation by a photon, from when it is formed sequentially by neutron capture and neutron emission. It appears likely that emission of a neutron from one spin state of the compound nucleus will be more probable than the other, because of neutron binding energy differences, leading to a greater frequency of second-chance fission from the resulting spin state in the fissioning nucleus than when that nucleus is formed directly. Similar considerations would apply to third-chance fission.

These differences would lead to different delayed neutron yields in second- and third-chance fission from those expected, thus resulting in erroneous predictions of the total yield as a function of energy.

The calculations by Alexander and Krick suggest that the delayed neutron yield from each compound nucleus is a function of excitation energy of that nucleus, and therefore, dependent on the incident neutron kinetic energy. This is explained as a consequence of a greater production of fission fragments with even atomic number, relative to those with odd atomic number, at low excitation energy, with a decrease in this effect as the excitation energy increases.

Thus, the failure of the partial cross section model to adequately reproduce the measured values with reasonable cross sections may be due to the simplistic use of constant (energy-independent) yield values for each of the compound nuclei involved.

Energy-dependent yield curves can be only estimations at this time, and several representations may be equally valid considering the uncertainties in the data. Cox (30) provides a form easily adapted to computer processing of the data. The yield is assumed to be constant in the low energy range (below ~ 4 MeV), linearly decreasing between about 4 to about 7 MeV, and then constant through 15 MeV to 20 MeV. As an alternative, Cox shows a somewhat greater yield above the intermediate energy transition region, with another linear decrease at 14-16 MeV.

The anomalous behavior of the yield for U-235 in different chemical forms, reported by Lukens and Bramblett, raises the question of differences in delayed neutron yields for reactors fueled with different fuel materials, with resultant systematic errors in the application of measured yields to reactor physics analysis of different reactors.

Lukens and Bramblett suggest that the differences observed may result from a modification in the de-excitation and decay modes of the delayed neutron emitter Kr-87 (daughter of the precursor Br-87, the major contributor to Group 1, the longest half-life group). In support of this suggestion, it was found that the gamma-ray emission following beta-decay of Kr-87 was greater for U308 than U02, indicating an increase in the beta-decay branch relative to neutron emission. The relative activities of two other fission products, I-134 and Mo-101, showed no difference. This effect would be the result of chemical modification of nuclear properties after fission.

This particular mechanism can produce only part of the observed difference. The fraction of delayed neutrons from Group 1, calculated for the irradiation, delay, and count times used, is 0.19. The observed change in Kr-87 activity, 6.6%, would therefore be expected to produce a corresponding change of 1.3% in the total delayed neutron counts. The greatest fraction of delayed neutron counts in these measurements result from Group 2 (0.78), which consists predominately of two precursors, Br-88 and I-137.

It has been observed that large differences in fission product yields can occur for the two different spin orientations of the captured neutron (31,32). Whether the differences in the atomic environment caused by the different oxides can alter the fission probability for thermal neutrons of different spin states is not clear.

The comparative measurements by Schrack provide a basis for continued reliance on the assumption of freedom from chemical effects. However, this question is of concern both in applications of the data and in the theory of fission, and measurements with a variety of compounds would be of value.

Since measurements of delayed neutron yields are now approaching accuracies of the order of the observed difference, the chemical form may have an impact on the derived yield value. The chemical forms used in delayed neutron measurements in the thermal and fast reactor energy range are listed in Table II.

This shows that forms other than metal have rarely been used and, in fact, have negligible effect on the evaluated yields. Only in the data of Brunson is there a possible indication of this effect. The values reported for Th-232 (metal), U-238 (metal), and Pu-239 (metal and PuO2) tend to be somewhat high relative to the weighted averages for these nuclides. The values reported for U-233 (U308) are low, while those for U-235 (metal and U308) are scattered. The deviations of the yields for the various nuclides, relative to their assigned uncertainties, show a pronounced difference: for the U-233 sample, all are negative, with an average value of -1.2, which is unusually large; for Th-232, the average is 0.3; for U-235, 0.3; for U-238, 0.4; and for Pu-239, 0.5. While this supports the contention that the chemical form may have an effect on the post-fission pnenomena, since the U-233 sample was U308, it could also result from a systematic error in the U-233 measurements. The accuracies involved (12-25%) are clearly inadequate for this to be anything more than a suggestion.

TABLE II

CHEMICAL FORM OF DELAYED NEUTRON SAMPLES

Measurement	^{232}Th	^{233}U	^{235}U	^{238}U	^{239}Pu
Snell			U308		
Hughes			metal		
Brunson	metal	U308	metal, U308	metal	metal, PuO2
Rose	metal?	metal?	metal?	metal?	metal?
Keepin	metal	metal	metal	metal	metal
Maksyutenko		metal?		metal?	metal?
Masters	metal	metal	metal	metal	metal
Notea	?	?	?		?
Cox	metal		metal	metal	
Conant		metal	metal		metal
Krick		metal	metal		metal
Cox			?	?	?
Clifford			metal	metal	
Besant			metal	metal	metal
Synetos			metal		

Another possible suggestion of this effect lies in integral measurements related to reactivities and the delayed neutron fraction. Fischer (33) finds that for several SNEAK assemblies fueled with UO2 and UO2-PuO2, there is better agreement between measured values of β_{eff} and values calculated using yields recommended in the previous evaluation (1) than those using Keepin's values, which are generally somewhat lower, by about 5%. Measurements at LASL, with metal assemblies, are consistent with the Keepin values (34). This would suggest a possible increase in yields for UO2 which would be consistent with the observed relative lower yield for U3O8.

REVISED EVALUATION

The present evaluation consists of a revision and updating of the previously reported evaluation. It reflects the current values of measured delayed neutron yields and has been expanded to include measurements made with D-T neutrons at about 14-15 MeV. The method used is the same: diverse measured values that have been adjusted to the extent possible to minimize systematic errors are combined in a weighted average based on consistent estimates of the uncertainties. Both relative and absolute measurements are utilized, with the relative values converted to interrelated ratios so as to fully distribute the information among the nuclides involved.

The yield measurements reported for fission caused by 14-15 MeV neutrons appear to form two groups: one of high values, measured prior to 1966, and one of low values, measured later. The cause for this discrepancy has apparently not been identified. The lower (more recent) group of values is in reasonable agreement with current predictions and may be assumed to have benefited from technical advances in the measurement methods and equipment relative to the older group. The higher group of values are consistent within themselves when compared between isotopes at 14-15 MeV. Therefore, only limited ratios, between isotopes for high-energy fission, have been derived from these values and used in the evaluation.

As in the previous evaluation, the present analysis shows expected uncertainties (those based on a weighted combination in quadrature of the individual measurement uncertainties), that are generally larger than the observed uncertainties (those based on the weighted standard deviation of the individual measurement values about the weighted average). For the five isotopes involved in the weighted averaging (with thermal and fast data combined), this is:

	^{232}Th	^{233}U	^{235}U	^{238}U	^{239}Pu
Expected, %	3.9	3.3	1.8	2.2	2.3
Observed, %	2.8	3.1	1.7	1.6	2.0

For the recommended delayed-neutron yields, the larger of the two uncertainties derived in the evaluation has been assigned to the value. The method of treating the interrelated ratios has been changed to more

properly reflect the weight of these entries in determining the uncertainty in the evaluated yield. This has resulted in increases in the estimated uncertainties compared to the previous evaluation.

The total delayed neutron yields for low excitation are well represented by an exponential function involving the mass number and proton number of the fissioning nucleus. This was first suggested by Moscati and Goldemberg (16) as exp-K(2Z-N), was modified to exp-K(3Z-A) by Caldwell and Dowdy (12), and recently has been described in detail by Pai (35). The yield for fission of a specific nuclide is proportional to the overall neutron emission probabilities of the resulting fission fragment chains. The individual probabilities are assumed by Pai to be proportional to exp-Bn/T, where Bn is the neutron binding energy of the delayed neutron emitter, and T is the nuclear temperature associated with the total beta decay energy. These parameters can be related to the fission fragment mass and proton numbers through a variational mass formula. Through averaging over the pairs of light and heavy fission fragments, Pai is able to show that the factor 3 in the variable (3Z-A) is an approximation to derived values of 3.11, 2.97, and 3.03, depending on the data set used.

Using the low-energy yield values for 17 reactions (neutron-fission, photofission, and spontaneous fission), the parameters obtained with a weighted least squares fit are:

$$\log Y = 11.29 + 0.3871(A_c - 3Z) \pm 11.7\% \quad .$$

Modifying the fitting variable to (Ac-3Z)(Ac/Z) reduces some of the variability associated with the different values of Z and results in a fitted equation of:

$$\log Y = 13.81 + 0.1754(A_c - 3Z)(A_c/Z) \pm 10.7\% \ ,$$

which has a slightly lower variance and so has been used for predictions of yields in this evaluation. This relation is shown in Figure 6. (The slope coefficient (0.1754) in this equation cannot be multiplied by an average value of (Ac/Z) as done by Pai for comparison with the slope coefficient (0.3871) in the other form, because the intercept values are significantly different.)

The validity of the systematic fit to low-energy yield data, using the parameter (Ac-3Z) (Ac/Z), for neutron-induced fission, photofission, and spontaneous fission may be tested exactly only for two pairs of reactions. These pairs and the corresponding (measured) delayed-neutron yields are:

U-233+n	0.00688 ± .00012
U-234+γ	0.00900 ± .00094
and	
U-235+n	0.01662 ± .00018
U-236+γ	0.01600 ± .00130

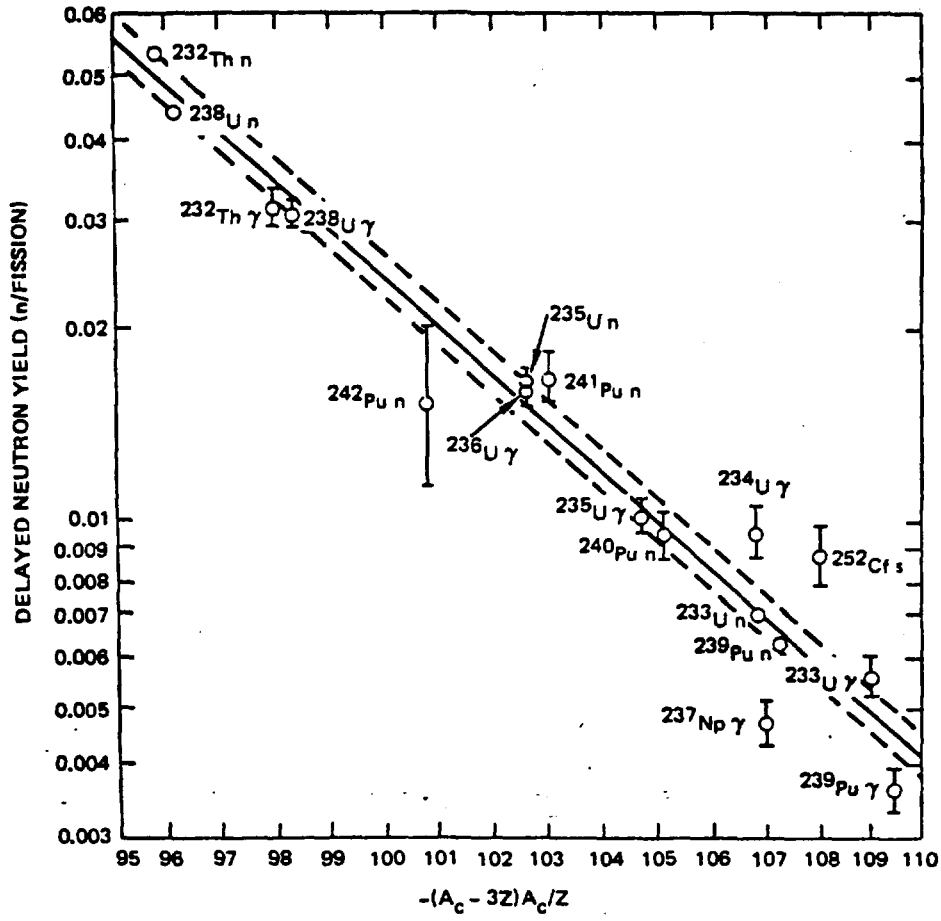

Figure 6. The relation between delayed neutron yield and the mass and proton numbers of the fissioning nucleus

For the first reaction pair, the difference in yields is 2.7 times its expected standard deviation, while for the second pair, the difference is only 0.5 times its expected standard deviation. Assuming a Gaussian distribution for these differences, the probability of these differences being this great or greater is 0.7% for the first and 62% for the second. Thus, the results of this comparison are ambiguous.

The chi-squared test, however, indicates a very low probability that the dispersion of the points about the fitted line would result from chance, given the assigned uncertainties. Therefore, this fit must be accepted at the present time as only a means for estimating yields and not a true representation of the behavior of the various fission reactions.

An interesting trio of reactions that could indicate the effect of the different fission reactions is:

Pu-239+n
Pu-240+γ
Pu-240 spontaneous fission

The characteristics of neutron-induced fission of Pu-239 and spontaneous fission of Pu-240 (except for delayed-neutron emission) have been compared in detail by Deruytter and Wegener-Penning (36). In these two reactions, the excitation energy of the fissioning nucleus differs by the binding energy of the neutron, about 6.4 MeV. Use of bremsstrahlung from electrons of 8 - 10 MeV would result in similar excitation energies for the photofission reaction as for the neutron-induced reaction.

The reactions for which predictions have been made using this equation are:

^{231}Pa (n,f)	0.0108 ± 0.0012
^{234}U (n,f)	0.0105 ± 0.0011
^{236}U (n,f)	0.0221 ± 0.0024
^{237}U (n,f)	0.0323 ± 0.0035
^{237}Pu (n,f)	0.00325 ± 0.00035
^{238}Pu (n,f)	0.00467 ± 0.00050
^{240}Pu (n,f)	0.0098 ± 0.0011
^{241}Pu (n,f)	0.0142 ± 0.0015
^{242}Pu (n,f)	0.0208 ± 0.00022

Some of these have been used to develop recommended values for significant nuclides or other nuclides which are candidates for measurements.

An alternative method of estimation may be applied to Pa-231. The delayed neutron yield for high-energy neutron fission (14.8 MeV) as

measured by Brown, et al., has an adjusted value of 0.0080 ± 0.0026. The ratio of high-energy fission yields to low-energy fission yields is relatively constant for the various nuclides for which information is available, lying in the range of 1.48 to 1.97. The weighted average is 1.69, with a standard deviation of 0.13. Using this ratio and the adjusted value from the measurements by Brown, an estimate of 0.0135 ± 0.0045 is obtained.

Combining these two predictions in a weighted average gives:

$$0.0111 \pm 0.0011 \quad .$$

As in the previous evaluation, two analytical predictions of the yield for Pu-242 have been combined with the single measurement to achieve a more accurate value. These three values are:

0.015 ± 0.005	measured by Krick and Evans (21)
0.0282 ± 0.0052	calculated by Bohn (37)
0.0208 ± 0.0022	present analysis

The resultant value is 0.0221 ± 0.0026, where the assigned uncertainty is that determined by the weighted standard deviation and is larger than expected from the assigned uncertainties. Because of the large uncertainty in the measured value (±33%), this value has little weight in determining the recommended value. This value is, therefore, poorly supported.

Analytical predictions, based on the logarithmic representation discussed earlier, have also been used to improve the quality of the yield values for isotopes with only one measurement. For Pu-240, the predicted value of 0.0098 ± 10.7% is combined with the measured value (Keepin 1957) of 0.0092 ± 11.8% to produce a recommended value of 0.0095 ± 7.9%. For Pu-241, the predicted value of 0.0142 ± 10.7% is combined with the measured value (Cox 1961) of 0.0161 ± 10.0% to produce a recommended value of 0.0152 ± 7.3%. While this value is recommended for both thermal and fast fission, it should be noted that there is no information regarding the energy dependence in this energy range.

The ratio between yields at high energy to those at low energy has been used to complete the estimates of high energy yields for isotopes for which no measurements have been made, U-234, U-236, Pu-238, and Pu-242.

The results of this evaluation are shown in Table III. The major sources of the changes noted in the current recommended values are the high-accuracy values reported by Besant et al., Synetos and Williams, and the elimination of Clifford's values. Yields determined partly or wholly on the basis of analytical predictions are indicated by parentheses.

The possibility of a difference in yields for thermal- and fast-fission (fission by thermal-spectrum neutrons and fast-reactor-spectrum

TABLE III

RECOMMENDED DELAYED-NEUTRON YIELDS*

Nuclide	Thermal	Fast	14 MeV
^{231}Pa	-	(0.0111 ± 0.0011) 10.0%	0.0080 ± 0.0026
^{232}Th	-	0.0531 ± 0.0023 4.2%	0.0285 ± 0.0013 4.6%
^{233}U	0.00667 ± 0.00029 4.3%	0.00731 ± 0.00036 4.9%	0.00422 ± 0.00025 5.2%
^{234}U	-	(0.0105 ± 0.0011) 10.7%	(0.0062 ± 0.0008) 13.3%
^{235}U	0.01621 ± 0.00050 3.1%	0.01673 ± 0.00036 2.1%	0.00927 ± 0.00029 3.1%
^{236}U	-	(0.0221 ± 0.0024) 10.7%	(0.013 ± 0.002) 13.3%
^{238}U	-	0.0439 ± 0.0010 2.3%	0.0273 ± 0.0008 2.9%
^{238}Pu	-	(0.0047 ± 0.0005) 10.7%	(0.0028 ± 0.0004) 13.3%
^{239}Pu	0.00628 ± 0.00038 6.0%	0.00630 ± 0.00016 2.5%	0.00417 ± 0.00016 3.7%
^{240}Pu	-	(0.0095 ± 0.0008) 7.9%	0.00671 ± 0.00050 7.5%
^{241}Pu	(0.0152 ± 0.0011) 7.3%	(0.0152 ± 0.0011) 7.3%	0.00834 ± 0.00070 8.4%
^{242}Pu	-	(0.0221 ± 0.0026) 11.8%	(0.0084 ± 0.0011) 13.3%

* Values influenced by empirical estimates are shown in parentheses.

neutrons, respectively) that was suggested, albeit weakly, in the previous evaluation has essentially disappeared in the present evaluation when the yield values are grouped according to thermal fission and fast (0-4 MeV) fission. Only U-233 shows a significant difference; U-235 suggests a difference, while Pu-239 shows essentially none.

However, energy dependence in this range may be obscured by the combination of results measured with broad-spectrum neutrons and monoenergetic neutrons over an extended energy range. Such energy dependence is supported by several individual measurements and the calculations of Alexander and Krick, as discussed earlier. These indications have been used to derive an alternate representation of the delayed-neutron yields for U-233, U-235, and Pu-239.

Evaluation of the data with the assumption of an increase in yield from thermal energy to 3 MeV followed by a decrease to a constant value from about 7 to about 11 MeV, with another decrease through 14 MeV, has resulted in a representation of the yields similar to that of Cox. These are shown in Figure 7. The energies and yields defining this representation are:

Energy	0	3	7	11	14.5
U-233	0.00680	0.00748	0.005	0.005	0.00422
U-235	0.01644	0.01738	0.010	0.010	0.00923
Pu-239	0.00622	0.00659	0.0048	0.0048	0.00417

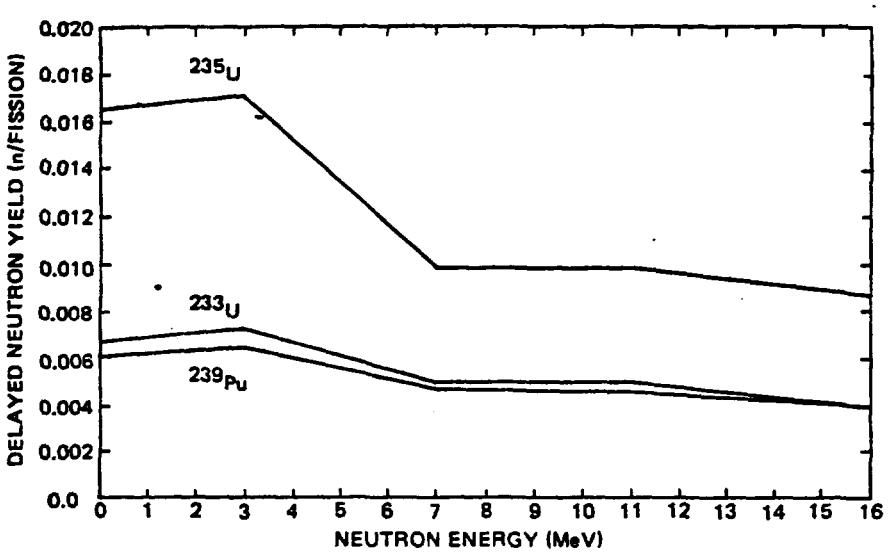

Figure 7. Representation of delayed-neutron yeilds for U-233, U-235, and Pu-239 with assumed energy dependence

RECOMMENDATIONS

There are significant gaps in the energy-dependent yield measurements, with no information between 4 and 14 MeV for Pu-239 and none at all between 7 and 14 MeV for any nuclides. This energy range should be investigated, preferably in conjunction with lower and higher energy measurements with the same samples and equipment. The low energy range is still poorly defined and high precision measurements are needed from a few keV to 4-5 MeV. The lower part of this range may be investigated by use of photoneutron sources such as Sb-Be (23 keV), Ga-D (140 keV), Na-D (265 keV), La-Be (770 keV), and Na-Be (964 keV), which provide well-established and stable neutron energy distributions.

Measurements should be made with additional nuclides. Those that appear practical for this purpose include Pa-231, U-234, U-236, Np-237, and Pu-238. The nuclide Pa-231 exists in nature in radioactive equilibrium with its parent, U-235. Significant quantities are accessible in high purity, both chemically and isotopically (38). It has a fission cross section comparable to that of Np-237 (39,40) and so is a possible candidate for delayed neutron measurements that would extend the range of (Z,A) for fast-reactor neutron fission.

The calculational method of Alexander and Krick should be applied to other nuclides for which the necessary data is available or can be estimated. This should be done especially for Pu-239, for which energy-dependent data are particularly lacking.

The accuracy of delayed-neutron yield measurements should be ±5% or better, or the results will not contribute significantly to the evaluated yields. Measurements should be as comprehensive in energy and include as many nuclides as possible. The spectrum of incident neutrons should be as well characterized as possible.

ACKNOWLEDGMENTS

The cooperation and assistance of many experimentalists, theoreticians, and data analysts is gratefully acknowledged. The encouragement of Dr. M. E. Remley and the support of Rockwell International have been greatly appreciated.

REFERENCES

1. R. J. Tuttle, Nucl. Sci. Eng. 56, 37 (1975)

2. A. Notea, "Research Laboratories Annual Report - January-December 1968," IA-1190, Israel Atomic Energy Commission (1969)

3. G. R. Keepin, T. F. Wimett, and R. K. Zeigler, J. Nucl. Energy, 6, 1 (1957); also, Phys. Rev. 107, 1044 (1957)

4. G. Herrmann, Proc. Panel Delayed Fission Neutrons, International Atomic Energy Agency, Vienna (1968)

5. L. A. Kull, R. L. Bramblett, T. Gozani, and D. E. Rundquist, Nucl. Sci. Eng. 39, 163 (1970)

6. O. P. Nikotin and K. A. Petrzhak, Soviet At. Energy, 20, 268 (1966)

7. M. G. Brown, S. J. Lyle, and E. B. M. Martin, Radiochim Acta, 15, 109 (1971)

8. D. A. Clifford, Ph. D. Thesis, Imperial College, London (1972)

9. M. H. McTaggart, Fast Integral Assembly Newsletter, No. 37 (1976)

10. M. H. McTaggart, personal communication, December 1978

11. E. T. Chulick and P. L. Reeder, Nucl. Phys. A173, 497 (1971)

12. J. T. Caldwell and E. J. Dowdy, Nucl. Sci. Eng. 56, 179 (1975)

13. J. T. Caldwell, E. J. Dowdy, and G. M. Worth, "Physics and Chemistry of Fission 1973," Vol. I, p 431, IAEA, Vienna (1974)

14. Y. Miyao, M. N. Martins, O. D. Goncalves, L. M Lunardi, S. Barros, and G. Moscati, 27th Annual Meeting of the Brazilian Society for the Advancement of Science, July 9-16, 1975, Sao Paulo

15. G. Moscati, personal communication, February 1979. The details of these measurements are reported in an unpublished M.S. thesis by Y. Miyao

16. G. Moscati and J. Goldemberg, Phys. Rev. 126, 1098 (1962)

17. H. R. Lukens and R. L. Bramblett, Nucl. Sci. Eng. 61, 426 (1976)

18. C. B. Besant, P. J. Challen, M. H. McTaggart, P. Tavoularidis, J. G. Williams, J. Br. Nucl. Energy Soc. 16, 161 (1977)

19. H. Rose and R. D. Smith, J. Nucl. Energy 1, 133 (1957)

20. G. S. Brunson, E. N. Petit, and R. D. McCurdy, "Measurement of Delayed Neutron Yields in Plutonium, Uranium-233, Uranium-238, and Thorium Relative to Yield in Uranium-235," ANL-5480, Argonne National Laboratory (1955)

21. M. S. Krick and A. E. Evans, Nucl. Sci. Eng. 47, 311 (1972)

22. J. G. Williams, IAEA Consultants Meeting on Delayed Neutron Properties, Vienna, March 1979

23. R. Schrack, International Conference on Neutron Physics and Nuclear Data for Reactors and Other Applied Purposes, Harwell, September 25-29, 1978.

24. S. Synetos and J. G. Williams, IAEA Consultants Meeting on Delayed Neutron Properties, Vienna, March 1979

25. D. R. Alexander and M. S. Krick, Nucl. Sci. Eng. 62, 627 (1977)

26. C. F. Masters, M. M. Thorpe, and D. B. Smith, Nucl. Sci. Eng. 36, 202 (1969)

27. W. G. Davey, Nucl. Sci. Eng. 44, 345 (1971)

28. D. G. Gardner, J. L. Brownless, and A. Delucchi in LMFBR Reaction Rate and Dosimetry 3rd Quarterly Progress Report December 1971, January, February 1972, compiled by W. N. McElroy, HEDL-TME 72-45, Hanford Engineering Development Laboratory (1972)

29. P. Möller and J. R. Nix, "Physics and Chemistry of Fission 1973," Vol. I, p 103, IAEA, Vienna (1974)

30. S. A. Cox, "Delayed Neutron Data - Review and Evaluation," ANL/NDM-5, Argonne National Laboratory (1974)

31. R. B. Regier, W. H. Burgus, and R. L. Tromp, Phys. Rev. 113, 1589 (1959)

32. R. B. Regier, W. H. Burgus, and B. H. Sorenson, Bull. Am. Phys. Soc. II, 5, 33 (1960)

33. E. A. Fischer, Nucl. Sci. Eng. 62, 105 (1977)

34. W. G. Davey, G. E. Hansen, J. J. Koelling, and T. P. McLaughlin, International Conference on Neutron Physics and Nuclear Data for Reactors and Other Applied Purposes, Harwell, September 25-29, 1978; LA-UR-78-2467, Los Alamos Scientific Laboratory (1978)

35. H. L. Pai, Ann. Nucl. Energy, 3, 125 (1976)

36. A. J. Deruytter and G. Wegener-Penning, "Physics and Chemistry of Fission 1973," Vol. II, p 51, IAEA, Vienna (1974)

37. E. M. Bohn, "Reactor Physics Division Annual Report - July 1, 1968, to June 30, 1969," ANL-7610, Argonne National Laboratory (1970)

38. D. A. Collins, J. J. Hillary, J. S. Nairn, and G. M. Phillips, J. Inorg. Nucl. Chem. 24, 441 (1962)

39. G. C. Wu and L. Ruby, Nucl. Sci. Eng. 68, 349 (1978)

40. A. Sicre, G. Barreau, R. Chastel, T. P. Doan, B. Leroux, J. C. Sageaux, "Physics and Chemistry of Fission 1973," p 71, IAEA, Vienna (1974)

Report for the Consultant's Meeting on Delayed Neutron Properties, IAEA, Vienna, 26-30 March 1979

Delayed-Neutron Branching Ratios of Fission Products - a Status Report

G Rudstam
The Studsvik Science Research Laboratory,
S-611 82 Nyköping, Sweden

Abstract

The delayed-neutron branching ratios of fission products have been reviewed, and the average values have been evaluated for 65 nuclides (including a few isomers). The report reflects the situation at the end of March, 1979.

1. *Introduction*

In my review on delayed neutrons at the IAEA meeting on fission product nuclear data at Petten in September 1977[1)] I drew the conclusion about branching ratios that only half of the precursors had ratios which could be considered to be known with good accuracy. As for the other half the ratios were either unknown or data from different investigators were in such a serious disagreement that remeasuring seemed necessary. Finally, cases with only one published ratio needed checking.

The reason for this rather unsatisfactory state of matters can sometimes be traced to indirect methods of determining sample strengths, notably by the intermediate use of fission yields for which estimated,and often quite unreliable, values have been used. However, also cases where direct methods for measuring the strengths have been used are occasionally unreliable and discrepancies amounting to factors of two or three, or tens of standard deviations, are not uncommon. The conclusion to be drawn is that the investigators have had a very incomplete knowledge about the uncertainties in their measurements, perhaps overlooking serious systematic errors.

The first condition for a successful determination of the branching ratio is that the precursors are obtained in a reasonably pure form, preferably by both chemical separation and mass separation. A good example of this is mass separation of alkali isotopes using surface ionization to remove other elements. Only mass-separated samples may also be acceptable although this usually implies resolving decay curves containing 2 - 3 components. Only chemical separation may also be used, but it is more difficult than only mass separation because the number of components in the decay curves becomes considerably larger.

As the branching ratio is simply the ratio between the number of neutrons emitted and the sample strength, the accuracy is determined by the accuracy which one can reach in the determination of those quantities, and here the reliability of the calibration of the counters becomes crucial. The uncertainty of the results is often determined by systematic calibration errors rather than by counting statistics.

2. Experimental methods

2.1 Neutron counting

The neutron counting is usually performed by means of ^{3}He- or BF_3-counters after moderating the neutrons. In these counters the neutrons give pulses which are larger

than pulses induced by gamma rays, and a discrimination against gammas can easily be made. The counters are very energy-sensitive, however, and their response will depend on the amount and arrangement of moderating material. Thus the response of the neutron detectors has to be determined as a function of neutron energy. This can be done by means of monoenergetic neutrons, for example, from (p,n)-reactions induced by protons from a Van de Graaff-accelerator. An example of the energy-dependence may be taken from Reeder et al[2] who give an efficiency of 47 % at 200 keV and 42 % at 800 keV for their detector. On the other hand, Ristori et al[3] find very little energy-dependence of their counter, or about 4 % in the range from zero up to 1.5 MeV. At any rate,the possible energy-dependence must be considered, and discrepancies between different determinations might have their roots in a negligeance of this effect.

With the energy-dependence of a counter determined one needs to know the neutron spectrum in order to apply the correction. If the response function is linear, however, it is sufficient to know the average neutron energy. This is easily seen if the efficiency function, i.e. the probability of detecting a neutron of energy E, is given by $\varepsilon(E)$, and the neutron spectrum is described by the normalized function $\varphi(E)dE$. Then, the probability P of detecting a neutron will be equal to

$$P = \int_0^{E_{max}} \varphi(E)\ \varepsilon(E)\ dE$$

and, if $\varepsilon(E) = a + bE$

$$P = a + b\bar{E}.$$

Measured average neutron energies range from about 200 keV to 600 keV[1]. A 10 % change between 200 and 800 keV would then correspond to an efficiency difference of 7.5 % between different precursors if we take the Reeder detector as an example. This estimate shows that the energy dependence of the response function must be taken into account.

A commonly used method is to use calibrated neutron sources for detector calibration. If this is done it is necessary to use a source with a spectrum which is typical for the delayed-neutron precursors. Thus, an americium-lithium source with an average neutron energy of about 400 keV is a proper choice whereas a plutonium-beryllium source with a much harder spectrum (average energy several MeV) would be unsatisfactory.

2.2 Determination of the sample strength

2.2.1 Beta counting

The sample strength is often determined by counting the number of beta decays in the sample and, if there are several beta-decaying components, to follow the decay of the sample decomposing the decay curve into its components. What is needed is then a calibrated beta-counter.

There is no need to discuss the calibration procedure here. It might only be mentioned that at Studsvik we have used the $\beta\gamma$-coincidence technique with mass-separated samples of isotopes of indium and tin (^{125,127}In, ^{125,127,129}Sn) for the purpose.

A correction for the presence of conversion electrons may occasionally be important.

2.2.2 Ion counting

Another method to determine the strength of a mass-separated sample is counting the ions which reach the collector. This method can only be used if there is just one kind of nuclides in the ion beam. This is the case when surface ionization is used to single out isotopes of rubidium and cesium.

A comparison between ion counting and beta counting, extended over several rubidium and cesium isotopes, gave a good agreement[2].

2.2.3 Determination of the number of atoms formed by decay

Several investigators have determined the number of atoms of a certain precursor in a sample by counting the number of atoms of a more long-lived decay product. This technique requires that the sample formed originally was free from daughter activities, or contained a known amount of such activities. An example of the method is given by Talbert, Tucker, and Day[4] who determined the number of ^{141}Xe and ^{141}Cs atoms in their samples by counting the gamma-rays of energy 1.36 MeV emitted by the isobar ^{141}La. Obviously, an accurate figure for the transition probability of the particular gamma-ray chosen for the measurement is needed, and the uncertainty of this branching ratio often limits the precision of the determination of the delayed-neutron branching ratio.

2.2.4 Indirect methods

Many of the older determinations of delayed-neutron branching ratios have been based on indirect determinations of sample strengths via fission yields. This is perfectly satisfactory if experimental values of the fission yields are used. The method is more doubtful, however, if it rests on estimations of fission yields, the reason being that an appreciable fine structure has been revealed in the yield pattern. The regular variation of the independent yields anticipated in earlier estimates has proved to be wrong, and the relative deviations from a smooth behaviour may reach 30 % [5]. There does not yet exist a sufficient amount of experimental data to make possible an estimate of the effect with the desired accuracy. Therefore, branching ratios determined by indirect methods involving estimated yields must be regarded with caution.

3. Analysis of delayed-neutron branching ratios

3.1 Outline of the analysis

In this chapter the branching ratios will be discussed for precursors from gallium to lanthanum. Published

or otherwise reported data are presented in a number of tables which also contain indications about the method used in the experiments, notably how the sample strength was determined. The neutron counting has been similar in all experiments, and there is no need to specify it.

In cases with several determinations their weighted average value is calculated and given at the bottom of the tables. When evaluating these averages the determinations which are based on estimated fission yields have been recalculated using recent fission yields for cases where the yield figures used are clearly stated in the articles (cf. ref.[6]). If the information necessary for a recalculation is lacking, or contradictory, the indirect values are excluded from the evaluation of the average value if direct measurements are also available.

The possible occurance of undetected systematic errors in the P_n-value measurements was pointed out in the introduction of this report. The presence of such errors is revealed by an unexpectedly large spread among the data, i.e. the sum of chi squares ($\Sigma\chi^2$) is larger than the number of degrees of freedom (n-1).In this review an attempt has been made to account for the systematic errors by multiplying the error deduced from the data by the correction factor

$$F = \sqrt{\Sigma\chi^2/(n-1)}$$

in cases with $F > 1$.

For easy reference the facility, or the laboratory, where the investigations have been carried out and the year of publication are also given in the tables. The names appearing there refer to the following techniques and places (within brackets: elements processed):

ARIEL	On-line isotope separator at CEN, Grenoble, (noble gases),
HARWELL	Chemical separation techniques used at Harwell,
LOHENGRIN	Recoil mass separator for unslowed fission products at ILL, Grenoble, (all elements),
MAINZ	Chemical separation techniques used at the University of Mainz,

MOL	Chemical separation techniques used at C.E.N., Mol,
ORSAY	Mass spectrometric techniques at Orsay (alkali metals),
OSIRIS	On-line isotope separator at Studsvik (wide range of elements),
OSTIS	On-line mass separator at ILL, Grenoble, (alkali metals),
SOLAR	On-line mass spectrometer at Battelle, Richland, (halogen and alkali elements),
SOLIS	On-line mass separator at Yavne (halogen and alkali elements),
RUSSIA	Russian work using chemical separation techniques (laboratory not stated in the article),
TRISTAN	On-line mass separator at Ames (halogen elements and noble gases).

3.2 Gallium isotopes

The information about branching ratios for gallium isotopes emanates from the OSIRIS grcup[7]. The method of sample strength determination has been beta counting. The results obtained are given in Table 1.

Table 1

Branching ratio of gallium isotopes

Nuclide	P_n-value, %	Comment
^{79}Ga	0.094±0.016	Contribution from ^{79}Zn (so far unknown) cannot be excluded
^{80}Ga	0.80±0.06	
^{81}Ga	11.9±1.0	
^{82}Ga	21.9±2.3	

3.3 Arsenic isotopes

For ^{84}As only one determination has been published. It is based on experimental fission yields[8]. The value obtained was 0.13±0.06 %. A recalculation using a new experimental yield value[9] decreases the P_n-value to 0.09±0.05 %. The still lower value 0.05±0.03 % is obtained using the yield 0.40 % communicated by Kratz[32].

Table 2

Branching ratio of ^{85}As

Determination	Result, %	Method	Reference
1	22±5	Estimated fission yields	Harwell-68 (10)
	78±8	Experimental yield from ref.[9]	(recalculated)
2	23±5	Estimated fission yield	Mainz-73 (8)
	62±10	Experimental yield from ref.[9]	(recalculated)
3	22±8	Experimental fission yields	Lohengrin-78 (11)

All the determinations seem to agree well. The first two are based on estimated fission yields which are considerably higher than a recent experimental value[9]. Using the latter brings the branching ratios up to 78 % (no. 1) and 62 % (no. 2), or about three times the determination no. 3. The average value deduced for the recalculated determinations and the determination no. 3 is 53±18 %. In this case the correction factor takes the high value of 7.7. A multiplication of the error by this factor leads to the trivial result that any P_n-value from zero to 100 % is compatible with the experimental determinations. Thus, we are left in a very unsatisfactory situation and have to put P_n = 50±50 %.

Table 3

Branching ratio of ^{86}As

Determination	Result, %	Method	Reference
1	$3.8^{+1.7}_{-1.0}$	Estimated fission yields	Mainz-73 (8)
	18^{+5}_{-3}	Experimental yield from ref.[9]	(recalculated)
2	10.5±2.2	Experimental fission yields	Lohengrin-78 (11)

The high value estimated for the fission yield in the first determination leads to a low P_n-value. An adjustment using an experimental value from ref.[9] gives the result 18 %. The average value is

$$P_n = 12 \pm 3 \text{ \%}.$$

With a value of 1.4 for the correction factor F the error increases to ± 4 %.

For ^{87}As only one value has been published: 44 ± 14 % (Lohengrin-78[11]). The method used for determining the sample strength is based on experimental fission yields.

3.4 Selenium isotopes

Table 4
Branching ratio of ^{87}Se

Determination	Result, %	Method	Reference
1	0.25±0.06	Experimental fission yields	Mainz-70 (12)
2	0.23±0.07	Comparison with P_n of daughter	Mol-70 (13)
3	0.16±0.03	Comparison with P_n of daughter	Harwell-71 (14

The average value of all the determinations is $P_n = 0.19 \pm 0.03$ %. The correction factor F is close to unity and does not change the error.

Table 5
Branching ratio of ^{88}Se

Determination	Result, %	Method	Reference
1	0.18±0.10	Comparison with P_n of daughter	Mainz-70 (1:
2	0.75±0.06	Comparison with P_n of daughter	Harwell-71 (1⁴

There is a large discrepancy between the experiments. Both are based on comparisons with the P_n-value of ^{88}Br for which too low figures have been used (no. 1: 4.0 %; no. 2: 4.7 %). Both determinations are therefore doubtful. As an average one obtains

P_n = 0.6±0.3 %

Because of the large spread the correction factor takes the high value of 3.9. A corrected error would then be $^{+1.2}_{-0.6}$ %.

For ^{89}Se there exists only one published value (Harwell-71[14]) which is

P_n = 5.0±1.5 %.

This value is based on a comparison with the P_n-value of ^{89}Br for which the low value 8.8 % was used. It must therefore be regarded with caution.

Also in the case of ^{91}Se only one value has been reported (Lohengrin-75[15]), and this is based on estimated fission yields. The value is

P_n = 21±8 %.

3.5 Bromine isotopes

Table 6

Branching ratio of ^{87}Br

Determination	Result, %	Method	Reference
1	3.1±0.6	Beta counting	Russia-64 (16)
2	2.1±0.3	Gamma-counting of long-lived daughter	Mol-71 (17)
3	2.3±0.4	Estimated fission yields	Mainz-72 (18)
	2.5±0.4	Experimental yield from ref.[9]	(recalculated)
4	2.5±0.3	Ion counting	Solar-77 (19)
5	2.6±0.4	Experimental fission yields	Mainz-78 (20)
6	2.33±0.14	Beta counting	Osiris-79 (7)

There is a satisfactory agreement among the investigators as regards the branching ratio of ^{87}Br. The average value of all determinations comes out to be

P_n = 2.38±0.08 %.

The correction factor F is less than unity and does not change the error.

Table 7

Branching ratio of ^{88}Br

Determination	Result, %	Method	Reference
1	6.0±1.6	Beta counting	Russia-64 (16)
2	4.3±0.5	Estimated fission yields	Mainz-72 (18)
	7.0±0.7	Experimental yield from ref.[9]	(recalculated)
3	7.4±0.5	Ion counting	Solar-77 (19)
4	6.5±0.7	Experimental fission yields	Mainz-78 (20)
5	6.3±0.4	Beta counting	Osiris-79 (7)

The average value is

$P_n = 6.7 \pm 0.2$ %.

The correction factor is less than unity and does not change the error.

Table 8

Branching ratio of ^{89}Br

Determination	Result, %	Method	Reference
1	7±2	Beta counting	Russia-64 (16)
2	7.2±1.8	Estimated fission yields	Mainz-72 (18)
	15.3±2.7	Experimental yield from ref.[9]	(recalculated)
3	16.9±1.7	Ion counting	Solar-77 (19)
4	12.5±2.0	Experimental fission yields	Mainz-78 (20)
5	13.8±0.9	Beta counting	Osiris-79 (7)

The average value of the determinations is

$P_n = 13.5 \pm 1.3$ %.

The low determination no. 1 gives a large contribution to the sum of chi squares, and the factor F becomes as large as 2.0. Thus, the corrected error is ± 2.6 %.

Table 9

Branching ratio of ^{90}Br

Determination	Result, %	Method	Reference
1	11±3	Estimated fission yields	Mainz-72 (18)
	56±10	Experimental yield from ref.[9]	(recalculated)
2	22.6±3.1	Beta counting	Lohengrin-75 (15)
3	18.9±3.9	Experimental fission yields	Mainz-78 (20)

In this case the recalculated value for determination no. 1 is excluded because of contradictory yield values. Ref.[9] reports the fission yield of ^{90}Br to be 0.287 % whereas Kratz[32] quotes 0.68 ± 0.08 %. The latter value leads to a P_n-value of 24±4 %, in agreement with the other determinations.

The average value of the determinations nos. 2 and 3 is

$$P_n = 21.2 \pm 2.4\ \%.$$

The factor F is less than unity.

Table 10

Branching ratio of ^{91}Br

Determination	Result, %	Method	Reference
1	9.9±2.0	Beta counting	Lohengrin-75 (15)
2	14.1±3.6	Experimental fission yields	Mainz-78 (20)

The average value of the determinations is

$$P_n = 10.9 \pm 1.8\ \%.$$

The correction factor is less than unity.

Table 11

Branching ratio of ^{92}Br

Determination	Result, %	Method	Reference
1	21±8	Beta counting	Lohengrin-78 (11)
2	24.5±10.2	Experimental fission yields	Mainz-78 (20)

The average value is

P_n = 22±6 %.

The correction factor is less than unity.

3.6 Krypton isotopes

Table 12

Branching ratio of ^{92}Kr

Determination	Result, %	Method	Reference
1	0.040±0.007	Gamma counting of long-lived daughter	Tristan-69 (4)
2	0.0323±0.0026	Beta counting	Ariel-75 (2

The average value of the two determinations is

P_n = 0.033±0.003 %.

The correction factor is less than unity.

Table 13

Branching ratio of ^{93}Kr

Determination	Result, %	Method	Reference
1	3.9±0.6	Estimated fission yields	Solis-68 (22)
2	2.6±0.5	Gamma counting of long-lived daughter	Tristan-69 (4
	2.8±0.5	Gamma branching ratio (recalculate from ref.[33])	
3	1.9±0.2	Beta counting	Lohengrin-75 (15)
4	1.92±0.14	Beta counting	Ariel-75 (21)

The indirect determination no. 1 is excluded giving, as an average of the other determinations, the branching ratio

P_n = 1.96±0.14 %.

By multiplication with the correction factor (1.2) the error increases to ± 0.17 %.

For ^{94}Kr a P_n-value of 5.7±2.2 % obtained using beta counting for the determination of the sample strength has been published (Lohengrin-75[15]). The same group also gives the value of 1.6±0.9 %, determined using estimated fission yields in the evaluation. This result is therefore indirect and, moreover, it is not independent of the first result since the neutron counting data were the same. The direct determination is preferred here although its error is larger than that of the other result. Thus

P_n = 5.7±2.2 %.

3.7 Rubidium isotopes

Table 14

Branching ratios of ^{92}Rb

Determination	Result, %	Method	Reference
1	0.012±0.004	Gamma counting of long-lived daughter	Tristan-69 (4)
2	0.0125±0.0015	Beta counting	Lohengrin-75 (15)
3	0.012 ± 0.002	Ion counting	Solar-77 (19)
4	0.0118±0.0008	Ion counting	Solar-79 (2)
5	0.0104±0.0012	Beta counting	Osiris-79 (7)

The average values of all determinations is

P_n = 0.0116±0.0012 %.

The correction factor is less than unity and does not change the error.

Table 15

Branching ratios of ^{93}Rb

Determination	Result, %	Method	Reference
1	2.6±0.4	Estimated fission yields	Solis-68 (22)
2	1.65±0.30	Gamma counting of long-lived daughter	Tristan-69 (4)
	1.75±0.32	Gamma branching ratio from ref.[33]	(recalculated)
3	1.43±0.18	Ion counting	Orsay-69 (23)
4	2.1±0.6	Estimated fission yields	Mainz-72 (18)
	1.77±0.50	Experimental yield from ref.[9]	(recalculated)
5	1.24±0.14	Beta counting	Orsay-74 (24)
6	1.16±0.08	Beta counting	Ariel-75 (21)
7	1.2±0.1	Beta counting	Lohengrin-75 (15)
8	1.86±0.13	Ion counting	Solar-77 (19)
9	1.66±0.13	Ion counting	Solar-79 (2)
10	1.97±0.22	Beta counting	Solis-79 (25)
11	1.39±0.08	Beta counting	Osiris-79 (7)

The average value of all the determinations except the indirect one (no. 1) comes out to be

$$P_n = 1.39 \pm 0.08\ \%.$$

In this case there is a considerable spread among the data, and the correction factor becomes 2.3. Thus, the error should be corrected to ± 0.18 %.

Table 16

Branching ratio of ^{94}Rb

Determination	Result, %	Method	Reference
1	11.1±1.1	Ion counting	Orsay-69 (23
2	11±2	Estimated fission yields	Mainz-72 (18
	10±2	Experimental yield from ref.[9]	(recalculated)
3	8.5±0.9	Beta counting	Orsay-74 (24
4	9.6±0.8	Beta counting	Lohengrin-75 (
5	13.7±1.0	Ion counting	Solar-77 (19
6	9.7±0.5	Beta counting	Ostis-78 (3
7	12.4±0.9	Ion counting	Solar-79 (2
8	11.1±0.9	Beta counting	Solis-79 (25
9	10.1±0.6	Beta counting	Osiris-79 (7

The average value of all the determinations is

$P_n = 10.4 \pm 0.6$ %.

The factor F is 1.8 giving the corrected error ± 1.1 %.

Table 17

Branching ratio of ^{95}Rb

Determination	Result, %	Method	Reference
1	7.1±0.9	Ion counting	Orsay-69 (23)
2	8.5±0.9	Beta counting	Orsay-74 (24)
3	8.4±0.5	Beta counting	Lohengrin-75 (15)
4	11.0±0.8	Ion counting	Solar-77 (19)
5	8.6±0.5	Beta counting	Ostis-78 (3)
6	10.8±0.8	Ion counting	Solar-79 (2)
7	8.2±0.8	Beta counting	Solis-79 (25)
8	8.8±0.6	Beta counting	Osiris-79 (7)

The average value of all the determination is

$P_n = 8.8 \pm 0.4$ %.

By multiplication with the correction factor 1.6 the error increases to ± 0.6 %.

Table 18

Branching ratio of ^{96}Rb

Determination	Result, %	Method	Reference
1	12.7±1.5	Ion counting	Orsay-69 (23)
2	13.0±1.4	Beta counting	Orsay-74 (24)
3	17.0±1.2	Ion counting	Solar-77 (19)
4	12.5±0.9	Beta counting	Ostis-78 (3)
5	17.7±1.3	Ion counting	Solar-79 (2)
6	14.2±1.2	Beta counting	Solis-79 (25)
7	13.5±0.9	Beta counting	Osiris-79 (7)

The average value of all the determination is

$P_n = 14.2 \pm 0.8$ %.

The correction factor is 1.8 which leads to a corrected error of ± 1.4 %.

Branching ratio of ^{97}Rb

Determination	Result, %	Method	Reference	
1	27.2±3.0	Beta counting	Orsay-74	(24)
2	35.9±2.6	Ion counting	Solar-77	(19)
3	25.2±1.8	Beta counting	Ostis-78	(3)
4	32.5±2.6	Ion counting	Solar-79	(2)
5	21.5±2.5	Beta counting	Solis-79	(25)

The average value of all the determinations is

P_n = 27.8±2.5 %.

The spread among the data is large and the correction factor becomes 2.3 which gives an increase of the error to ± 5.8 %.

Table 20

Branching ratio of ^{98}Rb

Determination	Result, %	Method	Reference	
1	13.3±2.1	Beta counting	Orsay-74	(24)
2	18.4±2.9	Beta counting	Ostis-78	(3)
3	16.5±2.3	Ion counting	Solar-79	(2)
4	16.7±1.6	Beta counting	Solis-79	(25)

The average value of all the determination is

P_n = 16.0±1.0 %.

The correction factor is less than unity.

Using an isotope separator attached to a reactor Peuser et al[26] have determined the branching ratio for the precursor ^{99}Rb to be

P_n = 15±3 %.

This value was obtained by a comparison with the P_n-value of ^{98}Rb.

3.8 Strontium isotopes

Branching ratios have been determined for ^{97}Sr and ^{98}Sr using beta counting of mass separated samples as a means to determine the sample strengths (Solis-79[25]). The results are

^{97}Sr: P_n = 0.27±0.09 %.

^{98}Sr: P_n = 0.36±0.11 %.

The branching ratio has been determined to 3.4±2.4 % for ^{99}Sr in an experiment where the sample strength was determined indirectly via estimated fission yields (Lohengrin-75[15]).

3.9 Yttrium isotopes

The SOLIS group (Solis-79[25]) also give branching ratios for ^{97}Y and ^{98}Y using beta counting for sample strength determination, arriving at the results

^{97}Y: P_n = 0.06±0.02 %.

^{98}Y: P_n = 3.44±0.95 %.

A value of 1.2±0.8 % has been determined for ^{99}Y (Lohengrin-75[15]) in an experiment using estimated fission yields for the strength determination.

3.10 Indium isotopes

The branching ratios of indium isotopes have been determined both at Yavne (Solis-79[25]) and at Studsvik (Osiris-79[7]). Both series of experiments were direct ones using beta counting to determine the sample strengths. There is a serious disagreement between the results, however, as is apparent from Table 21.

Table 21

Branching ratios of indium isotopes

Nuclide	P_n-value, % Solis-79	P_n-value, % Osiris-79	Comment concerning Osiris-79
^{127}In	< 0.15	0.65±0.05	(1/2$^-$ isomer)
		< 0.03	(9/2$^+$-isomer)
^{128}In	< 0.20	0.057±0.008	(mixture of 3$^+$-and 8$^-$-isomer with similar half-lives)
^{129}In	3.5±0.5		(not yet evaluated because of problems with the half-lives
^{130}In	4.3±1.4	1.38±0.09	(mixture of 3$^+$- and 8$^-$-isomer with similar half-lives)
^{131}In	5.5±1.5	1.73±0.26	(probably a mixture of two isomers)
^{132}In		4.3±0.9	

More work is needed to sort out the discrepencies. the cases are complicated because of the existence of isomers.

3.11 Tin isotopes

The LOHENGRIN group (Lohengrin-75[15]) gives two P_n-values for ^{134}Sn, 24±15 % and 15±8 %. Presumably, the sample strength determination is based on estimated fission yields in both cases. The determinations are not independent of each other, but a simple average is still taken giving

$$P_n = 17\pm7\ \%.$$

3.12 Antimony isotopes

Table 22

Branching ratio of 10.4 s isomer of ^{134}Sb

Determination	Result, %	Method	Reference
1	0.08±0.02	Estimated fission yields	Harwell-68 (10)
	0.09±0.03	Experimental yield (recalculated) from ref.[5]	
2	0.090±0.015	Experimental fission yields	Mainz-77 (27)
3	0.114±0.008	Beta counting	Osiris-79 (7)

The average value of the determinations is

$$P_n = 0.108\pm0.007\ \%.$$

The error is increased to ± 0.008% by multiplication with the correction factor 1.1.

Table 23

Branching ratio of ^{135}Sb

Determination	Result, %	Method	Reference
1	8±2	Estimated fission yields	Harwell-68 (10
	27±14	Experimental yield (recalculated) from ref.[5]	
2	19.9±2.1	Experimental fission yields	Mainz-77 (2
3	14±1	Beta counting	Lohengrin-78 (1
4	18.7±2.6	Beta counting	Osiris-79 (

The determinations give the average value

P_n = 15.6±1.4 %.

The correction factor 1.5 increases the error to ± 2.1 %.

Table 24

Branching ratio of ^{136}Sb

Determination	Result, %	Method	Reference
1	32±14	Estimated fission yields	Mainz-77 (27)
2	19±9	Estimated fission yields	Lohengrin-78 (11)

The average value of the determinations is

P_n = 23±8 %.

The factor F is less than unity.

3.13 Tellurium isotopes

Table 25

Branching ratio of ^{136}Te

Determination	Result, %	Method	Reference
1	0.7±0.4	Estimated fission yields	Mainz-77 (27)
2	2.0±1.0	Estimated fission yields	Lohengrin-78 (11)

The average value of the determinations is

P_n = 0.9±0.4 %.

The correction factor is less than unity.

Asghar et al (Lohengrin-75[15]) have published the value 2.5±0.5 % for the branching ratio of ^{137}Te. This was obtained using beta counting as a means of determining the sample strength, and it is preferred to the indirect (and not independent) value of 1.3±0.8 % given in the same reference.

The situation is similar for ^{138}Te where a direct determination of 6.3±2.1 % is preferred to an indirect determination of 4.6±2.5 % (Lohengrin-75[15]).

3.4 Iodine isotopes

Table 26

Branching ratio of ^{137}I

Determination	Result, %	Method	Reference	
1	3.0±0.5	Beta counting	Russia-64	(16)
2	4.7±1.0	Beta counting	Mainz-69	(28)
3	8.6±1.2	Gamma counting of long-lived daughter	Mol-71	(17)
4	5.2±0.7	Estimated fission yields	Mainz-72	(18)
	6.8±1.1	Experimental yield from ref.[5]	(recalculated)	
5	6.1±0.8	Beta counting	Lohengrin-75	(15)
6	8.5±0.9	Ion counting	Solar-77	(19)
7	6.1±0.5	Experimental fission yields	Mainz-78	(20)
8	6.7±0.4	Beta counting	Osiris-79	(7)

The determination no. 1 seems to be too low. It has been suggested[18] that this may be caused by the presence of short-lived isomers of ^{136}I, unknown at the time of the experiment, in the samples. This determination is therefore doubtful. As an average of all the other determinations is obtained

$$P_n = 6.6 \pm 0.4\ \%.$$

The correction factor becomes 1.4 which increases the error to ±0.6 %.

Table 27

Branching ratio of ^{138}I

Determination	Result, %	Method	Reference	
1	2.0±0.5	Beta counting	Russia-64	(16)
2	3.0±0.8	Estimated fission yields	Mainz-72	(18)
	5.1±1.9	Experimental yield from ref.[5]	(recalculated)	
3	2.58±0.22	Beta counting	Lohengrin-75 (15)	
4	6.0±3.5	Ion counting	Solar-77	(19)
5	4.5±0.9	Experimental fission yields	Mainz-78	(20
6	5.4±0.4	Beta counting	Osiris-79	(7)

The experimental P_n-values of ^{138}I are scattered with one set of values in the range 2 - 3 % and the others around 5 %. We may perhaps exclude the old determination no. 1 which might be low because of unsatisfactory techniques, but there is no reason to discard the value no. 3. Thus, the case is in an unsatisfactory state and needs further checking. Two average values are derived, one excluding no. 3 and the other including the same determination. The results are:

5.3±0.2 % (excluding no. 3)

3.3±0.6 % (retaining no. 3)

In the former case the correction factor is less than unity leaving the error unchanged whereas it becomes as large as 3.2 in the latter case increasing the error to ± 1.9 %.

Table 28

Branching ratio of ^{139}I

Determination	Result, %	Method	Reference
1	10±3	Estimated fission yields	Mainz-72 (18)
	18±6	Experimental yield from ref.[32]	(recalculated)
2	10.2±0.9	Beta counting	Lohengrin-75 (15)
3	10.1±3.6	Experimental fission yields	Mainz-78 (20)
4	8.9±0.6	Beta counting	Osiris-79 (7)

The average value of all determinations comes out to be

P_n = 9.4±0.5 %.

The correction factor is close to unity and does not change the error. The yield used for recalculating determination no. 1 is 0.51 ± 0.14 % (from ref.[32]).

Table 29

Branching ratio of ^{140}I

Determination	Result, %	Method	Reference
1	32±13	Estimated fission yields	Mainz-72 (18)
	51±32	Experimental yield from ref.[5]	(recalculated)
2	21.7±5.6	Experimental fission yields	Mainz-78 (20)

The average value of the determinations is

P_n = 23±6 %.

The correction factor is less than unity.

Kratz (Mainz-78[20]) has determined the branching ratio of ^{141}I to be

P_n = 39±13 %.

3.15 Xenon isotopes

Table 30
Branching ratio of ^{141}Xe

Determination	Result, %	Method	Reference
1	0.054±0.009	Gamma counting of long-lived daughter	Tristan-69 (4)
	0.070±0.012	Gamma branching ratio from ref.[34]	(recalculated)
2	0.0426±0.0023	Beta counting	Ariel-75 (21)

The average value of the determinations is

P_n = 0.044±0.005 %.

The error is adjusted to ± 0.011 % by means of the correction factor 2.2.

Table 31
Branching ratio of ^{142}Xe

Determination	Result, %	Method	Reference
1	0.45±0.08	Gamma counting of long-lived daughter	Tristan-69 (4)
	0.47±0.08	Gamma branching ratio from ref.[35]	(recalculated)
2	0.406±0.034	Beta counting	Ariel-75 (21)

The average value of the determinations is

P_n = 0.42±0.04 %.

The correction factor is less than unity.

3.16 Cesium isotopes

Table 32
Branching ratio of ^{141}Cs

Determination	Result, %	Method	Reference
1	0.073±0.011	Gamma counting of long-lived daughter	Tristan-69 (4)
	0.095±0.014	Gamma branching ratio from ref.[34]	(recalculated)
2	0.053±0.003	Beta counting	Ariel-75 (21)
3	0.043±0.007	Ion counting	Solar-77 (19)
4	0.034±0.002	Ion counting	Solar-79 (2)
5	0.028±0.002	Beta counting	Osiris-79 (7)

There is a wide spread among the data which indicates systematic errors. There is no reason to exclude any of the determinations, however. The average of all the determinations comes out to be

$$P_n = 0.036 \pm 0.005 \ \%$$

The correction factor is exceptionally high, or 4.1, which increases the error to ± 0.021 %.

Table 33
Branching ratio of ^{142}Cs

Determination	Result, %	Method	Reference
1	0.27±0.07	Gamma counting of long-lived daughter	Tristan-69 (4)
	0.28±0.07	Gamma branching ratio from ref.[35]	(recalculated)
2	0.285±0.020	Beta counting	Ariel-75 (21)
3	0.096±0.008	Ion counting	Solar-77 (19)
4	0.094±0.007	Ion counting	Solar-79 (2)
5	0.082±0.008	Beta counting	Solis-79 (25)
6	0.092±0.006	Beta counting	Osiris-79 (7)

The results are divided into two groups, almost a factor of three apart. It seems plausible that the lower values which have much lower limits of error, are the more reliable ones, and the average value has been evaluated from the determinations nos. 3 - 6. One possible source of error in the determinations nos. 1 and 2 is the similarity of the half-lives of ^{142}Xe and ^{142}Cs which might affect the analysis of the results.

Thus,

P_n = 0.091 ± 0.003 %.

The correction factor is less than unity.

It may be noted that retaining determinations nos. 1 and 2 would lead to an average value of 0.098 % with a corrected error of 0.067 %.

Table 34

Branching ratio of ^{143}Cs

Determination	Result, %	Method	Reference	
1	1.13±0.25	Ion counting	Orsay-69	(23)
2	1.95±0.14	Ion counting	Solar-77	(19)
3	1.74±0.12	Beta counting	Ostis-78	(3)
4	1.79±0.13	Ion counting	Solar-79	(2)
5	1.9±0.2	Beta counting	Solis-79	(25)
6	1.47±0.10	Beta counting	Osiris-79	(7)

The average value of all the determinations is

P_n = 1.68±0.10 %

The correction factor is 1.7 which increases the error to ± 0.17 %.

Table 35

Branching ratio of ^{144}Cs

Determination	Result, %	Method	Reference	
1	1.10±0.25	Ion counting	Orsay-69	(23)
2	4.3±0.3	Ion counting	Solar-77	(19)
3	2.95±0.25	Beta counting	Ostis-78	(3)
4	2.89±0.38	Ion counting	Solar-79	(2)
5	4.07±0.32	Beta counting	Solis-79	(25)
6	2.67±0.17	Beta counting	Osiris-79	(7)

The determination no. 1 definitely seems to be too low, and it is therefore excluded from the evaluation of the average value. The determination no. 2 is also excluded since it is disagreement with the new determination (no. 4) from the same group. The average value of the other determinations (nos. 3-6) is

P_n = 2.96±0.27 %.

The correction factor is 2.2, and the error is increased to ± 0.6 %.

Table 36

Branching ratio of ^{145}Cs

Determination	Result, %	Method	Reference
1	12.1±1.4	Beta counting	Orsay-74 (24)
2	21.8±1.5	Ion counting	Solar-77 (19)
3	12.5±3.0	Beta counting	Lohengrin-78 (11)
4	12.2±0.9	Beta counting	Ostis-78 (3)
5	13.0±0.9	Ion counting	Solar-79 (2)
6	19.5±1.5	Beta counting	Solis-79 (25)
7	13.2±0.9	Beta counting	Osiris-79 (7)

Determination no. 2 is excluded for the same reason as the corresponding determination for ^{144}Cs. The average value of the other determination is

$$P_n \doteq 13.3 \pm 0.9 \text{ \%}.$$

The factor F is 2.0 which increases the error to ± 1.8 %.

Table 37

Branching ratio of ^{146}Cs

Determination	Result, %	Method	Reference
1	14.2±1.7	Beta counting	Orsay-74 (24)
2	13.2±0.8	Beta counting	Ostis-78 (3)
3	11.3±2.5	Ion counting	Solar-79 (2)
4	13.1±1.3	Beta counting	Solis-79 (25)

The average value of all the determinations is

$$P_n = 13.2 \pm 0.6 \text{ \%}.$$

The correction factor is less than unity.

The only published branching ratio for ^{147}Cs (Ostis-78[28]) is

$$P_n = 25.4 \pm 3.2 \text{ \%}.$$

3.17 Barium and lanthanum isotopes

The SOLIS group (Solis-79[25]) has recently determined branching ratios for ^{147}Ba, ^{148}Ba, and ^{147}La

using beta counting as a means of determining the sample strengths. The results are

^{147}Ba: P_n = 5.21±0.52 %.

^{148}Ba: P_n = 23.9±2.1 %.

^{147}La: P_n = 0.50±0.17 %.

The branching ratios for the barium isotopes are surprisingly high in the light of mass formula predictions about the neutron window[36].

4. Summary of delayed-neutron branching ratios

All the average branching ratios discussed in the preceding chapter have been collected in Table 38 for easy reference. The corresponding values from the Petten review[1] are also included in the table.

Note that the errors of the P_n-values have been corrected by multiplying them by a factor of size square root of the sum of chi squares divided by the number of degrees of freedom. Therefore, the errors may sometimes appear large compared to the errors of the P_n-values given in the Petten review.

Table 38

Summary of average delayed-neutron branching ratios

Nuclide	P_n-value, % Petten-77	P_n-value, % Vienna-79	Comment
^{79}Ga	-	0.094±0.016	Possible contribution from ^{79}Zn
^{80}Ga	-	0.80±0.06	Only one determination
^{81}Ga	-	11.9±1.0	" " "
^{82}Ga		21.9±2.3	" " "
^{84}As	0.13±0.06	0.09±0.05	" " "
^{85}As	23±3	50±50	
^{86}As	10.5±2.2	12±4	
^{87}As	44±14	44±14	Only one determination
^{87}Se	0.21±0.03	0.19±0.03	
^{88}Se	0.15±0.09	$0.6^{+1.2}_{-0.6}$	Large discrepancy between experiments
^{89}Se	5.0±1.5	5.0±1.5	Only one determination
^{91}Se	21±8	21±8	" " "
^{87}Br	2.37±0.14	2.38±0.08	
^{88}Br	6.9±0.3	6.7±0.2	

Table 38 cont.

Nuclide	P_n-value, % Petten-77	P_n-value, % Vienna-79	Comment
^{89}Br	13.5±2.3	13.5±2.6	
^{90}Br	21.2±2.4	21.2±2.4	
^{91}Br	10.8±1.7	10.9±1.8	
^{92}Br	22±6	22±6	
^{92}Kr	0.033±0.003	0.033±0.003	
^{93}Kr	2.0±0.3	1.96±0.17	
^{94}Kr	2.2±1.4	5.7±2.2	
^{92}Rb	0.012±0.001	0.0116±0.0012	
^{93}Rb	1.38±0.11	1.39±0.18	
^{94}Rb	10.6±0.7	10.4±1.1	
^{95}Rb	8.9±0.5	8.8±0.6	
^{96}Rb	14.2±1.0	14.2±1.4	
^{97}Rb	30±3	28±6	
^{98}Rb	15.0±2.4	16.0±1.0	
^{99}Rb	-	15±3	Only one determination
^{97}Sr	-	0.27±0.09	" " "
^{98}Sr	-	0.36±0.11	" " "
^{99}Sr	3.4±2.4	3.4±2.4	" " "
^{97}Y	1.6±0.3	0.06±0.02	" " "
^{98}Y	-	3.4±1.0	" " "
^{99}Y	1.2±0.8	1.2±0.8	" " "
^{127}In	-	0.65±0.05 ($1/2^-$)	Two sets of data for indium isotopes, at variance with each other, have been reported (rfs. 7) and 25)). In this table ^{129}In is taken from ref. 25) and the others from ref. 7).
^{128}In	-	<0.03 ($9/2^+$) 0.057±0.008 ($3^+ + 8^-$)	
^{129}In	-	3.5±0.5	
^{130}In	-	1.38±0.09 ($3^+ + 8^-$)	
^{131}In	-	1.73±0.26	
^{132}In	-	4.3±0.9	

Table 38 cont.

Nuclide	P_n-value, % Petten-77	P_n-value, % Vienna-79	Comment
^{134}Sn	17±7	17±7	
^{134}Sb(10 s)	0.086±0.012	0.108±0.008	
^{135}Sb	13.9±2.4	15.6±2.1	
^{136}Sb	23±8	23±8	
^{136}Te	0.9±0.4	0.9±0.4	
^{137}Te	2.2±0.5	2.5±0.5	
^{138}Te	5.6±1.6	6.3±2.1	
^{137}I	6.7±0.5	6.6±0.6	
^{138}I	2.6±0.3	5.3±0.2	The value decreases to 3.2±1.9 if a value from ref.[15] is included.
^{139}I	10.2±0.9	9.4±0.5	
^{140}I	22±6	23±6	
^{141}I	39±13	39±13	Only one determination
^{141}Xe	0.043±0.003	0.044±0.011	
^{142}Xe	0.41±0.03	0.42±0.04	
^{141}Cs	0.053±0.004	0.036±0.021	
^{142}Cs	~0.18	0.091±0.003	
^{143}Cs	1.82±0.12	1.68±0.17	
^{144}Cs	3.0±0.7	3.0±0.6	
^{145}Cs	14.3±1.9	13.3±1.8	
^{146}Cs	13.4±0.7	13.2±0.6	
^{147}Cs	25±3	25.4±3.2	Only one determination
^{147}Ba	-	5.2 ±0.5	" " "
^{148}Ba	-	23.9±2.1	" " "
^{147}La	-	0.50±0.17	" " "

5. Estimates of P_n-values

If no P_n-value has been determined for a particular nuclide one may have to resort to theoretical or semi-empirical estimates of this quantity. Already before the Petten meeting it was shown by Rudolph and Kratz[29] that theoretical calculations of branching ratios did not lead to very accurate results. It seems to be just as good to use a simple semi-empirical approach based on the idea that the branching ratio should increase with increasing relative "neutron width", described by the parameter $(Q_\beta - B_n)/(Q_\beta - C)$ where Q_β is the total beta decay energy of the parent, B_n the neutron separation energy of the daughter and C a cut-off energy depending on the nuclear type involved. A commonly used approach (cf. ref.[30]) is to put

$$P_n = \left((Q_\beta - B_n)/(Q_\beta - C)\right)^n,$$

and to determine the exponent n empirically. Values of this exponent varying between wide limits - from 2 to 6 - have been found[11,19,30], and one cannot expect very accurate branching ratio estimates from this approach.

6. Discussion

On the whole the situation concerning delayed-neutron branching ratios has improved considerably since the Petten meeting in September 1977. Still, a matter of concern is the systematic deviations apparently present in the measurements of branching ratios and revealed by an unexpectedly large spread of data for several nuclides. This is an unsatisfactory situation.

Among the discrepancies might be mentioned the indium isotopes where we have two series of measurements, one at SOLIS, Yavne, and the other at OSIRIS, Studsvik, which are at variance with each other. It should be noted that the indium isotopes are difficult cases. Almost all of them have one or two isomers, and the half-lives of these states are often similar to that of the ground state. In addition, one may have to take the parent cadmium isotopes into account. Presumably, they will also be delayed-neutron precursors.

Other grave discrepancies appear for ^{85}As, ^{88}Se, ^{138}I, ^{141}Cs, ^{142}Cs, ^{144}Cs, and ^{145}Cs.

The list of known precursors for which no P_n-value has been reported is now very short. It consists of ^{83}Ga, ^{83}Ge, ^{84}Ge, ^{123}Ag, ^{133}Sn, and ^{143}Xe. This means that we now have measurements for 62 precursors, or more than 90 % of the 68 cases among the fission products. Since the Petten meeting in the Fall of 1977 14 new branching ratios have been determined. It would be of value, though, to check branching ratios by independent measurements in the cases where only one determination has been carried out (cf. table 38).

The recently detected nuclides ^{100}Rb, ^{100}Sr, and ^{148}Cs (ref.[31]) are presumably delayed-neutron precursors, and they have to be added to the list of precursors for which the P_n-value remains to be measured.

7. References

1) G Rudstam, Proceedings of the Second Advisory Group Meeting on Fission Product Nuclear Data, Petten 5-9 September 1977 (IAEA, Vienna, 1978) p. 567.

2) P L Reeder, private communication (1979).

3) C Ristori, J Crançon, K D Wünsch, G Jung, R Decker, and K L Kratz, Z Physik A290 (1979) 311.

4) W L Talbert, A B Tucker, and G M Day, Phys Rev 177 (1969) 1805.

5) S Amiel and H Feldstein, Phys Rev C11 (1975) 845.

6) T Izak-Biran and S Amiel, Nucl Sci Eng 57 (1975) 117.

7) E Lund, P Hoff, K Aleklett, and G Rudstam, work in progress (1979).

8) J V Kratz, H Franz, and G Herrmann, J Inorg Nucl Chem 35 (1973) 1407.

9) R B Strittmatter, thesis, University of Illinois at Urbana-Champaign (1978).

10) L Tomlinson and M H Hurdus, J Inorg Nucl Chem 30 (1968) 1649.

11) J Crançon, C Ristori, H Ohm, W Rudolph, K L Kratz, and M Asghar, Z Physik A287 (1978) 45.

12) J V Kratz and G Herrmann, J Inorg Nucl Chem 32 (1970) 3713.

13) P del Marmol and D C Perricos, J Inorg Nucl Chem 32 (1970) 705.

14) L Tomlinson and M H Hurdus, J Inorg Nucl Chem 33 (1971) 3609.

15) M Asghar, J P Gautheron, G Bailleul, J P Boquet, J Greif, H Schrader, and G Siegert, Nucl Phys A247 (1975) 359.

16) P M Aron, O I Kostochkin, K A Petrzhak, and V I Shpakov, Atomnaya Energiya 16 (1964) 368; Eng Trans Soviet J Atom Energy 16, 447.

17) P del Marmol, P Fettweis, and D C Perricos, Radiochimica Acta 16 (1971) 4.

18) H D Schüssler and G Herrmann, Radiochim Acta 18 (1972) 123.

19) P L Reeder, J F Wright, and L J Alquist, Phys Rev C15 (1977) 2108.

20) K L Kratz, Radiochimica Acta 25 (1978) 1.

21) M Asghar, J Crançon, J P Gautherin, and C Ristori, J Inorg Nucl Chem 37 (1975) 1563.

22) S Amiel, J Gilat, A Notea, and E Yellin, "Delayed Fission Neutrons" (Panel Proceedings) p. 115, IAEA, Vienna (1968).

23) I Amarel, H Gauvin, and A Johnson, J Inorg Nucl Chem 31 (1969) 577.

24) E Roeckl, P F Dittner, R Klapisch, C Thibault, C Rigaud, and R Prieels, Nucl Phys A222 (1974) 621.

25) G Engler, private communication (1979).

26) P Peuser, H Otto, M Weis, G Nyman, E Roeckl, J Bonn, L von Reisky, and C Spath, Z Physik A289 (1979) 219.

27) W Rudolph, K L Kratz, and G Herrmann, J Inorg Nucl Chem 39 (1977) 753.

28) H D Schüssler, H Ahrens, H Folger, H Franz, W Grimm, G Herrmann, J V Kratz, and K L Kratz, Proc 2nd Symp "Physics and Chemistry of Fission", p. 591, IAEA, Vienna (1969).

29) W Rudolph and K L Kratz, Z Physik A281 (1977) 269.

30) K L Kratz and G Herrmann, Z Physik 263 (1973) 435.

31) E Koglin, G Jung, G Siegert, R Decker, K D Wünsch, and H Wollnik, Z Physik A288 (1978) 319.

32) K L Kratz, private communication (1979).

33) D C Kocher, NDS 8 (1972) 527.

34) R L Auble, NDS 10 (1973) 151.

35) J K Tuli, NDS 25 (1978) 53.

36) Atomic Data and Nuclear Data Tables 17 (1976) nos. 5 and 6.

Acknowledgements

It is a pleasure to acknowledge the valuable assistance offered to my by many colleagues in the form of reports and communications. Also suggestions in the Vienna meeting have been very helpful, particularly the attempt to take systematic deviations into account by means of a correction of the errors of the branching ratios

Review of Delayed Neutron Energy Spectra

Karl-Ludwig Kratz
Institut für Kernchemie der Universität Mainz, Mainz, Germany

ABSTRACT

A brief review on fast neutron detection techniques is given, with particular emphasis on their application for measuring β-delayed neutron spectra from fission products. The effects of possible errors in the spectra from the two most common detection methods, proton-recoil spectrometry and ^{3}He(n,p) spectrometry, are discussed. The availability of experimental data on neutron energy spectra of individual precursors, group spectra and (near-) equilibrium spectra is surveyed. Some properties of individual delayed neutron precursors which are indirectly connected to application are reported and discussed, like β-strength functions and their influence on average energies of β- and γ-spectra, P_n-values and β-decay half-lives of short-lived fission products.

I) INTRODUCTION

Many authors have stressed the importance of delayed neutron energy spectra in reactor static and dynamic calculations. Recent reviews containing references to the work up to 1976 can be found in the papers of Saphier et al. |1| and Rudstam |2|. These evaluations are based on about 20 spectra of individual precursors measured by Shalev and Rudstam |3-7| who used ^{3}He(n,p) spectrometry. Since, on the one hand, a comparison of their spectra with those measured via ^{3}He(n,p) spectrometry by the Mainz-group |8-16| indicates differences especially in the low-energy spectrum parts, and on the other hand, both these data sets are in considerable disagreement with

spectra from proton-recoil spectrometry |17-19|, a critical review of the available neutron energy spectra seems to be worthwhile. As already pointed out |20|, this disagreement in the spectrum shapes may have strong influences on the calculations of the effective neutron energy distribution in nuclear fuel from either summation of individual spectra |1| or their analytical representations |2|, or from direct measurements of (near-) equilibrium spectra with different spectrometers |17,21-24|.

II) FAST NEUTRON DETECTORS

During the last years the interest in fast neutron detection techniques has considerably grown, and in many fields neutron spectroscopy became a standard method. The developments of the last years were mainly aimed at applicability and reliability of known detection techniques. In this respect there was remarkable success, however, there is still a growing need for much better accuracy of neutron experiments.

With respect to the principal detection methods one can still rely on earlier literature, e.g. |25,26|; a recent review on fast neutron detectors by Zeitnitz |27| can be found in the Proceedings of the Int. Conf. on the Interactions of Neutrons with Nuclei. Therefore the following survey will be restricted to the application for measuring β-delayed neutrons from fission products in the energy range 0.01 MeV to about 4 MeV. The most common techniques used are

a) proton-recoil spectromtery
b) time-of-flight measurements
c) $^{3}He(n,p)$ spectrometry.

a) Proton-recoil spectrometry

Very clean measurements of fast neutron energy spectra can be performed with recoil proton telescopes. In these spectrometers energy and direction

of the proton from a hydrogen rich material are measured with scintillators or semiconductor counters. Using pulse shape discrimination in a CsI(Tl) proton detector, for example, one is able to measure neutron spectra down to very lower energies |28|. However, the main reason why this technique is not commonly used in β-delayed neutron spectrometry, is the very low efficiency of the order of 10^{-5}.

The usual proton-recoil system uses methane or hydrogen filled proportional counters with several atmospheres pressure and γ-ray discrimination via pulse-shape analysis |17,18,22|. A typical electronic set-up for a two-parameter proton-recoil spectrometer |22| is shown in Fig. 1 and described further in Tab. 1. The system resolution is shown

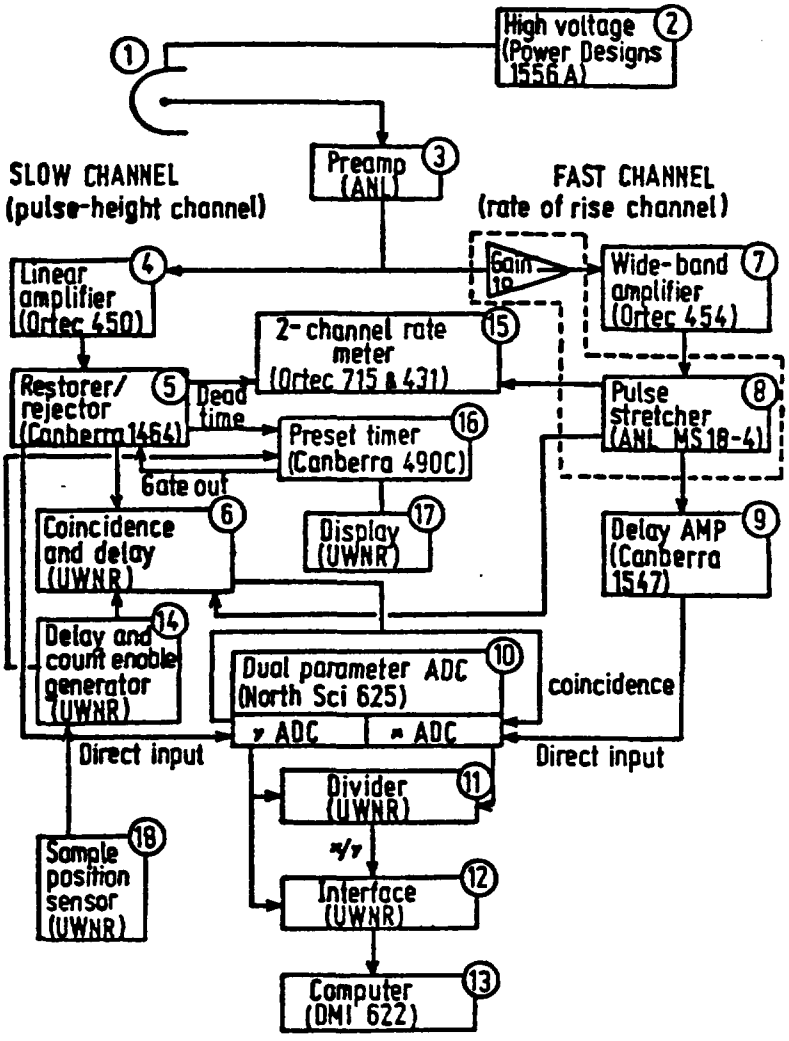

Fig. 1: Two-parameter proton-recoil spectrometer (from Ref. |22|).

Tab. 1: Two parameter components* of the proton-recoil spectrometer |22|.

1.	Proton-Recoil Detector
2.	Power Design 1556A—High voltage power supply for biasing detector, range of 0 to 6 kV.
3.	Wide-Band Charge-Sensitive Preamplifier—Designed by J. M. Larson of Argonne National Laboratory, Idaho Falls, Idaho. The device was built at UWNR using a circuit board supplied by J. M. Larson.
4.	ORTEC 450 Research Amplifier—A pole-zero-compensated semi-Gaussian linear amplifier. The differentiation and integration time constants were set to 3 msec.
5.	Canberra 1464 Restorer/Rejector—The active baseline restoration, busy, strobe, and linear-gate features of this device were used. This component was modified to provide a strobe-logic pulse, framing the linear output for the time the input pulse exceeded the discriminator level.
6.	Coincidence and Delay (UWNR)—This component was a combination of an ORTEC 418A Universal Coincidence unit and a shaping and delay circuit built at the UWNR. This combination ANDED the count enable signal, restorer strobe, and the fast side stretcher busy signal. These three conditions being true resulted in a logic pulse being sent to the coincident input of the ADC. The logic pulse was delayed and shaped so as to open the ADC linear gate during the peak amplitude for the fast and slow channels. The fast-channel rise time was such that the delay amplifier would ring. The delay time was selected to permit the ringing to settle out prior to opening the linear gate.
7.	ORTEC 454 Timing Filter Amplifier—This amplifier differentiated and amplified the preamplifier signal. The unit was modified to allow selection of 70-nsec differentiation time constants.
8.	ANL MS18-4 Pulse Stretcher—This unit provided for reshaping the differentiated preamplifier signal to a pulse width of ~10 μsec. The inverters in this component were modified to obtain a factor of 10 increase in gain.
9.	Canberra 1547 Delay Amplifier—The delay amplifier was used to provide the necessary time delay to obtain coincidence of the fast and slow channel signals.
10.	Northern Scientific 625 ADC—The ADC was used in the 256 × 256 two-parameter gated-coincidence mode. The *x* and *y* inputs were direct coupled and the linear gate was controlled by the coincidence input.
11.	Hardware Divider (UWNR)—This device was designed and built at the UWNR to calculate the digital ratio of the two 8-bit words supplied by the ADC.
12.	Computer-Divider Interface (UWNR)—This component provided an octal display of the information to be transferred to the computer and the necessary logic-level changes to transfer the data.
13.	Varian DMI 622 Computer—This machine is an 18-bit 8K machine. The primary functions were data storage and handling. The I/O capabilities included TTY, paper tape, and CRT display.
14.	Delay and Count Enable Generator (UWNR)—This component provided the count enable signal to the coincidence and delay unit after a preset delay. The sequence was initiated by a pulse from the sample position sensor.
15.	ORTEC 715 and 431 Dual Counter/Timer (715) and Timer/Scaler (431)—These units were used to monitor fast and slow channel count rates. The 715 was the master unit setting the time base.
16.	Canberra 490C Blind Timer—This device provided the system live time as displayed on 17. The timer was gated off during the 40-μsec signal processing time and during sample irradiation and cooling.
17.	Display (UWNR)—This unit displayed the live time accumulated by the blind timer.
18.	Sample Position Sensor (UWNR)—A photo-transistor device actuated by the linear motor armature indicating the sample was in the counting position. This output was used to start 14.

*Component numbers refer to labels in Fig. 1.

in Fig. 2; it includes both numerical unfolding effects and the intrinsic resolution of the detectors. With this system, time dependent neutron spectra from the thermal-neutron fission of ^{235}U were measured by Sloan

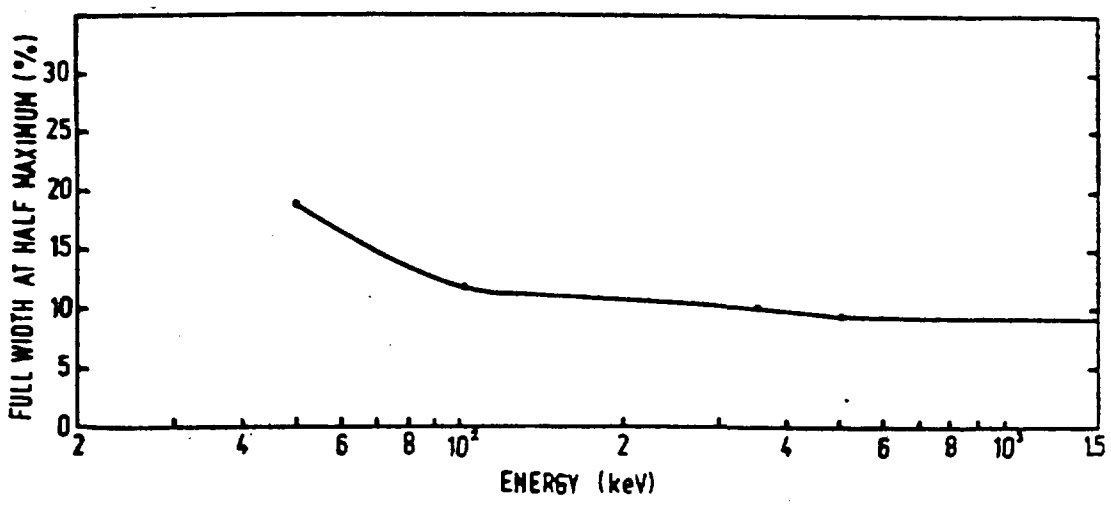

Fig. 2: Detector resolution of the two-parameter proton-recoil spectrometer from Ref. |22|.

and Woodruff |22|. This same system,following some modifications, was used by Eccleston and Woodruff |17| to measure two-parameter data of near-equilibrium delayed neutron spectra produced by fast-neutron-induced fission of different fissile isotopes. The main problem in analyzing these data is the transformation of the registered two-parameter data to one-parameter proton-recoil distributions. Examples of the two-parameter data of |17| are shown in Fig. 3. Events at low specific ionization values are induced by γ-rays, whereas neutrons produce events at higher values. After correction for the γ-ray pulses, the residual one-parameter proton-recoil distributions obtained from a weighted summing across the proton-recoil peaks are smoothed using frequency filtering |29| to improve the statistical properties of the data. Neutron spectra are then obtained by differentiating the proton-recoil distribution using the Bennett and Yule PSNS code |30|.

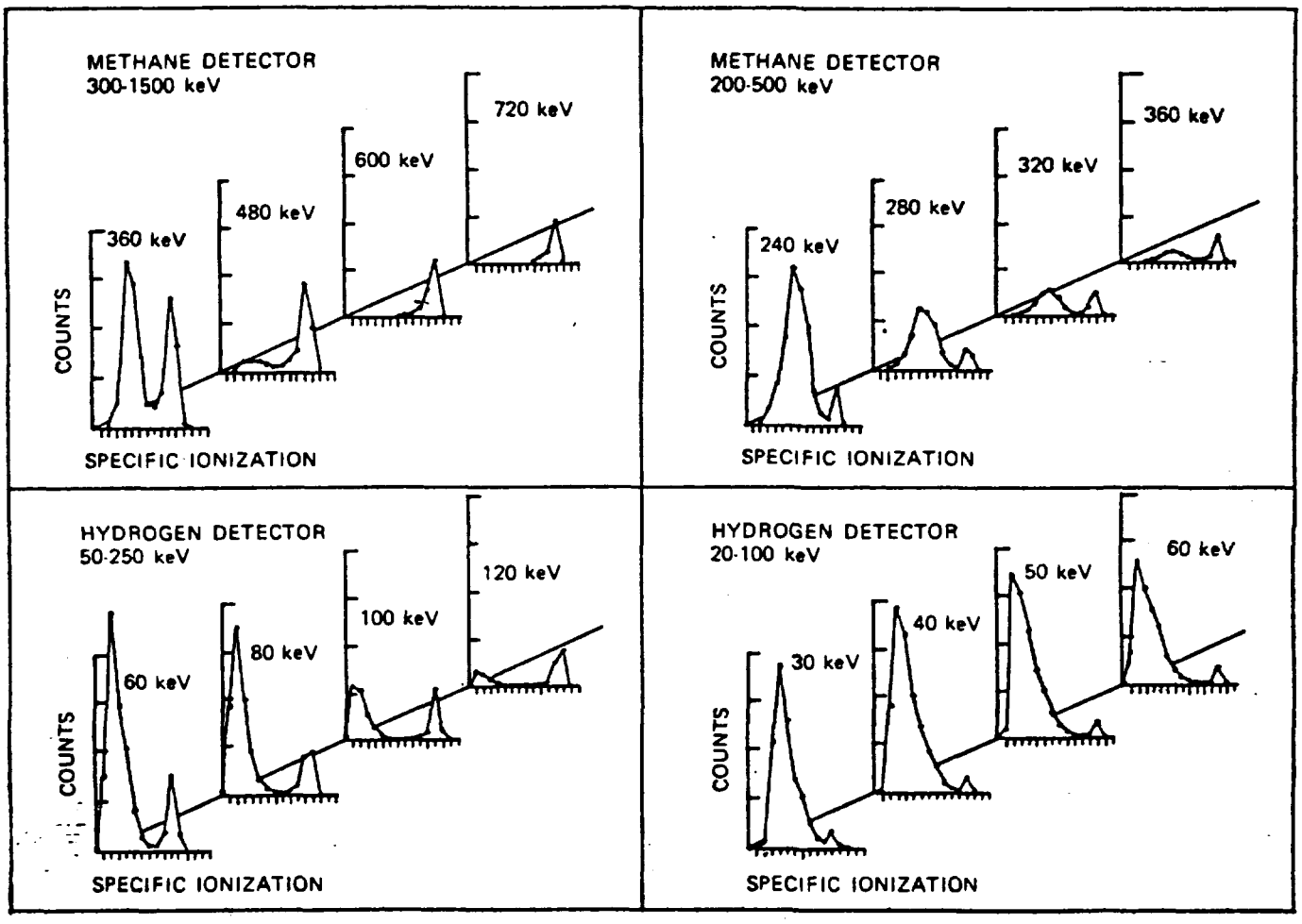

Fig. 3: Two-parameter data from a ^{235}U sample corresponding to four different energy intervals (from Ref. |17|).

A comparison of (near-) equilibrium delayed-neutron spectra obtained by proton-recoil spectrometry |17,22| with those from ^{3}He-spectrometry |1,21,23,24| show considerable differences in the energy distributions. Though Eccleston and Woodruff |17| have considered a number of possible bias effects in their spectra they conclude that there still remain unresolved differences especially in the low-energy portion of delayed neutrons (see Sec. III).

As an example for individual precursor spectra obtained with both techniques, in Fig. 4 the neutron spectra of ^{93}Rb and ^{94}Rb at low energies are given |31|. The proton-recoil spectra show some intriguing structure with good energy resolution, but unfortunately the poor statistical accuracy makes comparisons with the data from ^{3}He-spectrometry |12,31| rather inconclusive (see Sec. III).

A similar methane filled proton-recoil proportional counter was used by Ray and Kenney |18| to measure the delayed-neutron spectrum from ^{87}Br beyond 100 keV. Instead of discriminating pulses arising from γ-rays via pulse-shape analysis, they used a thick boric acid/paraffine neutron filter. When this filter was positioned between the source and the counter, the proton-recoil spectrometer represented events primarily induced by γ-rays. Data taken without the filter represented both γ-ray- and neutron-induced events. The difference between these two sets of data with proper corrections for neutron transmission through the filter and γ-ray scattering by the boric acid/paraffine mixture represented events induced by neutrons alone. The resultant energy distribution of ^{87}Br delayed neutrons, compared to the data from ^{3}He-spectrometry obtained by Shalev and Rudstam |3,7| is shown in Fig. 5. The spectrum from proton-recoil spectrometry differs significantly not only from that measured by Shalev and Rudstam, but also from that obtained by the Mainz group |10,11|. A detailed error analysis of the spectrum from proton-recoil spectrometry has been performed by Ray |19| to determine if bias in measurements might contribute to the apparent softness in the energy distribution compared to the data from ^{3}He-spectrometry.

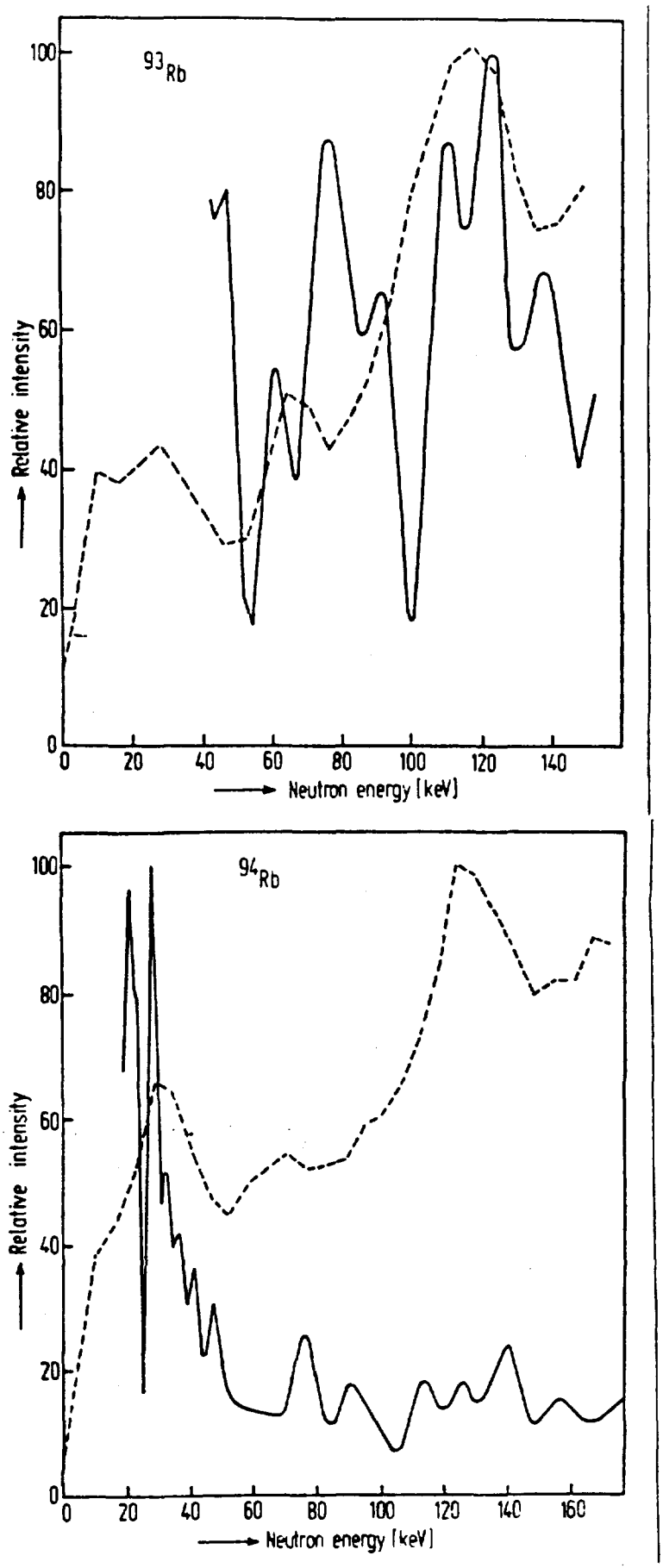

Fig. 4: Low-energy neutron spectra of ^{93}Rb (upper part) and ^{94}Rb (lower part); solid curve - from proton-recoil spectrometry |31|, dashed curve - from ^{3}He spectrometry |12|.

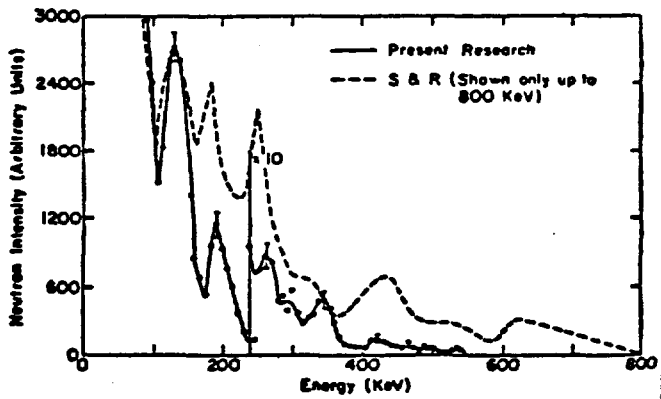

Fig. 5: Energy distribution of delayed neutrons from ^{87}Br (from Ref. |18|).

It is concluded, however, that the possible errors are not large enough to account for the large discrepancies between the different measurements (see Sec. III).

b) Fast neutron time-of-flight spectrometers

In principle, the best method for precise measurements of fast neutron energy spectra is the time-of-flight (TOF) technique |26,27|.Through the development of accelerators capable of delivering beam pulses of good quality, of large organic scintillation detectors, and of fast electronics, the energy resolution in TOF neutron spectroscopy has the same quality as that obtained for charged particles. The method is basically very simple: The flight time of a neutron ejected from a target is measured over a distance and the neutron energy calculated from it. The start pulse is taken from a pickup coil in front of the target or from an associated particle emitted in the reaction (in the case of delayed neutrons from the β-particles emitted $\geq 10^{-15}$s prior to the neutrons) and the stop pulse from the neutron detector.

The electronics of a typical TOF spectrometer consists of fast timing circuits for start and stop signals, a time-to-pulse height or a time-to-digital converter, and a circuit for pulse shape discrimination. The energy resolution ΔE is determined by the time uncertainty Δt, since the flight

distance d can be measured with high precision. The expected energy resolution is therefore |26,32|

$$\Delta E = -2E \frac{\Delta t}{t} = \frac{E^{3/2} \cdot \Delta t}{36.2\ d}$$

The real resolution in the experiments includes, of course, the energy spread of the beam and the target thickness, as in charged particle detection. However, the TOF technique is the only spectrometer type where the energy resolution is not an inherent factor of the system; it can essentially be defined by the experimentalist.

Though many large facilities are descibed in detail in the literature (for recent examples see Refs. given in the survey article of Zeitnitz |27|), it is somewhat astonishing that this technique has up to now not become a common detection method in β-delayed neutron spectroscopy.

During the past five years there have been reported a few (partly preliminary) TOF spectroscopic data by Crawford et al. |33-37|. In their latest experiments a specially fabricated thin plastic scintillation counter was used to detect β-particles, and two neutron counters were placed at different distances and angles from the β-detector. The first detector used a large liquid scintillator (NE 213 with 30 cm Ø x 2.5 cm thick) to cover the neutron energy range from about 200 keV upwards. It was placed 1 m from the β-detector. Three XP 1040 photo-multipliers operated in an "any 2 out of 3" coincidence mode viewed the liquid scintillator. A conventional zero-crossing type pulse shape discrimination system was used to reduce the efficiency of the liquid scintillator to the detection of γ-rays (by a factor of about 55) while having only small effects on the neutron detection efficiency. Pulses from the β-detector started a time-to-amplitude converter which was stopped by pulses from the neutron detector. The second detector used a lithium glass scintillator and covered the whole range from just above thermal neutrons. This detector is intensitive to γ-rays of less than 1 MeV but, unfortunately, does respond to photons of higher energy.

As an example the TOF neutron spectrum of ^{95}Rb from the liquid scintillator |37| is given in Fig. 6. It covers the energy range from about 100 to 1200 keV, and shows good overall agreement with the spectra obtained

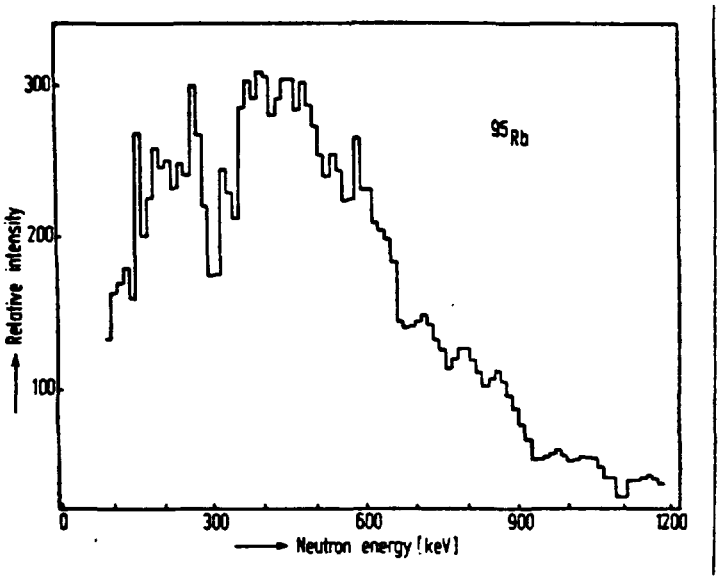

Fig. 6: Neutron spectrum of ^{95}Rb from the TOF-technique using a liquid scintillator |36|.

from ^{3}He(n,p) spectrometry |6,7,12,31| (see also Fig. 20 d in Sec. III). Though the analysis of the low-energy part of the ^{95}Rb spectrum from the lithium glass detector is not yet complete |37|, the raw spectrum given in Fig.7 exhibits some interesting features. In agreement with the results of the Mainz-group who used a ^{3}He ionization chamber |12|, there is a prominent group of delayed neutrons at 13.7±0.2 keV. The width of this group was found to be 0.9 keV. In addition there are further significant peaks in the low energy spectrum at 11.2 and 25.5 keV, their widths being about 2 keV, and numerous other peaks at higher energies. A complete analysis of these ^{95}Rb data, especially the determination of the detector efficiencies, is in progress.

Further preliminary TOF neutron spectra exist for the precursor isotopes ^{85}As, ^{89,90}Br, ^{94}Rb, ^{135}Sb and ^{137}I |34|.

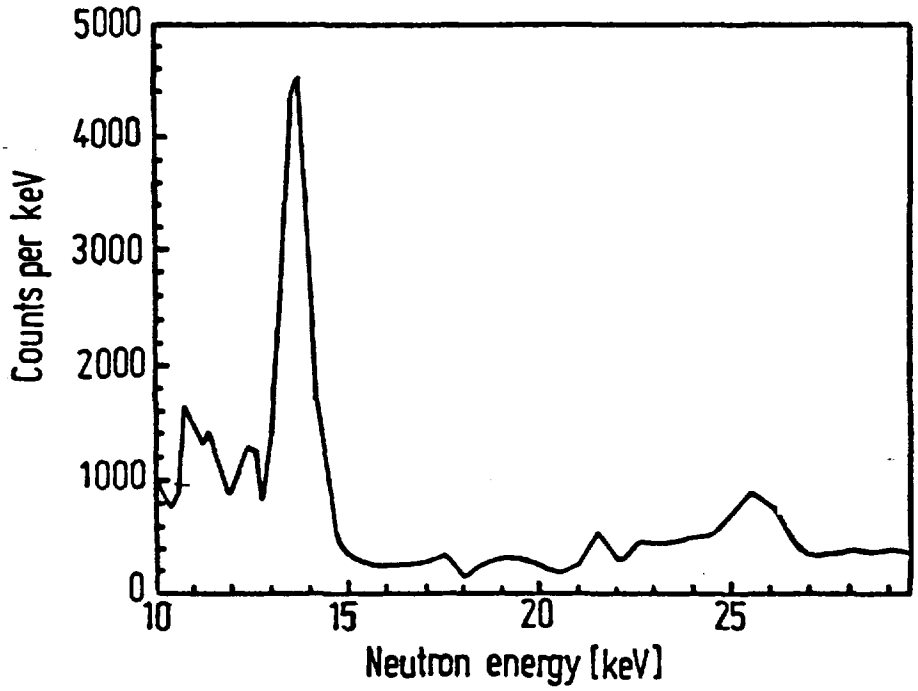

Fig. 7: Low-energy neutron spectrum of ^{95}Rb from the TOF-technique using a lithium glass scintillator (from Ref. |37|).

c) ^{3}He-Spectrometers

A few years ago, after a detailed study of various types of fast neutron spectrometric techniques, Shalev and Cuttler |21,38| decided that a ^{3}He gas proportional counter provided the best combination of energy resolution and detection efficiency for the spectroscopy of neutrons in the energy range 0 to 2 MeV. Though in the meantime several types of high-pressure ^{3}He proportional counters and ^{3}He ionization chambers have become available commercially, ^{3}He-spectrometry is not yet a straightforward technique and the properties of these detectors were up to recently not well understood.

With the $^{3}He(n,p)$ detection method neutron energy spectra for 33 individual precursors have been measured |3-16,31|, including those of primary interest for nuclear technology. However, for 14 out of these spectra the low energy part up to about 100 keV is lacking and there is a general discrepancy in the energy/intensity distributions between the OSIRIS- |3-7| and the Mainz-neutron spectra |8-16|. As noted in |20|, these discrepancies call for detailed studies of the ^{3}He-spectrometer characteristics with particular emphasis to detector resolution, efficiency and possible spectrum distortion effects. Recent publications on this subject can be found in Refs. |20,21, 24,39|.

The latest versions of the ^{3}He spectrometers |40,41| are cylindrical gridded ionization chambers with guard tubes to reduce fringing fields. Neutrons are detected through the reaction

$$^{3}He + n \rightarrow p + {}^{3}H + 763.8 \text{ keV}$$

This reaction has a smooth and rather well measured cross section in the energy range of the delayed neutrons. Competing reactions with comparative cross sections are $^{3}He(n,n')^{3}He$ and $^{1}H(n,n')^{1}H$.

The spectrometers are filled with a gas mixture of about 6.5 atm |40|, and 10 atm pressure |41|, respectively; the gas mixture consists mainly of ^{3}He, Ar and methane. The active volume of the ion chamber is 5 cm Ø x 15 cm. Because of the high sensitivity of the detector to thermal neutrons the Cuttler type spectrometer |41| is surrounded by a thermal neutron shield consisting of a 2 mm layer of boron nitride powder sandwiched between 0.5 mm sheets of cadmium. The boron is added to suppress epithermal neutrons. With this shield, the thermal neutron count rate is reduced by a factor of about 50, thus preventing possible neutron-neutron pile-up. The Shalev type detector is enclosed in a shield of boron carbide and cadmium which

reduces the thermal neutron response by a factor of 20 |24|. The influence of boron and cadmium on the detection efficiency is negligible above 1 keV. Further details on the construction of the ^{3}He detectors can be found in Ref. |21|.

The electronic system for delayed neutron spectroscopy with two identical ^{3}He-spectrometers of the Cuttler type |39| operated in parallel is outlined in Fig. 8. The anode and guard tubes are kept at 3000 V and the grid voltage at 850 V. A low-noise charge-sensitive preamplifier is connected directly to each ion chamber to minimize distortion due to pickup. Signals from the preamplifier are processed with a normal dc-coupled Gaussian amplifier and base line restoration is used to reduce low frequency pickup.

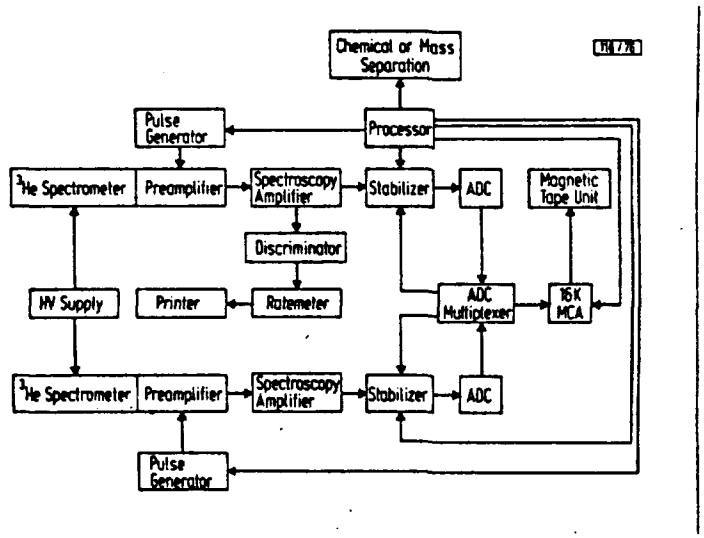

Fig. 8: Electronic system for delayed neutron spectroscopy with two ^{3}He spectrometers operated in parallel |39|.

The signals are then given to an analog-digital converter, and after passing an ADC-multiplexer the spectral data from both spectrometers are stored in a multichannel analyser. Other electronics normally used in the experiments are a ratemeter with a discriminator set arbitrarily at 76 keV

for monitoring the γ-ray counting rate and digital stabilizers with precision pulse generators for zero and gain stabilization. For delayed neutron spectrum measurements, the pulsers are only operated during intermission of the experiments. With stabilization the energy shift of the pulsers peaks can be kept within 0.2 keV over an energy range of 0-2 MeV during five days of operation |39|.

The energy calibration of the ^{3}He spectrometers and their response function to monoenergetic neutrons is usually obtained with neutrons from the $^{7}Li(p,n)^{7}Be$ reaction produced with Van de Graaff accelerators. In Ref. |39|, the result of an absolute calibration of the spectrometers which is accurate to about 0.1 % of the incident neutron energy served as the basis for a subsequent pulse height calibration of the electronic system with precision pulsers. The pulse generators (Ortec Model 448) were modified to give alternately two pulses with different analyser channel locations, one at the position of the thermal neutron peak and the other for the conversion gain. The pulse amplitudes were calibrated in keV by normalizing them to the location of the thermal neutron peak. By comparing these values with the absolute energy calibration from the $^{7}Li(p,n)^{7}Be$ measurements the linearity of the electronic system was determined.

The response function of the ^{3}He spectrometers |39| is shown in Fig. 9 for some examples. Scattered neutrons from the detector and the surrounding material and wall effects give a continuous pulse distribution between the fast and thermal neutron peak. Of major influence are recoil effects in the elastic scattering of neutrons with protons and ^{3}He nuclei. The recoiling nucleus can have energies from zero (grazing collision) to a maximum of 3/4 E_n (backscatter). An edge similar to that of the Compton edge familiar in Ge(Li)-spectra is observed in the spectrum at this latter energy. Because of the Q-value of 763.8 keV of the $^{3}He(n,p)^{3}H$ reaction, this recoil effect appears beyond the thermal neutron peak only for neutron energies larger than approximately 1.0 MeV.

The major difficulties with ^{3}He spectrometers which have an impact on neutron spectroscopy, especially the energy resolution, are:

a) wall effects resulting from incomplete energy loss of one or both reaction products within the active counter volume,

b) recoil effects from elastic scattering of neutrons with ^{3}He and ^{1}H nuclei,

c) spread in pulse rise time due to location and orientation of the reaction product tracks relative to the central wire,

d) γ-ray sensitivity; γ-rays interact with the spectrometer walls and the counter gas giving rise to pulses smaller than the thermal peak, but high γ-ray input rates cause spectrum distortion because of neutron-γ pile-up,

e) accoustic effects, which have a similar influence as γ-ray pile-up and may lead to spurious pulses in the neutron spectrum.

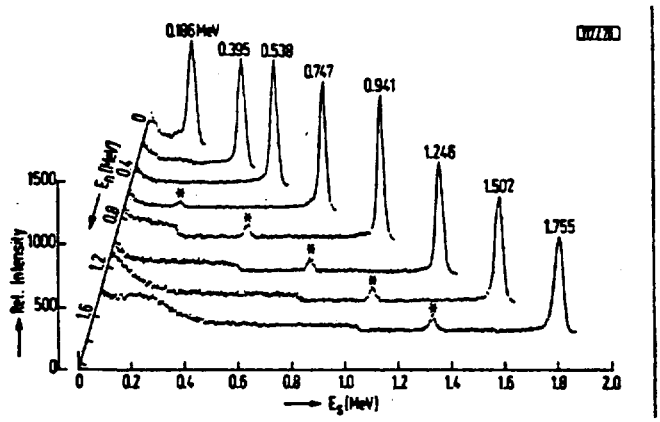

Fig. 9: Response of the ^{3}He ionization chamber to monoenergetic neutrons produced by the $^{7}Li(p,n)^{7}Be$ reaction. E_n is the incident neutron energy deduced from the measured proton energy and the reaction kinematics; E_s is the pulse height distribution obtained from monoenergetic neutrons with E_n. The peaks marked with an asterisk are due to a secondary reaction $^{7}Li(p,n)^{7}Be^{*}$ (from Ref. [39]).

Energy resolution

Variations of track orientation relative to the central anode wire produce a large spread in risetime of the pulses, e.g., 0.2-1 μs for thermal neutrons and up to 7 μs for 2 MeV neutrons. This relatively long charge collection time would imply long amplifier shaping times (8-10 μs), leading to problems with pile-up effects and base-line shifts. Short amplifier shaping times (∿ 2 μs) on the contrary improve the energy resolution at low energies at the expense of resolution at high energies. A compromise of T_{RC} = 5 μs was found to be the optimum for the particular application. Under normal experimental conditions an energy resolution of better than 12 keV for thermal neutrons and about 20 keV for 1 MeV neutron was achieved for the Cuttler type |39|. For the Shalev type a resolution of 14.6 keV for thermal neutrons and of about 45 keV for 1 MeV neutrons is reported by Weaver et al. |24|.

Pile-up effects

It is the advantage of the ^{3}He spectrometers that due to the intrinsic discrimination by the Q-value of 764 keV of the $^3He(n,p)^3H$ reaction, the pulse amplitudes of γ-ray quanta are well below the thermal neutron peak. At high counting rates two different pile-up effects leading to a distortion of the pulse height spectra can be expected: pile-up of γ- on γ-ray pulses and pile-up of neutron on γ-ray pulses. To visualize these effects, two pulse-height distributions of ^{92}Rb delayed neutrons with different γ-ray counting rates are given in Fig. 10.

Whereas γ-ray intensities up to about $5 \cdot 10^3$ cts/s at the 76 keV discriminator level do not interfere with the neutron spectrum, pile-up between photon and neutron pulses may severely degrade the resolution of the counter

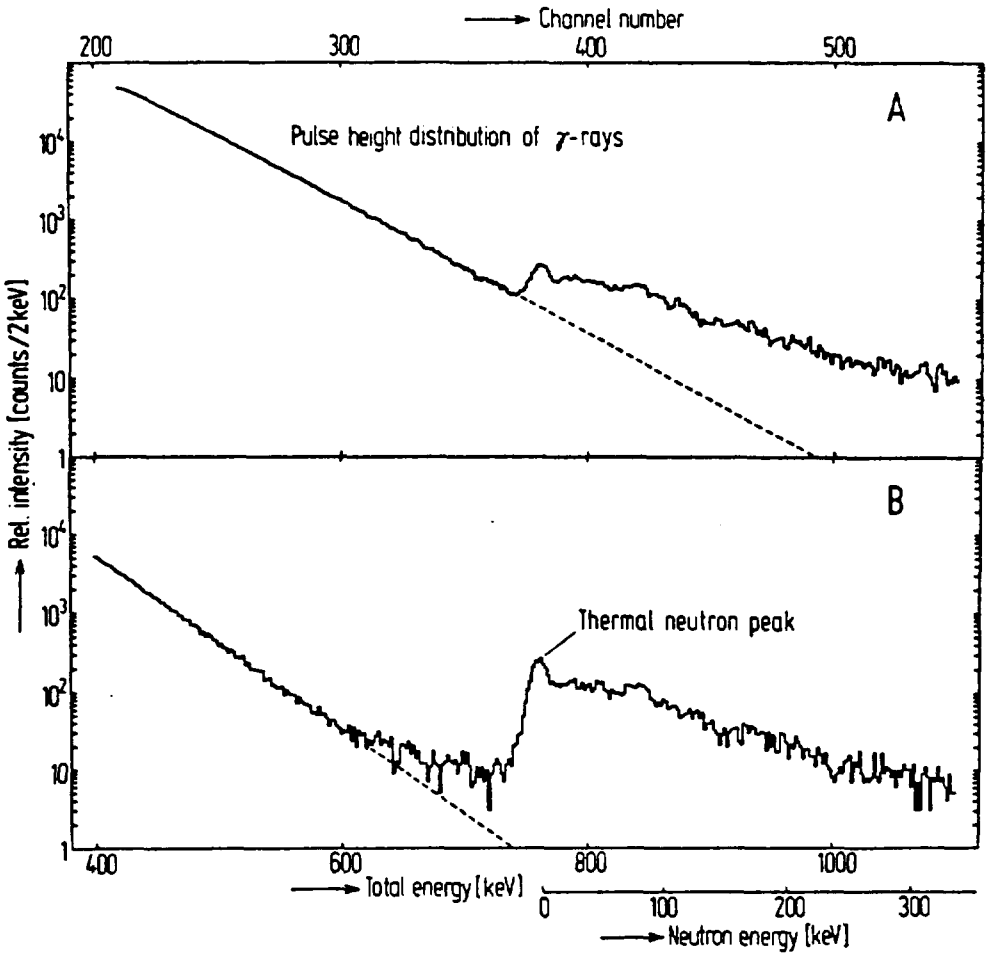

Fig. 10: Pulse height distributions of ^{92}Rb delayed-neutrons with different γ-ray counting rates (from Ref. |16|).

This distortion was measured for the thermal neutron peak of the Cuttler type spectrometer |39|. The pile-up leads to a broadening of the peaks (Fig.11) adding a tail to the high-energy shoulder which increases with the γ-ray counting rate. It can be fitted by an exponential function, and because of the proportionality of its relative amplitude to the γ-ray counting rate, a simple correction of the pulse height spectrum is possible |21|.

The positive energy shift ΔE due to the pile-up is shown in Fig. 12. The results indicate that γ-ray counting rates of 1500 counts/s can be tolerated without serious deterioration of resolution |39|.

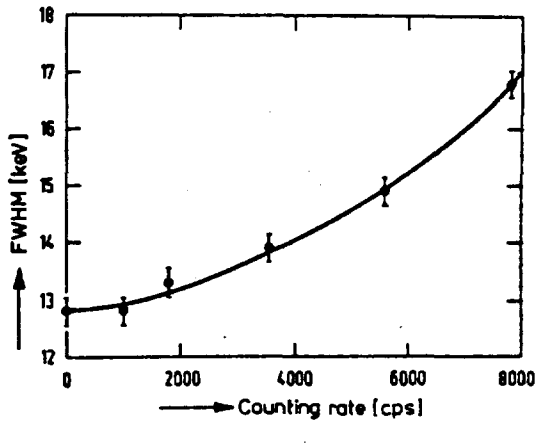

Fig. 11: Distortion of the thermal neutron peak by pile-up of neutron and γ-ray pulses plotted vs. the γ-ray counting rate at the 76 keV discriminator level (from Ref. |39|).

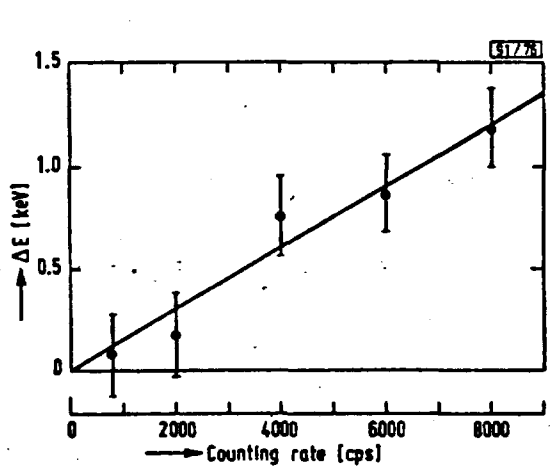

Fig. 12: Energy shift ΔE of the thermal neutron peak due to γ-ray pile-up plotted vs. the γ-ray counting rate at the 76 keV discriminator level (from Ref. |39|).

As delayed neutron emission is always accompanied by intense β- and γ-ray emission, the sensitivity of the spectrometer to pile-up from high-energy β-particles and γ-rays may be the limiting factor in delayed neutron spectroscopy. The total counting rate can be reduced by inserting lead between the source and the detector. Lead has, in addition to a high absorption cross section for β- and γ-rays, a high threshold energy for inelastic neutron scattering. The influence of lead absorbers on the energy resolution and the peak shape of monoenergetic neutrons was tested with neutrons from the $^{7}Li(p,n)^{7}Be$ reaction. A 2 mm thick lead absorber increases the tenth-width of the neutron peaks by approximately 10 %, whereas the half-width is not affected |21,39|.

In practice for low input-rates it was found sufficient to use 2-3 mm thick layers of lead. The influence of these absorbers on the peak shape, its energy and the spectrometer detection efficiency is negligible.

Microphonics

The long, thin anode wire of the spectrometer is very sensitive to vibration and accoustical noise resulting in significant deterioration in the detector resolution. These effects were studied for the Cuttler type detector with signals of various frequencies, obtained with an audio amplifier |39|. By observing the amplifier output, up to 30 resonance frequencies were found between 50 Hz and 26 kHz and were shown to cause an appreciable broadening of peaks produced by a pulse generator applied to the test input of the preamplifier. Fig. 13 shows a series of such peaks obtained without and with the influence of sound waves at 11.4 kHz of increasing signal-to-noise ratios. In addition to a considerable broadening of the peak already observed at a low signal-to-noise ratio, pulses of random amplitudes appear at higher ratios lying beyond and below the original peak. In practice these effects were observed during experiments at a fission fragment separator combined with a gas-jet transport system even though the noise level from pumps and eigen-vibration of the jet were lower than the noise level usually occuring at reactor installations.

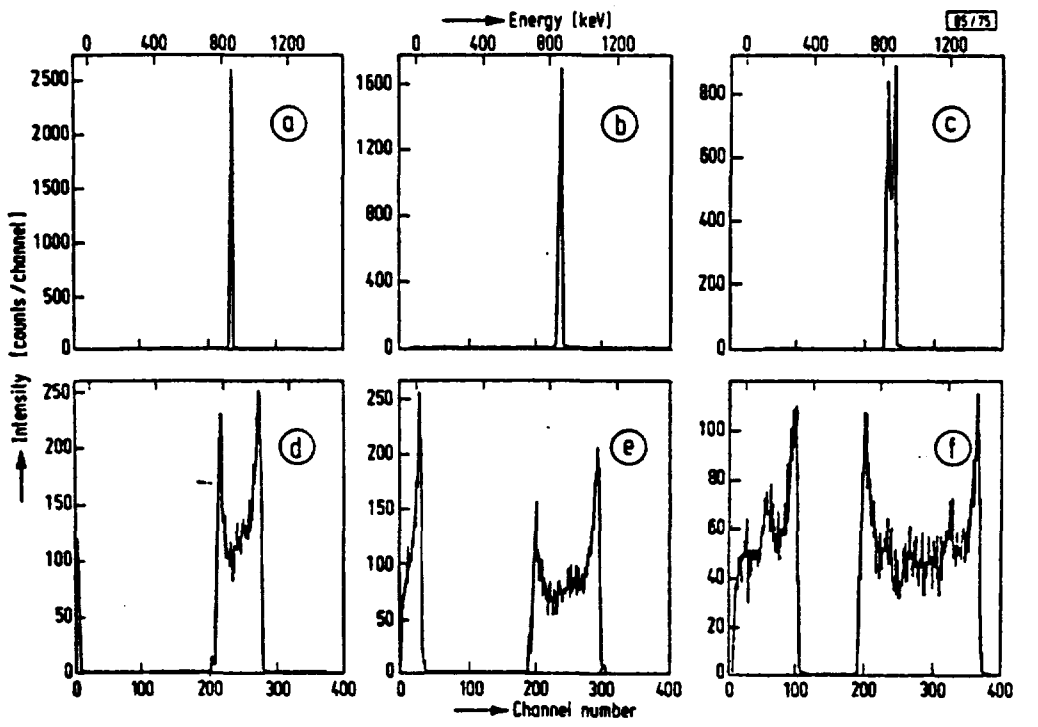

Fig. 13: Distortion of a precision pulser peak by sound waves at various sinus-to-noise amplitude ratios, U_s/U_n; sound wave frequency 11.4 kHz; (a) U_s/U_n = 0, (b) 1.3, (c) 3.8, (d) 10, (e) 13, (f) 20 (from Ref. |39|).

Neutron scattering

Distortion of neutron spectra due to room scattering and scattering from the experimental set-up and the counting sample itself is an important effect which cannot be suppressed but only minimized. To investigate this effect, the known delayed-neutron spectrum of ^{17}N |42| was measured under conditions particularly favourable to detection of scattered neutrons |39|. From Fig. 14 it is evident that the main intensity of the scattered neutrons is found in the thermal neutron peak region, exponentially decreasing

with increasing energy. For normal experimental conditions (Fig. 14, spectrum (a)), the amount of scattered neutrons with $E_n \geq 40$ keV is less than 7 %. However, strong spectral distortion is observed under conditions favouring neutron scattering (Fig. 14, spectrum (b)): The intensity of the thermal neutron peak is increased by a factor of 50, and neutron scattering also extends in energy to $E_n \simeq 1.1$ MeV.

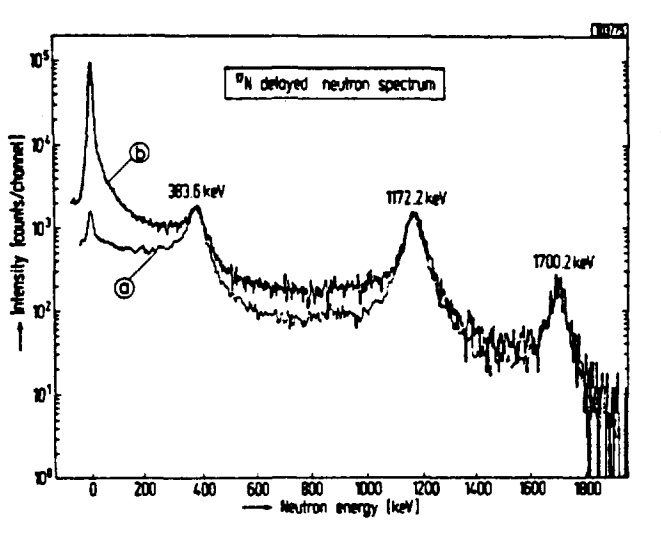

Fig. 14: Delayed neutron spectrum of ^{17}N; (a) measured under optimum conditions, (b) measured with a thick counting sample (from Ref. |39|).

Another even more serious effect is an appreciable increase of the half-width of the neutron peaks due to tailing on the low-energy side. If in the computer analysis of the spectra no provision is made for tailing effects, an appreciable shift of the calculated peak centroids follows. However, under the conditions applied to "normal" experiments peak shape distortion and energy shift lie within the standard deviations of the whole electronic system |39|.

Efficiency measurements

Data on the efficiency of the ^{3}He neutron spectrometers have been obtained by several authors |21,23,24,31,39|. The most complete set of data in the energy range 19 keV to 2.77 MeV from Franz et al. |39| is shown in Fig. 15 along with the ^{3}He(n,p)^{3}H cross section. Including un-

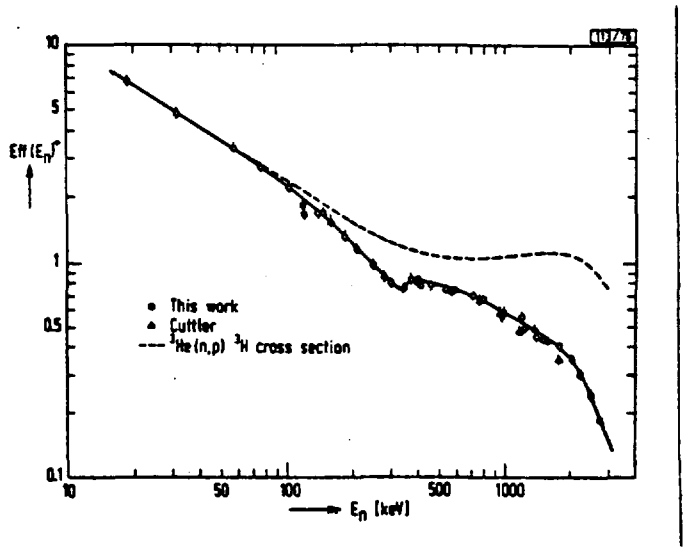

Fig. 15: Relative efficiency of the ^{3}He fast neutron spectrometer, normalized to previous measurements, along with the ^{3}He(n,p)^{3}H cross section (from Ref. |39|).

certainties in corrections applied for the magnet calibration data of the Van de Graaff, degradation of proton energy in the LiF target used, and the absolute efficiency of the BF_3 long counter, these efficiency measurements are reported to be accurate to about 5 %.

The most significant features of the efficiency variation are

a) a decrease at low energy which follows the 1/υ variation of the ^{3}He(n,p)^{3}H cross section, and the rapid decrease in efficiency above 1 MeV where wall effects due to charge collection problems become severe;

b) a departure from the smooth monotonic decrease in the efficiency with energy in the vicinity of $E_n \simeq 130$ keV and $E_n \simeq 340$ keV.

Working with spectrometers of the Shalev type |40|, a similar efficiency distribution in the vicinity of 350 keV was reported by Evans and Krick |23|, and Reeder |31|, and at about 250 keV by Weaver et al. |24|.

While the features noted in (a) are well understood, the mechanism(s) giving rise to the effect noted in (b) are not obvious. There are indications that these dips arise from the boron nitride/carbide shielding of the detectors.

Evans |43| also reported the presence of low energy "spurious" peaks in neutron spectra which seem to rise to a maximum intensity with neutron energies near 400 keV. In addition he noted that the intensities seemed to increase when an iron shield was inserted into the neutron beam. Franz et al. |39| have searched for such peaks in their spectra but find no clear evidence for them. For neutrons of similar energy a small increase in intensity above the thermal peak was noted but the effect appeared small compared to that observed by Evans. These observations suggest that differences in spectrometer construction may be important.

Wall effects and ^{3}He recoil distribution

In order to separate the continuous wall effect distribution and ^{3}He recoil events from the pulses produced by the ^{3}He(n,p) reaction dual parameter risetime and pulse height analyses in the delayed neutron spectrum measurements were performed by several authors |23,24,44,45|.

In the work of Ohm et al. |44| a pulse shape analyzer (Ortec Model 458) was used to analyze the risetime and pulse height distribution of the ^{17}N neutron spectrum |42| from a Cuttler type ^{3}He ionization chamber. Fig. 16 shows the distribution of the pulse risetimes for different pulse height intervals. For low pulse heights (energies) only one narrow component at

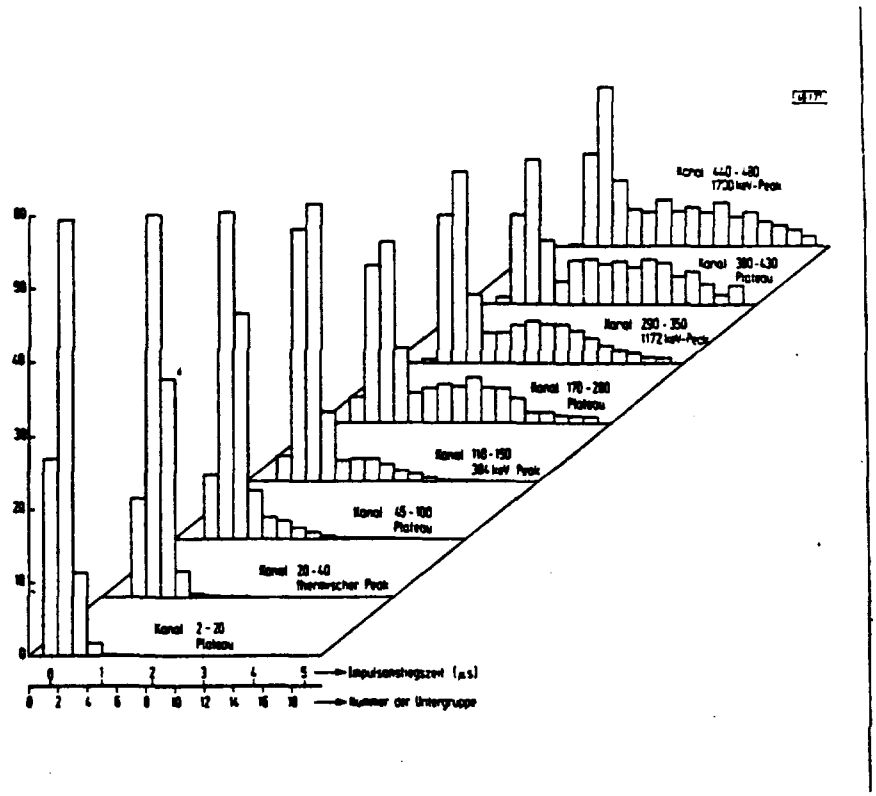

Fig. 16: Distribution of the pulse risetimes in the delayed-neutron spectrum of ^{17}N (from Ref. |44|)

about 0.5 µs is observed. With increasing pulse height its position changes only little, whereas its intensity decreases in favour of a broader component reaching up to 5 µs. This trend can easily be explained by the increasing ionization tracks in the spectrometer gas with increasing incident neutron energy. The analysis also showed that the centroids of the fast neutron peaks were not located in the same pulse height interval for all risetimes; however, the deviations were found to be considerably smaller than those reported by Weaver et al. |24|. Since, in addition, no significant deviation in the pulse risetimes between peaks and plateaus (due to wall effects and ^{3}He recoil) could be observed, the pulse shape analysis was regarded unnecessary for the Cuttler type spectrometer. Further tests on this subject are in progress, however.

In a contribution to this review article, Weaver et al. |24| describe a similar two dimensional analysis of pulse height and pulse risetime for a Shalev type detector which seccessfully eliminates ^{3}He recoil events. An apparent shift in the neutron peak centroid relative to the pulse risetime was also observed for their spectrometer, and after correction their dual parameter analysis yielded a resolution at 1 MeV improved by a factor of 1.7. A similar improvement of the final resolution of a Shalev type detector was also reported by Evans and Brandenberger |45|. Due to the lower gas pressure of this spectrometer compared to the Cuttler type, stronger wall effects appear, which were found by Weaver et al. |24| to be correctly described by the formula of Batchelor, Aves and Skyrme |46|. These predictions were used in their spectrum analysis for stripping the continuous wall effect distribution.

Analysis of the pulse height distribution

Several methods for spectral analysis may be applied. The most commonly used is an iterative technique originally developed by Greenberger and Shalev |47|. In their program a set of premeasured detector response functions for monoenergetic neutrons is taken to fit the entire spectrum in a least squares approach and to subtract the continuous pulse distribution below the respective fast neutron peaks. Similar subtraction processes applying fixed detector response functions are used by Evans and Krick |23|, Weaver et al. |24| and Rudstam |48|. Franz et al. |39| reported, however, that the actual response function (i.e. the ratio of continuum height to full-energy neutron peak) is very sensitive to the experimental conditions. Therefore they used response functions adapted to the experimental conditions during the spectrum measurements by varying the peak-to-plateau ratio.

Besides this continuum subtraction, corrections for thermal neutrons and γ-ray pile-up are considered by all authors |23,24,39,47,48|, before the residual 'net' pulse height distribution is converted to a neutron spectrum by division by the efficiency function of the detector.

The errors introduced by this unfolding procedure, including all possible uncertainties in response function, efficiency, correction for scattered and thermal neutrons and γ-ray pile-up, were estimated by Weaver et al. |24| to be about 7 % in the region 100 keV to 1 MeV. Below 100 keV the error is expected to be about 10 %, and above 1 MeV where the counting statistics are poorer about 10 to 20 %. From tests, Evans and Krick |23| obtained similar overall intensity uncertainties in the final spectrum.

However, though the main properties of the ^{3}He ionization chambers seem to be well understood by now, there still exist discrepancies between (near-) equilibrium and individual precursor neutron spectra accumulated by various authors with the same type of spectrometer, and there is disagreement among the data obtained with different detection methods.

As an - arbitrarily chosen - example, in Fig. 17 the ^{143}Cs delayed neutron spectrum accumulated by Shalev and Rudstam |6|, Reeder |31| and Ohm et al. |14| is shown. In comparing the spectrum measured by Ohm et al. with that of Shalev and Rudstam, fairly good agreement is found for peak energies and relative intensities in the energy range above 100 keV but disagreement exists for the absolute intensities. Part of this discrepancy may lie in the ∿17 % of the total intensity that lies below 100 keV which was not resolved from thermal and background events toward lower energies in the spectrum of Shalev and Rudstam. However, it would appear that this cannot account for the complete difference; it may be due to the additional effect of scattered neutrons in the energy range 100-400 keV giving rise to a considerably larger 'continuum' underlying the peak structure in their spectrum. Though in the spectrum of Reeder the low energy range seems to be well resolved, the strong 23 keV neutron peak seen in the spectrum of Ohm et al. is not observed, presumably due to poor counting statistics and worse energy resolution. Nevertheless, the overall spectrum shape, and probably also the average neutron energy $\bar{E}_n$, is in better agreement with the Mainz-spectrum than the OSIRIS-spectrum. These discrepancies in the data of individual precursors appear for most spectra measured by the latter two groups. They are probably due to spectrum distortion from background and scattered neutrons and insufficiently known response functions

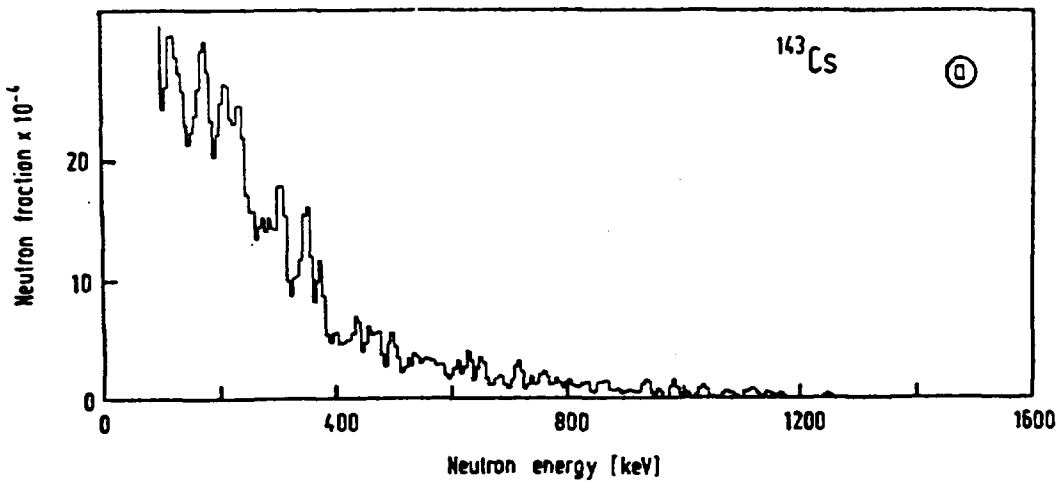

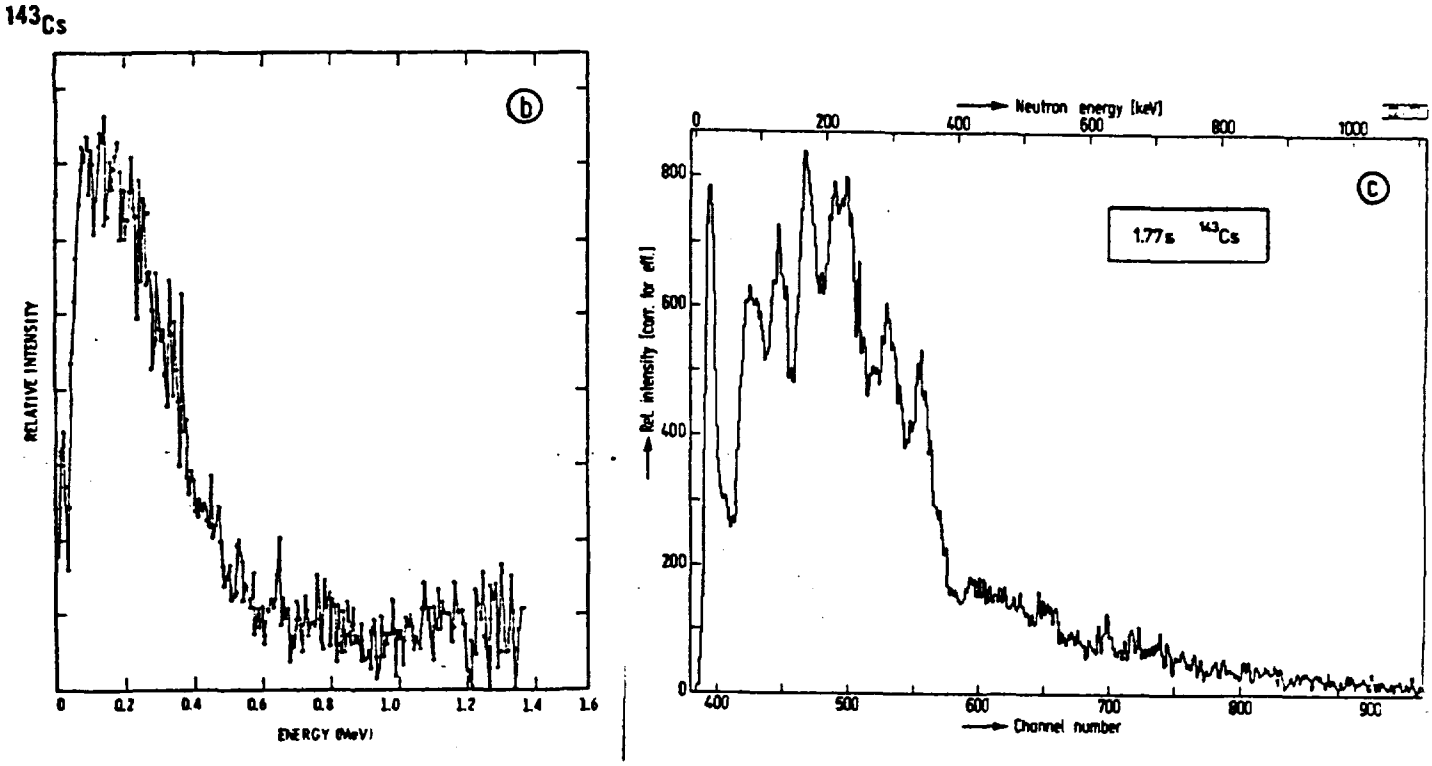

Fig. 17: Delayed neutron spectrum from ^{143}Cs decay:

a) from Shalev and Rudstam |6|

b) from Reeder |31|

c) from Ohm et al. |14|

which are most evident in the low energy part of the spectra. However, as has been shown |9-16,20,39| a considerably improved energy resolution down to $E_n \leq 10$ keV can be achieved by minimizing spectrum distortion effects. A further big advantage are the resultant small corrections (usually $\leq$ 10 % of the total spectrum intensity) required to account for the detector response function.

III) ENERGY SPECTRA OF INDIVIDUAL PRECURSORS

a) Experimental Spectra

It is only since a few years that neutron spectroscopy of individual precursors has become possible primarily due to the combination of fast separation techniques using radiochemical methods |49| or mass separation |50| with high-resolution ^{3}He ionization chambers |21,38|. As examples for neutron spectra measured after rapid chemical separation of individual precursors, those of the four nuclides ^{85}As, ^{87}Br, ^{135}Sb and ^{137}I which represent characteristic pairs in the light and heavy mass region in fission are shown in Figs. 18 and 19 |9-11,51,53|. The members of each pair differ only by a pair or protons and the corresponding neutron emitters have N = 51 or 83, respectively, leading to nuclei with major closed shells after neutron emission. For the nuclides ^{87}Br and ^{137}I the neutron decay proceeds entirely to the ground state of the final nucleus; for ^{85}As and ^{135}Sb, however, the large energy windows ($Q_\beta - B_n$) result in neutron emission to several excited states. While in the cases of ^{87}Br and ^{137}I the maximum neutron energies of about 1.3 MeV and 1.7 MeV, respectively, are in agreement with the energy range ($Q_\beta - B_n$) available for neutron emission, a dominant feature of the spectra from ^{85}As and ^{135}Sb is the absence of appreciable neutron intensity at high energies. For ^{85}As the intensity above 1.6 MeV is less than 3 % and for ^{135}Sb the intensity above 2.2 MeV is less than 4 %, respectively, of the total, even though ranges of 4.9 MeV (As) and 4.2 MeV (Sb) are possible. Through γ-ray studies is has been possible to demonstrate that this effect is due to strong neutron emission to excited final states |9,10,52|.

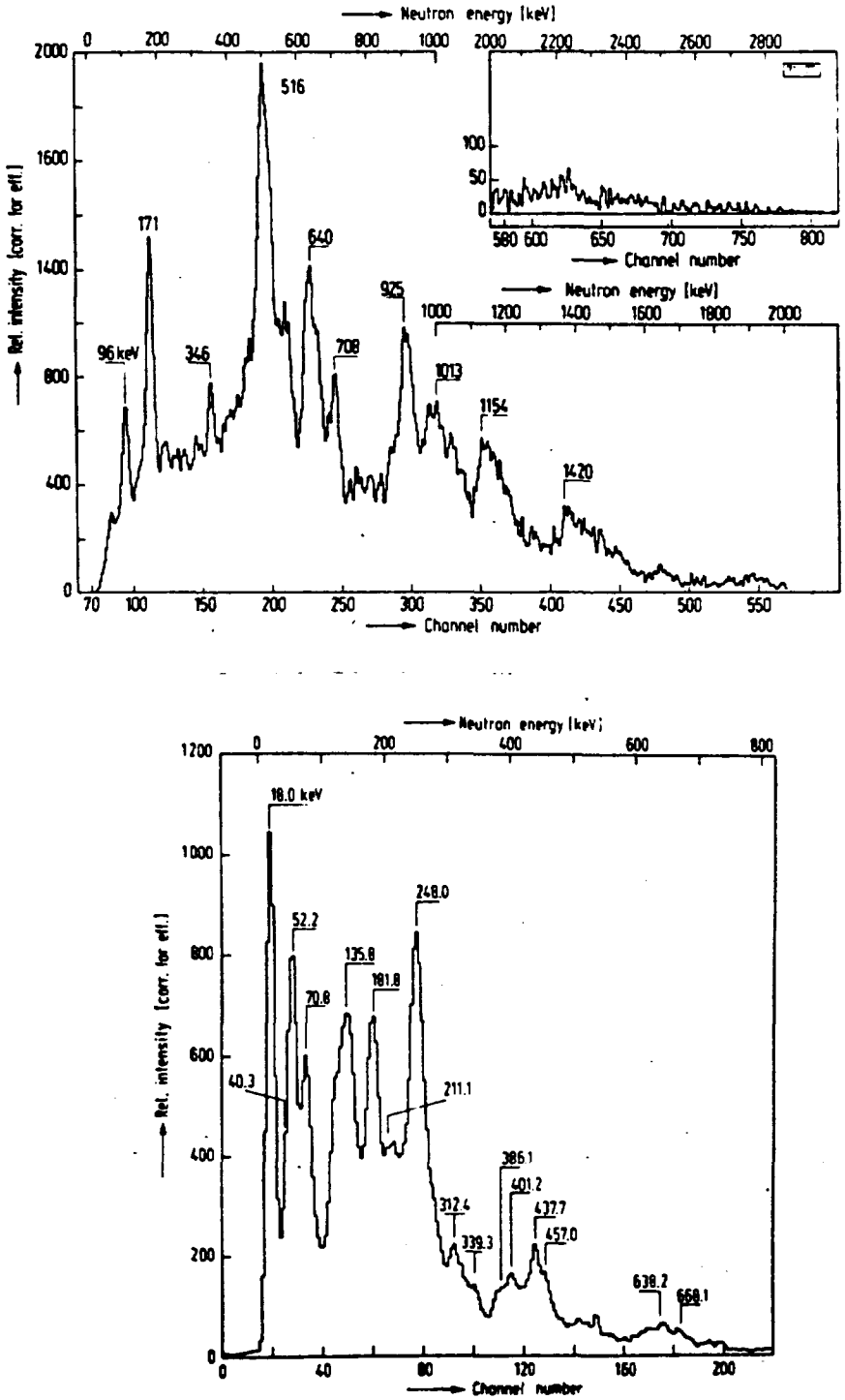

Fig. 18: Delayed-neutron spectra from ^{85}As (upper part) and ^{87}Br decay (lower part) after correction for detector response and thermal neutrons (from Refs. |11,51|).

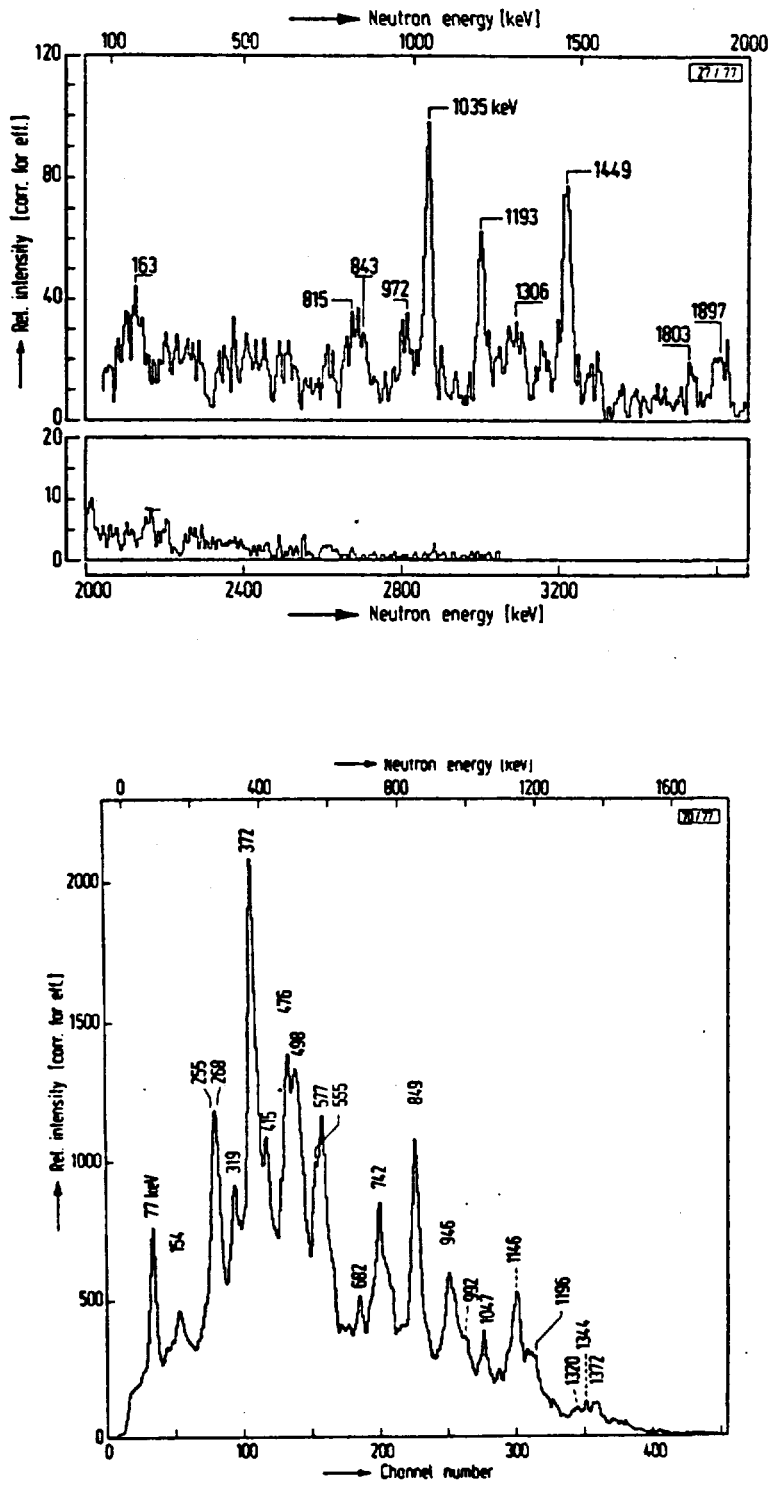

Fig. 19: Delayed-neutron spectra from ^{135}Sb (upper part) and ^{137}I decay (lower part) after correction for detector response and thermal neutrons (from Refs. |10,51|).

As examples for neutron spectra from isotope-separated precursors, the energy spectra from $^{92-98}$Rb are shown in Figs. 20 and 21 |12,16,53|. The number of neutrons counted with E_n > 10 keV lie between 25000 (^{96}Rb) and 970000 (^{95}Rb) total counts per spectrum. In order to demonstrate the good energy resolution obtained in these experiments, the pulse-height distribution from ^{95}Rb decay is shown in the upper part of Figure 20 d. A strong 13.6 keV peak containing 5 % of the total neutron intensity of the spectrum can still be resolved from the thermal neutron peak.

Two main features of the Rb neutron spectra are: Similar to ^{85}As and ^{135}Sb delayed-neutron spectra (see Figs. 18,19) only little high-energy neutron intensity is seen in all Rb spectra though energy ranges up to 5.8 MeV (^{98}Rb) are available for neutron emission. Moreover, a systematic variation of the peak structure and the overall spectrum shape with mass-number within this isotope sequence is observed. Neutron spectra of odd-mass Rb precursors decaying into even-even Sr nuclei exhibit prominent line structure accounting for the majority of the total neutron intensity. In all these spectra a sudden drop in neutron intensity above about 850 keV is evident. On the other hand, even-mass Rb precursors decaying into odd-mass Sr final nuclei show a larger continuous neutron distribution superimposed by only a few strong peaks which contain less than 20% of the total intensity. In these spectra the main neutron intensity is concentrated at energies below 400 keV.

As has originally been demonstrated by γ-ray singles measurements |12,31, 53| the strong neutron emission to excited states in the Sr Final nuclei explains the above mentioned absence of appreciable high-energy neutron intensity and the variation in the spectrum shape. As an example, Figure 22 shows the decay of $^{93-95}$Rb to levels in $^{92-94}$Sr. It is clearly seen that in the case of the even-even final nuclei ^{92}Sr and ^{94}Sr neutron emission can only lead to a few excited states which are widely spaced, whereas in the case of the final nucleus ^{93}Sr a total of about 30 narrowly spaced levels at excitation energies up to 3 MeV are available for neutron decay. Thus, many neutron branches with comparable intensities superimposed lead to the

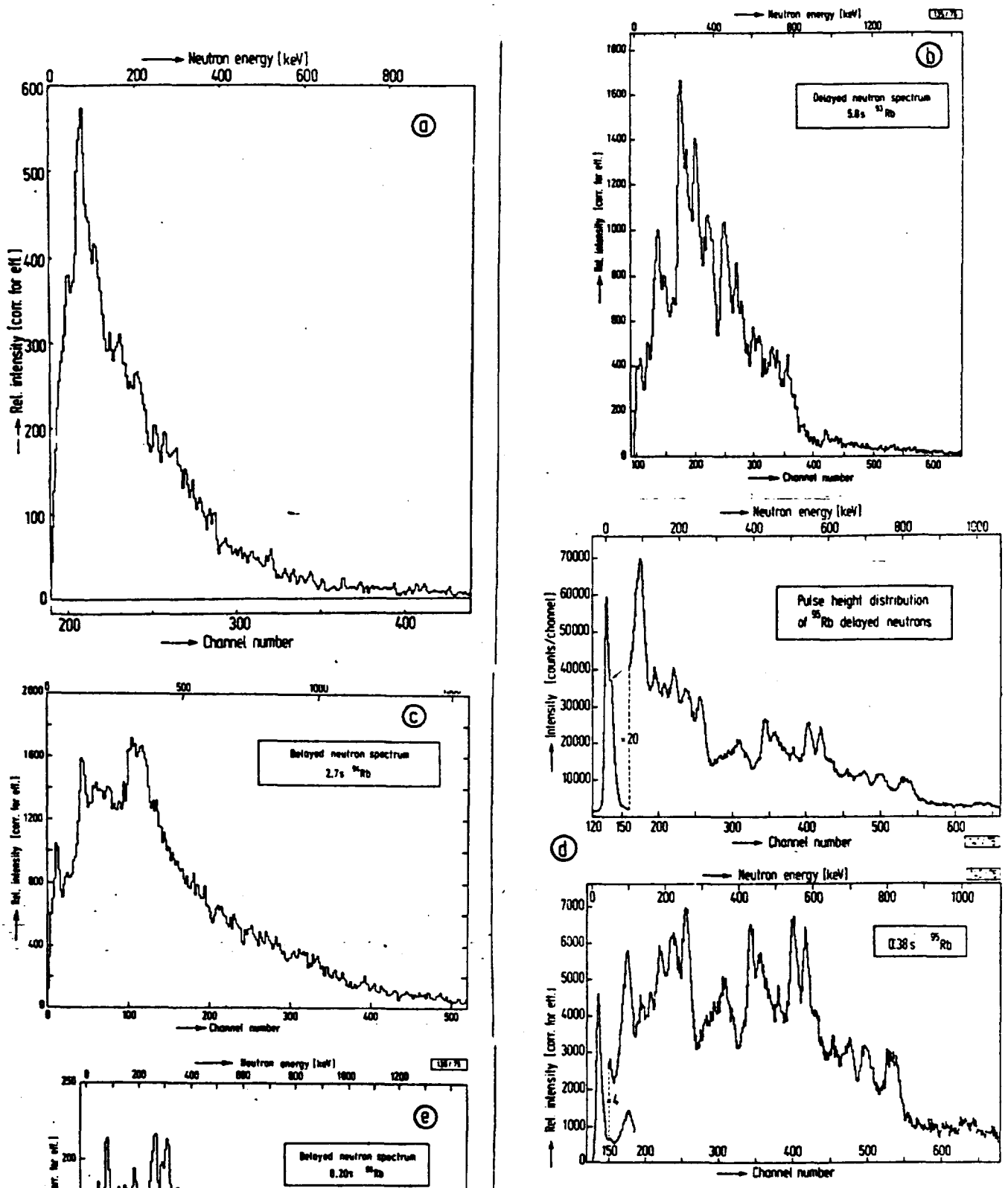

Fig. 20: Delayed-neutron spectra from the decay of

a) ^{92}Rb (from Ref. |16|);
b) ^{93}Rb (from Refs. |12,53|);
c) ^{94}Rb (from Refs. |12,53|);
d) ^{95}Rb (from Refs. |12,53|), upper part: pulse-height distribution, lower part: neutron spectrum;
e) ^{96}Rb (from Refs. |12,53|).

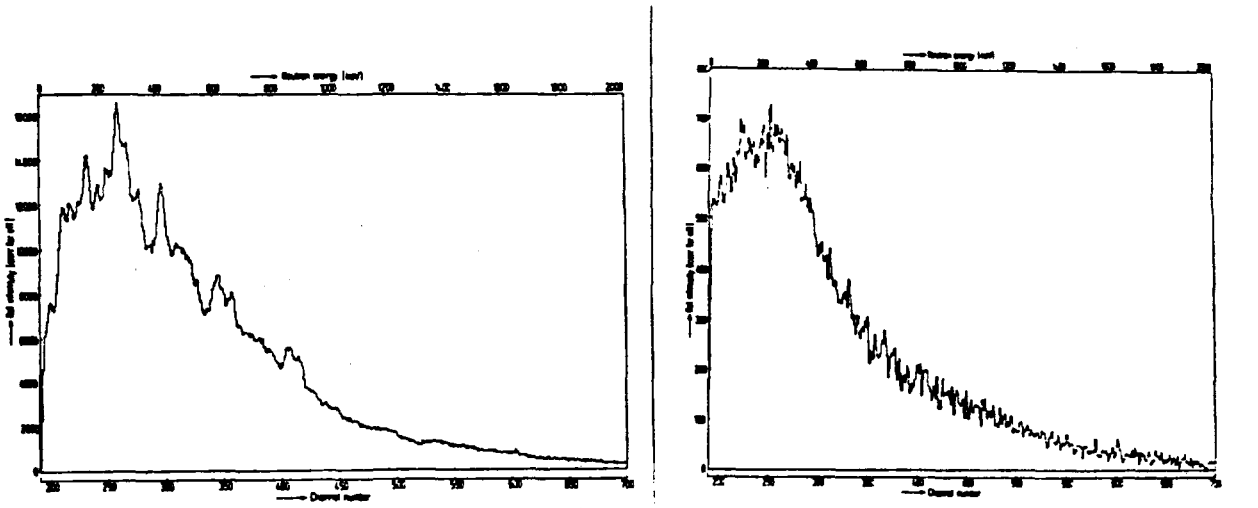

Fig. 21: Delayed-neutron spectra from the decay of ^{97}Rb (left side) and ^{98}Rb (right side), from Refs. |12,16,53| .

complex neutron spectrum of the even-mass precursor ^{94}Rb, with only a few strong neutron lines well resolved. Similar results were obtained for the partial neutron feeding of excited states in the other Sr final nuclei. This "odd-even effect" in neutron spectrum shapes is also observed for the bromine, iodine and cesium isotope sequences |4-6,10,13,14,16|.

Recently, neutron emission to excited final states has been demonstrated by Crawford et al. |54| using a direct βnγ-triple coincidence technique, and by the Mainz-group |12,53,55| measuring nγ-coincidence spectra. As examples, the results for ^{94}Rb and ^{95}Rb decay are given in the next figures. Fig. 23 shows the singles neutron spectrum of ^{95}Rb (upper part), together with the partial spectrum in coincidence with the 837 keV γ-rays corresponding to the $2^+ \rightarrow 0^+$ transition in ^{94}Sr (middle part) and the spectrum of neutron decay to the ground state of the final nucleus (lower part). Combining nγ-coincidence and γ-singles data |12,31,53|, one can deduce that about 59 % of the total neutron emission lead to the ground state of ^{94}Sr, about 37 % to the 2^+-state and only a total of 4 % feed the four higher

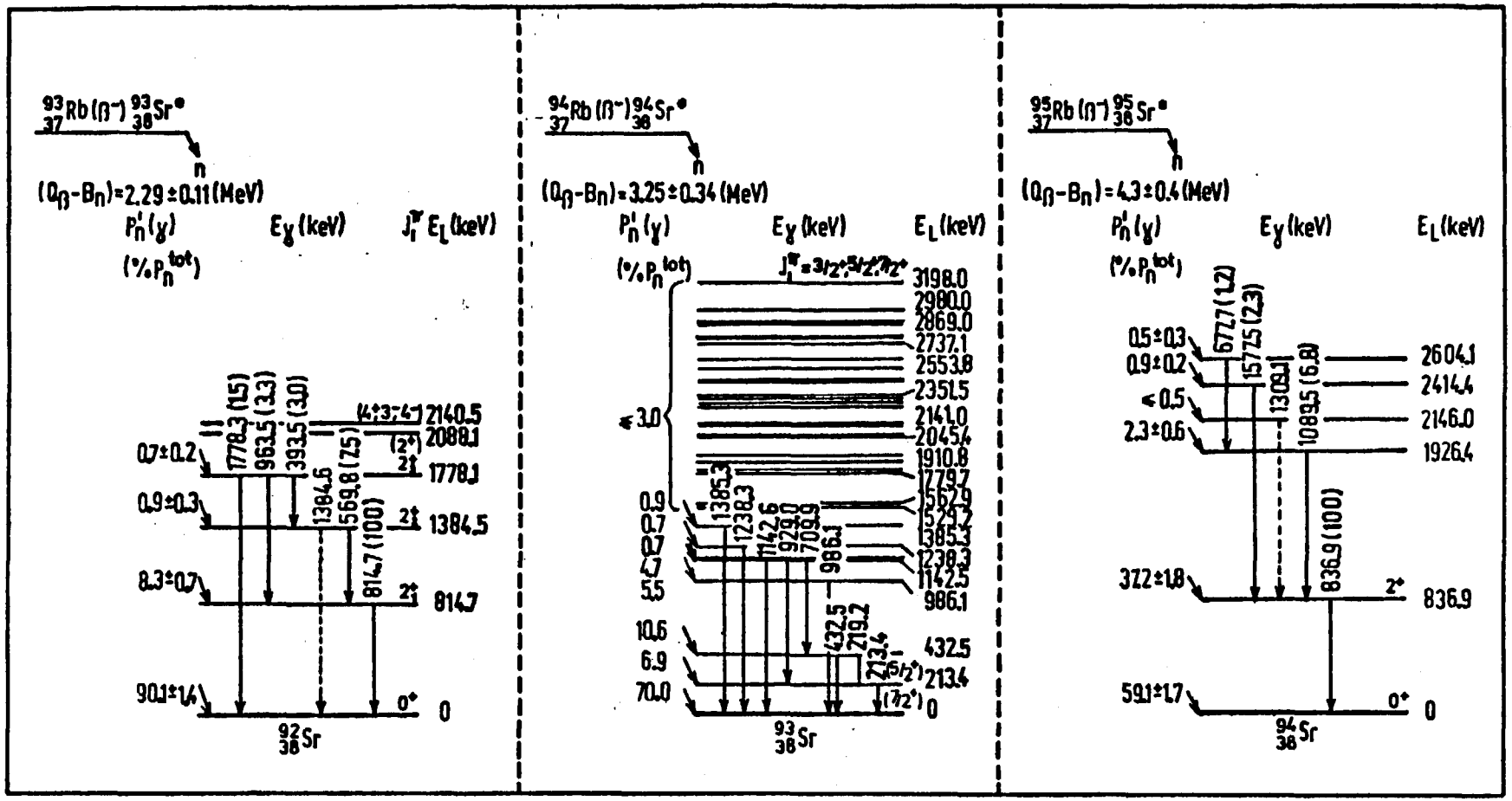

Fig. 22: Neutron emission to excited states in $^{92-94}$Sr (from Ref. |53|)

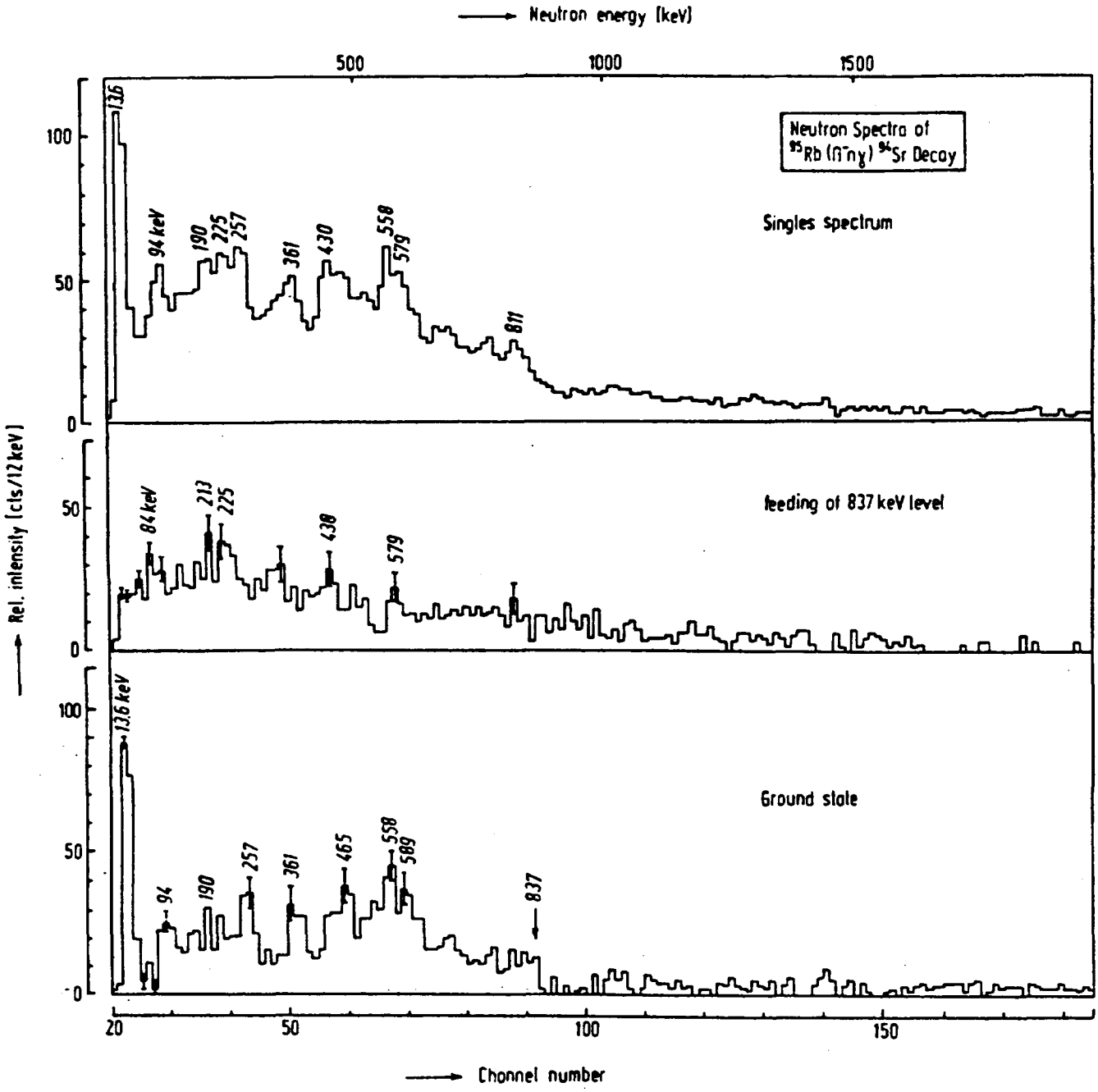

Fig. 23: Singles neutron spectrum of ^{95}Rb decay (upper part), and partial spectrum in coincidence with the 837 keV γ-rays corresponding to the $2^+ \rightarrow 0^+$ transition in ^{94}Sr (middle part). The partial spectrum of neutron decay to the ground state (lower part) was obtained by subtracting the coincidence spectrum from the singles spectrum (from Ref. |55|).

excited levels between 1926 and 2604 keV in ^{94}Sr (see Fig. 22). In this case the singles spectrum thus represents a superposition of only two intense partial spectra, their individual neutron peaks still being well resolved. The strongest neutron lines appearing in the singles spectrum are seen in only one or the other of the partial spectra, not in both. This is most clearly demonstrated for the 13.6 keV peak which surprisingly corresponds to a transition to the 0^+ ground state in ^{94}Sr though from the hindrance of the required f-wave neutrons at this low energy one would expect it to be seen in the partial spectrum to the 2^+-state where p-wave neutrons are dominating. As shown in Fig. 7 of Sec. IIb, recent results of Crawford et al. |37| who measured the low energy part of the ^{95}Rb delayed neutron spectrum with an energy resolution of 0.2 keV using the TOF-method confirm that the 13.6 keV peak consists of a single component. Another interesting feature of the partial spectrum to the ^{94}Sr ground state is the drop in neutron intensity at 837 keV, exactly corresponding to the energy difference of the ground- and the 2^+-state in the final nucleus. This supports the earlier qualitative explanation that the apparent lack of high-energy neutron intensity in the singles spectra is due to preferential neutron decay to excited final states |9,10,12,53|, their configurations being strongly connected to the main configurations of neutron-emitting states populated in β^--decay |56|.

Quite a different situation is found for ^{94}Rb($\beta^-n\gamma$)-decay, where many low-lying levels in the final nucleus ^{93}Sr can be reached after neutron emission as is indicated in Fig. 22. Fig. 24 shows several $n\gamma$-coincidence spectra (a-d) representing the neutron decay to the 4 lowest excited states in ^{93}Sr. The relative neutron branching ratios P_n^i to these levels are in general agreement with the previous results from γ-ray measurements. The partial spectrum of neutron decay to the ground state (e) was obtained by subtracting all coincidence spectra from the singles neutron spectrum of ^{94}Rb (f). Compared to the nearly continuous shape of this singles spectrum, the partial spectra exhibit clear peak structure, confirming the above mentioned explanation that the extent of fine structure in a singles neutron spectrum depends on the density of levels in the final nucleus accessible

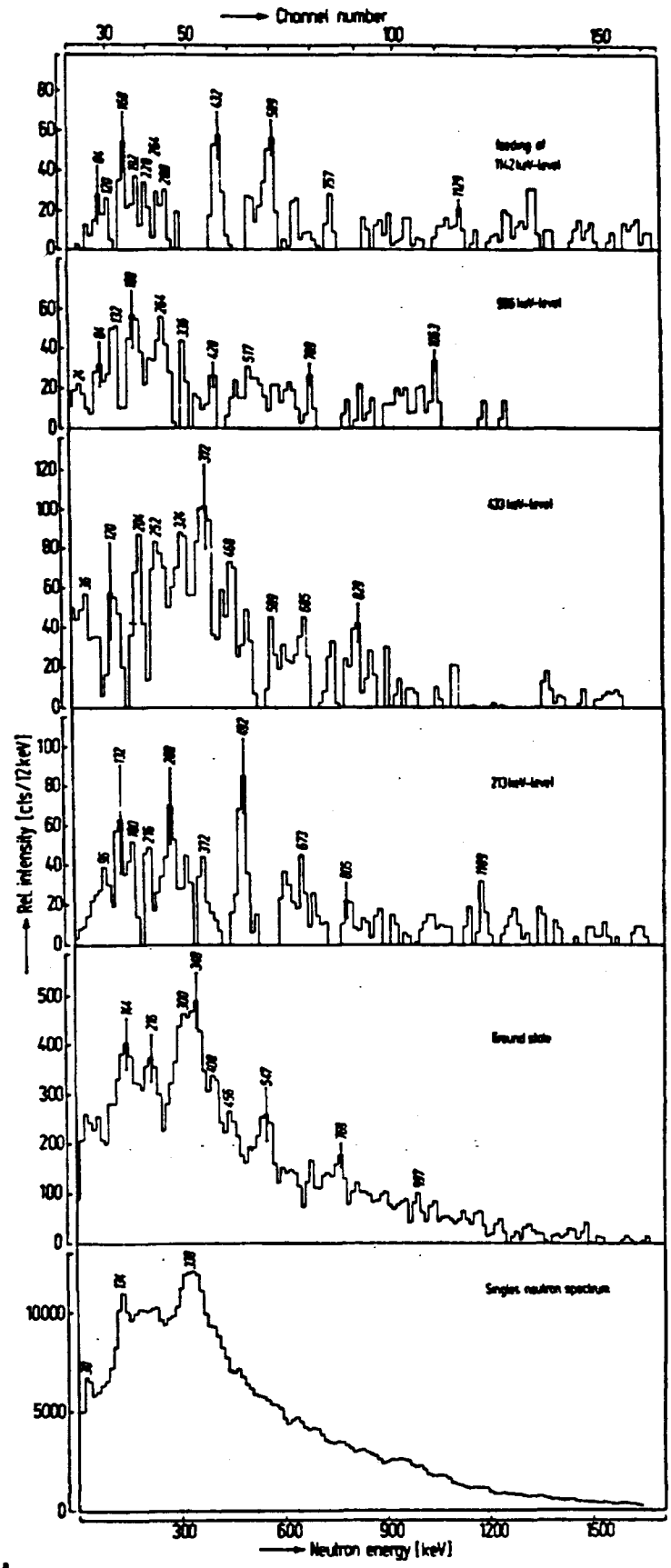

Fig. 24: ^{94}Rb partial neutron spectra in coincidence with γ-rays depopulating excited states in ^{93}Sr (a-d), neutron spectrum to the ground state in ^{93}Sr (e), and singles neutron spectrum (f), from Ref. |55|.

to neutron decay. In the case of ^{94}Rb the singles spectrum represents a superposition of 8 partial spectra containing about 95 % of the total neutron intensity $P_n^{tot} \approx 10$ %, and some further 20 partial spectra with very low P_n^i. Thus, with an average neutron detector resolution of about 18 keV in this experiment the individual peaks of the partial spectra can no longer be resolved in the singles neutron spectrum.

In the case of ^{94}Rb decay preferential neutron decay to the ^{93}Sr ground state is observed |55|, again indicating that partial widths for β-delayed neutron emission are not compatible with optical model transmission coefficients |57,58| as commonly assumed. In contrast to the ^{95}Rb(β^-n)-decay where the intermediate structure of the ^{95}Sr neutron-emitting states favours their decay to excited final states (2^+, 4^+, ...), the main configurations of the ^{94}Sr neutron-emitting states seem to be closer connected to the ^{93}Sr ground state ($7/2^+$) than to the first excited states ($5/2^+$, $7/2^+$, ...).

This "selectivity in neutron decay" |56|, together with the shape of the β^--strength function of the neutron emitters |12,51,53,59| and the Fermi-function essentially determine the general shape of the experimental neutron spectra.

b) Calculated Energy Spectra

Using statistical model considerations a substantial number of calculations of delayed neutron energy spectra |60-63| or "analytic fits" to the experimental data |2,4-7| have been performed with the assumptions of a β^--strength function (S_β) being constant, proportional to level density (ρ) or given by the gross theory of β-decay |64,65|. Since calculated neutron energy spectra are used to construct effective delayed neutron energy distributions in nuclear fuel or to deduce average neutron energies ($\bar{E}_n$) |2,7|, it is worth comparing those calculated spectrum envelopes with the experimental data.

When using the "analytical" representations of the neutron spectra measured by Shalev and Rudstam |2,4-7| in terms of fine structure peaks superimposed on a gross structure consisting of 1-4 different neutron wave components, one should have in mind the possible uncertainties due to the spectrum distortion in the energy range 100 to 300 keV and due to the cut of their spectra at about 100 keV and 1600 keV, respectively. Recent neutron spectrum calculations have been preformed by Gjøtterud et al. |61|, Hardy et al. |62| and Prussin et al. |63|. In these attempts, β-strength functions were assumed to be proportional to the level density and average values of partial widths for neutron emission were obtained using penetrability factors approximating the energy dependence of transmission coefficients. Level densities were calculated with the Gilbert and Cameron formulae |66|. In order to obtain detailed spectra, the β- and partial neutron widths were distributed amongst levels according to Porter-Thomas distributions and the levels were themselves scattered according to a Wigner distribution. Monte Carlo calculations were performed and the resultant spectra were smoothed to simulate that due to the finite detector resolution attendent to the experimental measurements. The results obtained by Gjøtterud et al. |61| and Hardy et al. |62| were remarkable in that the overall spectra bear, at first glance, a dramatic similarity to the experimental spectra. As far as the calculated neutron spectra are of interest to application, one can, however, restrict the discussion to an examination of spectrum envelopes and average values of neutron branching ratios P_n^i.

For those cases, where only one final level can be reached in neutron emission, the quality of the fit to experiment seems to be predominantly dependent on the β-strength function assumed. Taking ^{87}Br as an example, Gjøtterud et al. |61| and Hardy et al. |62| - both using a strength function proportional to level density - reported satisfactory qualitative agreement between experiment and statistical model calculations. Prussin et al. |63|, however, who performed similar calculations extensively testing the influence of reasonable variations in the shape of S_β, in optical model parameters and level densities, in Q_β within experimental errors and in γ-ray widths

over a large range, found that a strength function proportional to level density is not correct for ^{87}Br decay and even a constant strength function gave a better fit to experiment. From Fig. 25 it is clear that both these

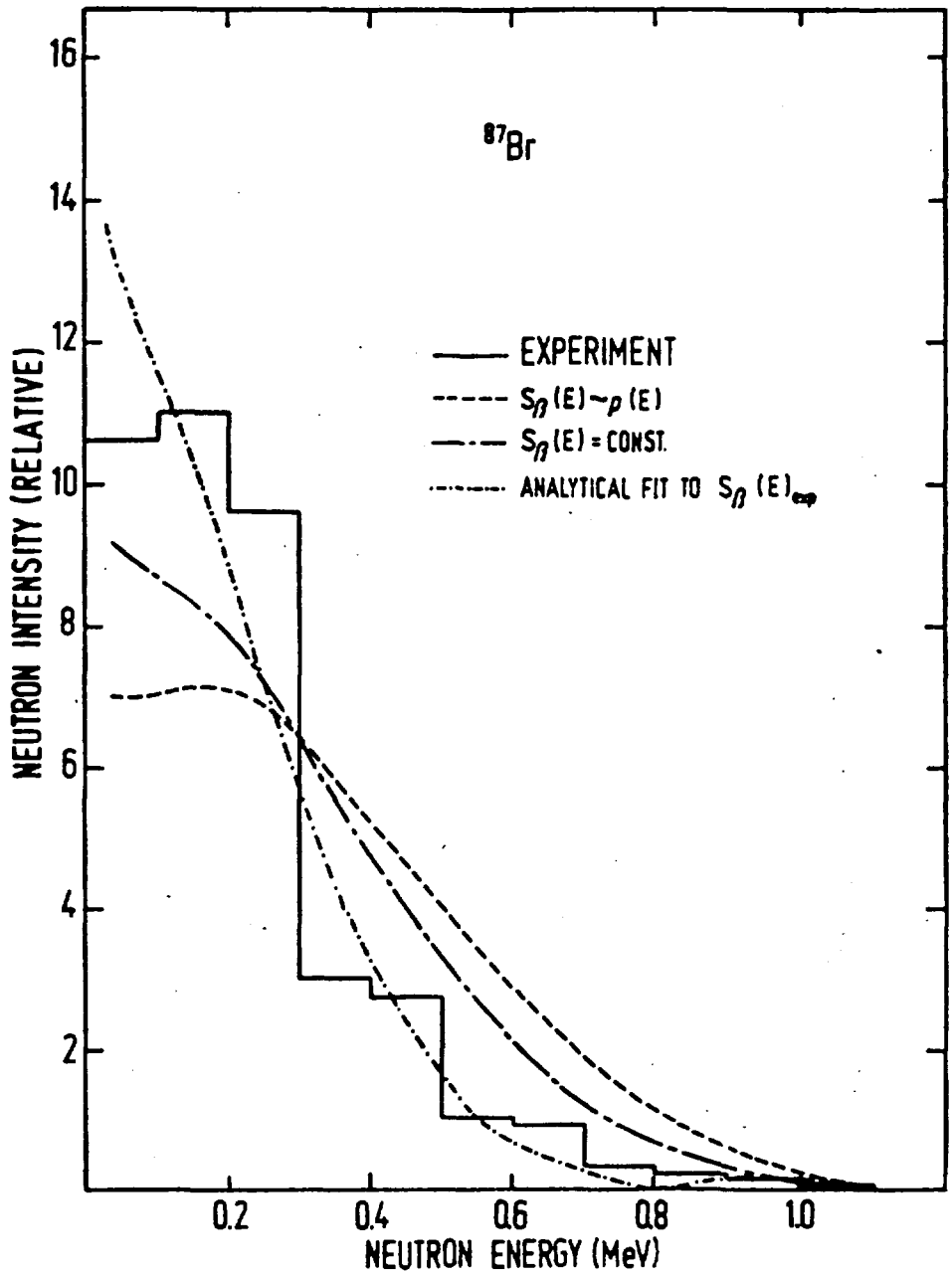

Fig. 25: The experimental neutron spectrum for ^{87}Br averaged over 100 keV intervals (histogram) and envelopes calculated with the assumptions $S_\beta(E) \sim \rho(E)$, $S_\beta(E)$=const., and with an analytical approximation to $S_\beta(E)_{exp}$ (from Ref. |63|).

model strength functions lead to overestimation in the intensity above 0.3 MeV and to underestimation at lower energies. Using an analytical representation of the experimental S_β |11,51| that possesses a resonance near B_n, however, gives a substantial improvement in the fit to experiment.

For those cases, where the energy window for neutron emission (Q_β-B_n) is large, the envelopes calculated under the assumption that only the ground state is populated |60| do not at all reproduce the tendency of the experimental spectra at high neutron energies, strongly overestimating the intensities in this range. As demonstrated by Gjøtterud et al. |61| introducing transitions to excited states in the final nuclei causes major changes in the calculates envelopes, increasing the intensities at lower neutron energies. Fig. 26 shows, as an example, the calculated neutron spectrum envelope of ^{143}Cs |61|, together with the experimental spectrum from Shalev and Rudstam and their older statistical model fit to this spectrum |6|. The sudden drops in experimental neutron intensity occuring at neutron energies corresponding to energy differences between states in

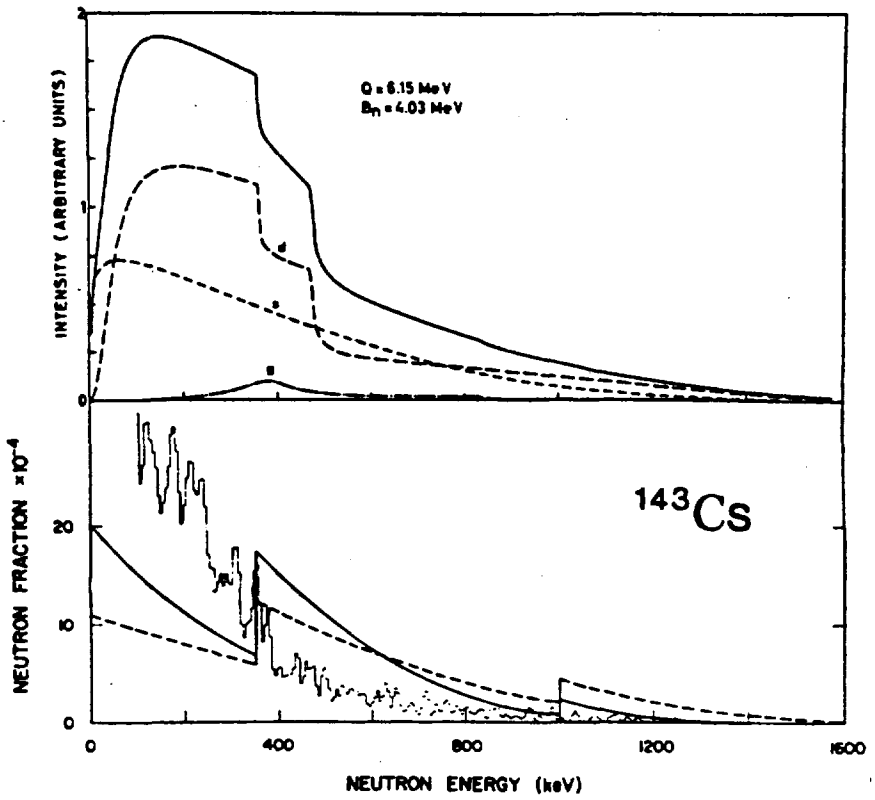

Fig. 26: Comparison of the calculated neutron spectrum envelope of ^{143}Cs with the experimental spectrum from Shalev and Rudstam (from Ref. |61|).

the final nucleus (see Sec. IIIa) are well reproduced in the calculations of Gjøtterud et al. |61|. Though generally "qualitatively satisfactory" agreement with the experimental data was reported |61|, for a considerable number of precursors with large $(Q_\beta - B_n)$ the model still predicts too much neutron intensity at higher energies. This was also found by other authors |51,53,63| who reported especially for the decay of odd-mass neutron precursors decaying into even-even final nuclei an average factor of 6 too much high-energy neutrons in the calculated spectra.

Several attempts exist to provide better fits to the relative population of excited states in the final nuclei. The results are demonstrated for the delayed neutron decay of ^{85}As. Gjøtterud et al. |61| propose to lower $(Q_\beta - B_n)$-values in order to obtain more resonable spectrum envelopes. As seen in Fig. 27, this indeed results in a considerable concentration of neutron intensity at lower energies, but consequently, results in an even greater disagreement between theoretical and experimental P_n^i. Similar statistical model calculations for ^{85}As were performed by Prussin et al. |63| in an attempt to simultaneously predict envelopes of neutron spectra and P_n^i-values to excited states with reasonable accuracy. Their calculated ^{85}As spectrum is shown in Fig. 28 along with a histogram representation of the experimental data |51,53|. The calculated P_n^i show a systematic decrease with increasing energy of the final state and, with some overestimation of the neutron intensity to the ground state, they decrease until, for the highest-excited level fed by neutrons, the calculations underestimate the P_n^i by a factor of 4-10. The calculated neutron spectrum is seen to be considerably harder than the experimental one, the fraction of the neutron intensity above 1.45 MeV being a factor of about 4 greater than found experimentally.

In an attempt to provide a better fit to the P_n^i the authors arbitrarily chose an exponential form for the β-strength function with a slope a factor of two greater than for an exponential fit to the energy dependence of the level intensity. The P_n^i were then in excellent agreement with experiment |51-53| but the calculated spectrum showed even worse agreement than that

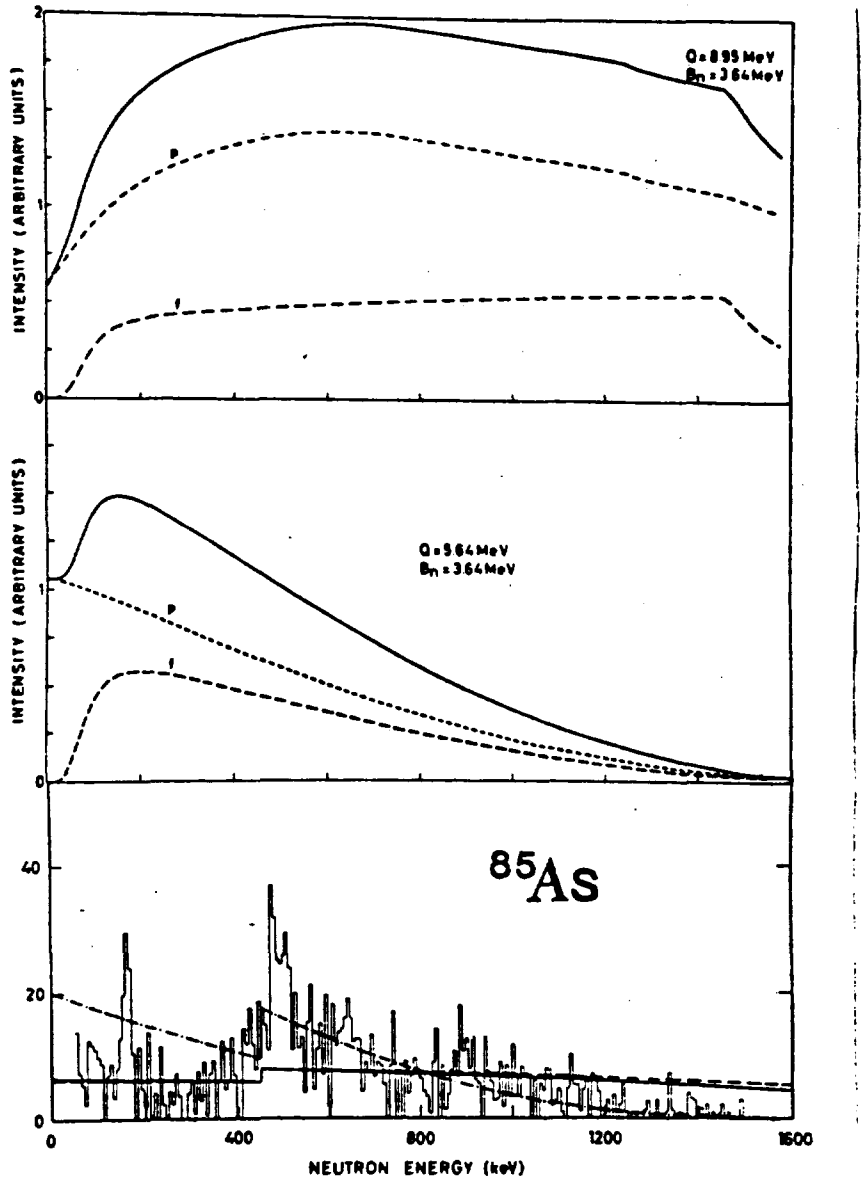

Fig. 27: The experimental spectrum of delayed neutrons from ^{85}As |8| and envelopes calculated with two different energy windows for neutron emission (from Ref. |61|).

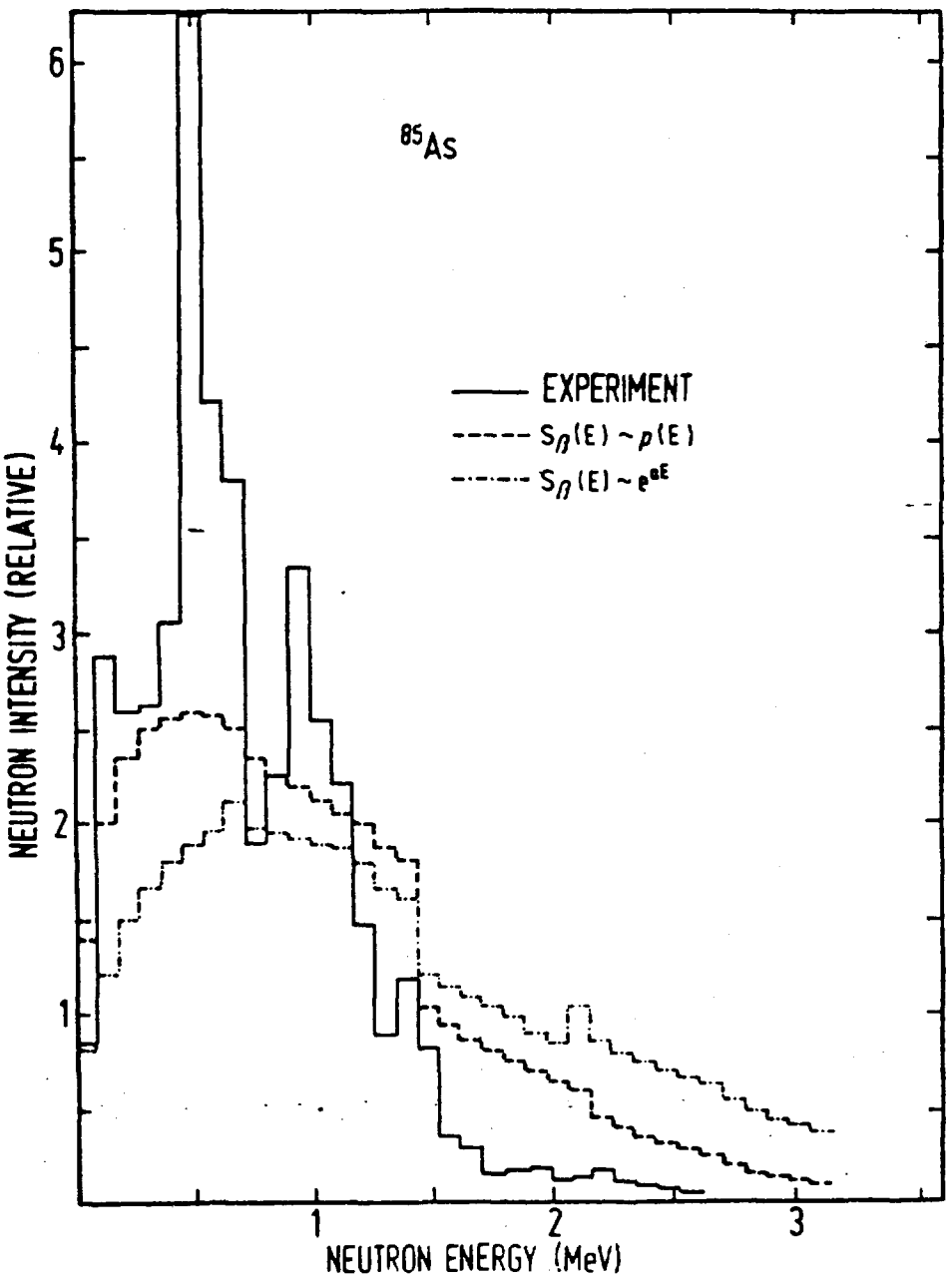

Fig. 28: The experimental neutron spectrum for ^{85}As averaged over 90 keV intervals (————) and envelopes calculated with the assumptions $S_\beta(E) \sim \rho(E)$ (----) and $S_\beta(E) \sim e^{aE}$ where the slope is a factor of 2 greater than for an exponential fit to the energy dependence of the level density (·····),(from Ref. |63|).

obtained with $S_\beta(E) \sim \rho(E)$. The fraction of intensity for $E_n > 1.45$ MeV in this case is a factor of about 7 greater than found in experiment. Although the shift of β-strength to higher energies results in greater neutron intensity to the higher-lying levels, the transmission coefficients still favour higher energy transitions. In addition, the authors have tried other strength functions, such as that derived from experiment |10,51,53|, but they were unable to simultaneously obtain good agreement with both the P_n^i and the neutron spectrum with this model.

From the above results, one can conclude that the simple statistical model generally used to describe delayed neutron emission is not, in fact, capable of explaining the experimental data. Consequently, one should be careful in using any "analytic fits" for individual spectra to construct delayed-neutron energy distributions in nuclear fuel |2,7|, since in these summation procedures the obvious discrepancies to the experimental data will accumulate. From a more scientific point of view, it seems reasonable to ask if the statistical model indeed should be able to reproduce the experimental data |63|. This model assumes that, to a good approximation, the matrix elements describing decay through all open channels are identical apart from statistical fluctuations. At sufficiently high energies there is a wealth of information that suggests this as a reasonable approximation, although some sort of pre-equilibrium emission has been well documented (see, for example, Ref. |67|). For the mass ranges and excitation energies considered here, however, this is not the case. The few channels open for neutron emission are associated with the lowest energy states of the final nuclei and substantial variations in their wave functions are found, the differences being most dramatic for levels of opposite parity where the major components in the wave functions cannot be the same |56|. Relative to levels at, or just above, the neutron binding energy, one can also expect that significant differences in the general makeup of wave functions can be found, at least over the energy range of a few MeV. It is therefore completely reasonable to expect that nuclear structure effects will be observable for these systems, and the calculations of Prussin et al. |63| support this conclusion.

c) Average Neutron Energies

As already pointed out in Ref. |20|, the discrepancies in the experimental neutron spectra from the Mainz-group and those from Shalev and Rudstam, as well as the results from an analytical description of these spectra have strong influences on the average neutron energies ($\bar{E}_n$) deduced from these data. Differences in the two sets of experimental data are mainly due to the fact that the Mainz-spectra cover the whole energy range from near thermal neutrons (E_n=10 keV) up to the full energy window for neutron emission ($E_n^{max} = |Q_\beta - B_n|$) whereas the OSIRIS-spectra are cut at 100 keV and 1600 keV, respectively, and due to the combined effects of insufficiently known detector response functions and high neutron background.

Since one of the recommendations of the Petten-meeting |2| was the reduction of uncertainties in average neutron energies, the sensitivity of $\bar{E}_n$ to response function correction and to the energy range of the measured spectrum was checked. In Fig. 29 the delayed-neutron spectra of the two non-fission products precursors ^{29}Na and ^{48}K are given |68|, the first one representing a 'hard', the second a rather 'soft' neutron spectrum. Both spectra consist of a few strong neutron peaks and a relatively small underlying continuum which represents the detector response and the neutron background distribution |39|. After subtraction of the continuum, in the residual 'net' spectrum $\geq$98 % of the respective total neutron intensity is contained in the peaks. In these cases a comparison of the average neutron energies obtained without and including response function subtraction may serve as an estimate of the possible uncertainties of $\bar{E}_n$ originating from these corrections (see Tab. 2): for the 'soft' spectrum the difference in $\bar{E}_n$ is less than 20 keV, for the 'hard' neutron spectrum about 45 keV. In addition, the sensitivity of $\bar{E}_n$ to the energy range of the spectrum is demonstrated in Tab. 2; the uncertainties are of the same magnitude (within 30 to 50 keV). As indicated in Ref. |39|, neutron background and response function (the ratio of continuum height to full-energy neutron peak) may strongly depend on the experimental conditions, and consequently may introduce uncertainties in the spectrum analyses, Therefore, in Tab. 2

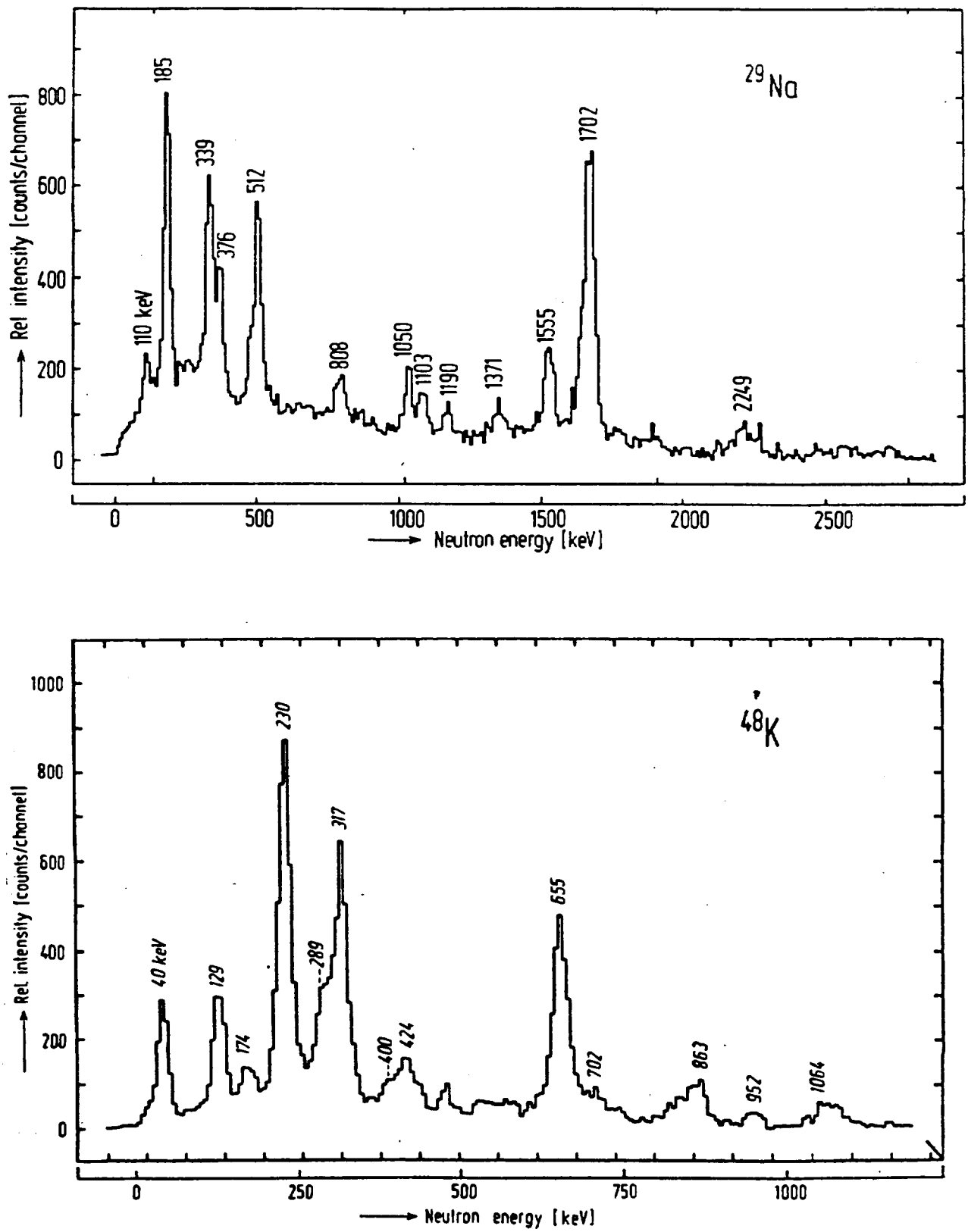

Fig. 29: Delayed-neutron spectra from ^{29}Na (upper part) and ^{48}K decay (lower part), (from Ref. [68]).

Tab. 2: Sensitivity of the average neutron energy ($\bar{E}_n$) to detector response function corrections and to the energy range of the spectrum

Precursor	Neutron energy range |keV|	Average neutron energy $\bar{E}_n$ |keV|	
		without response function corrections	‖ including response function corrections
^{29}Na	up to highest-energy peak at 2800 keV	927±13	970±14
	0 - 4000	992±14	
	0 - 4600	1010±14	
	0 - 5300	1017±14	
^{48}K	up to highest-energy peak at 1100 keV	396±12	413±12
	0 - 1385	422±12	
	0 - 2300	446±12	
^{85}As	0 - 1600	653±18	678±23
	0 - 2000	683±20	700±25
	0 - 2500	711±20	724±25
	0 - 3000	716±20	728±25

the possible errors of $\bar{E}_n$ of the fission product precursor ^{85}As are included. In the ^{85}As neutron spectrum a rather large amount of about 20 % of the total intensity is due to the detector response distribution. Again, the possible uncertainty in $\bar{E}_n$ is about 20 keV for the continuum correction, and less than 75 keV for different energy ranges chosen.

From these results one may conclude that the uncertainties in $\bar{E}_n$ from experimental neutron spectra are in the order of 20 keV for 'soft' spectra to maximum 100 keV for 'hard' neutron spectra. Compared to the average neutron energies deduced from the spectra measured by Shalev and Rudstam in the energy range 100 keV to 1600 keV, it can further be demonstrated (see Ref. |20|) that the discrepancies in $\bar{E}_n$ for rather 'soft' neutron

Tab. 3: Average neutron energy $\bar{E}_n$ from individual delayed neutron precursors

Precursor	This work	Average neutron energy $\bar{E}_n$ |keV| Rudstam |2| Experimental spectrum	Rudstam |2| Analytical representation	Reeder et al. |69| Method A	Reeder et al. |69| Method B
^{85}As	728^{+25}_{-50}	610*)	570		
^{87}Br	217±10	170	220		150±10
^{92}Rb	199±10			180±40	120±30
^{93}Rb	414±20	340	330	560±10	630±10
^{94}Rb	474±20	350	310	570±10	610±10
^{95}Rb	508±25	520	540	530±10	540±10
^{96}Rb	481±25			560±10	540±10
^{97}Rb	533±35			>720	>620
^{98}Rb	485±35				
^{135}Sb	1033^{+50}_{-100}	610	600		
^{136}Te	325±35	220	210		
^{137}I	579±25	510	490		530±50
^{138}I	467±30	390	370		
^{141}Cs	213±10	(270)	(320)		240±50
^{142}Cs	252±15	(200)	(200)	240±60	130±20
^{143}Cs	276±15	240	220	350±10	320±20
^{144}Cs	312±20	280	310	290±20	330±20
^{145}Cs	331±20			460±30	540±20
^{146}Cs	406±30				530±70
^{147}Cs	507±40				

*) from Ref. |8|

spectra are mainly due to neutrons from the energy range up to 100 keV, whereas for 'hard' spectra the influence of the high-energy neutrons is dominant.

In Tab. 3 the average neutron energies $\bar{E}_n$ deduced from the Mainz-spectra are presented, along with those obtained from the OSIRIS neutron spectra |2| and the results of Reeder at al. |69| who used a ^{3}He counter arrangement consisting of three detector rings with different amounts of paraffine moderator. It is seen that the Mainz neutron spectra are - for the above mentioned reasons - on the average 95 keV harder than those from Shalev and Rudstam. On the other hand, the results of Reeder et al. indicate even harder spectra than those measured by the Mainz group. A possible explanation of this discrepancy may lie in the fact that these authors calibrated their detector arrangement with the - obviously too soft - neutron spectra of Shalev and Rudstam. It is expected that, after a re-calibration of their system good agreement between the data of Reeder et al. and the Mainz-group can be achieved.

IV) INTEGRAL NEUTRON SPECTRA

A number of integral determinations of delayed-neutron spectra have been reported using either ^{3}He(n,p) spectrometry |21,23,24,70| or proton recoil spectrometry |17,22,71|. Among these, also spectra corresponding to different half-life groups have been measured |21,22,70|. Of special interest for reactor kinetics are the recent measurements of neutron spectra from fission of ^{235}U induced by neutrons of different energies |24|. These data are presented in a contributed paper to this review article.

Another approach has been used by Saphier et al. |1| who composed the effective delayed-neutron spectra of various fissile isotopes from the Shalev and Rudstam spectra of 21 individual precursors for thermal-neutron and fast-neutron fission, weighting the individual spectra by the abundances of the respective precursors. In addition, the authors constructed neutron spectra corresponding to the usual six half-life groups originally proposed by Keepin et al. |72|.

A third approach is to find a suitable analytical expression for individual delayed-neutron spectra describable by a small number of parameters |2,7|. By summing up these semi-calculated spectra weighted by the respective neutron abundances one is able to construct effective delayed-neutron distributions in nuclear fuel for any irradiation and cooling conditions.

Comparisons of the (near-) equilibrium spectra calculated by the technique used in Refs. |1,7| and the integral measurements |17,21-24| exhibit some disagreement. The spectra reported by Evans and Krick |23| and Weaver et al. |24| using ^{3}He-spectrometry are considerably harder than those obstined by Eccleston and Woodruff |17| using the proton-recoil technique. The reconstructed spectra of Saphier et al. |1| and Rudstam |2,7| seem to agree reasonably well with the other ^{3}He-spectrometry data |23,24| in the energy range 400 keV to 1600 keV; however, the semicalculated spectra do not extend below 100 keV and above 1600 keV, and too much intensity is found between 100 and about 400 keV due to neutron background (see Sec. II.c) As an example, the spectra from fast-neutron fission of ^{235}U from Refs. |1,17| are compared in Fig. 30. Besides the above mentioned sources of error in the spectra of Saphier et al. |1|, also the possible uncertainties in the neutron abundances (respectively in the fission yields) of the various precursors enter the calculations. Apart from this, the deviations from the spectra of Eccleston and Woodruff |17| may partly be connected to the complicated method of analysis of the proton-recoil data (see Sec. IIa).

The reconstructed spectra |1| corresponding to Keepins' six half-life groups of delayed-neutrons from thermal-neutron induced fission of ^{235}U are shown in Fig. 31. The authors claim that all important isotopic spectra have been measured. The missing spectra are for the short-lived isotopes contributing to Groups 5 and 6, mainly to Group 6. The contributors to Group 6 are ^{89}Se, ^{95}Rb, and ^{97}Rb, but only the spectrum of ^{95}Rb, which is also a contributor to Group 5, was available at that time. Therefore, in the sixth group, only ∿30 % of the spectral emission was taken into account, attributed to ^{95}Rb. All the neutrons emitted in delayed-neutron Group 1 were assumed to be from ^{87}Br. In Groups 1 and 2, 100 % of the spectra are known, and in Groups 3, 4, and 5, ∿98, 94, and 85 %,

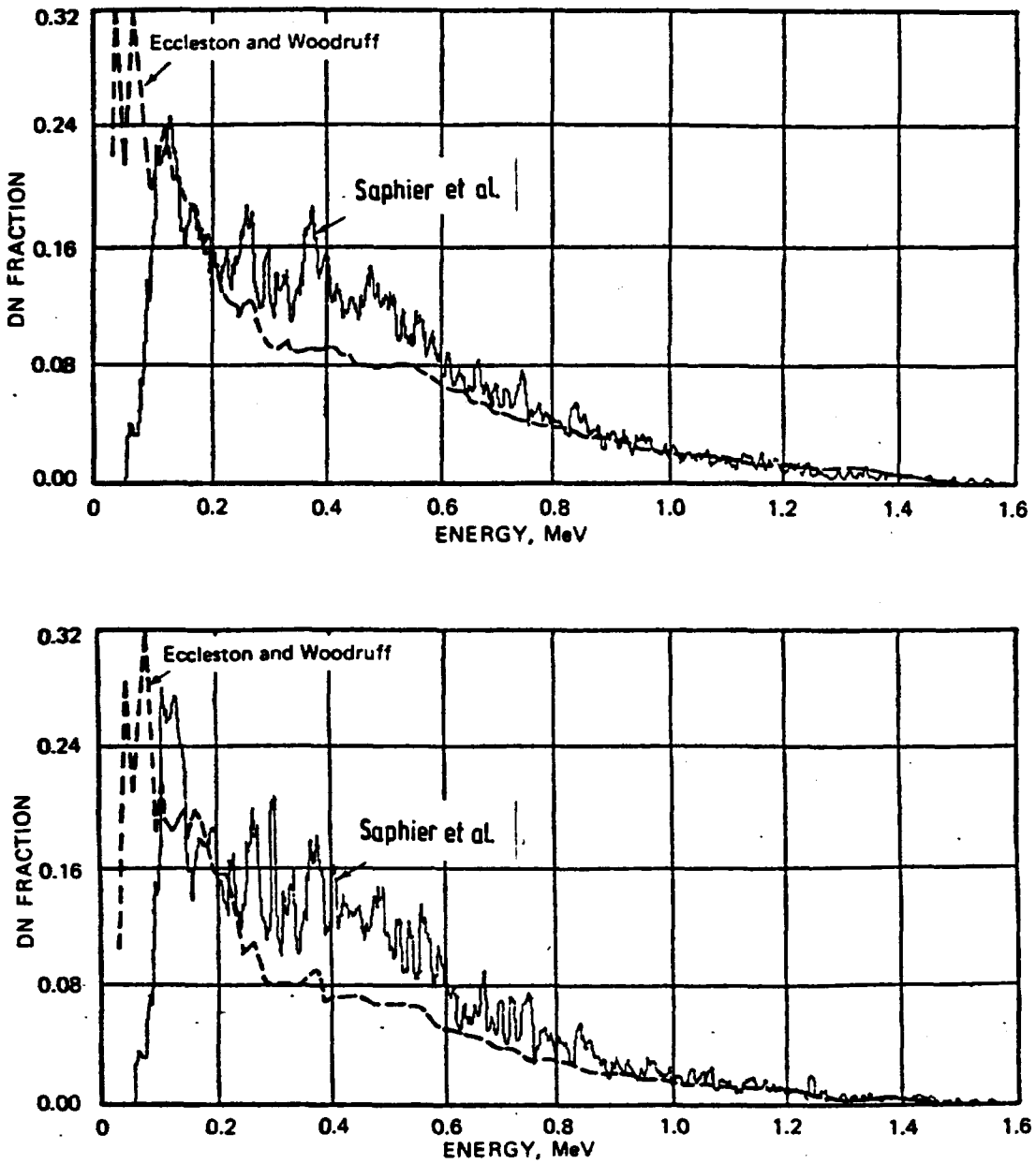

Fig. 30: Equilibrium delayed-neutron spectra from fast-neutron fission of ^{235}U (upper part) and ^{238}U (lower part), (from Ref. |1|).

respectively, of the spectra are known. Thus, the data presented in Ref. |1| were considered a complete set except for Group 6.

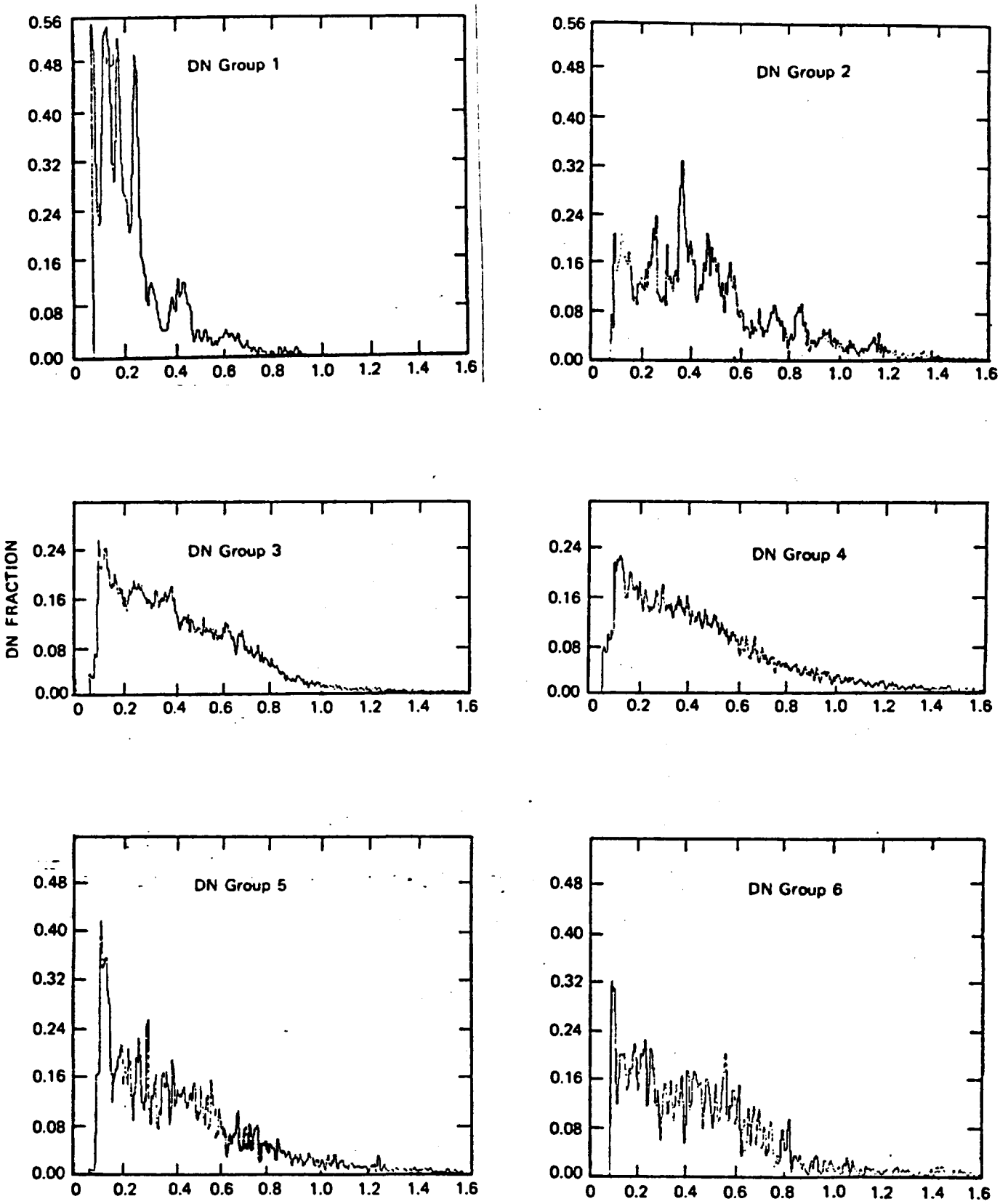

Abb. 31: Spectra of six groups of delayed neutrons from thermal-neutron fission of ^{235}U, (from Ref. |1|).

In the meantime further spectra of short-lived precursors have been measured, and for most of the other isotopes better quality data are available by now. An effort to reevaluate delayed-neutron spectra for reactor calculations using updated sets of delayed-neutron spectra, P_n-values |73|, and fission yields |74| would appear to be a worthwhile undertaking.

A direct way to determine energy spectra corresponding to the six half-life groups is the measurement of unseparated samples of fissile nuclides with different irradiation and cooling cycles |12,22,70|. Experiments of this kind can easily be performed at nuclear reactors or accelerators. Using automated fast rabbit systems, transit times of less than 100 ms are possible between irradiation and counting position |75,76|. Further advantages are the availability of pulsed neutron beams, as for example at the Mainz TRIGA reactor where neutron bursts of 30 ms width and thermal-neutron fluxes of up to $3 \cdot 10^{13}$ n_{th}/cm^2 can be produced |77|. As an example, the time dependent neutron spectra from a 2-s (Fig. 32) and a 10-s irradiation cycle (Fig. 33) for different cooling and counting intervals are shown |70|, together with the absolute number of delayed neutrons A_{DN} in units of $F_s(N/F)$ where F_s is the absolute fission rate of the ^{235}U sample and N/F the absolute delayed-neutron yield per fission. These measurements have been performed in 1970/71 using an old ^3He-proportional counter |78| with an energy resolution of about 70 keV for 1 MeV neutrons.

With the substantial improvement in ^3He spectrometers in the last few years, the measurements of time-dependent neutron spectra should be repeated for the most important fissile nuclides, for different primary neutron energies and various irradiation-counting cycles. Some studies of this kind are planned at Mainz.

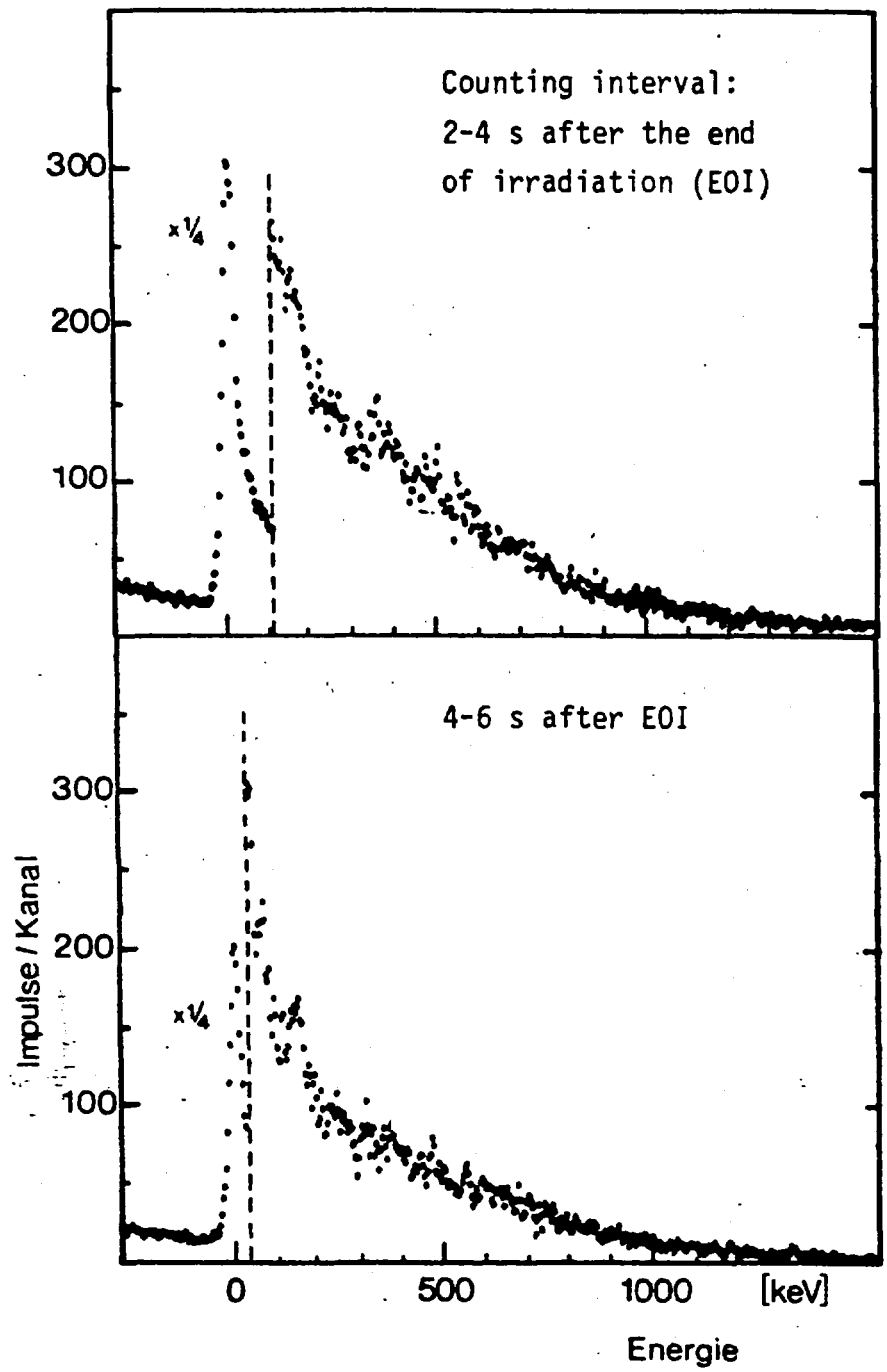

DN Group	$A_{DN}\|F_s(N/F)\|$
1	-
2	0.023
3	0.054
3	0.134

DN Group	$A_{DN}\|F_s(N/F)\|$
1	-
2	0.022
3	0.043
4	0.073

Fig. 32: $^{235}U(n_{th},f)$ delayed-neutron spectra: 2-s irradiation; together with the absolute number of delayed neutrons A_{DN} for each counting interval (from Ref. |70|).

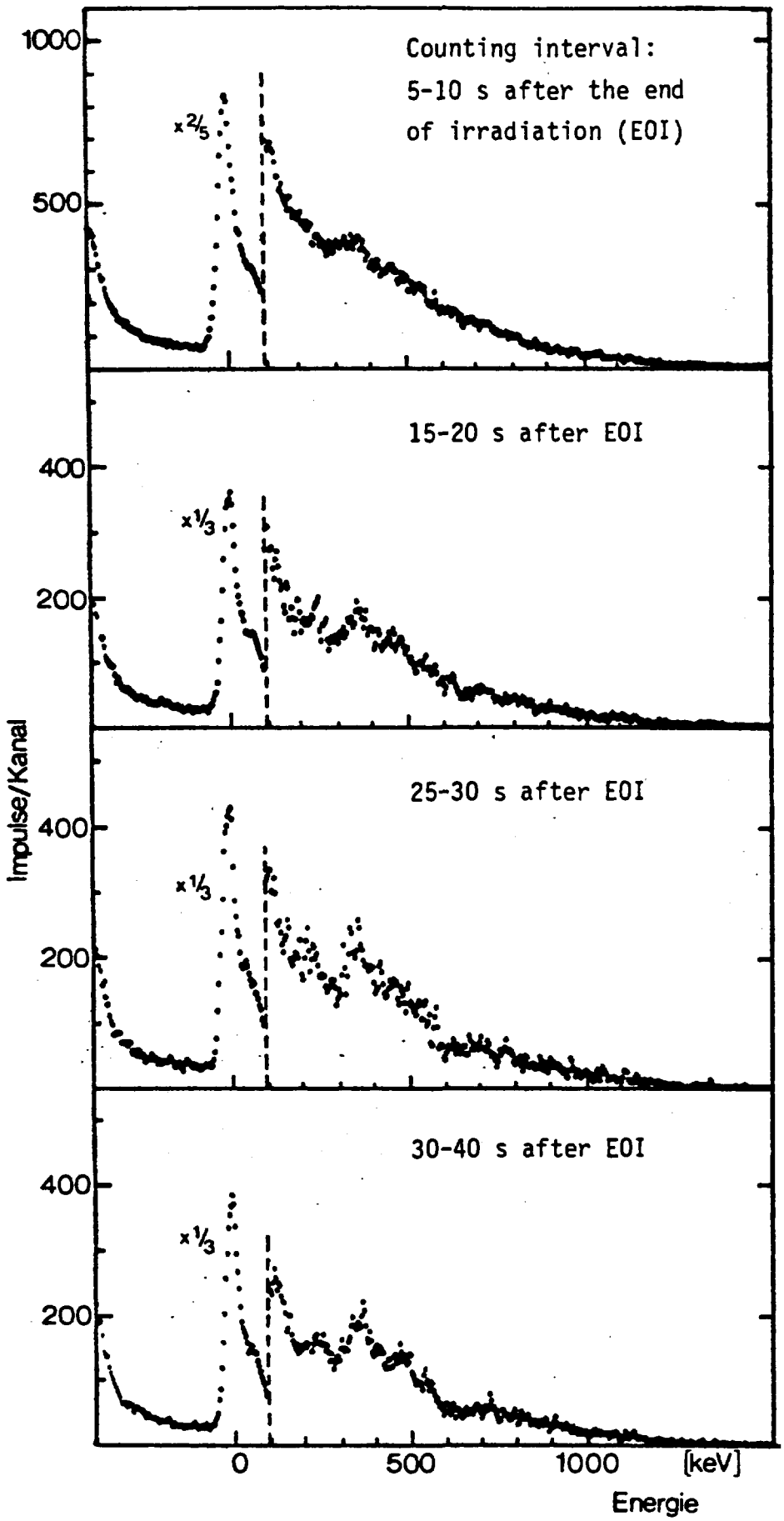

DN Group	$A_{DN}\|F_s(N/F)$
1	0.017
2	0.227
3	0.280
4	0.197
1	0.015
2	0.167
3	0.092
4	0.011
1	0.0135
2	0.123
3	0.030
4	-
1	0.248
2	0.197
3	0.027
4	-

Fig. 33: $^{235}U(n_{th},f)$ delayed-neutron spectra: 10-s irradiation; together with the absolute number of delayed neutrons A_{DN} for each counting interval (from Ref. |70|).

V) OTHER PROPERTIES OF BETA DELAYED NEUTRON DECAY

In the preceding sections those properties of delayed-neutron energy spectra have been discussed which are the most important ones for nuclear technology. However, there are other properties that more indirectly bear on problems of fission reactors but that are certainly of high scientific interest.

A large number of recent papers deal with the rather fundamental proble of statistical and/or structural influence on the β-delayed particle decay mode and on β-strength functions at high excitation energies. One theoretical concept for high-energy β-decay starts with statistical nuclear reaction theories |60-62,79-81|. For nuclei far away from stability the energy available for β-decay is very large. The decay can therefore procee to a very large number of excited levels. One is thus concerned with individual states of the same type as the resonances observed in the neutron capture process. The individual transition probabilities and the level spacings show pronounced local fluctuations, and the most convenient appoa is then to treat only averages over a large number of states. A very usefu quantity is the strength function defined |82| as

$$S_{\lambda c} = (\gamma^2_{\lambda c})\rho_{\lambda},$$

where $\gamma^2_{\lambda c}$ denotes the square of the overlap integral between two sets of nuclear wave functions, ρ_{λ} the level density of the states λ, and c the possible exit channels. The overlap integrals are normally referred to as reduced widths since they are factors of the observed partial widths $\Gamma_{\lambda c} = 2P_c\gamma^2_{\lambda c}$. The factor $2P_c$ is the barrier penetrability in the exit channel. For the beta decay a convenient definition of the strength function has been given |79| as the energy distribution of the reciprocal ft value,

$$S_{\beta}(E) \equiv b(E)/|f(Z,Q_{\beta}-E)\cdot T_{1/2}|,$$

where b(E) is the absolute β-intensity per MeV of states at excitation E, Q_β is the energy available for β-decay, $T_{1/2}$ the half-life in seconds, and f(Z,Q-E) is the statistical rate function. The strength functions describe the average behaviour of the nucleus over many final levels at a given excitation energy. The individual transition probabilities and the spacings between the states have wide distributions, and the finite number of resonances contributing to the average will then give rise to fluctuations in the observed intensity. Such fluctuations have been observed in the slow-neutron average cross-sections |83|; and it is generally accepted by now that they are the origin of the fine structure observed in the delayed particle spectra |11,61,62,79-81|.

In some work on β-delayed particle emission and high-energy β-decay the "gross theory" developed by Yamada and Takahashi |64,65,84| has been used. In their approach they combine a simplified single-particle model with a superimposed giant resonance behaviour and determine the absolute strength with the use of sum rules. This theory has proved to be useful in giving a rough overview on the general β-decay properties of nuclei far from stability. For most delayed-particle work up to now further simplifications of the gross theory which do not even fulfill sum rules have been used |4-6,60-62,79,81| in attempts to interpret experimental β-strength distributions. Especially in the recent paper of Hardy et al. |62|, it was concluded, that the examined experimental delayed-neutron data were consistent in all important aspects with statistical model calculations, assuming a smooth β-strength function proportional to level density. In particular, the authors concluded that no nuclear structure effects in either the β-decay or neutron emission are required to account for experiment.

The other theoretical concept starts with general nuclear structure considerations |51,56,85-87|. A recent survey on structures in S_β can be found in Ref. |86|. In β-decay a neutron-hole proton or a proton-hole neutron excitation is created. As in the case of neutron-hole neutron and proton-hole proton states, the coherent movements of the single nucleons will concentrate the main part of the transition strength for the different multipolarities in small regions of transition energy i.e. in giant resonances (GR). These collective $\bar{n}p$ and $\bar{p}n$ states forming the β-strength

function have been discussed by Ikeda et al. |88| in a generalized Brown-Bolsterli model and by Petersen and Veje |89| in the random phase approximation. The GR will deprive the β-decays to levels outside the resonance of their single-particle strength. One consequence of this for β^--decay is the occurence of only small low-lying resonances together with the giant resonance. Some of these "pygmy" resonances were discussed in the early analysis of hindrance effects from giant resonances |88,90-92|. Today they have been observed in γ-decay of isobaric analog states (IAS) in nuclei near stability (see for example Refs. |93-95|), in charge exchange reactions |96|, and also directly in β-decay of nuclei far off the stability line |10,11,51,53,59|. Although these "pygmy" resonances may not strongly affect the ground state to ground state hindrance factors they will become increasingly important for nuclei with larger Q_β i.e. for nuclei far off stability. When lying inside the Q_β window they are expected to completely determine the β-decay properties of the nucleus |85|.

As an example, in Fig. 34 the experimental β^--strength functions of odd-mass Rb precursors are presented in terms of reduced β-transition probabilities $B'(GT) = (4\pi/g_A^2)\cdot B(GT)$ versus excitation energy, integrated over 100 keV intervals |53,59|. As expected from the concept of a strength function in β-decay |79| and from the prediction of single particle models |51,56,87|, S_β- for the decay of neighbouring Rb isotopes shows a systematic behaviour as a function of mass number and β-decay energy Q_β. The most interesting feature is the appearance of resonances, in Fig. 34 a-e indicated by dotted Gaussian curves with centroid μ and half-width σ. Due to the relatively low Q_β values |97| of ^{89}Rb and ^{91}Rb, only the lower resonance is accessible to β-decay of these isotopes (Fig.34 a,b), whereas for the decay of the heavier precursors (Fig.34 c-e) in addition a second, stronger resonance centered about 2 MeV beyond the first one becomes visible. From ^{89}Rb to ^{97}Rb decay the centroid of the lower resonance is but little shifted towards higher excitation energies and the half-width of the fitted Gaussian curves increases only slightly. The second resonance in ^{93}Rb to ^{97}Rb decay located at 6 MeV shows similar trends. These data suggest that - at least in the vicinity of A = 90 - the resonances in S_β are still

well separated so that they become directly 'visible'. With increasing mass number, however, the structures in S_β seem to be more and more smeared out, so that for nuclei very far from stability a smoothly increasing strength function may be expected. Notwithstanding this 'disappearance' of the resonances due to increasing level density and configuration mixing, there remains the fact that, compared to the gross theory strength distribution, the experimental β^--strength of the heavier Rb precursors contains about five times more strength in the energy range 4 to 8 MeV. On the other hand, at lower excitation energies the gross theory systematically overestimates the β-strength. These deviations can, of course, only be extracted from quantitative analyses and were therefore not observed in the hitherto rather qualitative statistical model treatments |4-6,60-62|. Comparing the shapes of the experimental β-strength functions with the reduced β-transition probabilities from shell model calculations |56,98|, qualitative agreement is observed. For the lighter Rb precursors (^{89,91}Rb) the calculations suggest that besides the scattering of valence neutron pairs ($\nu g_{7/2} \rightarrow \pi g_{9/2}$) only the ($\nu p_{1/2} \rightarrow \pi p_{3/2}$) transition lies below 5 MeV in the Sr emitters. Going away from the β-stability line, the low lying $\nu g_{7/2} \rightarrow \pi g_{9/2}$ single particle strength increases by about a factor of ten due to the increase of neutron pairs in the valence orbital. In the same way the $\nu g_{7/2} \rightarrow \pi g_{9/2}$ strength increases, whereas the strong $\nu g_{9/2} \rightarrow \pi g_{9/2}$ strength at about 6.7 MeV remains constant. In addition, further single particle configurations in the range 7.5 to 8 MeV become accessible to β-decay.

Summarizing this part, one must conclude that the β^--strength function of nuclei far from stability indeed shows "pygmy" resonances and that this concentration of β-strength can be explained by specific shell model configurations, i.e. collective core polarization (CP) and spin flip (SF) states, strongly mixing with the antianalog states (AIAS).

Besides "selectivity in β-decay" also "selectivity in neutron emission" has been discussed. As already mentioned in Sec. III, γ-spectroscopic data and recent nγ-coincidence spectra have indicated preferential neutron

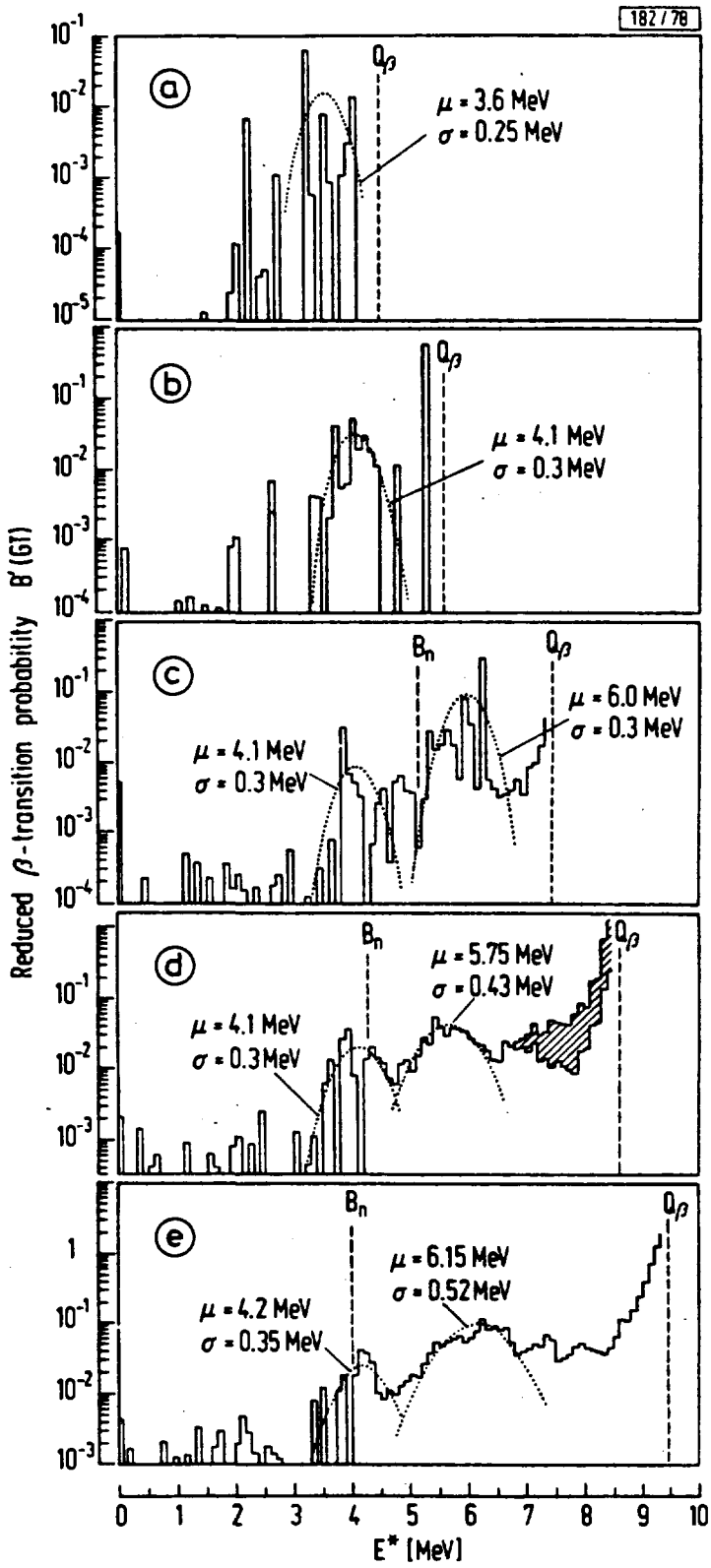

Fig. 34: Experimental β^--strength functions in terms of B'(GT) from the decay of odd-mass rubidium precursors 89-97 (from Refs. [53,59]).

decay to certain states in the final nuclei |12,53,55|. As pointed out by Shihab-Eldin et al. |56| for neutron emission to even-even final nuclei, the strong feeding of low-lying excited states may be explained by the magnitude of particle-hole excitations in the wave functions of the accessible levels. To illustrate this, the ground state shell model configuration for a typical precursor (^{85}As, ^{95}Rb, etc.) is shown to the left of Fig. 35. Allowed single particle GT β-transitions lead to configurations labelled "doorway states". The upper doorway state in Fig. 35a involves a valence neutron transition into an identical proton orbital, while the lower doorway state in Fig. 35b represents core neutron β-transitions. These latter configurations are frequently referred to in the literature as core polarization (CP) and spin flip (SF) states. It is apparent that the principal part of the β-strength to levels above B_n populates CP and SF configurations. Neutron emission from these "pure" intermediate CP and SF configurations is absolutely forbidden, and therefore it can occur only through admixtures in the wave functions of intermediate states obtained via scattering events that lead to a neutron in an unbound state. In Fig. 35 (to the right), such configurations are shown that can result from simple one-step, two-nucleon collisions. In Fig. 36, typical configurations of the

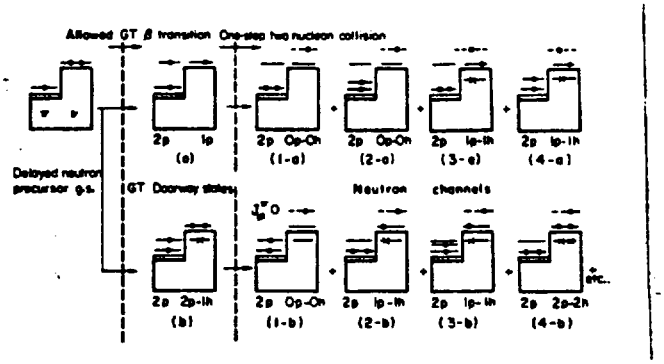

Fig. 35: Schematic of precursor β-decay to core polarization and spin flip states followed by one-step, two-nucleon collisions to neutron unbound configurations (from Ref. |56|).

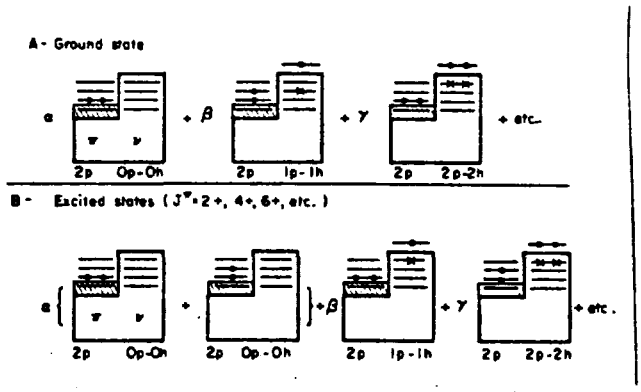

Fig. 36: Leading term configurations for ground states and low-lying excited states in final nuclei (from Ref. |56|).

leading terms for the ground state (A) and excited states (B) in the final nucleus are given. The amplitudes for these configurations are roughly inversely proportional to the degree of complexity (excitation) as indicated by the number of particle and hole excitations in each configuration (pairing correlations are implicitly assumed). Thus, $\alpha >> \beta >> \gamma$, etc. If one assumes that one-step collisions are reponsible for predominant admixtures i.e., intermediate structure, it can be clearly seen, from comparison of Fig. 35 and Fig. 36, that one-step collision admixtures in CP and SF configurations can lead to first-order (and higher) terms in the excited states of the final nucleus, but only to second-order (and higher) terms in the ground state. Therefore, preferential neutron emission to excited states is expected in this simple picture |56|.

Quite the opposite situation seems to exist for neutron decay to odd-mass final nuclei. As is discussed in Ref. |55|, for the case of ^{94}Rb(βn) decay preferential ground state neutron feeding is observed (see Tab. 4) indicating that the main configurations of the ^{94}Sr neutron emitting states are closer connected to the ^{93}Sr ground state ($7/2^+$) than to the first excited states ($5/2^+$, $7/2^+$ ...). However, with the emission of predominantly p-wave neutrons as required from angular momentum considerations, moderate agreement

between experimental and calculated envelopes of partial neutron spectra to different final states can be obtained as shown in Fig. 37, and as is further indicated by their first moments (Tab. 4). These comparisons of statistical

Table 4: Experimental and calculated neutron intensities (P_n^i) to different states in the final nucleus ^{93}Sr, and comparison of the first moment ($\bar{E}_n$) of the respective partial neutron spectra (from Ref. |55|).

Level in ^{93}Sr |keV|	P_n^i |%| of P_n^{tot}		$\bar{E}_n$ |keV|	
	exp.	calc.[a]	exp.	calc.[a]
ground state	70.0	52.4	440	489
213	6.9	24.5	568	584
433	10.6	14.5	422	595
986	5.5	3.6	516	540
higher levels	7.0	5.0	-	-

[a] Calculated with $S_\beta \sim \rho(E)$ assuming p-wave neutrons

model predictions with experimental partial neutron spectra open the possibility of studying 'neutron spectroscopic factors'; and with the determination of angular momenta of the emitted neutrons indirectly the spins and parities of the final states can be deduced.

The above experimental results and the fact that one is unable to fit spectra and neutron branching ratios to excited states with any reasonable β-strength function |63| shows that β-delayed neutron emission does not follow the trends predicted by optical model transmission coefficients, the same coefficients which apparently represent well low energy neutron reactions in the same mass ranges. It follows from this and the observations above, that discrete structure effects (i.e., intermediate structure) must be considered in the description of β-delayed neutron emission.

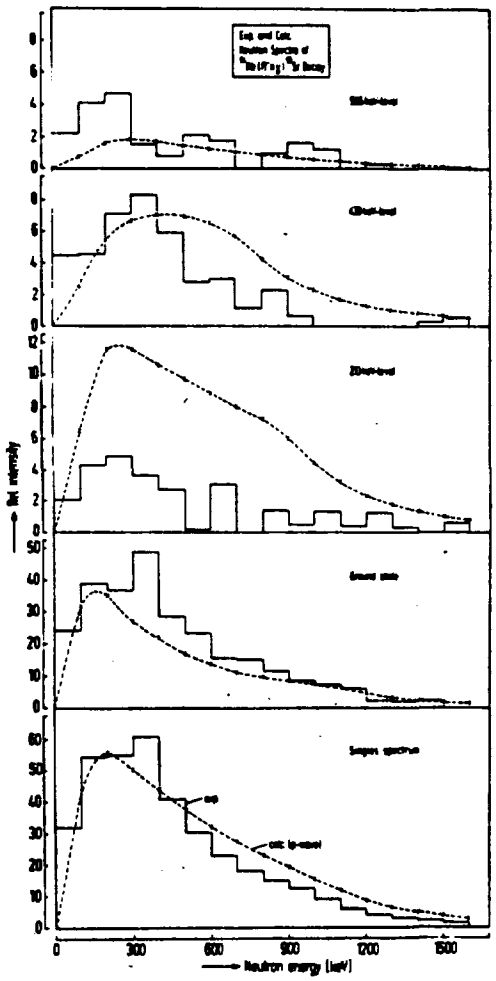

Fig. 37: Comparison of experimental and calculated neutron spectrum envelopes of ^{94}Rb decay (from Ref. |55|).

This does not say that statistical properties are unimportant, but only that a purely stastistical approach is unable to satisfactorily describe β-delayed neutron emission. Very recent results on lighter delayed-proton |99| as well as delayed-neutron precursors |68| support the 'non-statistical' interpretation. As mentioned above, nuclear structures in S_β have direct consequences on the decay properties of neutron-rich nuclei, for example β-decay half-lives and β-delayed neutron emission |51,53,59,85,86|. According to its definition |79| the β-strength is inversely proportional to the ft-value, and the neutron emission probability P_n is given as the ratio of β-strength above the neutron binding energy B_n and of total β-strength, corrected for the Fermi-integral. Whereas in the latter case the above mentioned concentration of strength in the energy range 4 to 8 MeV - in the single particle picture mainly due to the $p_{1/2}$ and $g_{9/2}$ transitions - is decisive in determining the P_n-values |98,100|, the β-decay half-lives are predominantly determined by the position and magnitude of the low-lying $g_{7/2}$ single particle configuration.

Fig. 38 shows a comparison of theoretical Rb P_n-values from different model assumptions with recent experimental data |100|. In the case of the gross theory, the neutron emission rates λ_n |65| were transformed to emission probabilities using for the half-lives experimental data (A) and values from the gross theory calculations (B) |84|. Both attempts, however, result in P_n-values roughly one order of magnitude too small. The P_n-slope from $S_\beta \sim \rho(E)$ is too steep, and the absolute values of the lighter isotopes are systematically underestimated whereas those for heavier nuclides (with large Q_β) are overestimated. It seems somewhat embarrassing that next to the shell model P_n-values those from the assumption S_β=const. including the cut-off energy C |79| give 'best' agreement with the experimental data. In the light of these results any agreement of theoretical P_n-values from statistical model calculations with experimental data must be regarded as fortuitous, since the neutron emission probability strongly depends on the location of Q_β and B_n relative to the position of the resonances in S_β. As for example shown in Ref. |101|, for those precursors in the vicinity of A = 90 where structures in the

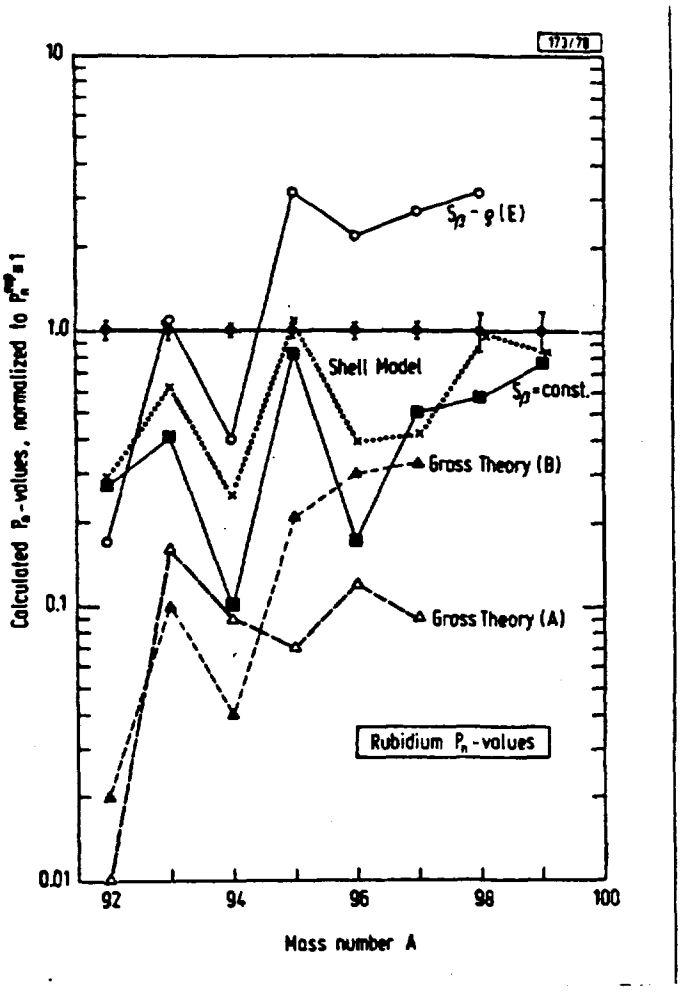

Fig. 38: Comparison of experimental rubidium P_n-values |100| with predictions from different nuclear models |65,89,101| (from Ref. |59|).

strength function are contained within a relatively small energy window for neutron emission ($Q_\beta - B_n$), the experimental P_n-values are found to be considerably higher (factors of 5-20 for ^{87}Se, ^{87}Br, ^{92}Kr, ^{92}Rb, ^{97}Y, for example) than the caluculated values. The systematic deviations of P_n-values derived from statistical model calculations must therefore be considered as an inherent result of the structureless shape of S_β assumed in these approaches.

As recently stated by Wohn et al. |102| and demonstrated in Fig. 39, within an isotope sequence the gross theory |84| underestimates half-lives ($T_{1/2}$) near the β-stability line, whereas it systematically overestimates this quantity for very neutron rich isotopes. The simple shell

model approach |100| strongly underestimates the half-lives (by factors of about 10 to 50) which clearly is the effect of neglecting residual interactions, but the trend of the half-life decrease with increasing neutron number follows fairly well the experimental data. To visualize this tendency in direct comparison with the experimental and the gross theory half-lives, the shell model half-lives were normalized to the experimental value of ^{93}Rb. In the single particle approach the β-decay half-lives are roughly inversely proportional to the strength of the lowest lying $\nu g_{7/2} \rightarrow \pi g_{9/2}$ transition originating from neutron pair scattering out of the valence orbital. With the closure of the $d_{5/2}$ neutron subshell in ^{93}Rb (N = 56) the magnitude of the $g_{7/2}$-strength increases by a factor of 5 in ^{95}Rb (N = 58). Besides this shell effect, the position of Q_β is important for determining the β-decay half-life due to the rapid variation in the Fermi function which is roughly proportional to $(Q_\beta - E)^5$. However, as can be shown for the ^{93}Rb/^{95}Rb pair (and similar for other N = 56/N = 58 pairs) a good choice of the Q_β-values alone can in no way account for the sudden $T_{1/2}$ decrease by a factor of 15, which is well reproduced by the single particle model (factor of 12). In Ref. |102|, for example, the effect of Q_β on the gross theory half-lives of Rb isotopes is demonstrated. One set of Q_β-values therein is within 50 keV and 390 keV,

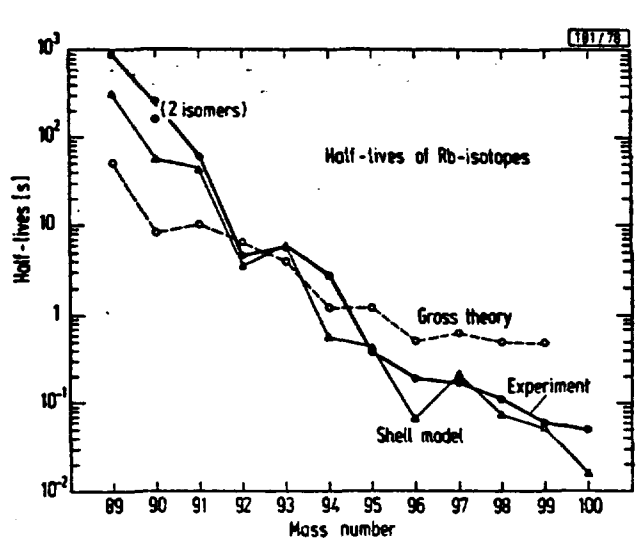

Fig. 39: Beta-decay half-lives of rubidium isotopes; comparison of experimental data with predictions from the 'gross theory' |84| and shell model calculations |98| (from Refs. |53,59|).

respectively, equal to the experimental data for ^{93,95}Rb |100| used in the shell model attempt |98|, and the resulting gross theory half-lives are shown to decrease only by a maximum factor of 3.2. The $T_{1/2}$ comparison in Tab. 5 clearly demonstrates that without doubt the N = 56 shell effect exceeds possible Q_β effects in defining the β-decay half-lives for nuclei in this mass region.

Tab. 5: Comparison of gross theory |103|, single particel model |98| and experimental |97| β-decay half-lives of $^{93-98}$Rb.

Isotope	Gross theory |103| Q_β^{calc}(MeV)	rel. $T_{1/2}$ (a)	rel. $T_{1/2}$ (b)	Single particle model |98| Q_β^{exp}(MeV)	rel. $T_{1/2}$	Experiment|100| rel. $T_{1/2}$
^{93}Rb	7.49	1.00	1.00	7.44	1.00	1.00
^{94}Rb	10.30	0.47	0.32	10.27	0.08	0.47
^{95}Rb	8.98	0.39	0.32	8.59	0.09	0.06
^{96}Rb	11.76	0.22	0.13	11.60	0.02	0.03
^{97}Rb	9.91	0.24	0.16	9.53	0.04	0.03
^{98}Rb	13.18	0.12	0.06	10.85	0.01	0.01

The fact that only the single particle approach is able to provide consistent agreement with experimental data suggests that this model can account for the real shape and general locations of 'pygmy' resonances of the β^--strength in the A = 90 mass region. As demonstrated above, these nuclear structures in S_β are decisive in predictions of β-decay half-lives and β-delayed neutron emission. Furthermore, the shape of S_β also has consequences on the average γ-ray energies and the β-spectra of short-lives isotopes, the first being systematically higher, the second systematically softer than those predicted from a strength function according to the gross theory |64|.

All these data bear on several problems of fission reactors, in particular on loss-of-coolant accidents and the associated problem of decay heat from radioactive decay of the fission products. To design emergency cooling systems to compensate for this heat production, one approach is to identify those short-lived isotopes that produce the decay heat and then to calculate

the rate of heat production. Prussin et al. |104| have examined the contribution and their uncertainties from individual isotopes produced from ^{235}U fission products for a burst irradiation and for cooling times (t_c) of 10 and 100 s. For t_c of 10 s, more than 97 % of the total decay power is due to about 84 isotopes. By summation of individual contributors, 26 isotopes account for 94 % of the total energy variance, among these being the short-lived halogen and alkali isotopes extensively studied by the Mainz-Grenoble-Berkeley collaboration. This data base may be extremely useful for the flexible and efficient design of next-generation reactors.

As can be seen from Tab. 6, recent γ-ray measurements at Livermore |104| extending up to high excitation energies on the properties of short-lived Sb isotopes associated with reactor-safety indicate that compared to previously accepted average γ-decay energy data the new values lie up to 45 % higher. Again these data support our finding that in the β^--strength function a considerable amount of strength is concentrated above about 4 MeV. In the light of these results, recent calculations on emergency cooling systems of nuclear reactors |105| based on the gross theory of β-decay should be regarded with some caution.

Tab. 6: Changes in average γ-ray energies of isotopes associated with reactor-safety decay heat (from Ref. |104|).

Value	Isotope $^{132}Sb^m$	$^{132}Sb^g$	^{133}Sb	^{134}Sb
E_γ, MeV/fission (previous work)	2.344	2.488	1.874	2.086
E_γ, MeV/fission (present work)	2.799	2.535	2.531	2.632
Percent change	19	1.9	45	26

A discussion of the relevance of the study of neutron-rich nuclei would not be complete without mentioning that the shape of the β^--strength function is also decisive in predictions of β-delayed fission probabilities and in this way for the production rates of heavy nuclides by astrophysical processes and by thermonuclear explosions |85,86,106-108|.

VI SUMMARY AND RECOMMENDATIONS

Considerable progress on delayed-neutron energy spectra has been made in the past few years. By now, 33 spectra of individual precursors have been measured, including those of primary interest for nuclear technology. However, for 14 out of these spectra the low energy part up to about 100 keV and the energy range above 1600 keV is lacking. These spectra should be remeasured, the most important for reactor technology being $^{79-81}$Ga, $^{88-91}$Br, ^{134}Sn, ^{139,140}I. Further precursors still requiring measurement of neutron spectra are ^{92}Br, ^{93,94}Kr, $^{98-100}$Sr, $^{97-100}$Y, ^{137,138}Te, ^{141}I. However, there seems to be no strong motivation from a technical point of view to study these precursors |2|.

As was requested at the Petten meeting, further work on assessment of the properties of different neutron spectrometer types has been done, especially concerning response function and detector efficiency of the ^{3}He-spectrometers and on error analysis of the spectra measured with proton-recoil and ^{3}He(n,p) techniques. The analyses have not succeeded in clarifying the apparent differences in neutron intensities. However, one should have in mind that by now the main properties of the ^{3}He(n,p) spectrometry seem to be well understood, whereas in the case of the proton-recoil technique spectrum subtraction or two-parameter to one-parameter transformations are not straightforward and may possibly be subject to errors. One possibility for clarifying the discrepancies could be the measurements of neutron spectra from individual light-mass precursors like ^{16}C, ^{17}N or ^{29}Na, ^{49}K, all exhibiting very simple line-structure without measurable complex or continuous neutron distributions.

Average neutron energies ($\bar{E}_n$) from individual precursor spectra can by now be determined within $\pm$10 keV for 'soft' and $\pm$50 keV for 'hard' spectra. However, there still remain (the above mentioned) precursors where a considerable reduction of the uncertainties in $\bar{E}_n$ is required. For direct determinations, like with neutron counter ring arrangements (SOLAR-group), an energy recalibration using the latest spectral data seems to be necessary.

Because of the still existing discrepancies in neutron spectra measured by different techniques a considerable improvement in the knowledge of (near-) equilibrium and time-dependent spectra for different fissile isotopes at various primary neutron energies is urgently required. Summation methods using experimental spectra or 'analytical representations' contain rather large uncertainties, last not least due to the generally insufficiently known total delayed-neutron yields and individual precursor neutron abundances. A new evaluation with updated sets of delayed-neutron energy spectra, P_n-values and fission yields would appear to be a worthwhile undertaking. However, with the experimental possibilities available at many laboratories, direct measurements of (near-) equilibrium and time-dependent spectra are to be preferred.

Summarizing, one may conclude that the data set on neutron spectra is on the average sufficiently complete to permit a satisfactory evaluation of the macroscopic effects of delayed neutrons in nuclear fuel. Before defining new specific requirements, at the moment further sensitivity studies needed to formulate those accuracy requirements for the time dependence and the energy spectra seem to be of highest priority.

ACKNOWLEDGEMENTS

It is a pleasure to acknowledge the valuable assistance offered to me by Profs./Drs. G.I. Crawford, H. Franz, G. Friedlander, P.G. Hansen, J.C. Hardy, G. Herrmann, P. Hoff, B. Jonson, E.S. Kenney, H.V. Klapdor, M.S. Krick, F.M. Nuh, G. Nyman, A.C. Pappas, S.G. Prussin, P.K. Ray, P.L. Reeder, C. Ristori, E. Roeckl, W. Rudolph, G. Rudstam, D. Saphier, A.A. Shihab-Eldin, K. Takahashi, D.R. Weaver, H. Wollnik, G.L. Woodruff and K.D. Wünsch in form of - partly unpublished - manuscripts, communications and suggestions.

This work was a supported - in part - by the German Bundesministerium für Forschung und Technologie (BMFT).

REFERENCES

|1| D. Saphier, D. Ilberg, S. Shalev, S. Yiftah; Nucl. Sci. Eng. 62 (1977) 660.

|2| G. Rudstam; Proc. of the 2nd Advisory Group Meeting on Fission Product Nuclear Data (FPND)-1977, IAEA-213, Vol. II (1978) 567.

|3| S. Shalev, G. Rudstam; Phys. Rev. Lett. 28 (1972) 687.

|4| S. Shalev, G. Rudstam; Nucl. Phys. A230 (1974) 153.

|5| G. Rudstam, S. Shalev; Nucl. Phys. A235 (1974) 397.

|6| S. Shalev, G. Rudstam; Nucl. Phys. A275 (1977) 76.

|7| G. Rudstam; J. Radioanal. Chem. 36 (1977) 591; The Swedish Research Councils'Laboratory Report LF-70 (1976).

|8| H. Franz, G. Herrmann, J.-V. Kratz, K.-L. Kratz; J. de Phys. 33 (1972) C5-31.

|9| H. Franz, J.-V. Kratz, K.-L. Kratz, W. Rudolph, G. Herrmann, F.M. Nuh, S.G. Prussin, A.A. Shihab-Eldin; Phys. Rev. Lett. 33 (1974) 859.

|10| K.-L. Kratz, W. Rudolph, H. Ohm, H. Franz, C. Ristori, M. Zendel, G. Herrmann, F.M. Nuh, D.R. Slaughter, S.G. Prussin; Proc. 3rd Int. Conf. on Nuclei far from Stability, Cargèse 1976, CERN-Report 76-13 (1976) 304.

|11| F.M. Nuh, D.R. Slaughter, S.G. Prussin, H. Ohm, W. Rudolph, K.-L. Kratz; Nucl. Phys. A293 (1977) 410.

|12| K.-L. Kratz, H. Ohm, W. Rudolph, K. Sümmerer, M. Zendel, K.D. Wünsch, G. Jung, H. Wollnik, C. Ristori, J. Crançon; Proc. Int. Workshop on Gross Properties of Nuclei and Nuclear Excitations V, Hirschegg, Austria, AED-Conf. 77-017-35 (1977) 208; Annual Report 1976, Inst. f. Kernchemie, Univ. Mainz (1977) 37; Annex to the Annual Report, ILL Grenoble (1977) 32.

|13| H. Ohm, C. Ristori, K.-L. Kratz, W. Rudolph; Annual Report 1975, Inst. f. Kernchemie, Univ. Mainz (1976) 55.

|14| H. Ohm, K.-L. Kratz, C. Ristori, J. Crançon, K.D. Wünsch, G. Jung; Annual Report 1977, Inst. f. Kernchemie, Univ. Mainz (1978) 59; Annex to the Annual Report, ILL Grenoble (1977) 21.

|15| M. Zendel, H. Ohm, E. Stender, N. Trautmann; Annual Report 1976, Inst. f. Kernchemie, Univ. Mainz (1977) 10.

|16| A. Schröder, W. Ziegert, K.-L. Kratz, G. Nyman, L.C. Carraz, P.G. Hansen, B. Jonson, H.L. Ravn; Annual Report, 1978, Institut f. Kernchemie, Univ. Mainz (1979).
|17| G.W. Eccleston, G.L. Woodruff; Nucl. Sci. Eng. 62 (1977) 636.
|18| P.K. Ray, E.S. Kenney; Nucl. Instr. Methods 134 (1976) 559.
|19| P.K. Ray; contributed paper to RP 4.
|20| K.-L. Kratz; Contributed paper to RP 13 of the 2nd Advisory Group Meeting on Fission Product Nuclear Data (FPND)-1977.
|21| S. Shalev, J.M. Cuttler; Nucl. Sci. Eng. 51 (1973) 52.
|22| W.R. Sloan, G.L. Woodruff; Nucl. Sci. Eng. 55 (1974) 28.
|23| A.E. Evans, M.S. Krick; Nucl. Sci. Eng. 62 (1977) 652.
|24| D.R. Weaver, J.G. Owen, J. Walker; Contributed Paper to RP 4.
|25| J.B. Marion, J.L. Fowler; Fast Neutron Physics, Wiley, New York (1960).
|26| E. Finck; 'Nuclear Spectroscopy and Reactions', Part B, ed. J. Cerny, Academic Press, New York and London (1974).
|27| B. Zeitnitz; Proc. Int. Conf. on the Interactions of Neutrons with Nuclei, Lowell, USA (1976).
|28| P. Harihar; Nucl. Instr. Methods 127 (1975) 387.
|29| W.R. Sloan, G.L. Woodruff; Nucl. Instr. Methods 150 (1978) 253.
|30| E.F. Bennett, T.J. Yule; Report ANL-7763, Argonne National Laboratory (1971).
|31| P.L. Reeder; Report BNL-50844, Brookhaven National Laboratory (1978).
|32| K.H. Beckurts, K. Wirtz; Neutron Physics, Berlin (1964).
|33| G.I. Crawford, M. Asghar, S.J. Hall, J.D. Kellie, J. Crançon, J.P. Gautheron, C. Ristori, G. Bailleul, J.P. Boquet, J. Greif, H. Schrader, G. Siegert; Annex to the Annual Report, ILL Grenoble (1974) 10.
|34| G.I. Crawford, M. Asghar, S.J. Hall, J.D. Kellie, J. Crançon, J.P. Gautheron, C. Ristori, G. Bailleul, J.P. Bocquet, J. Greif, H. Schrader, G. Siegert; Fission Information Meeting and Workshop, ed. M. Asghar, ILL Grenoble (1974) 95.
|35| G.I. Crawford, S.J. Hall, K.-L. Kratz, W. Rudolph, M. Asghar, J. Crançon, C. Ristori; Annex to the Annual Report, ILL Grenoble (1975) 17.
|36| G.I. Crawford, M. Asghar; priv. communication (1976).
|37| G.I. Crawford, J.D. Kellie, S.J. Hall, K.D. Wünsch, E. Koglin, M. Asghar; Annex to the Annual Report, ILL Grenoble (1977) 57.

|38| S. Shalev, J. Cuttler; Trans. Am. Nucl. Soc. 14 (1971) 373.
|39| H. Franz, W. Rudolph, H. Ohm, K.-L. Kratz, G. Herrmann, F.M. Nuh, D.R. Slaughter, S.G. Prussin; Nucl. Instr. Methods 144 (1977) 253.
|40| Technion, Israel Institute of Technology.
|41| Seforad Applied Radiation Ltd., Emek Hayarden, Israel.
|42| H. Ohm, W. Rudolph, K.-L. Kratz; Nucl. Phys. A274 (1976) 45.
|43| A.E. Evans; priv. communication (1975).
|44| H. Ohm, W. Rudolph, K.-L. Kratz; Annual Report 1976, Inst. f. Kernchemie, Univ. Mainz (1977) 54.
|45| A.E. Evans, J.D. Brandenberger; Bull. Am. Phys. Soc. 23, No.8 (1978) 1056.
|46| R. Batchelor, R. Aves, T.H.R. Skyrme; Rev. Sci. Inst. 26 (1955) 1037.
|47| S. Greenberger, S. Shalev; Technion Haifa Report TNSD-R/407 (1969).
|48| G. Rudstam; The Swedish Research Councils' Laboratory Report LF-57 (1974).
|49| N. Trautmann, G. Herrmann; J. Radioanal. Chem. 32 (1976) 533.
|50| G. Rudstam, S. Shalev, O.C. Jonsson; Nucl. Instr. Methods 120 (1974) 333.
|51| K.-L. Kratz, W. Rudolph, H. Ohm, H. Franz, M. Zendel, G. Herrmann, S.G. Prussin, F.M. Nuh, A.A. Shihab-Eldin, D.R. Slaughter, W. Halverson, H.V. Klapdor; Nucl. Phys. A, in press.
|52| K.-L. Kratz, W. Rudolph, H. Ohm, H. Franz, G. Herrmann, C. Ristori, J. Crançon, M. Asghar, G.I. Crawford, F.M. Nuh, S.G. Prussin; Phys. Lett. 65B (1976) 231.
|53| K.-L. Kratz; Habilitationsschrift, submitted to Univ. Mainz (1978).
|54| G.I. Crawford, S.J. Hall, J.D. Kellie, M. Asghar, R. Decker, K.D. Wünsch; Annex to the Annual Report, ILL Grenoble (1977) 61.
|55| A. Schröder, H. Ohm, K. Sümmerer, U. Tharun, W. Ziegert, K.-L. Kratz, K.D. Wünsch, G. Jung, J. Crançon, C. Ristori, S.G. Prussin; Proc. Int. Workshop on Gross Properties of Nuclei and Nuclear Excitations VII, Hirschegg, Austria (1979); Annual Report 1978, Inst. f. Kernchemie, Univ. Mainz (1979); Annex to the Annual Report, ILL-Grenoble (1978).
|56| A.A. Shihab-Eldin, F.M. Nuh, W. Halverson, S.G. Prussin, W. Rudolph, H. Ohm, K.-L. Kratz; Proc. 3rd Int. Conf. on Nuclei far from Stability, Cargèse 1976, CERN-Report 76-13 (1976) 317; Phys. Lett. 69B (1977) 143.
|57| E.H. Auerbach, F.G.J. Perey; Report BNL-765, Brookhaven National Laboratory (1962).

|58| N. Glendenning; OPTIC-code, priv. communication (1976).

|59| K.-L. Kratz, H. Ohm, A. Schröder, S.G. Prussin, C. Ristori, G. Jung, K.-D. Wünsch; Proc. Int. Workshop on Gross Properties of Nuclei and Nuclear Excitations VII, Hirschegg, Austria (1979); Report NEANDC(E)-192 U, Vol. 5 (1978) 72; Annual Report 1978, Inst. f. Kernchemie, Univ. Mainz (1979).

|60| A.C. Pappas, T. Sverdrup; Nucl. Phys. 188 (1972) 48.

|61| O.K. Gjøtterud, P. Hoff, A.C. Pappas; Nucl. Phys. A303 (1978) 281 and 295.

|62| J.C. Hardy, B. Jonson, P.G. Hansen; Nucl. Phys. A305 (1978) 15.

|63| S.G. Prussin, Z.M. Oliveira, K.-L. Kratz; Nucl. Phys.,in press.

|64| K. Takahashi, M. Yamada; Progr. Theoret. Phys. (Kyoto) 41 (1969) 1470.

|65| K. Takahashi; Progr. Theoret. Phys. (Kyoto) 47 (1972) 1500.

|66| A. Gilbert, A.G.W. Cameron; Can. J. Phys. 43 (1965) 1466.

|67| M. Blann; Ann. Rev. of Nucl. Sci., Vol. 25, ed. E. Segre, p. 123 (1975).

|68| W. Ziegert, A. Schröder, H. Ohm, K.-L. Kratz, G. Nyman, L.C. Carraz, P.G. Hansen, B. Jonson, H.L. Ravn; Annual Report 1978, Inst. f. Kernchemie, Univ. Mainz (1979).

|69| P.L. Reeder, J.F. Wright, L.J. Alquist; Phys. Rev. C15 (1977) 2098.

|70| H. Franz; Doctoral Dissertation, Univ. Mainz (1972).

|71| G. Fieg, J. Nucl. Energy 26 (1972) 585.

|72| G.R. Keepin, T.F. Wimett, R.K. Zeigler; Phys. Rev. 107 (1957) 1044.

|73| G. Rudstam; Review Paper 3 of this meeting.

|74| J.G. Cunninghame; Proc. of the 2nd Advisory Group Meeting on Fission Product Nuclear Data (FPND)-1977, IAEA-213, Vol. I (1978) 251.

|75| H.-D. Schüssler, W. Grimm, M. Weber, U. Tharun, H.O. Denschlag, G. Herrmann; Nucl. Instr. Methods 73 (1969) 125.

|76| H.J. Kreiner; Nucl. Instr. Methods 141 (1977) 119.

|77| H. Menke, N. Trautmann, W.J. Krebs; Kerntechnik 17 (1975) 281.

|78| S. Shalev, J.M. Cuttler, Y. Dagan, S. Greenberger, D. Barak; Technion Haifa Report TNSD-R/412 (1969).

|79| P.G. Hansen; Adv. Nucl. Phys. 7 (1973) 159.

|80| J.C. Hardy; Proc. 3rd Int. Conf. on Nuclei far from Stability, Cargèse 1976, CERN-Report 76-13 (1976) 267.

|81| B. Jonson, E. Hagberg, P.G. Hansen, P. Hornshøj, P. Tidemand-Petersson; Proc. 3rd Int. Conf. on Nuclei far from Stability, Cargèse 1976, CERN-Report 76-13 (1976) 277.

|82| A.M. Lane, R.G. Thomas, E.P. Wigner; Phys. Rev. 98 (1955) 693.

|83| P.A. Egelstaff; Proc. Phys. Soc. 71 (1958) 910.

|84| K. Takahashi, M. Yamada, T. Kondoh; Atomic Data and Nucl. Data Tables 12 (1973) 101.

|85| H.V. Klapdor; Proc. 3rd Int. Conf. on Nuclei far from Stability, Cargèse 1976, CERN-Report 76-13 (1976) 311; Phys. Lett. 65B (1976) 35.

|86| H.V. Klapdor, C.O. Wene; subm. to J. Phys.

|87| P.O. Martinsen, J. Randrup; Nucl. Phys. A195 (1972) 26; A207 (1973) 209.

|88| K. Ikeda, S. Fujii, J.I. Fujita; Phys. Lett. 2 (1962) 169 and 3 (1963) 271; Phys. Rev. 133B (1964) 549 and 176 (1968) 1277.

|89| D.F. Petersen, C.J. Veje; Phys. Lett. 24B (1967) 449.

|90| J.I. Fujita, Y. Futami, K. Ikeda; Progr. Theoret. Phys. 38 (1967) 107.

|91| I.S. Towner, E.K. Warburton, G.T. Garvey; Annals of Physics 66 (1971) 674.

|92| H.Ejiri; Nucl. Phys. A166 (1971) 594 and A178 (1972) 350.

|93| C. Gaarde et al.; Nucl. Phys. A143 (1970) 497 and A184 (1972) 241.

|94| H.V. Klapdor et al.; Nucl. Phys. A223 (1974) 365, A245 (1975) 133 and A263 (1976) 477.

|95| Y.W. Naumow, O.E. Kraft; Sov. J. Part. Nuclei 6 (1976) 361.

|96| R.R. Doering, A. Galonsky, D.M. Patterson, G.F. Bertsch; Phys. Rev. Lett. 35 (1975) 1691.

|97| K.D. Wünsch, R. Decker, H. Wollnik, J. Münzel, G. Siegert, G. Jung, E. Koglin; Z. Physik A288 (1978) 105, and priv. communication.

|98| W.J. Halverson; Masters Thesis, Univ. of California, Berkeley (1975), and S.G. Prussin et al.; to be published.

|99| D.J. Vieira, R.A. Gough, J. Cerny; Phys. Rev. C19 (1979) 177.

|100| C. Ristori, J. Crançon, K.D. Wünsch, G. Jung, R. Decker, K.-L. Kratz; Z. Physik, in press.

|101| W. Rudolph, K.-L. Kratz; Z. Physik A281 (1977) 269.

|102| F.K. Wohn, K.D. Wünsch, H. Wollnik, R. Decker, G. Jung, E. Koglin, G. Siegert; Phys. Rev. C17 (1978) 2185.

|103| T. Kondoh, M. Yamada; Suppl. Progr. Theoret. Phys. 60 (1976) 136.

|104| S.G. Prussin, F.M. Nuh, R.A. Meyer; priv. communication (1978).
|105| T. Yoshida; Nucl. Sci. Eng. 63 (1977) 376.
|106| H.V. Klapdor, C.O. Wene, I.N. Isosimow, Y.W. Naumow, Phys. Lett. 78B (1978) 20.
|107| W. Hillebrandt, K. Takahashi, T. Kodama; Astron. and Astrophys. 52 (1976) 63.
|108| J.B. Blake, D.W. Schramm; Ap. J. 209 (1976) 846.

Delayed neutron yield and decay constants for thermal neutron induced fission of ^{235}U.

S. Synetos and J.G. Williams
University of London Reactor Centre
Imperial College, University of London.

Abstract

Delayed neutron yield and decay constants were measured using foils of ^{235}U irradiated in a thermal column of the University of London Reactor. The samples were transferred pneumatically to and from the irradiation position where a constant thermal neutron flux was maintained. After each irradiation the delayed neutron emission rate was measured in a detector consisting of a water bath containing BF_3 counters. The geometry of the detector was chosen to minimize the neutron energy dependence of its response, and the efficiency of the detector was measured using a calibrated Am/Li source.

The number of fissions in the foils was measured using a gamma spectrometer to determine their ^{140}La activity, relative to that of calibration foils irradiated in an absolute fission chamber.

The measured delayed neutron decay curve was fitted to the sum of five exponential groups by the least squares method. The total yield of the five groups was 0.0151 ± 0.0007 delayed neutrons per fission. No sixth group was observed because of the transfer time of 380 ms before counting commenced. When the six group parameters of Keepin and Wimett were used together with the total counts observed in this experiment the total yield found for the six groups was 0.0156 ± 0.0010, where the difference from the previous value is attributable to the presence of the sixth group.

The period-reactivity relationship was calculated for positive periods between 0.2 and 900 seconds using both the five group data and the six group data. These were found to give equal reactivities within 1% except for periods less than one second.

Introduction

Measurements of delayed neutron emission rates from unseparated fission products provide the basis for calculations of time dependent reactor performance[1]. In addition one of the two commonly used methods of establishing reactivity worth in reactors, and the only method usually available in power reactors relies on a knowledge of delayed neutron parameters[2].

Recently knowledge of yields and decay constants of individual delayed neutron precursors has improved[3] and it is possible to explain the main features of the neutron emission from unseparated fission products by means of these data. It seems unlikely, however, that such data will replace the delayed neutron parameters obtained from measurements of gross delayed neutron emission rates in reactor physics applications. On the other hand the delayed neutron parameters for unseparated fission products do provide a useful check on the accuracy and consistency of more detailed but less precise information obtained from separate isotopes.

The parameters used for reactor calculations usually represent the delayed neutron emission by means of six groups, each characterized by a single yield and decay constant, so that twelve parameters are needed for each fissioning isotope. Often these are obtained by combining the data from thermal and fast neutron induced fission, since no difference in parameters has been conclusively demonstrated for incident neutron energies below the threshold for second chance fission[4]. The most recent evaluation of delayed neutron data for reactor physics[5] does state that differences between measured delayed neutron yields from thermal and fast neutron induced fission are statistically significant, but this may be due to the shortage of recent measurements using thermal neutrons.

The use of six groups to describe delayed neutron decay data has followed the practice of Hughes et al[6] and Keepin and Wimett[7], although other measurers have reported data in four or five groups. For a particular set of experimental data the only proper test of how many parameters should be used is whether or not a significant improvement in the fit to the data can be achieved by increasing the number. Since this test will yield different results for different experiments, depending on their statistical precision and on the time domain covered, it should not be surprising that values are reported for a variety of numbers of groups. A practical difficulty does arise, however, for the evaluator who wishes to make use of more than one measurement to obtain a recommended set of parameters, since it is not obvious how to compare parameters when the number of groups is different. Indeed, even for sets of results reported using the same number of groups it is by no means clear that averaging the parameters is a justifiable procedure. Probably because of these difficulties in combining data, it has been usual to recommend only the data of Keepin and Wimett to describe the time dependence of delayed neutron emission. These relative yields and decay constants are often combined with values of total yield obtained by including data from other sources[5].

The present experiments were undertaken with the aims of measuring the total delayed neutron yield from ^{235}U thermal neutron fission to an accuracy of approximately ±4% (1σ), which is better than that of any existing measurements using thermal neutrons, and similar to that of recent measurements with fast neutrons[8], and of measuring the decay parameters sufficiently well to enable the period-reactivity relationship to be calculated to similar accuracy.

Experimental Arrangements

Foils of ^{235}U were irradiated for ten minutes in a steady thermal neutron flux in a thermal column of the University of London Reactor. Samples were transferred pneumatically to and from the irradiation position. After each irradiation the delayed neutron emission rate was measured in a detector consisting of a water tank containing BF_3 counters. The arrangement is shown schematically in Fig. 1. The count rate was recorded in 2048 multiscaler channels during the first 380 seconds after the end of each irradiation. The samples arrived at the detector after a flight time of 380 ms. Because of this delay the sixth group of Keepin and Wimett would not be detectable in this experiment, but this group has no important effect on the period-reactivity relationship in thermal reactors.

The samples used in the experiment consisted of metal foils of 7.5 mm diameter and weighing approximately 35 mg. The material was 95.54% ^{235}U. Experiments were done using one, three or ten of these foils wrapped in aluminium. The number of fissions was only determined for the experimental runs in which single foils were used. The total delayed neutron yield was determined from the total delayed neutron counts in these runs, together with decay parameters determined from the combined data of runs using also three and ten foils.

The irradiation position was at the centre of a spherical cavity in one of the graphite thermal columns. The neutron flux at this position was approximately $10^8 cm^{-2} s^{-1}$ with a gold cadmium ratio of 700. The angular distribution of the flux was known to be of the form $\phi(\mu) = \phi(o)\ (1+a\mu)$, where μ is a direction cosine measured in the radial direction from the reactor core and a is a constant. Under such conditions the self shielding correction for a foil is the same as it would be in an isotropic flux. The neutron temperature at the irradiation position was not measured, but was assumed to be 300 ± 10°K.

The samples were mounted in polythene capsules with internal aluminium spacers. The total weight of the capsule was approximately 12g, which was the minimum compatible with adequate strength to sustain the decelleration at either end of the pneumatic transfer. To obtain adequate counting statistics it was essential to perform approximately 20 sequences of irradiation and decay in one experimental run. Irradiation and decay times were ten minutes each in all runs. The capsule was arrested at either end of its flight in an aluminium tube .5 mm thick and 26 mm O.D. An outer concentric aluminium tube of 44.5 mm O.D. was used to carry the gas supply for the return flight. At the detector position the two concentric aluminium tubes were immersed in a cylindrical water tank 650 mm deep and 580 mm in diameter. The sample was arrested at the centre of this tank for counting. (See Fig. 1)

The Neutron Detector System

The neutron detector consisted of one or two BF_3 counters placed in cylindrical aluminium tubes of outer diameter 26 mm, and immersed in the water tank parallel to the axial tube in which the sample was carried. The detectors used were of active length 310 mm and 25 mm O.D. filled with 96% enriched boron-10 trifluoride at a pressure of 70 cm Hg. The supplier was 20th Century Electronics Ltd., and their type number was 31 EB 70 G. The counters were insulated externally using polythene tape and inserted in their aluminium tubes so that the centre of their active volume was at the same height as the arrest position of the sample. The radial distance of the centre of the counters from the centre of the samples was 74 mm. This distance was chosen on the basis of ANISN[9] calculations as the one which would provide the least energy dependence in the neutron efficiency in the range 50 keV to 2 MeV.

The BF_3 counters were operated at 2.4 kV which gives a gas multiplication of about 40. Pulses were amplified using a differentiating amplifier with a time constant of 0.1 μs. A pulse height discriminator was used to reject pulses below about half the height of those at the peak of the pulse height distribution. The threshold setting was chosen so that the count rate was exactly halved when the threshold voltage was doubled. This method of setting provides good reproducibility and insensitivity to drifts of amplifier gain or E.H.T. voltages. The lack of gamma sensitivity was checked by showing that the pulse height distribution obtained from delayed neutron measurements was the same as that obtained using an Am/Be source which is not a strong gamma emitter. For some measurements two BF_3 counters were connected together to a single channel of electronics, but for the calibration of the detector only one BF_3 counter was used, and the same single counter was used in all the delayed neutron runs used to establish the absolute yield. The second counter remained in position in the detector at all times, however. The reason only one counter was used in the most critical runs was that it was then easier to ensure reproducibility of the electronic settings.

The output of the discriminator was connected to a scaler, used to record total counts and for background measurements, and to a LABEN 8000 multichannel analyser used as a multiscaler. The multiscaler was triggered using a pulse from a control circuit of the transfer system. The delay between this trigger and the actual movement of the capsule from the irradiation position was determined in a calibration experiment in which a small gamma source was placed in the capsule and a NaI gamma detector was placed near the irradiation end of the transfer system. By multiscaling the pulses from the gamma detector it was possible to determine the time the capsule left the irradiation position. In the delayed neutron experiments the samples had to pass through the thermal column for a distance of approximately 1m before leaving the neutron flux, so this portion of the flight tube was surrounded with cadmium. The analyser was capable of using up to three different channel widths during a single run, with a total of 4096 channels. The channel widths chosen were 500 at 10 ms, followed by 500 at 80 ms, followed by 1048 at 320 ms. Thus a total of 2048 channels were used, covering a total counting time of 380s. In the analysis of the data each channel count was treated as a measurement of count rate at the time corresponding to the centre of the channel. The error in this approximation is negligible for the channel widths used.

The dead time of the counting system was measured using the two source method. A 1Ci Am/Be source and a 10 μg ^{252}Cf source were used in positions near enough to the BF_3 counter to provide high count rates, without being close enough to interfere, by scattering, with each other. This was done for a number of source positions and count rates, and the dead time was found to be 1.50 ± 0.09 μs. The highest count rate used in the experiment was a few thousand counts per second, so that the uncertainty introduced because of the uncertainty in the dead time correction was very small.

Calibration of the Neutron Detector

A calibrated Am/Li neutron source was used for the determination of the detector efficiency. This source was hired from the National Physical Laboratory where it was calibrated, using a manganese sulphate bath, with an accuracy of ± 0.5%. The reported source strength was 2.084×10^5 neutrons per second. The source was fabricated at the Radiochemical Centre, Amersham. It is made of a compacted mixture of americium oxide, nominally 5Ci, with lithium hydride, doubly encapsulated in stainless steel. The dimensions are 30 mm diameter and 60 mm height and the capsule is designated type X14. This type of source was chosen because the spectrum of a similar one has been measured by Werle[10] using proton recoil proportional counters, and the reported spectrum is very similar to that of delayed neutrons.

The Am/Li source was placed in the delayed neutron detector so that the centre of its active volume was at the same position as the counting position of the ^{235}U foils. The count rate of the detector was measured several times and the count rate from a 30 mCi Am/Be source was also measured before and afterwards. This Am/Be source was then used to check the detector settings each time a delayed neutron measurement was made.

A number of corrections have to be made to the detector efficiency obtained using the Am/Li source, and the uncertainty associated with each of these must be estimated. These corrections and uncertainties arise as follows:

(a) Volume correction

The Am/Li source is much larger than the foils which constitute the delayed neutron source. Since the ^{235}U foils can be regarded as effectively point sources we need to correct the efficiency of the detector measured with the Am/Li source to find the efficiency for a point source. Since we could not have a small Am/Li source of adequate strength we used a small ^{252}Cf source to estimate this correction by measuring the detector efficiency when the ^{252}Cf source was at the centre of the system and when it was displaced radially and axially from the centre. By numerically averaging these results over a volume equal to the volume of the Am/Li source we obtained the efficiency that the detector would have for a ^{252}Cf source of the same size as the Am/Li source. This was found to be 1.4% smaller than that measured with the small ^{252}Cf source at the centre of the system. The Am/Li source has a different spectrum from the ^{252}Cf source but since the correction is a small one we feel justified in assuming that the correction for the Am/Li source is the same, with an uncertainty equal to 50% of the correction. Thus we apply a correction factor of 1.014 ± .007 to the measured efficiency.

(b) Neutron Self Absorption

The source strength reported by the N.P.L. is the emission rate of the source in vacuo, obtained after correction for neutron self absorption occurring in the manganese sulphate bath. When the source is placed in the delayed neutron detector some of the neutrons will scatter back into the source and be absorbed. This correction was estimated by calculating the number of neutrons absorbed and their effect on the detector efficiency using ANISN. The reduction was found to be 1.0%, so a correction factor of 1.010 ± .005 was applied to the measured efficiency.

Neutron self absorption and multiplication in the ^{235}U foils was negligible.

(c) Anisotropy of neutron emission

Because of the size and shape of the Am/Li source it does not emit neutrons equally in all directions. Data were supplied by A.G. Bardell of the N.P.L. on the relative emission rates measured at 10^{o} intervals from the cylindrical axis of the source. These figures were used in an ANISN calculation to find the difference between the efficiency for an isotropic source from that using the measured angular distribution. The correction factor was 0.998. Because the correction is so small no uncertainty was assigned.

(d) Energy spectrum effects

Because the detection efficiency is not independent of neutron energy we need to correct the measured detection efficiency to account for the difference between the spectra of neutrons from the Am/Li source and of delayed neutrons. Three types of uncertainty also need to be considered: that due to the uncertainty of the Am/Li neutron spectrum, that due to the uncertainty of the delayed neutron spectrum, and that due to the uncertainty of the detector response function.

The detector response function calculated by ANISN was subject to considerable uncertainty due to the approximations introduced in modelling the detector in a one dimensional geometry. In order to check the response function the efficiency of the detector to ^{252}Cf neutrons was measured in order to find the ratio of this efficiency to that for Am/Li neutrons. This ratio was found experimentally to be 0.75 instead of 0.93 which was the value obtained from the ANISN calculation. An adjusted calculation was then made with the effective moderator thickness changed by trial and error to reproduce the observed ratio of 0.75 for the ratio of the ^{252}Cf to Am/Li efficiencies. When the delayed neutron spectrum reported by Saphier et al[11] was used the efficiency obtained using the original ANISN calculation was 1.011 times that for the Am/Li source. The adjusted ANISN calculation gave 1.008 for the same ratio, a difference of only 0.3% which is so small because of the close similarity between the Am/Li spectrum of Werle and the delayed neutron spectrum recommended by Saphier et al. If instead of the Saphier spectrum the much softer spectrum reported by Eccleston and Woodruff[12] is used the unadjusted ANISN calculation gives a ratio of 0.979 for the delayed neutron efficiency relative to the Am/Li efficiency and the adjusted ANISN calculation gives a ratio of 1.022. The uncertainty due to the uncertainty of the Am/Li spectrum as reported by Werle was also calculated and was found to be ± 0.25%. In view of these results it was decided to apply no correction to the Am/Li efficiency and to assign an uncertainty of ± 2.2% to the detector efficiency due to the combined effect of uncertainties in the neutron spectra and the detector response function.

The corrections and uncertainties found for the detector efficiency are summarized in Table 1.

The Fission Measurements

The number of fissions in the ^{235}U foil during an experimental run was found by measuring the ^{140}La activity relative to that in a calibration foil irradiated in an absolute ionisation chamber.

The ^{140}La activity was measured about 12 days after irradiation, by which time the ^{140}La activity is equal to that of its parent ^{140}Ba with a half life of 12.789 days. This half life is sufficiently long that the activity is a good integrating monitor of fissions produced during the period (up to seven hours) of an experimental run. A Ge(Li) spectrometer was used to find the intensity of the 1596 keV photopeak. Foils were counted with their aluminium wrappings, which acted as catchers of fission products leaving the surface of the foils.

The calibration foils were irradiated inside a demountable parallel plate fission chamber, where they were positioned close behind the centre of a thin 20 mm diameter ^{235}U deposit of known mass. The irradiation position was the same as that used in the delayed neutron measurements, with the pneumatic transfer system removed. The flux gradient in this position was known to be small and in the direction parallel to the planes of the foil and deposit. The fission rate in the deposit was determined by counting ionization pulses and correcting in the usual way[8] for undetected fissions due to non zero discriminator bias and fission fragment absorption in the deposit. Counts were also made when no calibration foil was in the chamber, and no difference in count rate, relative to a monitor counter, was found. The deposit used was one of a series intercompared with NBS deposits and its mass was deduced from this intercomparison[8].

The fission rate in the calibration foil was deduced from that found in the deposit, after correcting for self shielding in the calibration foil. The calibration foil was similar to the ones used in the delayed neutron measurements, having a thickness of 73 mg cm^{-2}. The correction was found using the third order exponential integral[13] and an absorption cross section of 673.5b, corresponding to a neutron temperature of 300°K. The effect of scattering was negligible. The correction was found to be 0.81 ± 0.01.

The number of fissions in the calibration foil being known, the number of fissions in the foils used in the delayed neutron measurements was found directly from the relative measurements of ^{140}La activity. Since the two measurements were not made on the same day a ^{137}Cs source was used to check the stability of the gamma counting system.

A summary of uncertainty contributions in the fission determinations is given in Table 2.

Derivation of Decay Parameters

The delayed neutron count rate at time t after the end of a saturation irradiation is given by

$$C(t) = \varepsilon \cdot \frac{F}{T} \cdot \nu . \sum_i \beta_i \exp(-\lambda_i t) + u(t)$$

where
- ε = the detector efficiency
- F = the number of fissions
- T = the duration of the irradiation
- ν = the number of neutrons per fission
- β_i = the delayed neutron fraction for the i^{th} group
- λ_i = the decay constant of the i^{th} group
- $u(t)$ = the statistical discrepancy of the count rate from its expectation value.

If we measure $C(t)$ at many times t_j then

$$C_j = \varepsilon . \frac{F}{T} \cdot \nu . \sum_i \beta_i \cdot \exp(-\lambda_i t_j) + u_j \quad ,$$

where the subscript j refers to values at time t_j and if we can estimate σ_j^2, the variance of u_j, from the usual laws of counting statistics, then we wish to find the values of $\nu.\beta_i$ and λ_i which minimize

$$\chi^2 = \sum_j (u_j^2/\sigma_j^2) = \sum_j \frac{1}{\sigma_j^2} . \left[C_j - \varepsilon . \frac{F}{T} \cdot \sum_i \nu.\beta_i . \exp(-\lambda_i t_j)\right]^2$$

To find the relative yields of the delayed neutron groups, α_i, and the group constants λ_i, the count rates C_j, corrected for background and dead time, were obtained from the sum of many runs in which one, three or ten foils were irradiated. Because the total counts accumulated for the latest channels was less than 100, these channels were combined in groups of 8 reducing the total number of data points to 1334. This was done so that σ_j, the standard deviation on the counts, could be estimated using the square root of the counts in the usual way.

Since the number of fissions in all the runs used was not known the function minimized was actually

$$\chi^2 = \sum_j \frac{1}{\sigma_j^2} \cdot \left[C_j - N. \sum_i \alpha_i \cdot \exp(-\lambda_i t_j)\right]^2$$

where N is an arbitrary normalizing constant. The solution was found for the values of $N\alpha_i$ and λ_i. The values of α_i were subsequently deduced by setting $N = \sum_i N\alpha_i$, so that $\sum_i \alpha_i = 1$.

The minimization made use of the subroutine E04 GAF of the NAG library[14], which is based on the Marquardt technique[15]. Five groups of delayed neutrons were fitted using as a starting guess the values for the first five of Keepin and Wimett's groups. Other starting guesses were also tried and these always led to the same results. Six group fitting was also tried, but these did not produce smaller χ^2 values and two of the decay constants always came out nearly the same as each other.

The covariance matrix of the ten parameters was printed by the program and it was found that the non-diagonal elements were all very small compared with the diagonal elements, so the parameters were essentially uncorrelated. This is so for the values of λ_i and $N\alpha_i$, but not for the parameters α_i, because correlations are introduced by the normalization which makes these sum to unity. The solution of this problem is as follows.

Given independent quantities x_i and their diagonal covariance matrix $|X_{ij}|$, we have to find α_i and their covariance matrix $|A_{ij}|$, where

$$\alpha_i = x_i / \sum_i x_i = x_i / N$$

and N is the normalizing value $= \sum_i x_i$

So $$\frac{\partial \alpha_i}{\partial x_i} = 1/\Sigma_i x_i - x_i/(\Sigma_i x_i)^2 = 1/N - x_i/N^2 \qquad (1)$$

And $$\left|\frac{\partial \alpha_i}{\partial x_{i'}}\right|_{i' \neq i} = -x_i/(\Sigma_i x_i)^2 = -x_i/N^2 \qquad (2)$$

Now $A_{ij} = \langle \delta\alpha_i \cdot \delta\alpha_j \rangle$, where the brackets < > stand for the expectation value.

$$\delta\alpha_i = \Sigma_{i'} \frac{\partial \alpha_i}{\partial x_{i'}} \delta x_{i'}$$

and $$\delta\alpha_j = \Sigma_{j'} \frac{\partial \alpha_j}{\partial x_{j'}} \delta x_{j'}$$

So $$A_{ij} = \Sigma_{i'} \Sigma_{j'} \frac{\partial \alpha_i}{\partial x_{i'}} \cdot \frac{\partial \alpha_j}{\partial x_{j'}} \cdot \langle \delta x_{i'} \cdot \delta x_{j'} \rangle$$

$$= \Sigma_{i'} \Sigma_{j'} \frac{\partial \alpha_i}{\partial x_{i'}} \cdot \frac{\partial \alpha_j}{\partial x_{j'}} \cdot X_{i'j'}$$

Substituting from (1) and (2) and assuming $X_{i'j'} = 0$ if $i' \neq j'$ we find

if $i \neq j$, $$A_{ij} = -\frac{1}{N^3} x_j X_{ii} - \frac{1}{N^3} x_i X_{jj} + \frac{1}{N^4} x_i x_j \Sigma_\kappa X_{\kappa\kappa}$$

and $$A_{ii} = \frac{1}{N^2} X_{ii} - \frac{2}{N^3} x_i X_{ii} + \frac{1}{N^4} x_i^2 \Sigma_\kappa X_{\kappa\kappa}$$

These values were calculated and used to find the correlation matrix $|r_{ij}|$ such that

$$r_{ij} = A_{ij}/(A_{ij}^{\frac{1}{2}} \cdot A_{jj}^{\frac{1}{2}}),$$

and the standard deviation $\sigma_i = (A_{ii}^{\frac{1}{2}})$.

The results of the analysis described above are shown in Table 3 where the Keepin and Wimett 6 group data are also shown for comparison. The comparison shows that although the parameters for the first two groups agree the rest do not. This is not surprising since we know that these groups do not necessarily have any physical meaning except when used to calculate the gross neutron emission rates or other desired functions of these such as the period-reactivity relationship. We note that the uncertainties given in Table 3 are generally smaller for the present data than for the Keepin and Wimett data and that the uncertainty information for the latter is incomplete, since we do not know how the parameters are correlated, although we may be sure that significant correlations do exist, at least for the relative yields. On the other hand the present data lack information on the sixth group, and this may be significant for very short reactor periods.

Total Delayed Neutron Yield

The total delayed neutron yield was obtained from the total counts recorded over the period during which the decay was measured, using only the data from the single foil runs for which the number of fissions in the sample was known.

The number of counts expected in a time interval t_1 to t_2 after a saturated irradiation is given by

$$C_{12} = \varepsilon \cdot \frac{F}{T} \cdot y \int_{t_1}^{t_2} \sum_i \alpha_i \exp(-\lambda_i t)dt$$

where $y = \nu . \sum_i \beta_i$, is the total delayed neutron yield per fission.

$$\therefore \quad C_{12} = \varepsilon \cdot \frac{F}{T} \cdot y \sum_i \frac{\alpha_i}{\lambda_i} (\exp(-\lambda_i t_1) - \exp(-\lambda_i t_2))$$

$$\therefore \quad y = T \cdot C_{12}/\varepsilon \cdot F \cdot \sum_i \frac{\alpha_i}{\lambda_i} (\exp(-\lambda_i t_1) - \exp(-\lambda_i t_2))$$

The times t_1 and t_2 were .380s and 380s respectively. The values α_i and λ_i used were those derived from the decay as explained in the previous section. The uncertainty calculated for y took into account the uncertainties in the total counts, σ_c , the detector efficiency, σ_ε , the number of fissions, σ_F , and the decay parameters, $\sigma_{\alpha i}$ and $\sigma_{\lambda i}$. For the decay parameters it was also necessary to take account of the correlations, r_{ij} , of the relative yield, and these have the effect of reducing the uncertainty in y because the off diagonal elements are predominantly negative.

The standard deviation, σ_y , of the yield was given by

$$(\sigma_y)^2 = (\frac{\partial Y}{\partial C} \cdot \sigma_c)^2 + (\frac{\partial Y}{\partial \varepsilon} \cdot \sigma_\varepsilon)^2 + (\frac{\partial Y}{\partial F} \cdot \sigma_F)^2 + \sum_i (\frac{\partial Y}{\partial \lambda_i} \cdot \sigma_{\lambda i})^2$$

$$+ \sum_i \sum_j (\frac{\partial Y}{\partial \alpha_i} \cdot \frac{\partial Y}{\partial \alpha_j} \cdot r_{ij} \cdot \sigma_{\alpha i} \cdot \sigma_{\alpha j})$$

No uncertainty was assigned to the value of T , the irradiation ti (600 seconds) or of t_1 and t_2, because the contribution of each of these was negligible. The size of each of the contributions to the total uncertainty is given in Table 4.

The value obtained for the delayed neutron yield was,

$y = 0.0151 \pm .0007$ (4.6%), for five groups.

This value must be qualified by the statement that it refers to the total yield of the five delayed neutron groups detected and should be used together with the five group parameters reported in the previous section. It may not be directly compared with values for total yield of the six Keepin and Wimett groups. While it is true that the values of the yield and the five group parameters reported above are the best representation of the results of the present experiments, it may arise that in combining the present results with other data it will be convenient to use the six group parameters of Keepin and Wimett. For this reason we have calculated a second value of the total yield, using this time the Keepin and Wimett group constants shown in Table 3. The result was

$$y_6 = 0.0156 \pm .0010 \ (6.6\%), \text{ for six groups.}$$

The increase of 3.3% from the previous value is attributable to the inclusion of group six. The difference is not quite equal to the 4.4% increse one would find by simply adding the group six yield, since presumably part of the contribution from group six has been accounted for in the five group parameters. The last value of the yield is the one which should be used with the six group parameters. In calculating the uncertainty in this value the uncertainties in the six group parameters shown in Table 3 were used and the relative yields were treated as uncorrelated.

The Period-Reactivity Relationship

The most stringent requirement for delayed neutron yield and decay data arises in their use, via the period-reactivity relationship, to establish the reactivity scale in operating power reactors. In addition to the type of data reported here it is necessary to calculate, from a knowledge of the delayed neutron spectra, importances of delayed neutrons of each group relative to prompt neutron importance. The importance weighting factors, w_i , obtained from such calculations are normally slightly greater than one for thermal reactors. For the purpose of comparison between the present five group data and the six group data of Keepin and Wimett we will here set those weighting factors to unity and also neglect the effect of prompt neutron lifetime. The period-reactivity relationship is then:

$$\rho = \frac{y}{\nu} \sum_i \frac{\alpha_i}{1 + \lambda_i T}$$

Values of this function are given in Table 5 for the five group parameters and yield measured in this work. We have also calculated the reactivities using the Keepin and Wimett six group parameters together with our yield value obtained using these. The differences between these two sets of results are remarkably small and show that the five group parameters reported here are essentially equivalent to Keepin and Wimett's six group parameters except for reactor periods of less than one second.

Conclusions

The measurements reported here have resulted in values of the yield and decay parameters of delayed neutrons from ^{235}U thermal neutron fission in good agreement with the values of Keepin and Wimett reported twenty two years ago, although the precision of the present values is somewhat better.

Only five groups of delayed neutrons were observed because of a delay of 380 ms before counting commenced. The total yield of the five groups was found to be 0.0151 ± 0.007 delayed neutrons per fission.

When the six group parameters of Keepin and Wimett were used the total yield of these six groups was found to be 0.0156 ± 0.0010 delayed neutrons per fission. This is the value which should be used in any future evaluation of yield based on six group parameters.

The period reactivity relation arising from the measured yield was calculated using both the five group decay parameters discovered here and the six group parameters of Keepin and Wimett. The results were the same within 1% for positive reactor periods equal to or greater than one second. It is believed that the present experimental results do very nearly meet the present target accuracies[16] for the calculation of reactivities in thermal reactors, so far as this isotope is concerned.

Acknowledgement

The authors wish to express their appreciation of the work of the Operating Staff and other colleagues at the University of London Reactor Centre, and of Mr. A.G. Bardell at the National Physical Laboratory.

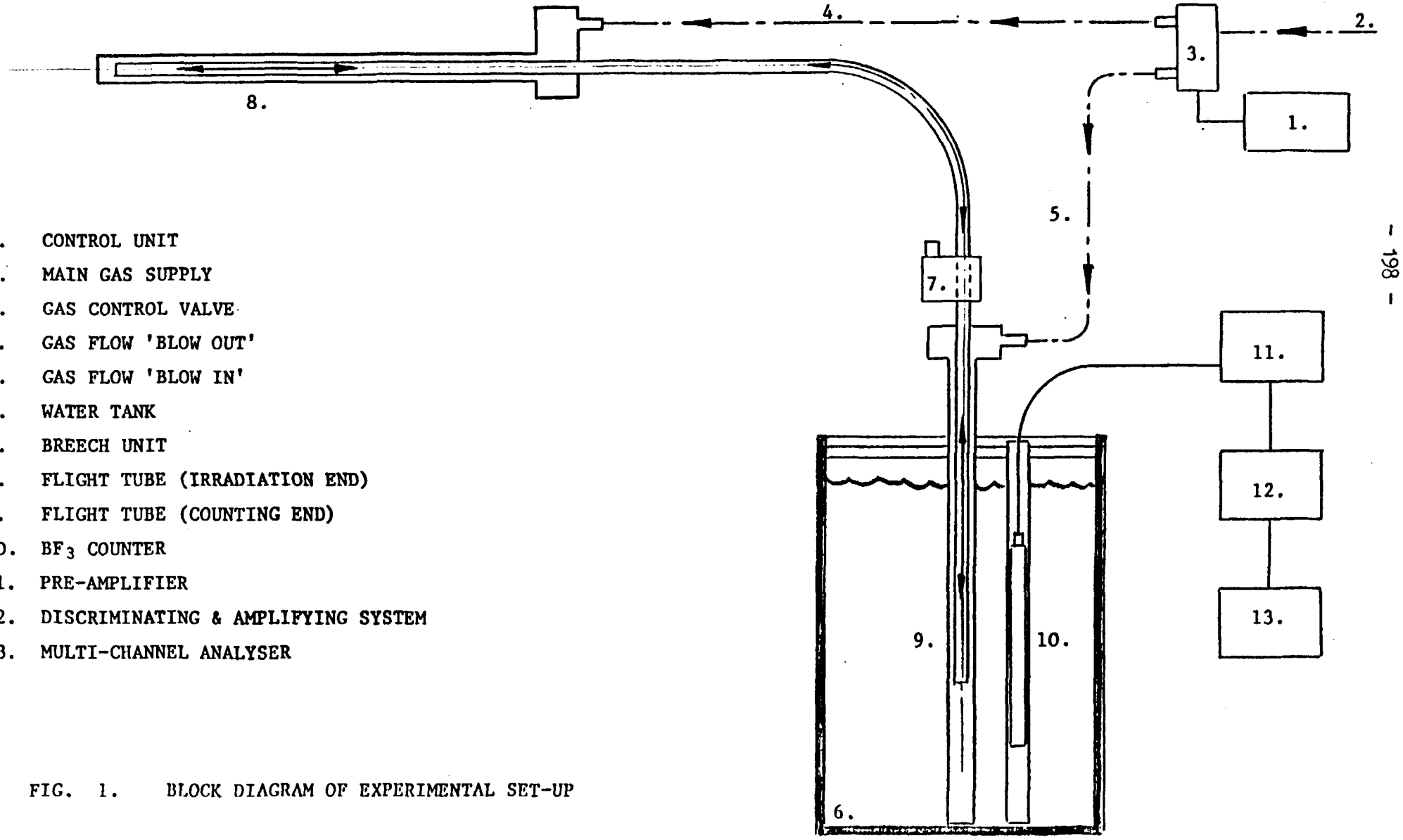

1. CONTROL UNIT
2. MAIN GAS SUPPLY
3. GAS CONTROL VALVE
4. GAS FLOW 'BLOW OUT'
5. GAS FLOW 'BLOW IN'
6. WATER TANK
7. BREECH UNIT
8. FLIGHT TUBE (IRRADIATION END)
9. FLIGHT TUBE (COUNTING END)
10. BF_3 COUNTER
11. PRE-AMPLIFIER
12. DISCRIMINATING & AMPLIFYING SYSTEM
13. MULTI-CHANNEL ANALYSER

FIG. 1. BLOCK DIAGRAM OF EXPERIMENTAL SET-UP

TABLE 1 The efficiency of the neutron detector

Am/Li source measured efficiency	$1.696 \times 10^{-2} \pm 0.55\%$
Volume correction factor	$1.014 \pm 0.7\%$
Self absorption correction factor	$1.010 \pm 0.5\%$
Anisotropic emission correction factor	$0.998 \pm$ NIL
Energy response correction factor	$1.000 \pm 2.2\%$
Efficiency of the detector for delayed neutrons	$1.733 \times 10^{-2} \pm 2.4\%$

TABLE 2 Uncertainties in the fission determinations

Source of uncertainty	Uncertainty ± (1σ)
Deposit mass	1.30%
Dead time corrections	0.50%
Fission fragment absorption correction	0.35%
Extrapolation to zero bias correction	0.20%
Self shielding correction	1.20%
Foil mass	0.03%
γ-counting in stability	0.70%
γ-counting statistics (ratio of two foils)	1.00%
Total uncertainty	2.2%

TABLE 3 ^{235}U thermal fission decay parameters

Group	Keepin et al[7]		This work						
	α_i	$\lambda_i(s^{-1})$	α_i	$\lambda_i(s^{-1})$	Correlation matrix for α_i				
1	.033 ± .004*	.0124 ± .0004	.035 ± .002	.01226 ± .00012	1.	.63	-.42	.27	-.15
2	.219 ± .013	.0305 ± .0015	.227 ± .009	.0310 ± .0004	.63	1.	-.54	.32	-.20
3	.196 ± .033	.111 ± .006	.148 ± .023	.099 ± .011	-.42	-.54	1.	-.62	-.38
4	.395 ± .016	.301 ± .016	.403 ± .017	.254 ± .020	.27	.32	-.62	1.	-.38
5	.115 ± .013	1.14 ± .22	.187 ± .017	.90 ± .11	-.15	-.20	-.38	-.38	1.
6	.042 ± .012	3.01 ± .43	-	-					

*Probable errors reported by Keepin et al[7] converted to standard deviation using the formula:

probable error = 0.6745 x standard deviation.

TABLE 4 Contributions to the total yield uncertainty

Source of uncertainty	Contribution to σ_y $\pm$
Fission measurement	2.2%
Detector efficiency	2.4%
Counting statistics in total counts	0.9%
Decay parameter uncertainties	3.1%
Total uncertainty, σ_y	4.6%

TABLE 5 Period-reactivity relation

Period (sec)	Reactivity		
	y = .0156 6 group parameter[7]	y = .0151 5 group parameter	ratio= $\frac{5 \text{ group}}{6 \text{ group}}$
.2	.00605	.00594	.981
.5	.00562	.00555	.988
1	.00511	.00507	.992
3	.00400	.00398	.994
7	.00300	.00299	.996
10	.00258	.00258	1.000
30	.00147	.00147	1.000
70	.000838	.000836	.998
100	.000640	.000639	.998
300	.000252	.000252	1.000
700	.000115	.000115	1.000
900	.000090	.000090	1.000
-900	-.000098	-.000098	1.000
-700	-.000182	-.000183	1.003
-200	-.000529	-.000531	1.004
-100	-.00180	-.00187	1.038

Errors : The errors due to detector efficiency and fission determination and statistical error on the total count are common to columns 2 and 3 and total 3.4%. The errors due to decay parameters are not shown, but are independent between columns 2 and 3. ν has been taken as 2.41.

REFERENCES

1. Keepin, G.R., "Physics of Nuclear Kinetics". Addison Wesley (1965).

2. Saphier, D., and Yiftah, S. "The effect of errors in the delayed-neutron data on fast reactor static and dynamic calculations". Nucl. Sci. and Engng., 42, 272-277 (1970).

3. Rudstam, G., "Status of delayed neutron data". IAEA Advisory Group Meeting on Fission Product Nuclear Data, IAEA-213, 567-626 (1977).

4. Krick, M.S.-and Evans, A.E., "The measurement of the total-delayed neutron yields as a function of the energy of the neutron inducing fission". Nucl. Sci. and Engng., 47, 311-318 (1972).

5. Tuttle, R.J., "Delayed-neutron data for reactor-physics analysis". Nucl. Sci. and Engng., 56, 37-71 (1975).

6. Hughes, D.J., Dabbs, J., Cahn, A., and Hall, D., Phys. Rev., 73, 111 (1948).

7. Keepin, G.R., Wimett, T.F., and Zeigler, R.K., J. Nucl. Energy, 6, 1, (1957).

8. Besant, C.B., Challen, P.J., McTaggart, M.H., Tavoularides, P., and Williams, J.G., "Absolute yields and group constants of delayed neutrons in the fast fission of ^{235}U and ^{238}U and ^{239}Pu", J. Br. Nucl. Energy Soc. 16, 161-176 (1977)

9. Engle, W.W., "A user's manual for ANISN. A one-dimensional discrete ordinates transport code with anisotropic scattering". USAEC Report, K-1693 (1967).

10. Werle, H., Oak Ridge National Laboratory, INR-41/70-25 (1970).

11. Saphier, D., Ilberg, D., Shalev, S., and Yiftah, S., "Evaluated delayed neutron spectra and their importance in reactor calculations". Nucl. Sci. and Engng., 62, 660-694 (1977).

12. Eccleston, G.W., and Woodruff, G.L., "Delayed-neutron spectra from ^{232}Th, ^{233}U, ^{235}U, ^{238}U, and ^{239}Pu". Trans. Am. Nucl. Soc., 23, 492 (1976).

13. Beckurts, K.H., and Wirtz, K., "Neutron Physics", Springer-Verlag (1964).

14. "NAG Library Mk. 5 Manual". Numerical Algorithms Group, Oxford, England (1976).

15. Marquardt, D.N., "An algorithm for least squares estimation of non-linear parameters". J. Soc. Industrial and Applied Math., 11, 431-441 (1963).

16. Rowlands, J.L., "Needs and accuracy requirements for FPND in the physics design of power reactor cores". IAEA Advisory Group Meeting on Fission Product Nuclear Data, IAEA-213, 41-60 (1977).

Note to the participants of the IAEA Consultant's Meeting on Delayed Neutron Properties, 26-30 March 1979

A correction to the delayed neutron yields of Besant et al.

J.G. Williams, March 1979

The measurements reported by Besant et al[1], for delayed neutron yields in the fast fission of ^{235}U, ^{238}U and ^{239}Pu made use of the same Am/Li neutron source for the detector calibration as used in the measurements reported at this meeting by Synetos and Williams[2]. As stated in ref. 2 this source does not emit neutrons isotropically because of scattering and absorption within the source material. This was not taken into account previously.

The effect of this on the detector calibration and on the yield values reported in ref. 1 has been calculated using a Monte Carlo Code, MONK[3]. The resulting correction factor to the efficiency of the detector was 0.986 ± .0015, so the yield values should all be multiplied by 1.014. The total reported errors are not changed.

1. Besant, C.D., Challen, P.J., McTaggart, M.H., Tavoularides, P., and Williams, J.G., J. Br. Nucl. Energy Soc. 16, 161-176 (1977).

2. Synetos, S., and Williams, J.G., This meeting

3. Sherriffs, V.S.W., "MONK - A general purpose Monte Carlo neutronics program". SRD R 86, UKAEA, (1978).

Delayed Neutron Spectrum Measurements using a ^{3}He Spectrometer

D.R. Weaver, J.G. Owen and J. Walker

A contributed paper for the IAEA Consultants' Meeting on Delayed Neutrons

Vienna - March 1979

Abstract.

Measurements have been made of the delayed neutron spectra from fission of ^{235}U induced by primary neutrons of 940, 1440, 1760 and 6000keV. A ^{3}He spectrometer was used, for which supplementary measurements had shown the fast neutron resolution to be 27keV at 1MeV and had determined the detector efficiency as a function of energy. Two-dimensional analysis of pulse height and pulse rise time was used to eliminate ^{3}He recoil events. The Birmingham Radiation Centre Dynamitron accelerator produced suitable fluxes of primary neutrons by bombarding a tritium target with a proton beam that was pulsed 0.8s on, 1.0s off; this gave a near-equilibrium production of delayed neutrons.

1. Introduction.

In nuclear reactor kinetics, the delayed neutron contribution enters directly into the source term of the neutron balance equation and as a result the time constant for flux variation caused by a small change in reactivity proves to be dependent on the delayed neutron lifetimes rather than the history (through slowing down and diffusion) of a prompt neutron despite the greater intensity of the prompt neutrons. The difference in the energy spectrum of delayed and prompt neutrons is not particularly significant in thermal reactors, but in fast reactors the average neutron energy in the core is close to the mean delayed neutron energy and it has been suggested[1] that the delayed neutron spectrum assumed can radically alter the prediction of time dependent fluxes under fault conditions.

The existing information on the spectra of delayed neutrons from fission is sparse, with only a few measurements with primary neutron energies in the fast region[2,3]. Using a ^{3}He spectrometer measurements have been made on a ^{235}U sample at four primary neutron energies: 940, 1440, 1760 and 6000keV, and the results compared with those of other workers. Owing to the disagreement between spectra accumulated by various authors with different spectrometers, a fact which was remarked upon at the Petten meeting on Fission Product Nuclear Data[4], particular emphasis has been made in this contribution to the methods employed for determining the resolution and efficiency of the ^{3}He spectrometer.

2. Spectrometer details.

The ^{3}He gridded ionization chamber was supplied by Technion in Israel and is of the Shalev type[5]. It contains 4.2 atmospheres of ^{3}He, 2.1 atmospheres of argon and 0.3 atmospheres of methane, and with anode and grid potentials of 2250 and 450V respectively it gave a resolution (F.W.H.M.) of 14.6keV for thermal neutrons. The efficacy of the grid in giving good resolution was shown by monitoring thermal neutrons with the grid disconnected, when a resolution of 65keV was obtained. The reaction in the detector:

$$^{3}He + n \rightarrow p + T \qquad Q = 764keV$$

leads to long tracks in the gas and consequently there is a noticeable wall effect; indeed, in this detector, neutrons of energy greater than 2MeV give proton tracks comparable with the dimensions of the counter and above 2.5MeV the fast peak has almost completely disappeared. The predictions of Batchelor, Aves and Skyrme[6] were found to be appropriate for the wall effect contribution for neutron energies right up to 1.8MeV and were used extensively in the analysis of spectra obtained.

The slow charge collection in this type of counter means that long time constants must be used with the electronics. This results in the system being particularly sensitive to electrical noise and vibration. Considerable care was taken with the earthing of the detector, preamplifier and power supplies and the spectrometer was mounted on an assembly of two thick steel plates separated by glass fibre mounted on rubber feet which successfully restricted vibrational transmission. Franz et al[7] have reported on the effect of microphonics on the resolution of these detectors.

^{3}He spectrometers are particularly sensitive to thermal neutrons, and in order to minimise their detection the counter was enclosed in a shield of boron carbide and cadmium which reduced the thermal neutron response by a factor of 20. The dual parameter (pulse height and rise time) analysis reduced the thermal efficiency still further, as is explained below.

Gamma rays alone do not interfere with the neutron spectrum but, if there is an intense gamma flux, pile up between photon and neutron pulses severely degrades the resolution of the counter, e.g. in a gamma flux of 7×10^{5} photons cm^{-2} s^{-1} the thermal peak becomes 84keV wide. Shalev[5] has proposed the use of the count rate at an energy equivalent of 76keV in a gamma-broadened spectrum of thermal neutrons (C_{76}) as a guide to the effect of pile up on resolution, little influence being seen for C_{76} less than 8 counts s^{-1}

keV^{-1}. Owing to the gamma flux from the irradiated uranium, it was necessary to place a lead shield between the uranium and the spectrometer. It was found that 5cm of lead reduced C_{76} to about 1 counts $s^{-1}keV^{-1}$ for the delayed neutron spectra measurements which is well below Shalev's figure of 8. The lead shield does have the effect of degrading the resolution of the counter system by multiple scattering of neutrons prior to their reaching the detector; all measurements of resolution efficiency and delayed neutron spectra were therefore performed with the same counter arrangement which is shown in Figure 1.

3. Resolution measurements.

a) Single parameter.

The dual parameter analysis was not used in the initial resolution measurements as at that stage it was not appreciated quite how marked an influence this technique has on the width of pulses detected. The single parameter measurements will be described first. They were performed in the 'low scatter cell' of the Birmingham Radiation Centre which is a room approximately 9m x 9m x 8m, bisected by a grid floor. A proton beam from the 3MV Dynamitron accelerator was used to produce neutrons in the centre of the room by means of the $^{7}Li(p,n)$ and T(p,n) reactions. The detector was mounted sufficiently far from the neutron source to ensure that the energy spread from the angle subtended was small. Measurements with a shadow cone showed that the room-return flux consisted largely of thermal neutrons and a very small quantity of fast neutrons of random energy. The lithium target was an evaporated layer of lithium carbonate which was shown to be 8keV thick by measurements of the rise in yield at 0^{o} at threshold; this therefore contributed an energy spread very much less than the detector resolution. The thinnest tritium target available as tritium absorbed in titanium from the Radiochemical Centre, Amersham, England, proved to be 68keV thick at threshold. This was

comparable with the detector resolution but comparisons with measurements made with the lithium target giving the same neutron energy showed that the effect of the tritium target thickness could be successfully stripped from measured spectra to give a consistent value for the detector resolution. Measurements were made with neutrons at twelve energies from 130 and 1766keV. The spectra obtained were found to be well represented by two Gaussians plus a continuous wall effect distribution, the last being correctly predicted by the formula of Batchelor, Aves and Skyrme[6]. It was shown that a continuum, as used by other workers for the wall effect, was not a good representation. The reason why two Gaussians are required for the main peak is not certain, but it is a similar result to that found in the fitting of gamma spectra in Ge(Li) detectors. The wall effect was stripped from the spectra, and the FWHM of the resultant peaks obtained. The results are shown in Figure 2 and were disappointing, the 1MeV resolution, for example, being about 45keV. No improvement resulted from different combinations of voltage on the grid and anode and by running the getter built into the detector.

b) Dual parameter.

It was known that it would be necessary to employ dual parameter rise time and pulse height analysis in the delayed neutron spectrum measurements in order to separate the unwanted ^{3}He recoil events in the detector from the pulses produced by the $^{3}He(n,p)T$ reaction. Without this technique, neutrons of energies greater than 1MeV could produce ^{3}He recoils of energy greater than 764keV and the recoil spectrum would thus obtrude into the neutron spectrum above the thermal peak. However, separation is possible because the ^{3}He recoil tracks in the gas are on the whole shorter than the proton and triton tracks and therefore produce pulses which rise faster. The electronics system used is shown in Figure 3 and a typical resolution function measurement spectrum is shown in Figure 4 where the pulse height increases from left to right, and the rise time is short to the rear of the display and long to the front (the pulses

in rise time channel 1 are missed coincidences and were ignored). The Canberra 1412 amplifier provided a fast pulse, the rise of which above a threshold was detected by the Ortec 473 constant fraction discriminator. The resultant timing pulse was delayed and formed the stop pulse for an Ortec 467 time-to-amplitude converter (hence the short rise times were at high rise time channel numbers). The start pulses for the T.A.C. were obtained from the cross-over of a bipolar pulse from an Ortec 410 amplifier. The double differentiation time constants required in the 410 were set at 2 and 5μs in the light of the analysis of Cuttler et al[8]. It can be seen from Figure 4 that rise time channels 2 to 11 contain no ^3He recoils and so these rise times alone were used in all subsequent resolution, efficiency and delayed neutron spectrum measurements.

This analysis also showed that the centroid of the fast neutron peaks did not occur at the same pulse height channel for all rise times. Figure 5a shows the effect for neutrons of 1306keV where the fast neutron peaks from successive rise time channels have been superimposed; this phenomenon was, in fact, reported by Shalev[9]. It is no doubt due to the long rise time pulses being clipped by the 6μs time constant shaping circuit of the Ortec 472 amplifier; a longer time constant was not used as it was found to make the detector even more sensitive to electrical and vibrational noise and the resolution, in fact, became worse. Therefore further resolution measurements were made with the same target arrangement as before but now using the dual parameter electronics. It was found that the shift in the centroid relative to rise time channel 11 was linear with neutron energy for each rise time channel (see Figure 6) making it possible to correct all the results on to the same energy scale, the result of which is shown in Figure 5b. After this correction all rise time channels from 2 to 11 were combined and the wall effect prdicted by Batchelor, Aves and Skyrme stripped off (it was found that the rise time analysis only marginally altered the predicted wall effect

observed in the rise time channels above the ^{3}He recoils). A double Gaussian fit was performed as in the single parameter work and the final FWHM values obtained are shown in Figure 7; it can be seen that the dual parameter analysis has improved the resolution at 1MeV to the value of 27keV.

A second benefit of the dual parameter analysis can also be seen in Figure 4; the vast majority of thermal neutron pulses are of short rise time and by selecting only rise time channels 2 to 11 most of them are removed from the spectra. This greatly assists in analysing the delayed neutron results at energies close to the thermal peak.

4. Efficiency measurements.

The efficiency of the spectrometer was measured by comparison with a de Pangher Precision Long Counter[10] which had been calibrated against the one at the National Physical Laboratory, London, England[11]. A similar experimental arrangement to that used in the resolution measurements was employed, although higher count rates were obtained by having the detector nearer the neutron source. The tritium target was used at all neutron energies except below 300keV where the lithium target was used in order to avoid the region where the T(p,n) reaction produces two neutron energies at each laboratory angle (this regime extends from threshold to proton energies at 1160keV).

The Birmingham long counter has an efficiency within 5% of that of the NPL counter and as, so far, no attempt has been made to obtain more than the relative efficiency of the ^{3}He spectrometer, the NPL calibration figures of Hunt[11] were used directly. Corrections for room in-scattering and air out-scattering for the long counter are complementary and it is felt that their overall effect is small compared with the total error on each efficiency value.

When defining the efficiency of the ^{3}He counter it is essential to be specific about the region of pulses which are being counted. In the two-parameter analysis it is clear that some of the wall effect pulses are lost in the high level of low energy events. Therefore a total efficiency has been

defined which allows for all wall effect events by extrapolating from high energies by the form given by Batchelor, Aves and Skyrme. All rise time channels are then summed and the relative efficiencies obtained in this way are shown in Figure 8. It will be noted that the efficiency rises sharply at low energies, a fact which has previously limited the lowest energy to which ^{3}He spectra could be unfolded. These results confirm the observation by Franz et al[7] that the measured efficiency falls off more rapidly than the ^{3}He(n,p)T cross section.

At about 250keV there is a departure from the smooth monotonic decrease in efficiency. Despite a search of the cross sections for all the elements likely to attenuate a direct beam (boron, carbon, lead, iron) no clear reason can be found for this observation. Franz et al[7] saw similar dips at 130 and 340keV, whilst Evans and Krick[3] noted one between 350 and 400keV. Shalev[12] has suggested these may be due to iron in the construction of some counters but he believes this should not affect the Birmingham device which is of different construction. Clearly, there is some variation in the behaviour of ^{3}He spectrometers.

As selected rise time channels were used in the delayed neutron experiments, the total efficiency as defined above is inappropriate as it includes events at all rise times. Therefore 'effective efficiency' has been defined by taking only the results in rise time channels 2 to 11 inclusive and considering only those events above a neutron energy of 15keV, that discriminator level having been chosen as the lowest energy that could reasonably be identified without contamination by the thermal peak. The results of this analysis are shown in Figure 9 and it will be seen that the efficiency no longer rises at low energies but, in fact, falls because of the operation of the 15keV discrimination. The shape of the curve can be understood as the combined effect of the ^{3}He(n,p)T cross section and the tendency of wall effect counts to fall above the 15keV cut-off as neutron energy increases; this accounts for the

maximum observed at about 600keV and the slight minimum around 1000keV. So far measurements have been made only up to 1300keV but at higher energies the efficiency can be expected to be moderately flat as the cross section only varies by 6% between 1300 and 2000keV and at these energies most of the wall effect pulses lie above 15keV. Therefore in the analysis of the delayed neutron experiments a flat efficiency has been used above 1300keV and the least squares fitted fifth order polynomial shown in Figure 9 used from 15 to 1300keV*.

5. Delayed neutron spectrum measurements.

For the measurements with primary neutrons of 940, 1440 and 1760keV a proton beam from the Dynamitron was used to bombard a thick tritium target containing about 3.3×10^{19} tritium atoms cm^{-2} of the titanium layer (Radiochemical Centre, Amersham, target TRT100). At zero degrees with 2MeV protons this gave a yield of about 1.2×10^{7} n $sr^{-1}\mu A^{-1}s^{-1}$ and in the experimental arrangement used resulted in an energy spread of about 300keV at the uranium. For the 6000keV experiment a deuteron beam was used on a thick deuterium absorbed on titanium target (Radiochemical Centre, Amersham, target DBT100) and this produced a similar yield per microamp but an energy spread nearer 700keV.

The uranium sample was kindly loaned by AERE, Harwell, and of a total mass of 105g, 100g were ^{235}U(96.54% ^{235}U, 3.46% ^{238}U). It was double wrapped in polythene film to contain fission products and positioned 2cm from the neutron source. The detector was 8cm behind the uranium, the separation being necessitated by the lead shield. A cadmium shield was used round the uranium to minimise thermal fission by neutrons moderated in the walls of the experimental area.

It is obviously impossible to detect delayed neutrons in the presence of the source neutrons and those emitted at the time of fission. The Dynamitron accelerator was therefore pulsed by deflecting the beam emerging from the ion source prior to acceleration with an electrostatic potential applied to a plate in the high-voltage terminal. Timing was by an external circuit, with control

* The results presented in Vienna took account of new efficiency measurements between 1300 and 2000keV.

information being fed to the terminal by an optical link. The reduction in primary neutron source strength from the beam-on to beam-off conditions was better than 10^6:1. The cycle consisted of a beam-on period of 0.8s and a beam-off time of 1.0s. Delayed neutron counting took 0.8s and began 0.1s after the beam was turned off; this permitted the detector to recover from the huge overload of the beam-on period and allowed the source neutrons to die away. The detector recovery proved to be a limiting factor on the intensity of primary neutrons that could be employed; if the source rate was increased above a critical level the recovery period would suddenly increase to 0.2s or more, which was not acceptable. For beam currents of less than 50μA the recovery time was always less than 0.1s. This cycle produced a near equilibrium distribution of delayed neutron groups and therefore corresponds closely to that produced by continuous irradiation. Table 1 shows the contributions expected according to Keepin's six group formalism[13] for this experiment, equilibrium conditions and the cycle used by Eccleston and Woodruff[2].

Figure 10 shows a typical two-parameter spectrum, the fissions having been induced by primary neutrons of 1440keV. The spectra from all the experiments were corrected for the energy shift with rise time as described in section 3(b) above and the rise time groups 2 to 11 inclusive summed; the results are shown in Figures 11-14 (the 6MeV run contains significantly fewer counts as the detector recovery limitation on primary source strength was particularly severe at that energy). Figures 11-14 also show tentative assignments of the energies of prominent peaks and in Table 2 comparison is made with peaks determined from spectra of separated precursors measured by Franz et al[7], Kratz et al[14,15], Rudstam and Lund[16,17] and Shalev and Rudstam[18-20]. The peaks observed in the spectra from ^{235}U by Evans and Krick[3] and Sloan and Woodruff[21] and Shalev and Cutler[5] are also listed in Table 2. The agreement is good below about 1MeV but above this energy few peaks have been observed by other workers; however, the structure is believed to be genuine, particularly since many of

the peaks appear in one more than one spectrum.

The pulse height distributions were converted to delayed neutron spectra by applying an iterative technique similar to that used by Rudstam[22] where the required response functions were derived from the resolution and efficiency measurements noted earlier. A number of corrections were considered before final analysis.

a) Source multiplication.

The uranium constitutes a multiplying system and some of the fissions taking place must be the result of prompt neutrons from one fission inducing a second. There is little that can be done to correct for this effect in the present situation of poor knowledge of the variation of emitted spectra with primary neutron energy. Calculations based on the mean chord length in the uranium sample indicated an 8% contribution from prompt neutron fission.

It is simple to show that an effect of similar magnitude arises from the fissions induced in the uranium by delayed neutrons during the beam-off period. Allowance was made by stripping off the appropriate amount of prompt fission neutron spectrum, but it was appreciated that this was not ideal as much of the prompt spectrum is at energies greater than the operational limit of the spectrometer and would thus give only wall effect pulses. As it has not been possible to predict the shape of the spectrum from these high energy pulses, no correction has been applied. Nor is it possible to predict whether ^{3}He recoil pulses of sufficiently long rise time to fall in the selected channels can be caused by neutrons of energies greater than 2MeV; experiments to check these issues are required.*

The corrections applied here are in general agreement with those determined by Sloan[23] but the multiplication quoted by Evans and Krick[3] appears to be several times that predicted by the mean chord length method.

b) Neutron scattering.

The effect of scattering in the lead and iron of the detector assembly

* Measurements have recently been made with a ^{252}Cf source and prompt neutron corrections are now based on these results.

was taken into account by the efficiency and resolution measurements. The additional scattering introduced by the uranium sample itself is thought to be small in comparison with the effect of the lead. It has been mentioned that the uranium was wrapped in two layers of polythene in order to contain fission products; this results in 0.5 to 1% of delayed neutrons being scattered in traversing this material.

c) Neutrons generated by energetic gamma rays.

The high thresholds for photo fission and (γ,n) reactions make the probability of contamination of the delayed neutron spectra small.

d) Delayed neutrons from ^{238}U.

3.5% of the uranium sample is ^{238}U and although the lowest primary energy measurements are not expected to have much ^{238}U reaction contribution owing to the low level of the ^{238}U fission cross section at these energies, the 1760 and 6000keV experiments may have about a 3% addition from ^{238}U fission.

e) Low energy fission.

The cadmium layer around the uranium sample is expected to have removed all but 7×10^{-10} of thermal neutrons and even at 1eV less than 0.06 of the incident flux should have been transmitted.

f) Room return neutrons.

Measurements of the die away of source neutrons indicated that the 0.1s delay between the beam turning off and the delayed neutron counting being started was sufficient for room return neutrons to be reduced to a negligible level. Room return of delayed neutrons is estimated to be less than 0.1% of detected delayed neutrons.

g) Source neutrons.

The reduction in the source strength was better than 10^6:1 when switching from beam-on to beam-off. The absence of any structure in the measured spectra at energies corresponding to the source further confirm that the source flux was sufficiently attenuated.

h) Incomplete rise time discrimination.

Good experience has been obtained with the dual parameter analysis system; however, the unfolding of spectra is particularly sensitive to any variations in the rise time analysis system and it is felt that further investigation of the magnitude of errors associated with jitter in the rise time analysis is required before the effects can be properly quantified.

i) Incomplete discrimination against the thermal peak.

A low energy limit of 30keV was employed in the unfolding at which level a single thermal peak would only contribute 1.5×10^{-5} of its maximum value. Gamma rays might broaden the peak by adding an exponential tail but at the level of gamma flux encountered in the experiment the size of this tail is expected to have been negligibly small.

j) Errors introduced by the unfolding procedure.

The combination of uncertainties on the response function and efficiency variation are expected to result in an overall error of 5% for the whole energy range. This must be combined with the statistical variation in the number of counts in the pulse height spectra and results in a final error of $\pm$7% in the region 100 to 1000keV. Below 100keV the error is expected to be larger as a result of not being able to predict correctly the effect of scattering. Above 1MeV statistics are poorer and there is greater uncertainty in the wall effect subtraction; thus a final uncertainty of $\pm$15 to 20% is expected here.

6. Discussion of results and comparison with other workers.

Figure 15 shows all the spectra measured in this work; they have been normalised to contain the same number of counts in the region 210 to 1200keV as the absolute delayed neutron emission rate has not been measured. The results are also given in Table 3. One particular feature is the peak at around 370keV which is present in the 940, 1440 and 1760keV experiments, but is absent at 6000keV. If the assignment to ^{137}I in Table 2 is correct it

must imply the ^{137}I fission yield or the mode of decay alters as the primary neutron energy rises. The occurrence of other ^{137}I peaks in the 6000keV spectrum makes the latter possibility the more likely. Figure 16 comparss the 1760keV spectrum with that of Eccleston and Woodruff[2] and Figure 17 compares the same one with the spectrum reconstructed by Saphier et al[1] from separated precursor measurements. It is clear that reasonable agreement exists between these spectra at delayed neutron energies between 200 and 900 keV but that this work and Eccleston and Woodruff suggest a higher contribution than Saphier at lower energies. In fact, even more low energy delayed neutrons are seen here than by Eccleston and Woodruff. Above a delayed neutron energy of 1MeV these results compare better with Evans and Krick[3] in that considerable numbers of neutrons are seen; it may be that the proton recoil counter used by Eccleston and Woodruff[2] did not respond well to these high energy particles. However, the structure seen at around 370keV by Evans and Krick[3] is not reproduced here despite similar experimental and spectrometer conditions being used in both cases. Finally, it is clear that variations do exist in the delayed neutron spectra as the primary neutron energy is raised and that significant quantities of both low and high energy neutrons appear in the spectra.

References.

1. Saphier D. et al, Nucl. Sci. and Eng., 62, 660-694 (1977).

2. Eccleston G.W. and Woodruff G.L., Nucl. Sci and Eng., 62, 636-651 (1977).

3. Evans A.E. and Krick M.S., Nucl. Sci. and Eng., 62, 652-659 (1977).

4. Rudstam G., Proceedings of the 2nd Advisory Group Meeting on Fission Product Nuclear Data, Petten, 1977.

5. Technion - Israel Institute of Technology, manufacture taken over by Seforad - Applied Radiation Ltd., Emek Hayarden, Israel. Shalev S. Technion Report TNSD-R/421, Technion, Haifa, Israel (1971).

6. Batchelor R., Aves R. and Skyrme T.H.R., Rev. Sci. Inst., 26, 1037-1047 (1955).

7. Franz H. et al, Nucl. Instr. Meth., 144. 253-261 (1977).

8. Cutler J.M. et al, Nucl. Instr. Meth., 75, 301-311 (1969).

9. Shalev S., Technion Report TNSD-R/412, Technion, Haifa, Israel (1970).

10. de Pangher J. and Nichols L.L., Pacific Northwest Laboratories Report BNWL260 (1966).

11. Hunt J.B., National Physical Laboratory Report RS5, London, England (1976).

12. Shalev S. - private communication.

13. Keepin G.R., "Physics of Nuclear Kinetics", Addison Wesley (1965).

14. Kratz K-L. et al, Proceedings of International Workshop V on Gross Properties of Nuclei and Nuclear Excitations, Hirschegg, Klein Walsertal, Austria, January 1977.

15. Kratz K-L. et al, Proceedings of 3rd International Conference on Nuclei far from Stability, Cargese, France, May 1976.

16. Rudstam G. and Lund E., Nucl. Sci. and Eng., 64, 749-760 (1977).

17. Lund E. and Rudstam G., Phys. Rev., C13, 1544-1551 (1976).

18. Shalev S. and Rudstam G., Nucl. Phys., A230, 153-172 (1974).

19. Shalev S. and Rudstam G., Nucl. Phys., A275, 76-92 (1977).

20. Rudstam G. and Shalev S., Nucl. Phys., A235, 397-409 (1974).

21. Sloan W.R. and Woodruff G.L., Nucl. Sci. Eng., 55, 28-40 (1974).

22. Rudstam G., The Swedish Research Councils' Laboratory Report LF-57 (1974).

23. Sloan W.R. at al, Trans. Am. Nucl. Soc., 13, 759-760 (1970).

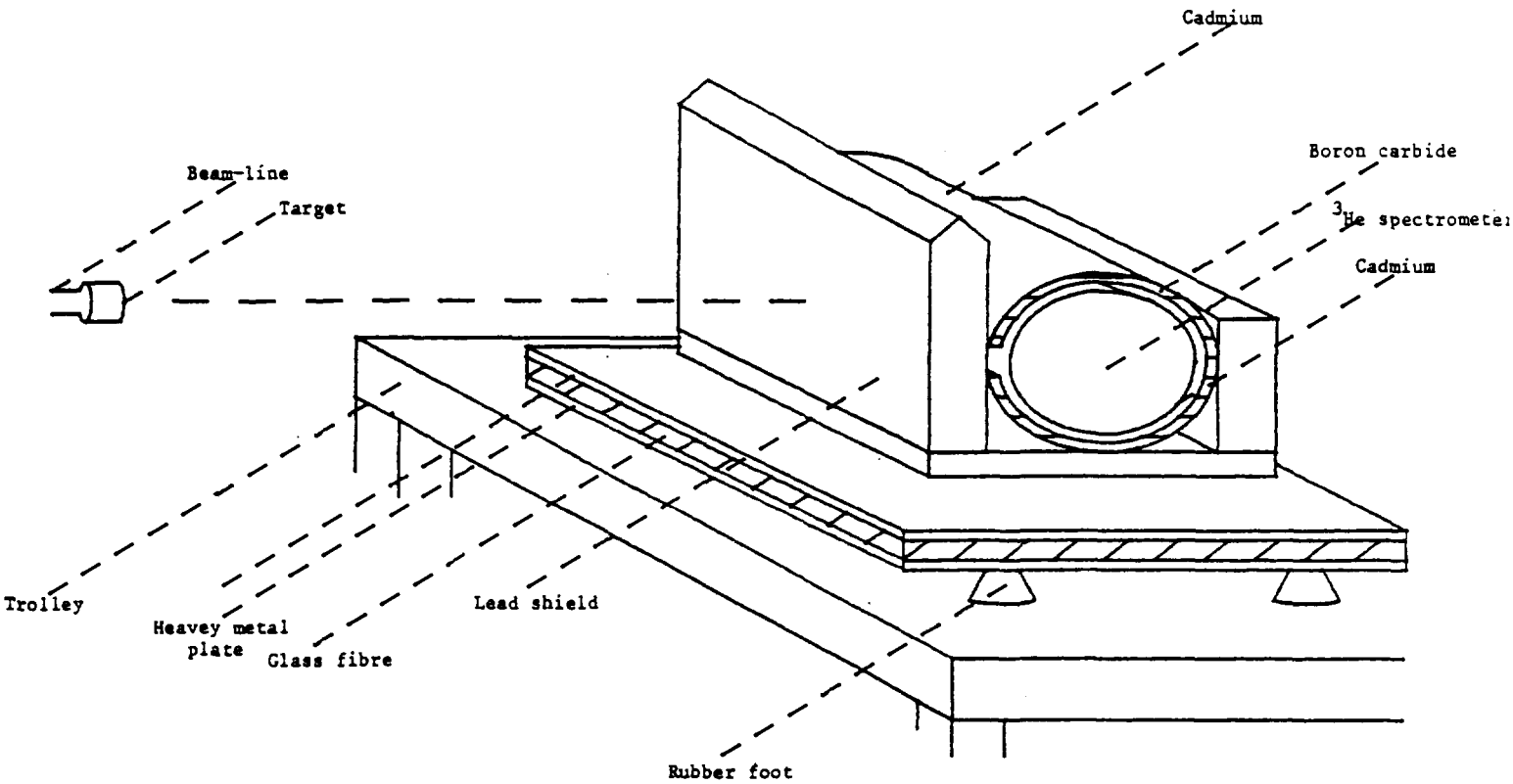

Figure 1: The ^{3}He spectrometer, shielding and mounting.

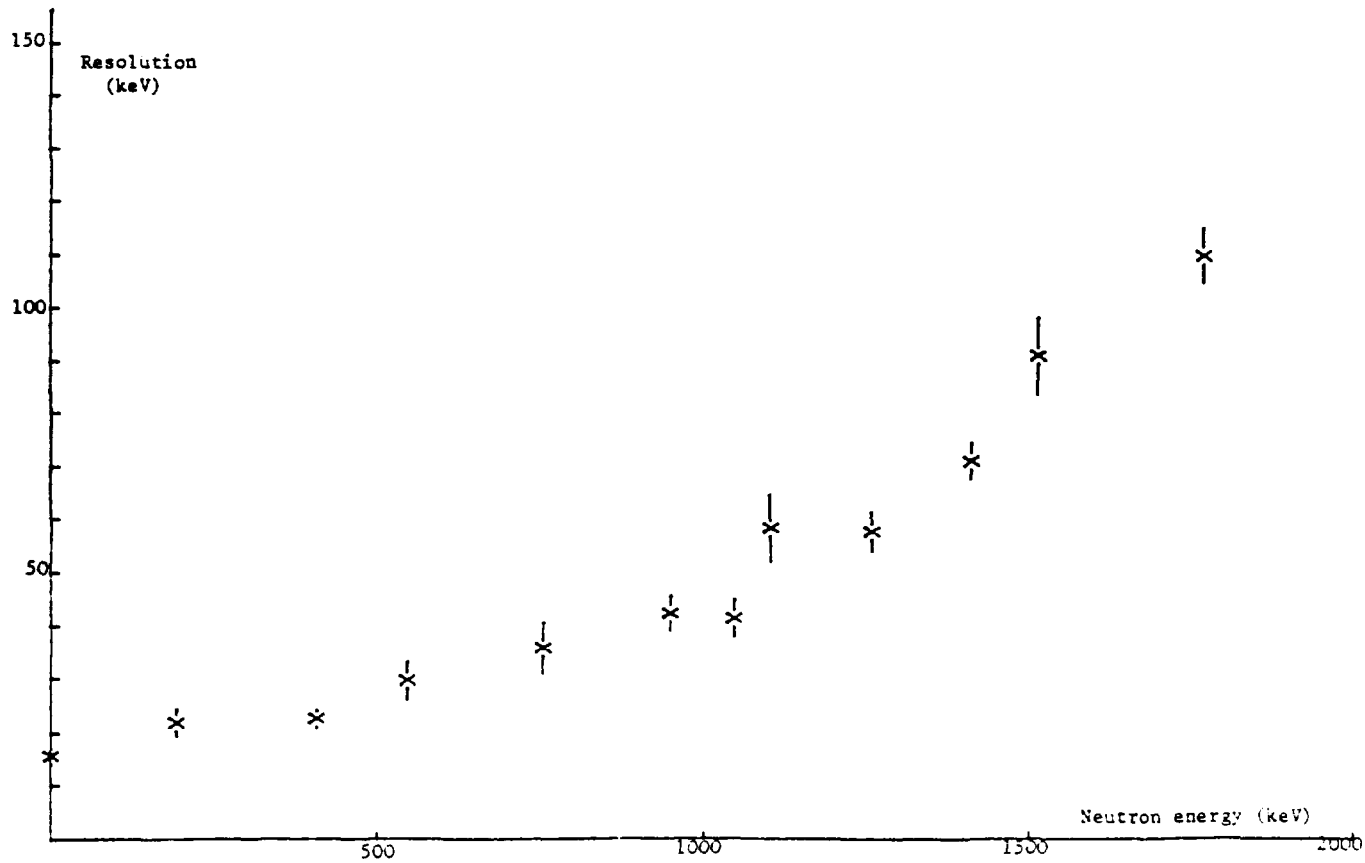

Figure 2: Resolution (F.W.H.M) of the ^{3}He spectrometer from the 'single parameter' measurements.

FIGURE 3: THE ELECTRONICS ASSOCIATED WITH THE ^{3}He SPECTROMETER.

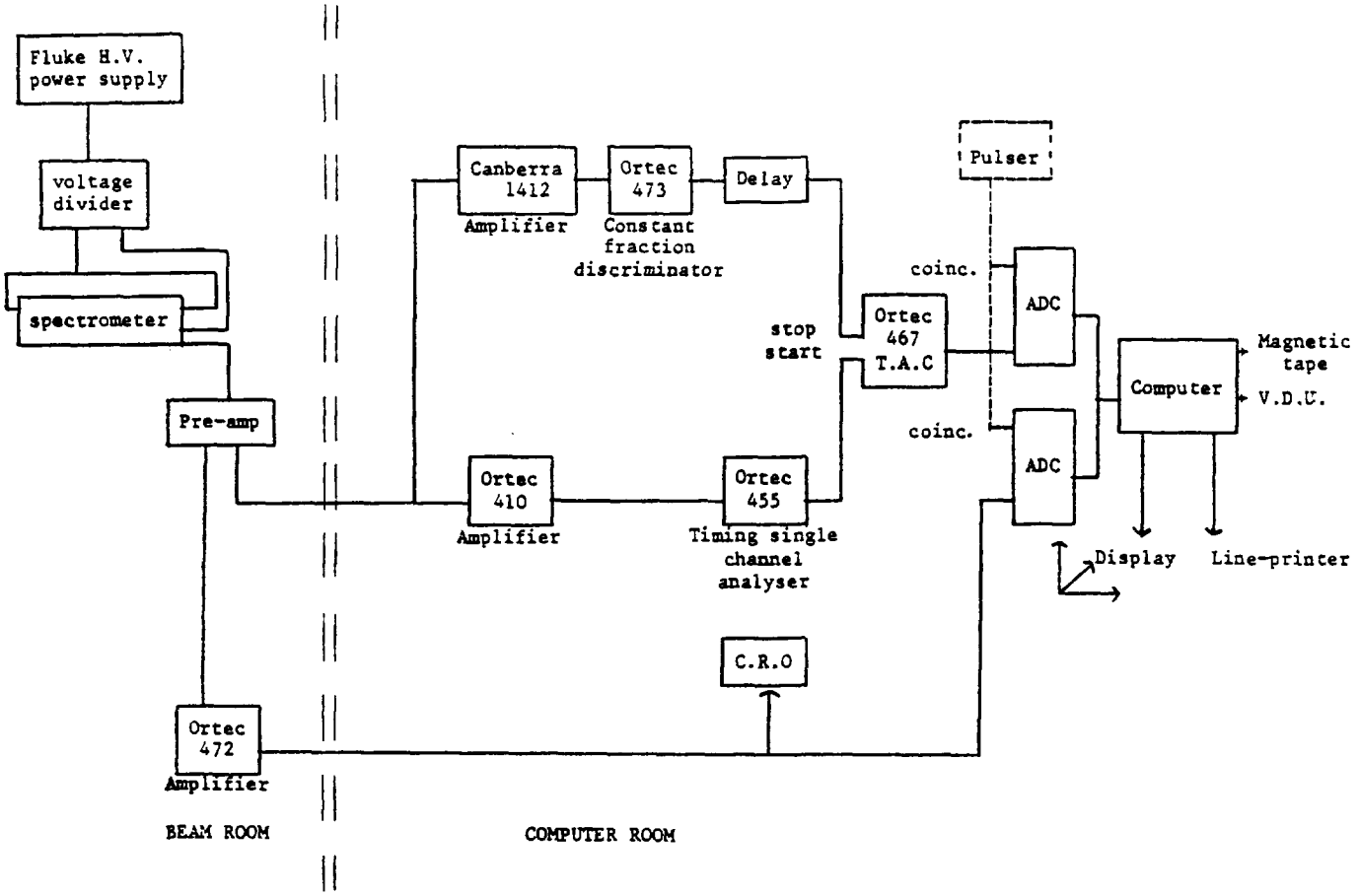

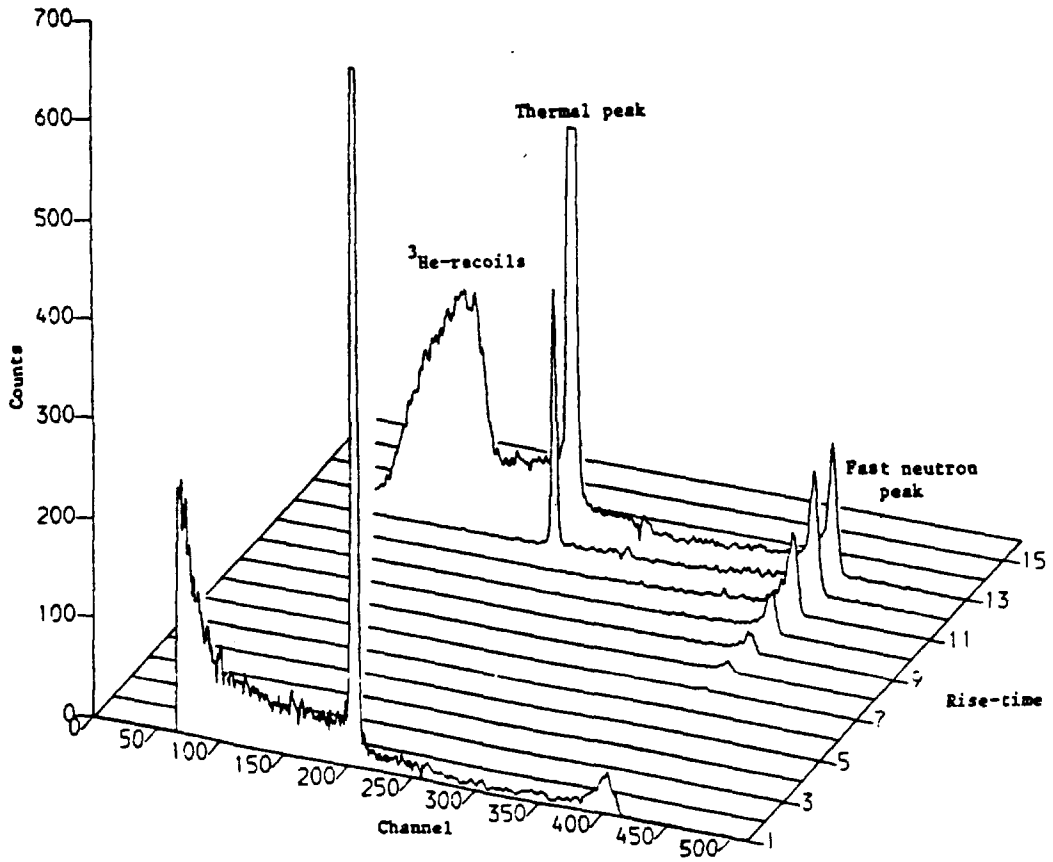

Figure 4: ^{3}He spectrometer response to a flux of 755keV neutrons

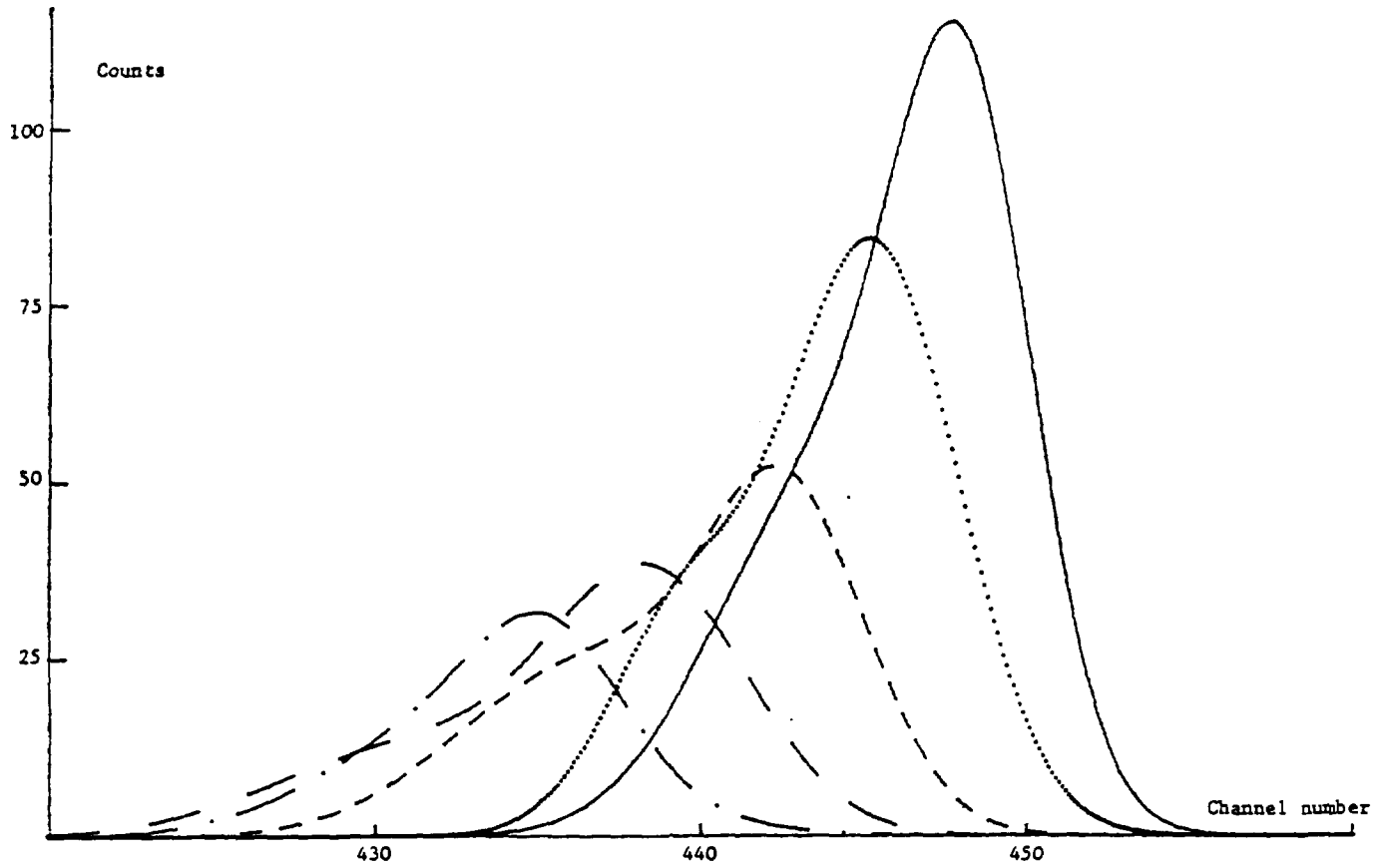

Figure 5a: The rise time variation in the position of the fast neutron peaks generated by a neutron flux of 1306keV.

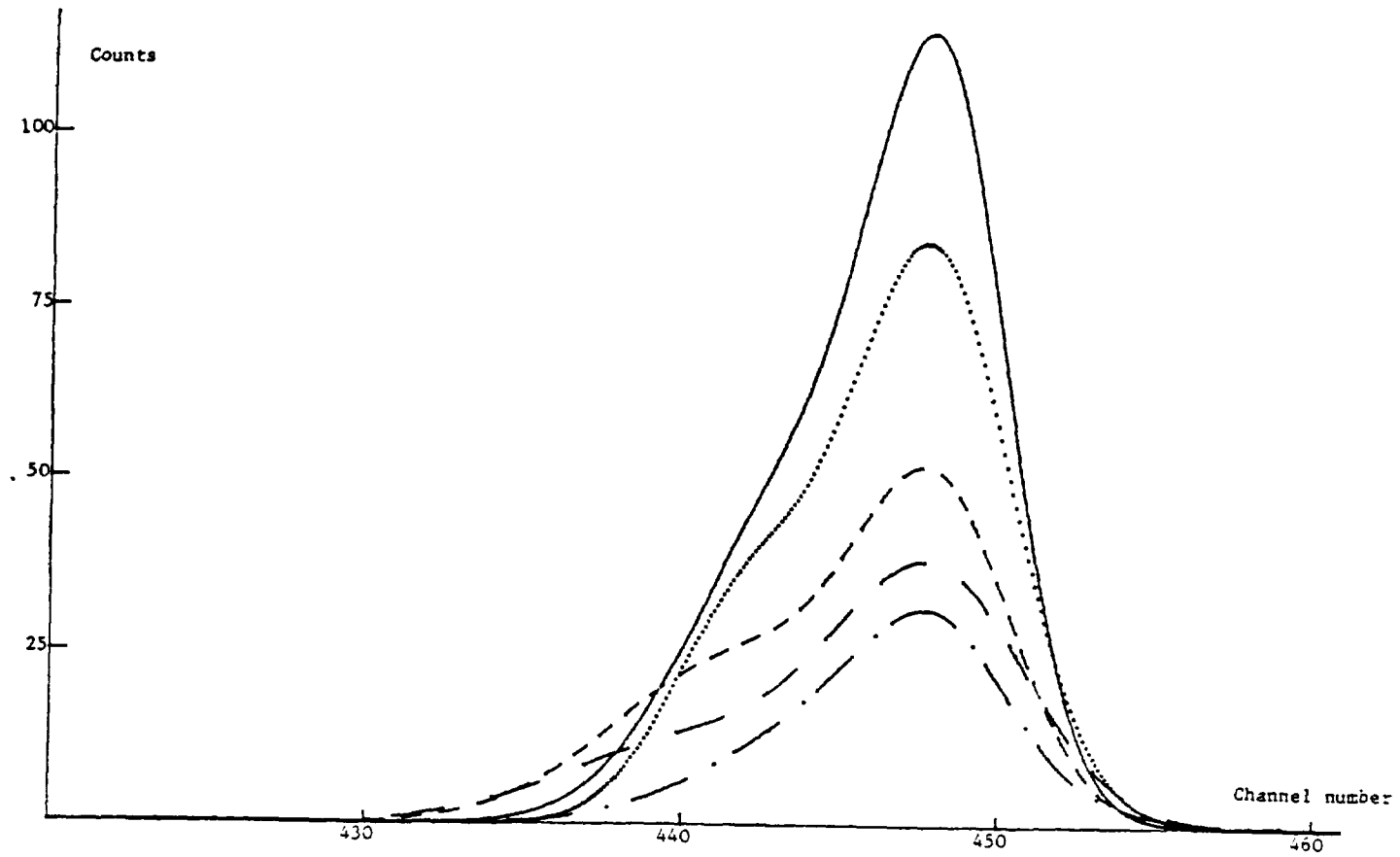

Figure 5b: The fast neutron peaks generated by 1306keV neutrons after correction for the rise time shifts.

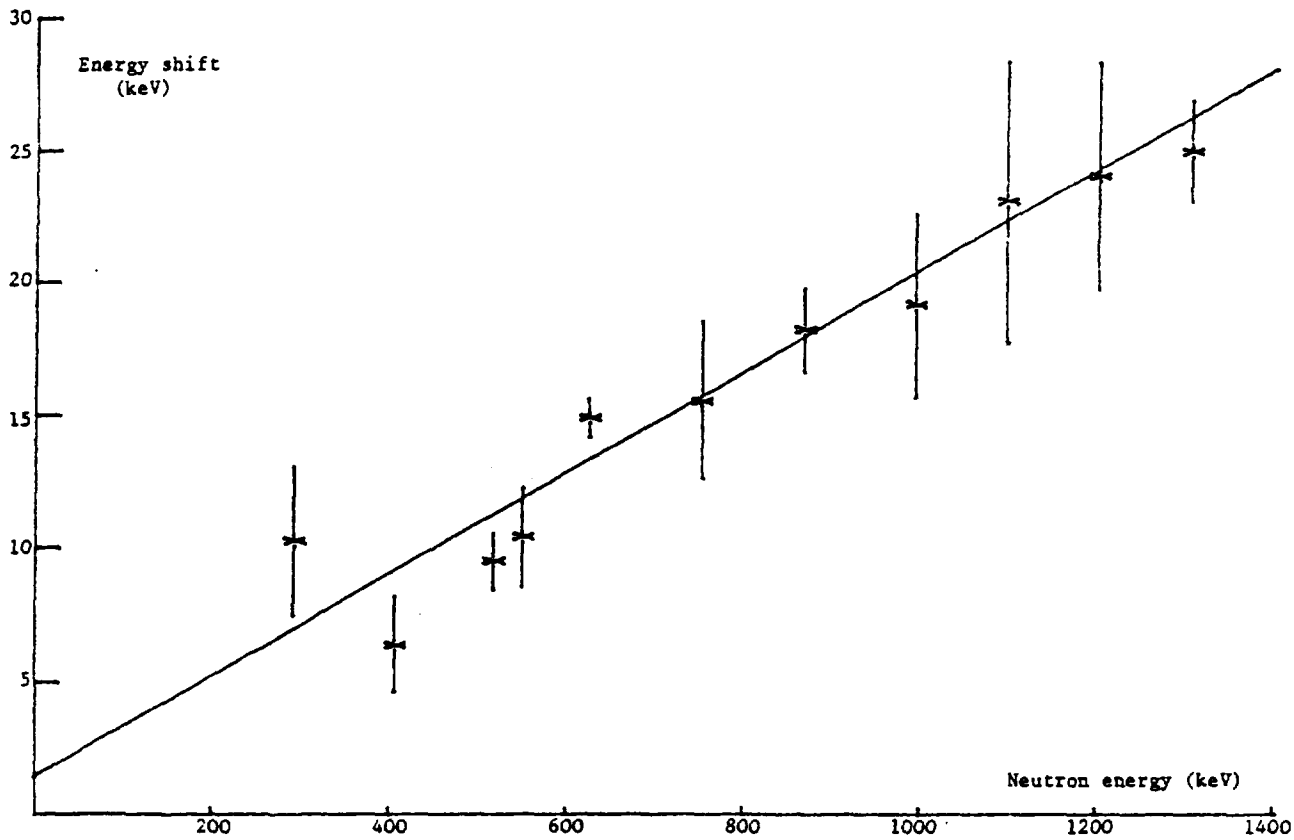

Figure 6: The energy shift associated with neutron energy for rise time channel 9.

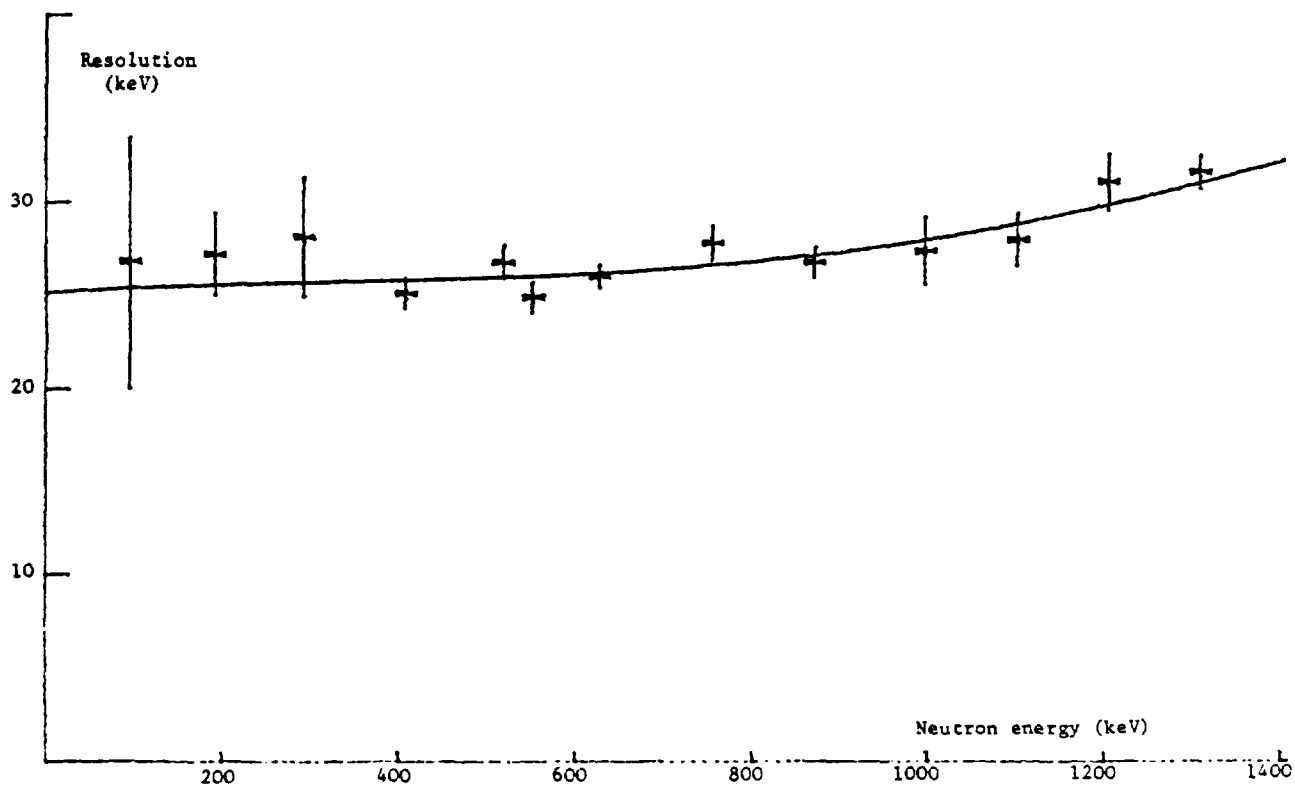

Figure 7: Resolution of the ^{3}He spectrometer as a function of neutron energy.

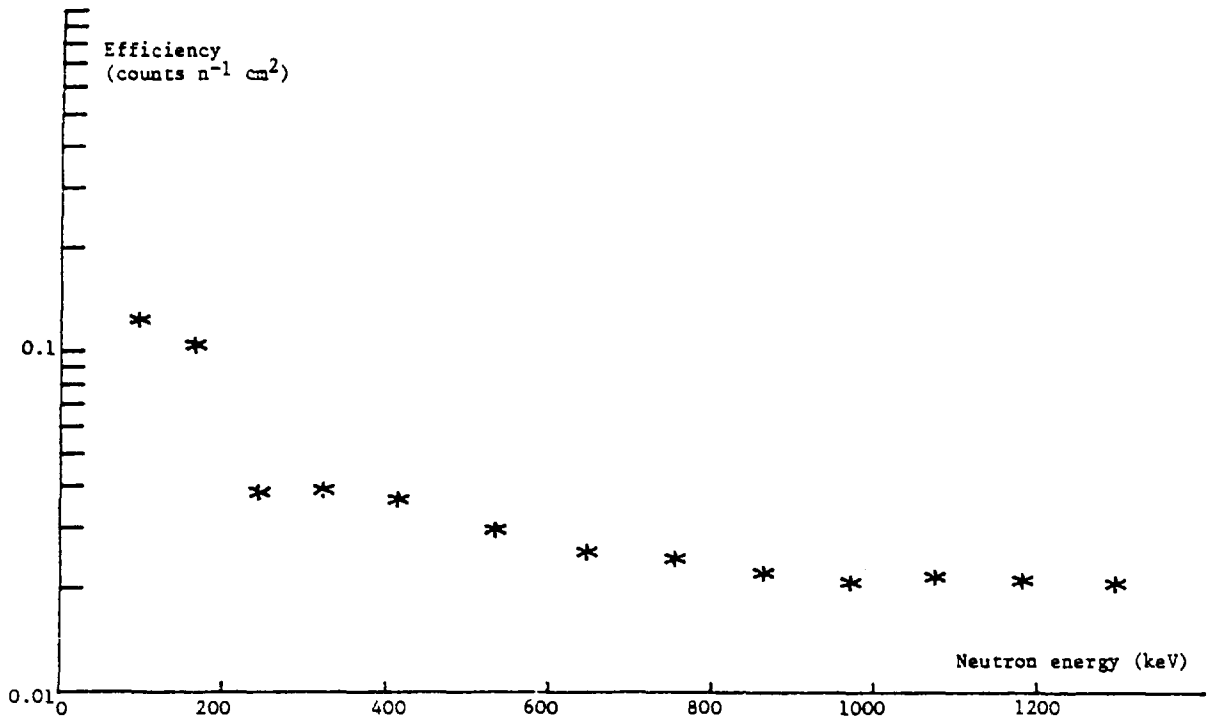

Figure 8: The total efficiency of the ^{3}He spectrometer.

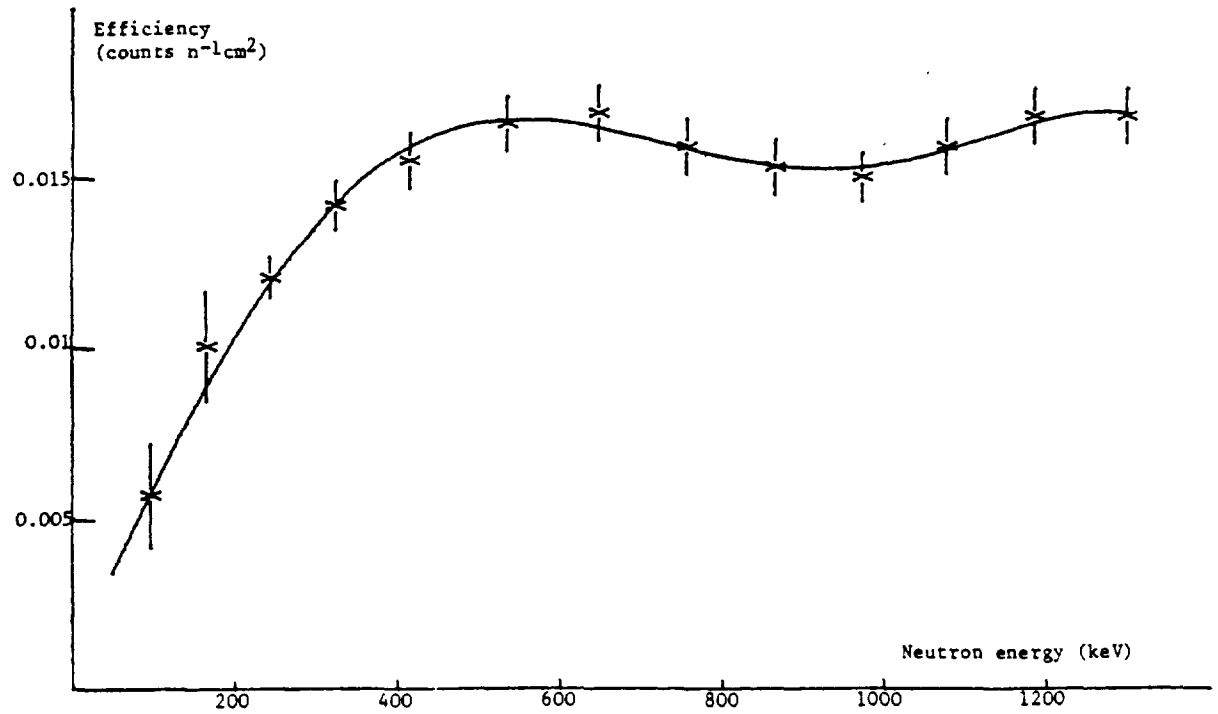

Figure 9: The efficiency of the ^{3}He spectrometer resulting from counts in the correct rise-time channels with energies greater than 15keV.

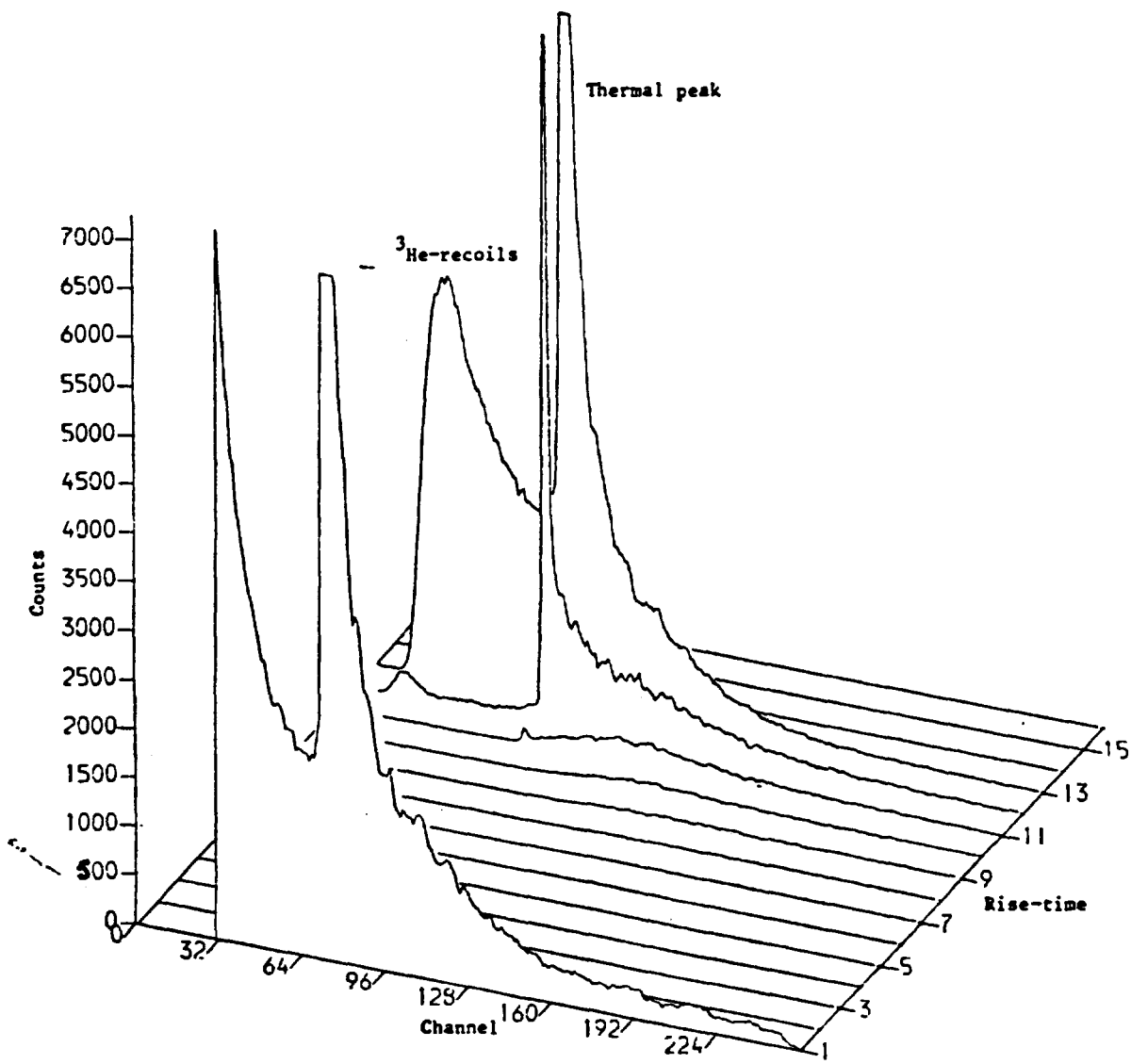

Figure 10: ^{3}He spectrometer response to a delayed neutron spectrum

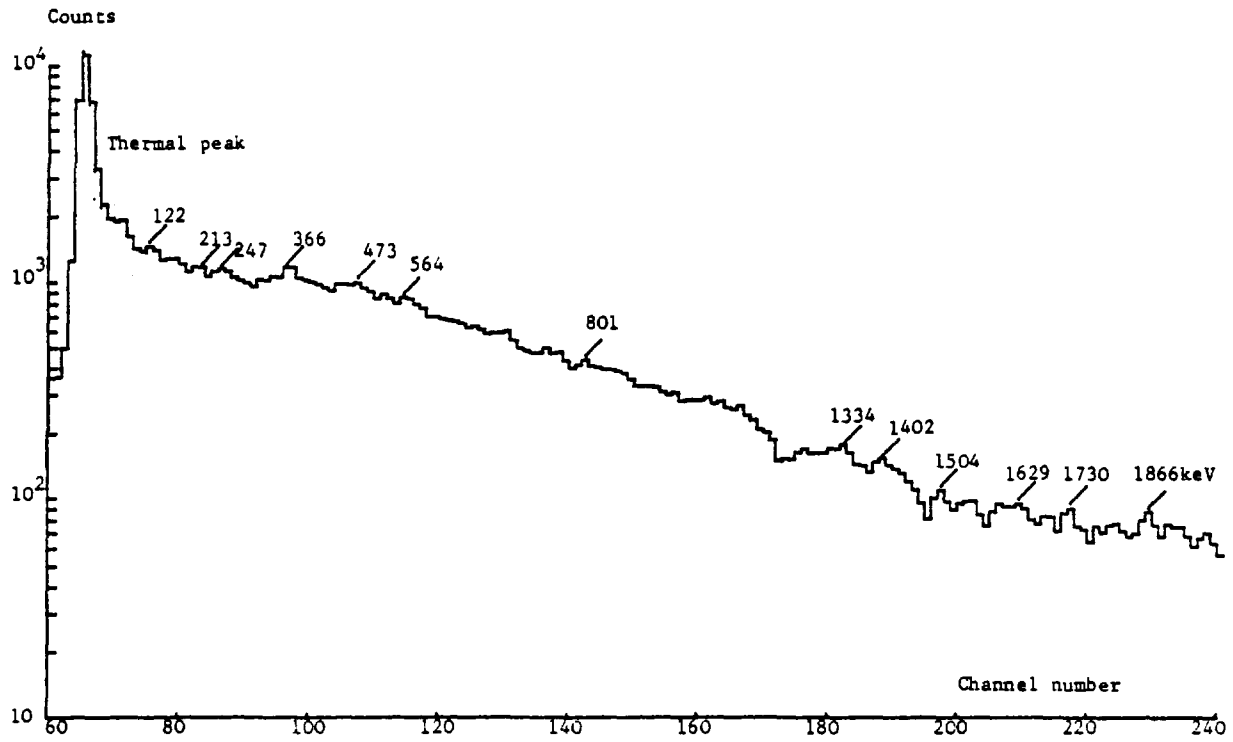

Figure 11: Delayed neutron pulse-height distribution for a fission energy of 940keV.

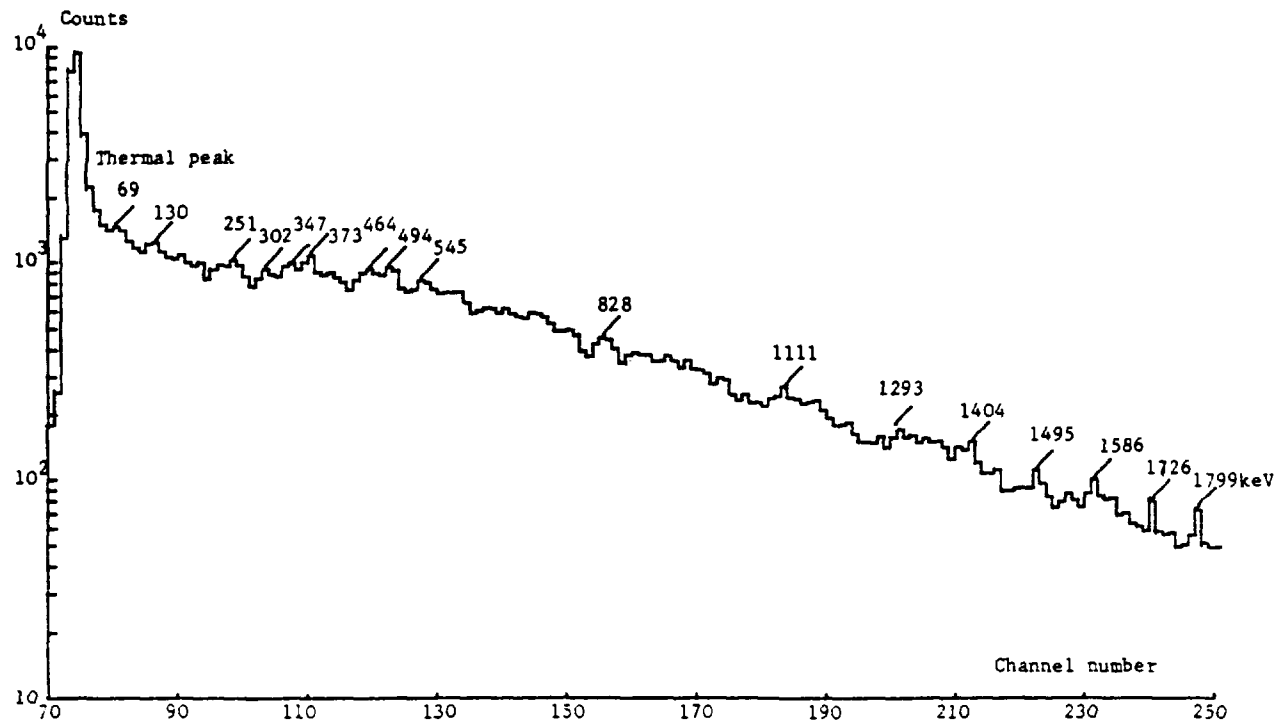

Figure 12: Delayed neutron pulse-height distribution for a fission energy of 1440keV.

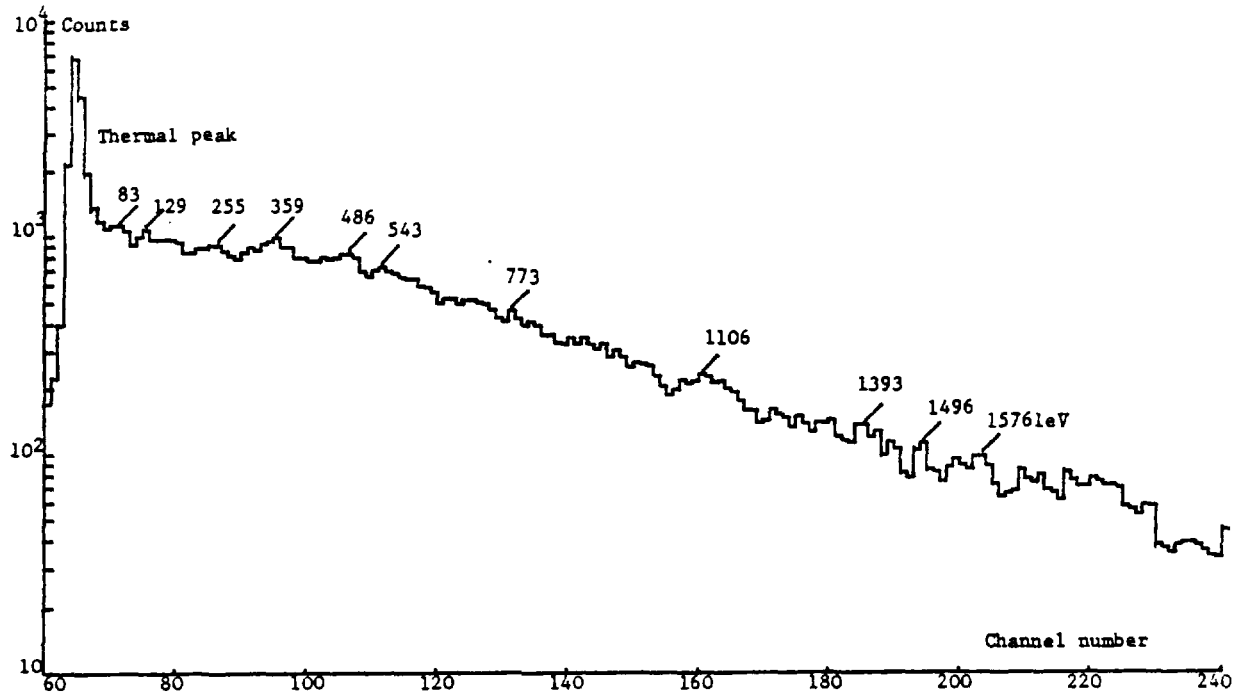

Figure 13: Delayed neutron pulse height distribution for a fission energy of 1760keV.

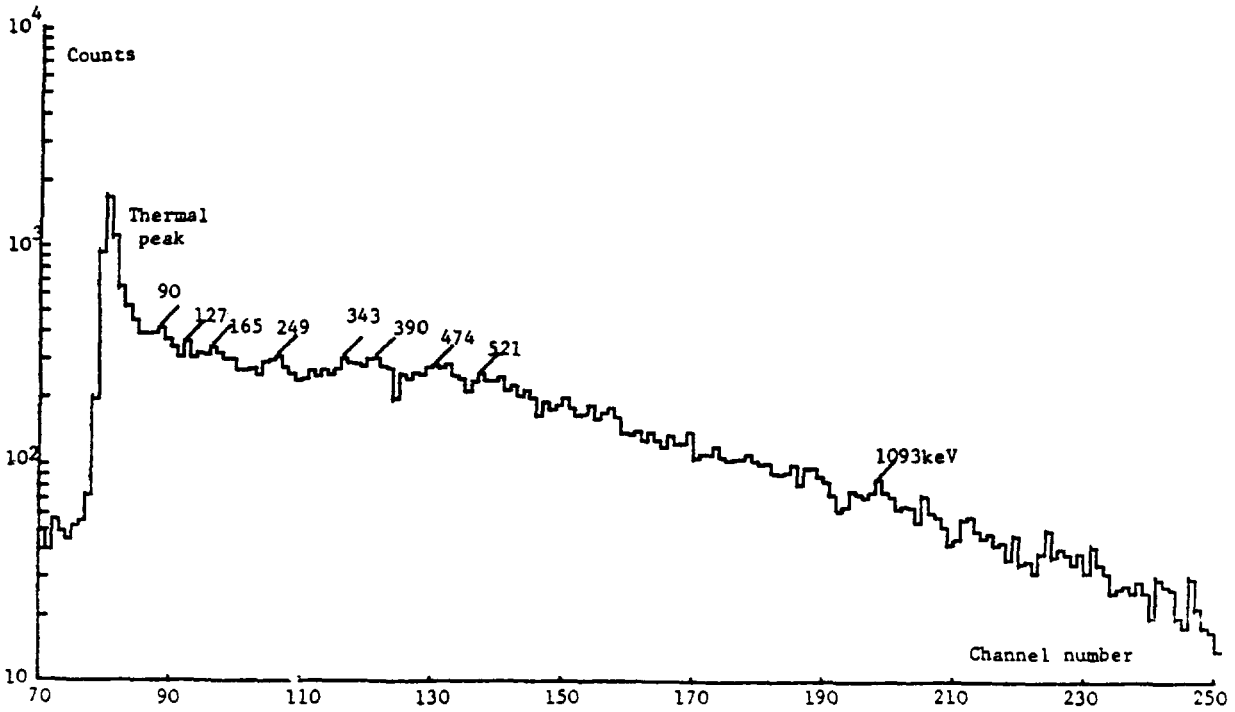

Figure 14: Delayed neutron pulse height distribution for a fission energy of 6MeV.

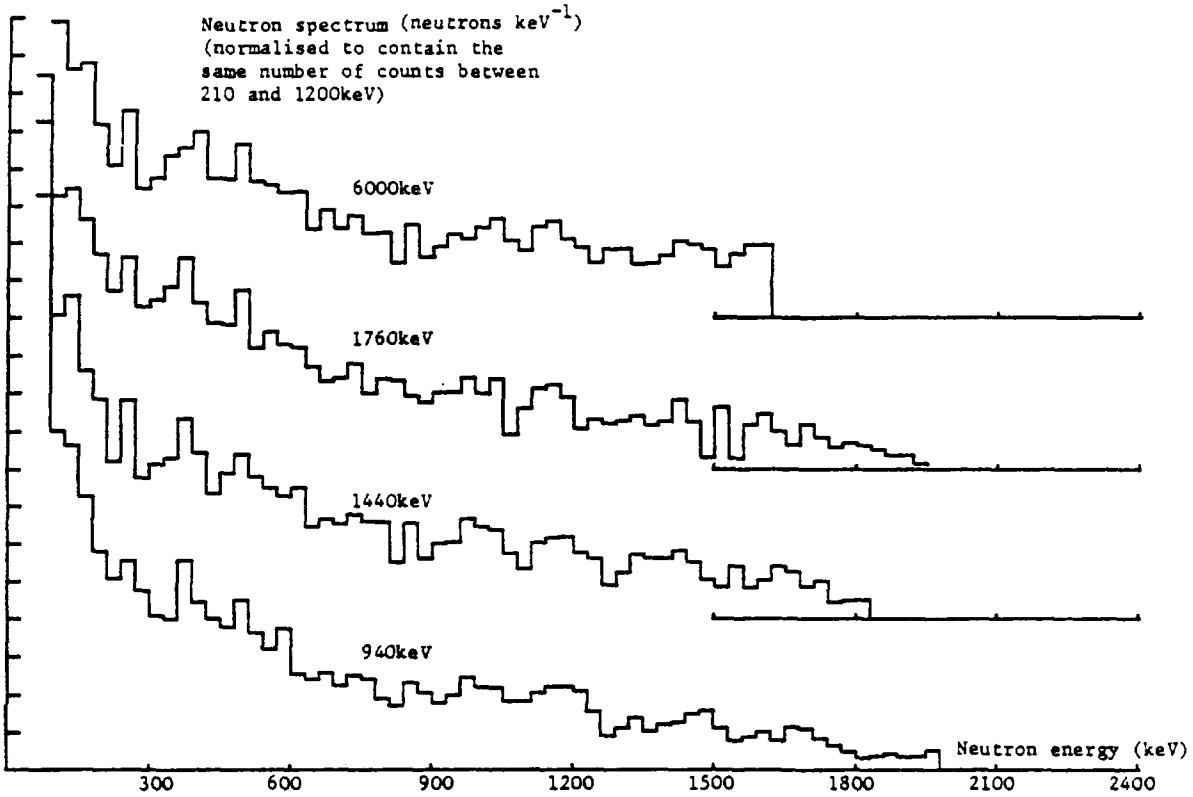

Figure 15: Final results, delayed neutron spectra produced at four primary neutron energies. (Estimates of uncertainties are given in the text).

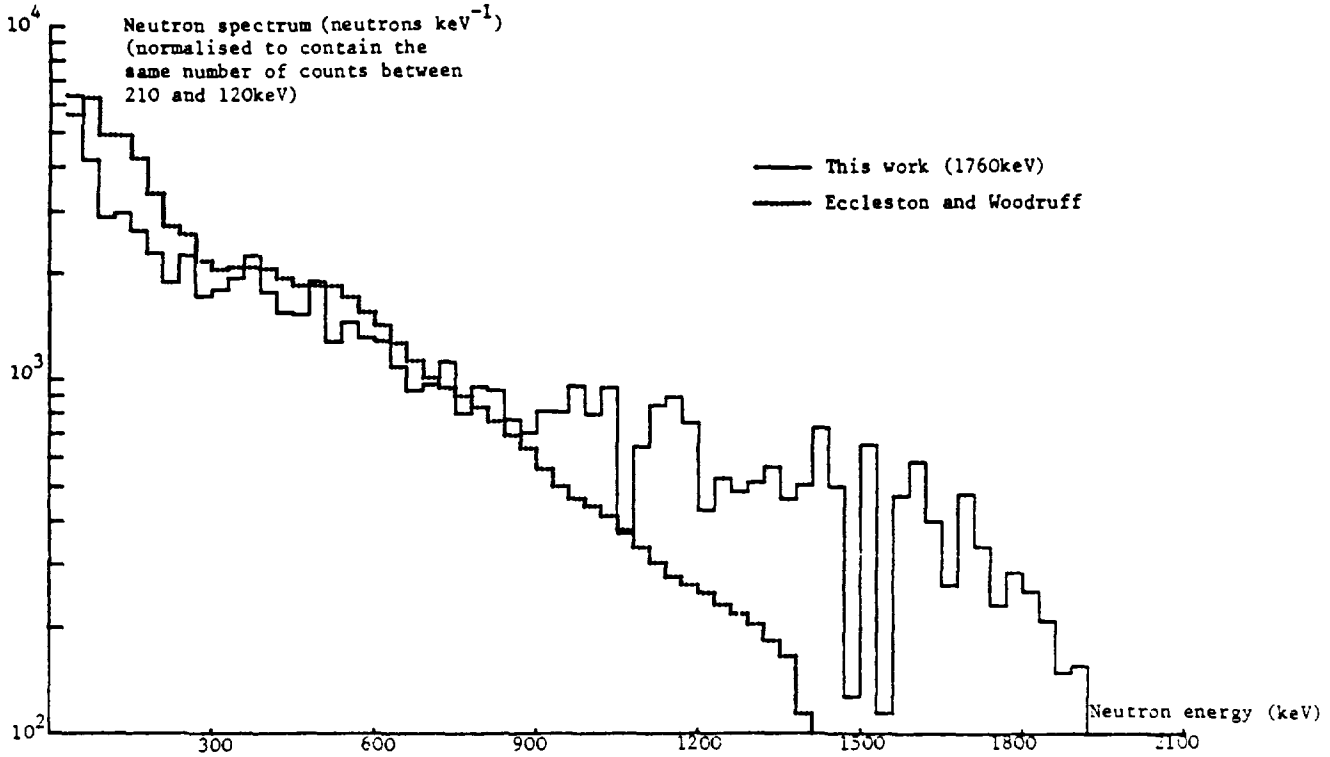

Figure 16: Comparison of this work and that of Eccleston and Woodruff.

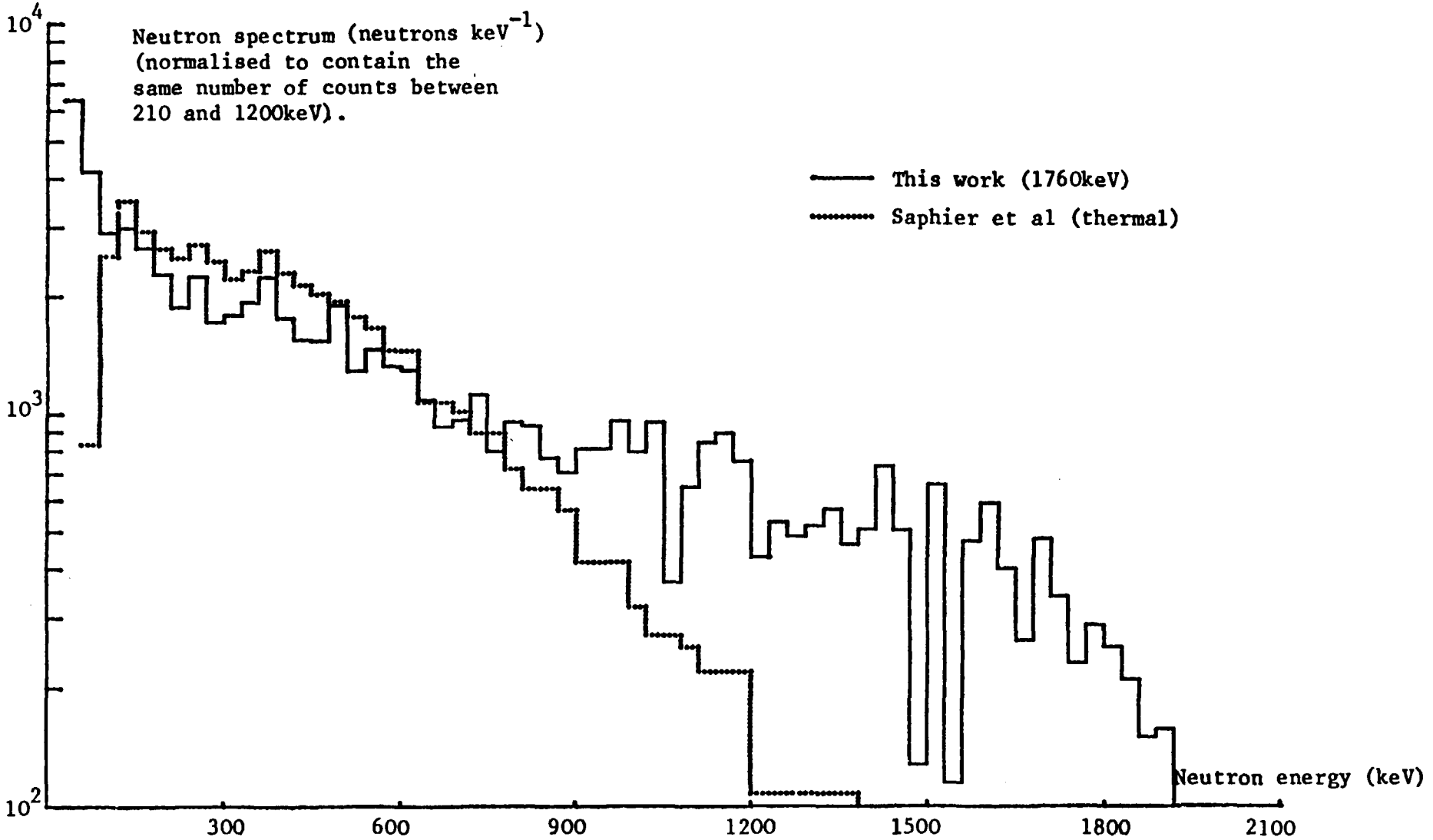

Figure 17: Comparison of this work and that of Saphier et al.

TABLE 1

Group Yields

Yields expected according to Keepin's group structure for this experiment, the work of Eccleston and Woodruff (reference 2), and the equilibrium yields from continuous irradiation.

Group	This Work	Eccleston and Woodruff	Equilibrium
1	0.039	0.040	0.038
2	0.221	0.224	0.213
3	0.195	0.197	0.188
4	0.419	0.421	0.407
5	0.114	0.108	0.128
6	0.012	0.010	0.026

TABLE 2

The Principal Peaks in the Delayed Neutron Spectra

(All energies are in keV)

THIS WORK				POSSIBLE PRECURSOR	Evans and Krick (3)	Shalev and Cuttler (5)	Sloan and Woodruff (21)
E_f=940keV	E_f=1440keV	E_f=1760keV	E_f=6.0MeV	(Peak energy in brackets)			
							33
							41
							60
	68			$^{137}I(77)$	68	75	76
		82	90				90
							103
128	130	129	127	$^{87}Br(130), ^{94}Rb(130),$			
				$^{89}Br(130), ^{141}Ga(140),$	125	125	129
				$^{139}I(130)$			
			165	$^{137}I(168), ^{95}Rb(155)$		170	161
					178	180	183
213				$^{87}Br(211), ^{93}Rb(200)$	205		210
247	251	255	249	$^{87}Br(248), ^{137}I(255,268)$	255	255	240

Table 2 continued.

THIS WORK				POSSIBLE PRECURSOR (Peak energy in brackets)	Evans and Krick (3)	Shalev and Cuttler (5)	Sloan and Woodruff (21)
E_f=940keV	E_f=1440keV	E_f=1760keV	E_f=6.0MeV				
						268	283
	302			^{87}Br(312), ^{93}Rb(305) !			
						320	
						325	
	342		343	^{87}Rb(339), ^{93}Rb(330)	343	355	351
366	373	360		^{137}I(372), ^{93}Rb(365)	370	375	
			390	^{137}I(390), ^{141}I+^{141}Cs(395)	380	390	
					418	420	420
						440	
473	464		473	^{87}Br(457), ^{93}Rb(460), ^{137}I(476)	467		
		486		^{139}I(485)	488	480	
	495			^{137}I(498), ^{134}Sn(500), ^{93}Rb(490), ^{85}As(495)	503	500	
			520	^{137}I(514), ^{85}As(516), ^{93}Rb(520)			

Table 2 continued.

THIS WORK				POSSIBLE PRECURSOR (Peak energy in brackets)	Evans and Krick (3)	Shalev and Cuttler (5)	Sloan and Woodruff (21)
E_f=940keV	E_f=1440keV	E_f=1760keV	E_f=6.0MeV				
	545	543		$^{89}Br(540), ^{137}I(555)$			552
564				$^{137}I(577)$	560	570	
					610		
						680	
					753	750	
		773		$^{137}I(767,756), ^{93}Rb(775)$			
	828						
					858	850	
881				$^{137}I(874)$			
					958	950	
			1093	$^{137}I(1092)$			
	1111	1106		$^{85}As(\simeq 1110)$			
					1160	1145	
	1293			$^{135}Sb(1280)$			
1334				$^{137}I(1320,1344)$			

Table 2 continued.

THIS WORK				POSSIBLE PRECURSOR	Evans and Krick (3)	Shalev and Cuttler (5)	Sloan and Woodruff (21)
E_f=940keV	E_f=1440keV	E_f=1760keV	E_f=6.0MeV	(Peak energy in brackets)			
1402	1404	1393					
1504	1495	1496					
	1586	1576					
1629							
1730	1728						
	1799						
1866				^{135}Sb(1897)			

TABLE 3

Results from the delayed neutron spectrum measurements

The relative counts per channel are given for 30keV wide channels. The base of the first channel corresponds to 30keV. No normalisation has been performed between separate measurements.

E_f = 940keV (± 378keV)

9815	5683	3352	3211	2702	2154	1890	2060
1773	1522	1483	2066	1659	1491	1404	1674
1350	1187	1391	950	897	960	834	936
896	712	642	860	765	669	746	910
818	809	684	689	766	826	821	779
584	338	423	522	388	456	478	557
596	421	286	336	387	292	434	413
311	239	177	120	144	163	128	139
195	0	0	0	0	0	0	0

E_f = 1440keV (± 324keV)

8647	5439	3319	3527	2702	2399	1731	2386
1554	1698	1766	2188	1827	1382	1605	1809
1569	1438	1344	1446	1005	1087	1034	1141
1053	1049	619	1042	661	828	839	1083
999	962	714	543	830	884	895	719
656	369	505	704	659	663	745	619
425	347	569	346	427	574	514	352
418	186	206	223	0	0	0	0

E_f = 1760keV (± 362keV)

5383	3543	2461	2529	2248	1931	1594	1903
1456	1518	1638	1897	1492	1306	1292	1603
1086	1231	1115	1089	920	785	818	944
676	806	787	651	597	688	686	812
673	803	313	546	714	755	638	363
445	408	435	480	391	428	619	423
108	553	97	397	495	338	222	402
287	195	242	214	177	127	133	47

Table 3 continued.

E_f = 6.0MeV (± 734keV)

2399	1680	1112	933	957	729	578	779
490	530	614	645	703	527	524	655
515	502	473	477	337	409	339	386
319	323	207	350	231	270	317	296
342	377	292	254	344	367	297	265
207	259	263	202	207	236	291	276
257	192	240	277	273	0	0	0

Uncertainties:

The combination of uncertainties on the efficiency and response function measurements are expected to give rise to ± 5% in the final spectra over the whole energy range. When combined with statistical variations in the number of counts in the pulse-height spectra a final ± 7% is expected in the 30keV bin width results for the energy region 100keV to 1MeV. Above 1MeV the poorer statistics cause a final uncertainty of 15-20%. Below 100keV the error is expected to be greater than 7% due to uncertainty in the scattering correction.

(Revision note: These data were presented graphically in Vienna, and supercede those in the original version of this paper. The revision incorporated new detector efficiency measurements from 1300 to 2000keV, later estimates of the peak shift in the various rise-time slices, and better correction for prompt neutron contributions by use of counts obtained from a Cf-252 source. Further measurements of the detector efficiency at energies below 100keV are in progress).

MEASUREMENT OF AVERAGE NEUTRON ENERGIES BY A COUNTING RATE RATIO TECHNIQUE *

P. L. Reeder and R. A. Warner

Pacific Northwest Laboratory
Richland, WA 99352

February 1979

ABSTRACT

Ratios of counts in rings of counter tubes embedded in different thicknesses of moderator are used to measure average energies of neutrons from spectral sources. This method offers a rapid technique for surveying a large number of spectral sources. Consistent agreement between average energies measured by the ring ratio technique and average energies calculated from the available spectra for Rb and Cs delayed neutron precursors has been achieved. Data for $^{92-98}$Rb and $^{141-147}$Cs are reported.

* Work Supported by The U. S. Department of Energy, Nuclear Sciences Division, under Contract EY-76-06-1830

MEASUREMENT OF AVERAGE NEUTRON ENERGIES BY A COUNTING RATE RATIO TECHNIQUE

I. INTRODUCTION

The concept of using the ratio of counts in banks of counter tubes embedded in different thicknesses of moderator has been used previously as a technique for obtaining average energies ($\bar{E}$) of neutron sources.[1] In a previous paper[2] (called "Paper I" hereafter) this ring ratio technique was applied to the measurement of $\bar{E}$ from precursors produced by the on-line mass spectrometer facility "SOLAR". The average energies reported in Paper I showed significant variations from one precursor to another as expected from the predictions of a simple model based on the "energy window" available for neutron emission. However, absolute values of $\bar{E}$ were dependent on a calibration curve of ring ratio versus neutron energy. This calibration curve was determined from measurements of monoenergetic neutrons from photoneutron sources, but significant corrections were required to account for weighting by the shape of the delayed neutron spectrum. The values for $\bar{E}$ determined by the ring ratio technique differed significantly from $\bar{E}$ values calculated from the spectra measured by Shalev and Rudstam by use of a ^{3}He ionization chamber spectrometer.[3] Because the corrections to the ring ratio calibration curve also were based on the Shalev and Rudstam spectra, it was disturbing that the two techniques generated inconsistent results.

Since the publication of Paper I, new measurements of the energy spectra of delayed neutrons from Rb and Cs precursors have become available from the OSTIS group.[4] These new spectra have much greater statistical accuracy, better resolution and extend as low as 10 keV in neutron energy. With the aid of several refinements to the ring ratio technique and the use of the new spectral data to correct the calibration curve, we are now able to get internal consistency between the ring ratio technique and $\bar{E}$ values calculated from spectral data. This gives us greater confidence in reporting $\bar{E}$ values measured by the ring ratio technique for several precursors for which spectral data do not exist.

Although it is clearly more desirable to have complete spectral data for all precursors, there are situations involving low neutron emission prob-

abilities or low fission yields where obtaining the spectral data would be quite difficult. The ring ratio technique, although limited to the measurement of $\bar{E}$ only, can give results after short running times and is useful for surveying a large number of precursors.

II. TECHNIQUE

The SOLAR on-line mass spectrometer facility has been described previously[5] and the ring ratio technique was discussed in Paper I. In the following discussion, we briefly review the ring ratio technique and describe the modifications which give greater reliability. The new calibration curve of ring ratio versus energy is given and results of ring ratio measurements for Rb and Cs delayed neutron precursors are presented.

A. Neutron Counter

The SOLAR Neutron Counter (SNC) described in Paper I contained 42 counter tubes embedded in polyethylene moderator. The tubes were arranged in three concentric rings about a central beam hole with 9 tubes in the inner ring, 9 tubes in the middle ring and 24 tubes in the outer ring. For the new series of measurements, only 40 tubes were available so two of the counter holes in the outer ring were filled with polyethylene rods. In order to increase the efficiency of the inner ring, extra polyethylene liners were added between the outer wall of the beam tube and the inner wall of the central beam hole. The liner downstream from the source was 10.8 cm long by 1.27 cm thick while the upstream liner was 12.1 cm long by 1.91 cm thick. A schematic diagram of the modified SNC is shown in Figure 1. The liner caused a large increase in the efficiency of the inner ring, a small increase in the efficiency of the middle ring, and almost no change in the efficiency of the outer ring. The effect of the liner was to increase the total efficiency for a typical delayed neutron spectrum by about 19%.

The counter tubes in each ring were connected in parallel to a separate preamplifier for each ring. The signals from each of the three preamplifiers went to separate amplifiers, discriminators, and scalers for each ring. Standard NIM electronics were used in place of the older elctronics used previously. Each day before taking data, the pulse height spectrum was checked for each ring. The standard procedure was to adjust the amplifier

gains to center the neutron peak in channel 90 of a 100 channel spectrum. The discriminator was adjusted to cut off pulses below channel 40 which was well above any noise pulses or gamma-ray pile up pulses. This gave about a 6% improvement in neutron counting efficiency over the use of channel 50 as was done in Paper I. With the discriminator set in channel 40, 87% of the neutron pulses were counted.

B. Absolute Efficiency of SNC

The absolute efficiency of the SNC was redetermined using the same procedures as given in Paper I. Photoneutron sources were calibrated against a known ^{252}Cf source by use of the Hanford precision long counter H2. The calibration experiments were performed in a large sub-basement room with the reactor off. The photoneutron source intensities were about the same as those used in Paper I, but the room background was about a factor of 10 lower. The background taken with a bare gamma source in the standard source position was less than 2% of the photoneutron count rate. Corrections of 2.9-3.6% were made for the room-return neutrons. The energy dependence of the precision long counter was taken from Ref. 6. The sources, neutron energies, emission rates and corresponding relative efficiencies of the precision long counter are given in Table I.

In Paper I, the energy of the $^{24}NaD_2O$ source was taken as 0.27 MeV which is based on the energy of the ^{24}Na gamma-ray and the binding energy of the neutron in deuterium. Because of concern whether the finite size of the photoneutron sources might degrade the neutron energy, the energy spectra of the $^{24}NaD_2O$ and $^{24}NaBe$ sources were measured using a ^{3}He ionization chamber detector. The measured FWHM for the $^{24}NaD_2O$ source was .043 MeV and for the $^{24}NaBe$ source, it was .036 MeV. The FWHM for the thermal neutron peak was .030 MeV. These data indicate that the neutron energy of the $^{24}NaD_2O$ source was considerably broader than the neutron energy from the $^{24}NaBe$ source. Moreover, by calibrating the energy scale with the thermal neutron peak as zero and the $^{24}NaBe$ peak as 0.83 MeV, the $^{24}NaD_2O$ peak was determined to be 0.22 MeV. Changing the $^{24}NaD_2O$ neutron energy from 0.27 MeV to 0.22 MeV had a relatively small effect on the efficiency curve but made a significant change in the ring ratio calibration curve.

TABLE I. Neutron sources used for absolute calibration

Source	Neutron energy (MeV)	Neutron emission rate (n/sec)[b]	Relative Efficiency of Long Counter
^{124}SbBe	0.024	7.4×10^3	.933
^{24}NaD_2O	0.22	1.5×10^3	.957
^{24}NaBe	0.83	6.4×10^2	.998
^{252}Cf	2.35[a]	1.92×10^5	.970
RaBe	3.9[a]	3.8×10^3	.896

[a]Average over neutron spectrum

[b]Emission rate calculated for 00:00 on June 8, 1978

The ^{252}Cf source was calibrated against a Hanford standard source as described in Paper I. The emission rate was measured with an uncertainty of 2%. No new calibrations were performed - the emission rate given in Table I was calculated from the previous value using the ^{252}Cf half-life of 2.63 yr. Because the ^{252}Cf source had decayed by almost a factor of 2, it was possible to count the ^{252}Cf source directly in the SNC although dead time corrections of up to 13% were required. The dead time of the SNC was determined by measuring the counting rates with 1, 3, 4, 5 and 9 tubes in the inner ring. The counting rate per tube was plotted versus number of tubes and the true count rate per tube was obtained by extrapolating this plot to zero tubes. The dead time was calculated for each of the five measurements and an average value of 5.15 μsec was obtained for the dead time.

All the sources listed in Table I were counted in the SNC at the position corresponding to the deposition point of the delayed neutron precursors. The neutron sources were also counted at a position 1.27 cm from the standard position inside the SNC in order to determine the slope of the efficiency versus position. The average value for the percentage change in efficiency was 2.7% per cm along the axis of the counter; i.e., a 1 cm uncertainty in source position causes a 2.7% uncertainty in counting efficiency

The efficiency of each ring is plotted as a function of neutron energy in Figure 2. The uncertainty in the efficiency for the ^{252}Cf is estimated to be 4% due to the 2% uncertainty in emission rate and 3.5% uncertainty in positioning the source in front of the precision long counter. The photoneutron sources were not point sources so an additional uncertainty of 5.5% was added to give an overall uncertainty of about 7%. The errors shown in Figure 2 include these uncertainties in absolute source strength. The efficiency curves for the monoenergetic sources in Figure 2 have been extrapolated to include the ^{252}Cf data even though ^{252}Cf is a spectral source.

Because the energy dependence of the inner and outer ring efficiencies are quite different, the ratio of counts in the outer to counts in the inner is a sensitive measure of the energy of the neutrons being counted. Likewise, the ratio of counts in the outer ring to the counts in the middle ring is an independent measure of the neutron energy. The uncertainty in the

absolute source strength cancels out when taking a ratio of counts in separate rings. Therefore, the errors shown on the absolute efficiency curves in Figure 2 do not apply to the ring ratio measurements.

C. Calibration of Ring Ratio Versus Energy

As discussed in Paper I, the ring ratio versus energy curve determined with monoenergetic sources does not represent the calibration curve required for sources having an energy spectrum such as the delayed neutron precursors. For monoenergetic sources, the ring ratio is just the ratio of counting efficiencies in the corresponding rings. However, for sources with a spectrum of neutron energies, the ring ratio is the ratio of effective efficiencies where the effective efficiency is defined as

$$\epsilon_{eff} = \frac{\int N(E)\ \epsilon(E)\ dE}{\int N(E)\ dE} \qquad (1)$$

In Eq. 1, N(E) is the neutron intensity as a function of energy and $\epsilon(E)$ is the efficiency of a particular ring as a function of energy. In Paper 1, the corrected calibration curve was obtained by calculating ratios of effective efficiencies using a number of delayed neutron spectra published by Shalev and Rudstam.[3] The calculated ring ratios were plotted versus the average energies of the Shalev and Rudstam spectra. Greatly improved spectra are now available from the work of Kratz, et al.[4] In particular, their measurements extend as low as 10 keV whereas the earlier spectra did not go below about 100 keV. Many important neutron peaks have been found in this low energy region. In the present work, we have used the new Rb and Cs delayed neutron spectra to calculate effective efficiencies for each ring. In Figure 2, these effective efficiencies are plotted versus the average energies calculated from the new spectra. The effective efficiencies for the inner ring lie above the curve based on monoenergetic sources while the effective efficiencies for the outer ring lie below the corresponding outer curve. Thus, a significant shift in the outer/inner ring ratio is observed between monoenergetic sources and spectral sources. The shift is not as great for the outer/middle ring ratio since the effective efficiencies of the middle ring lie close to the curve for monoenergetic sources.

The calibration curves corrected for neutron spectra are shown in Figure 3 for the outer/inner ring ratio and in Figure 4 for the outer/middle ring ratio. The ^{252}Cf and RaBe ring ratios lie on a single straight line with the calculated ring ratios for the delayed neutron sources. Thus the calibration curves are now valid up to much higher energies than were the curves in Paper I.

The slight scatter of points in Figure 3 and Figure 4 from the straight lines is an indication of the magnitude of the effect of different shape spectra on the calculated ring ratio. From among all the spectra available from the OSTIS group, the worst discrepancy in calculated ring ratios due to different spectral shapes occurs with ^{97}Rb and ^{85}As. For these two precursors, the calculated average energies are within 2% of each other. However, the calculated outer/inner ring ratios differ by 5.5% leading to a 25.4% difference in average energies obtained from the calibration curve of Figure 3. The calculated outer/middle ring ratios differ by 4.0% leading to a 23.1% difference in average energy obtained by use of the calibration curve in Figure 4. Generally, the deviations from the calibration curve are much less than the numbers given for ^{97}Rb and ^{85}As.

Kratz, et al,[4] have already noted that odd mass precursors tend to have more peaks in the energy spectrum than the even mass precursors. In Figure 3 and Figure 4, the odd mass precursors are shown as closed points and the even mass precursors as open points. The differences due to odd or even character do not appear to affect the calculated ring ratios to any great extent.

III. APPLICATION

A. Data Collection

Experimental values for the ring ratios of Rb and Cs delayed neutron precursors were measured in conjunction with measurements of P_n values to be reported elsewhere. Neutron counts from each of the three rings were recorded continuously during repetitive cycles of ion beam-on and ion beam-off.

During beam-on, the ions were deposited on the first dynode of an electron multiplier located inside the beam hole of the SNC. During beam-off, the ion beam was stopped at an electrostatic deflector and slit assembly located about 2.4 m from the SNC. In Paper I, the ion beam had been switched off at the ion source. However, a test showed that having ion beam present at the electrostatic deflector increased the background in the SNC by 5%. Thus switching the ion beam off at the deflector more truly represented the actual background during beam-on. Background rates were determined after each data run by counting for 300 sec in the beam-off mode. Background rates were constant as long as the oven was kept at a constant temperature. Background counts measured on the same day at the same temperature were combined to give greater statistical accuracy. Background rates in the present experiments were about 10 times higher than the rates obtained in Paper I. This was due to the 10-times higher neutron flux at the target and the corresponding increase in the production of neutral gaseous fission products which diffused into the counter in spite of two stage differential pumping. (See Appendix I.)

The performance of the SNC was monitored daily with the ^{252}Cf source before starting any data runs. The ^{252}Cf source could not be counted at the ion beam deposition point when the SNC was in place on the SOLAR beam pipe. However, a new position for the source was established which could be accurately reproduced without removing the SNC from the beam pipe. The ratio of ^{252}Cf counts in each of the three rings between the new standard position and the ion-beam deposition position was carefully determined. With the new electronics, the SNC was very stable over the four month data collection period and only minor adjustments to the amplifer gains were necessary to keep the neutron peak amplitude fixed relative to the discriminator level. The count rates in each of the three rings were constant to within 1% and no unexplained variations in ring ratios were observed.

Most of the ring ratio data reported here were taken with a 17-stage electron multiplier and its tube base located in the SNC beam hole. However, a set of 11 data runs was taken using a thin Al window and a Si beta detector in place of the electron multiplier. The ring ratios taken with the Si detector in place were significantly different from those taken with the electron multiplier in place. The effects could be explained by assuming

that the electron multiplier and its associated beam pipe and tube base caused a 6.9% reduction in the efficiency of the inner ring, a 2.1% reduction in the efficiency of the middle ring and no change in the efficiency of the outer ring. The above changes in efficiency can not be explained by any possible change in ion beam deposition point between the two configurations. The most likely cause for absorbtion of neutrons is probably the presence of boron in the glass liner used to insulate the electron multiplier from the walls of the beam tube. This liner was not present when the Si detector was in place nor during the calibration experiments with photoneutron sources. The above normalization factors for the inner and middle rings were therefore applied to all the data taken with the electron multiplier.

The ratios of net outer counts to net inner counts and net outer counts to net middle counts were calculated for each data run. Weighted average outer/inner and outer/middle ring ratios were calculated for each precursor. Weighting factors were based solely on the statistical counting uncertainties.

B. Results

The weighted average ring ratios for the Rb and Cs precursors measured in the present experiments are listed in Table II. The error for an experimental ring ratio was based on the formula:

$$\sigma = (\Sigma\, \sigma_i^{-2})^{-\frac{1}{2}} \qquad (2)$$

where σ_i was taken only from the counting statistics. The distribution of individual results was accounted for by multiplying Equation 2 by the square root of chi-square per degree of freedom whenever this factor exceeded unity. Also listed in Table II are the calculated ring ratios based on the effective efficiencies calculated according to Equation 1 using the energy spectra of Kratz, et al.[4] It can be seen that the measured ring ratios are in reasonable agreement with the calculated ring ratios which implies that the corresponding average energies will also be in agreement.

The experimental ring ratios were converted to average energies by use of the calibration curves shown in Figure 3 and Figure 4. A simple exponential expression was obtained by a least squares fit to the data points shown in each figure. Average energies and uncertainties were calculated from the analytical expression. The average energy for a given precursor was taken as the unweighted average of the values from the outer/inner and outer/middle

TABLE II. Ring ratios for delayed neutron precursors in SNC

Mass	O/I (Exp.)[a]	O/I (Calc.)[b]	O/M (Exp.)[a]	O/M (Calc.)[b]
		Rb Precursors		
92	.509±.027 (3)		1.066±.108 (3)	
93	.678±.003 (6)	.658	1.197±.005 (6)	1.167
94	.678±.002 (14)	.688	1.201±.003 (14)	1.203
95	.666±.004 (14)	.660	1.190±.007 (14)	1.189
96	.678±.016 (9)	.652	1.212±.025 (9)	1.167
97	.728±.008 (3)	.737	1.248±.018 (3)	1.269
98	.693±.172 (1)		1.662±.557 (1)	
		Cs Precursors		
141	.556±.030 (3)	.564	1.045±.094 (3)	1.054
142	.526±.014 (6)	.579	1.016±.031 (6)	1.075
143	.573±.005 (8)	.593	1.103±.008 (8)	1.086
144	.561±.006 (9)	.608	1.085±.017 (9)	1.110
145	.625±.006 (7)	.630	1.149±.021 (7)	1.128
146	.656±.040 (5)	.640	1.237±.083 (5)	1.151
147	.697±.303 (1)			

[a]Numbers in parentheses are number of determinations

[b]Calculated from absolute efficiency curves for SNC and delayed neutron spectra from Kratz, et al.[4]

TABLE III. Average energies (keV) of delayed neutron spectra determined by ring ratios in the SNC and by calculations from spectra measured by ^{3}He spectrometers.

Mass	SOLAR (SNC)	SOLAR (^{3}He)[a]	OSTIS (^{3}He)[b]	OSIRIS (^{3}He)
		Rb Precursors		
92	200±85			
93	482±11	390	414	340
94	486± 7	420	474	350
95	454±15	470	508	520
96	500±59		481	
97	650±46		754	
98	>303			
-		Cs Precursors		
141	216±76		213	270
142	182±24		252	200
143	267±10	390	276	240
144	245±16		312	280
145	356±27		331	
146	500±183		406	
147	>69			

[a]Ref. 7

[b]Ref. 4

[c]Ref. 8

ring ratios. The experimental average energies from the ring ratio technique are listed in Table III. The symmetric errors associated with the experimental ring ratios give rise to non-symmetric errors when converted to average energy. For simplicity, the errors shown with the average energy in Table III are just an average of the errors resulting from both ring ratios. The errors do not take into account possible deviations from the calibration curve due to different spectral shapes. As discussed in Section II C above, the uncertainties due to spectral shape are thought to be less than ±10% of the energy quoted in Table III. In two cases, the errors on the ring ratios were large and only the lower limit of the average energy is given.

C. Discussion

The average energies obtained by the ring ratio technique and shown in Table III can be compared to average energies calculated from measured delayed neutron spectra. Spectra measured with ^{3}He ionization chamber detectors have been reported by three laboratories. The first set of spectra were reported by Shalev and Rudstam working at the OSIRIS on-line separator facility.[3] Average energies calculated from these spectra may be suspect because the spectra could not be measured below 100 keV and may also be contaminated by scattered neutrons. The spectra measured by Kratz and co-workers at the OSTIS facility have good statistics, excellent resolution and extend as low as 10 keV.[4] The statistical and systematic errors in the average neutron energy are thought to be 20 to 50 keV. The four spectra which we have measured at the SOLAR facility suffer from poorer statistics and not quite as good resolution but do extend down to about 20 keV.[7] All three groups have had to measure the efficiency of their ^{3}He spectrometers in separate experiments using monoenergetic neutrons from accelerators.

Because the calibration curve for the ring ratio technique is based on the effective efficiencies calculated using the OSTIS spectra, one might expect close agreement between the two techniques. To illustrate the degree of agreement or disagreement, we have plotted in Figure 5 the average energies determined by the ring ratio technique versus average energies from the OSTIS spectra. Many of the data points do fall on a 45^{o} line as expected, but five points deviate outside the estimated error from counting statistics.

In two cases, ^{95}Rb and ^{97}Rb, the deviations are comparable to what one expects from the scatter of calculated ring ratios relative to the least squares fitted calibration curve. This scatter was ascribed to spectral shape differences in Section II C. For ^{93}Rb, the deviation is more than four times the deviation expected from the spectral shape dependence and about 8 times the statistical uncertainty. For this odd mass precursor, the deviation is toward a higher $\bar{E}$ measured by the ring ratio technique. For the even mass precursors ^{142}Cs and ^{144}Cs, the deviations are toward lower $\bar{E}$ values measured by the ring ratio technique. For ^{142}Cs and ^{144}Cs, the combined rms uncertainty due to counting statistics is ±10.5%, whereas the rms deviation of the experimental $\bar{E}$ values from the $\bar{E}$ calculated from the spectra is 25.6%. The rms deviation expected from spectral shape considerations is only 2.9% - far less than the actual deviations. Overall, the present data suggest the possibility that spectral shape differences related to odd/even mass character are more pronounced than the present spectral data allow. However, additional data are needed to clarify this situation.

IV. CONCLUSION

In this work we have shown that by use of a few well known delayed neutron spectra, a calibration curve can be derived for the average energy as a function of ring ratio. This calibration curve gives consistent agreement between the average energies determined by ring ratios and average energies calculated from the spectra used to derive the calibration curve. The calibration curve can then be used to determine average energies from ring ratio data for those precursors for which spectral data do not exist. In the present work we have used this procedure to determine the average energy of ^{92}Rb and lower limits for the average energies of ^{98}Rb and ^{147}Cs.

The significant changes which improved the calibration curve beyond the one used in Paper I were:

a. The use of spectral data from the OSTIS group
b. The normalization of ring ratio data taken with an electron multiplier in the SNC beam hole to ring ratio data taken in a configuration more closely representing the calibration con-

figuration (Si beta detector in SNC beam hole).

c. The shift of the energy of the $^{24}NaD_2O$ monoenergetic source from 0.27 MeV to 0.22 MeV.

ACKNOWLEDGMENT

We wish to acknowledge the kind assistance of Professor O. K. Harling of MIT in providing the loan of the 40 ^3He counter tubes used in this work.

APPENDIX I

Average Energy of Gaseous Fission Products

The background in the neutron counter can be attributed to three sources - cosmic ray and electronic noise, operation of the TRIGA reactor, and delayed neutrons from neutral gaseous fission products. The relative contributions from each source are given in Table A1.

TABLE A1. BACKGROUND COUNTING RATES (COUNTS/SEC) DUE TO VARIOUS SOURCES

Ring	Cosmic ray and Noise	Reactor	Kr, Xe
Inner	.38	.57	2.34 - 6.15
Middle	.11	.50	1.36 - 3.40
Outer	.29	1.17	1.57 - 4.08
Total	.78	2.24	5.27 -13.63

The gaseous background depended on the operating temperature of the oven. At each temperature the cosmic ray and reactor contributions were subtracted from the measured background counting rates to give a set of counts representing only the contribution from gaseous activities. Outer/inner and outer/middle ring ratios were calculated for this gaseous component and plotted versus inner background count rate (which was found to be a function of oven temperature). No significant trends could be observed in these plots. Either the distribution of gaseous fission products was independent of oven temperature or else the ring ratio was insensitive to whatever changes might have occurred. It was therefore assumed that the average value of all the gaseous background ring ratios was indicative of the average delayed neutron energy

of whatever gaseous fission products were present. The average values for the outer/inner and outer/middle ring ratios were 0.632 ± .008 and 1.174 ± .014 respectively for 13 measurements. From the calibration curves of Figures 3 and 4, a final value of 390 ± 25 keV is obtained for the average energy of the delayed neutrons from gaseous precursors.

It is possible to estimate the contributions of individual gaseous precursors to this background. If decay losses prior to the activities reaching the neutron counter are ignored, one can consider three Kr and three Xe precursors as contributing. These precursors are listed in Table A2 along with their half-lives, cumulative fission yield (CFY), delayed neutron emission probabilities per precursor decay (P_n), and calculated delayed neutron yields (DNY).

TABLE A2 GASEOUS DELAYED NEUTRON PRECURSORS

Precursor	Half-Life (sec)	CFY[a] (%)	P_n[b] (%)	DNY = (CFY)(P_n) (10^{-4})
^{92}Kr	1.85	1.697	.033	.056
^{93}Kr	1.29	.524	2.1	1.10
^{94}Kr	.208	.254	2.2	.56
^{141}Xe	1.73	1.329	.043	.057
^{142}Xe	1.24	.447	.406	.181
^{143}Xe	.30	.054	2.6	.139

[a]Recommended cumulative fission yield from M. E. Meek and B. F. Rider NEDO-12154-2, Jan.(1977) (unpublished).

[b]Ref. 8

The time required for neutral gases to diffuse from the oven to the neutron counter (a distance of about 7 m) is not known precisely. However, the precursors ^{94}Kr and ^{143}Xe with half-lives much less than 1 sec are not expected to contribute significantly. Of the remaining gaseous precursors, ^{93}Kr probably contributes about 80% of the observed background and is primarily responsible for the measured average energy of 390 $\pm$ 25 keV.

APPENDIX II

Average Neutron Energy of Delayed Neutron Precursors from Revised 1976 Ring Ratio Data

The average energies based on ring ratio data published in Paper I were redetermined using the modifications described in this paper. Specific changes were 1) the use of 0.22 MeV for the energy of the $^{24}NaD_2O$ source and 2) the use of the delayed neutron spectra from OSTIS to calculate effective efficiencies. No correction for the presence of the electron multiplier was needed here. The 1976 data were not taken with polyethylene liners close to the glass liner of the electron multiplier so neutrons were probably not being thermalized in the vicinity of the glass (with its unknown boron content).

In Paper I, data taken with three neutron scalers were treated separately from experiments done with only two scalers available. For this revised analysis, this distinction was not made.

The revised average energies are presented in Table A3. The errors shown in Table A3 are somewhat larger than those given in Paper I because we now take the distribution of independent results into account when calculating the error of a mean. The average energies for Rb and Cs precursors now agree well with the recent ring ratio data. Table A3 includes some values for Br and I precursors which were not measured in our recent work.

Table A3. Average Energy of Delayed Neutrons Based on 1976 Ring Ratio Data

Precursor	$\bar{E}$ (keV)
^{87}Br	131 ± 30
^{88}Br	231 ± 57
^{89}Br	552 ± 377
^{92}Rb	112 ± 41
^{93}Rb	477 ± 41
^{94}Rb	461 ± 26
^{95}Rb	460 ± 24
^{96}Rb	474 ± 32
^{97}Rb	750 ± 99
^{98}Rb	> 89
^{137}I	> 94
^{141}Cs	101 ± 41
^{142}Cs	62 ± 23
^{143}Cs	254 ± 23
^{144}Cs	215 ± 19
^{145}Cs	382 ± 26
^{146}Cs	> 550

APPENDIX III

Summary of Average Neutron Energies of Fission Product Delayed Neutron Precursors.

In Table A4 are presented the existing data on average neutron energies measured for separated precursors. The 1976 and 1978 SOLAR data are based on the ring ratio technique. Three groups have reported delayed neutron spectra taken with ^{3}He ionization chambers. Average energies have been calculated from the experimental spectra.

Table A4. Summary of Average Neutron Energies of Delayed Neutron Precursors

Z	A	1976 SOLAR[a]	1978 SOLAR[b]	^{3}He SOLAR[c]	^{3}He Mainz[d]	^{3}He OSIRIS[e]
Zn, Ga	79					250
Ga	80					240
Ga	81					370
As	85				728	610
Br	87	131 ± 30			217	170
Br	88	231 ± 57				260
Br	89	550 ± 380				470
Br	90					460
Br	91					510
Kr	93		390 ± 25			
Rb	92	112 ± 41	200 ± 85			
Rb	93	477 ± 41	482 ± 11	442	414	340
Rb	94	461 ± 26	486 ± 7	460	474	350
Rb	95	460 ± 24	454 ± 15	527	508	520
Rb	96	474 ± 32	500 ± 59		481	
Rb	97	750 ± 99	650 ± 46		754	
In	129					550
In	130					420
Sn	134					540
Sb	135				1033	610
Te	136				325	220
I	137				579	510
I	138				467	390
I	139					370
I	140					450
Cs	141	101 ± 41	216 ± 76		213	270[f]
Cs	142	62 ± 23	182 ± 24		252	200[g]
Cs	143	254 ± 23	267 ± 10	390	276	240
Cs	144	215 ± 19	245 ± 16		312	280
Cs	145	382 ± 26	356 ± 27		331	
Cs	146		500 ± 183		406	

a. P. L. Reeder, J. F. Wright and L. J. Alquist, Phys. Rev. C 15, 2098 (1977) (Data revised in 1979 by P. L. Reeder and R. A. Warner)

b. P. L. Reeder and R. A. Warner, to be published.

c. P. L. Reeder, in Proceedings of Ames-BNL Workshop on ISOL Systems, BNL 50847. (Revised data - 1979).

d. K. L. Kratz, in Proceedings of Second Advisory Group Meeting on FPND, Petten, September 1977.

e. G. Rudstam, in Proceedings of Second Advisory Group Meeting on FPND, Petten, September 1977.

f. Combined ^{141}Cs + ^{141}I

g. Combined ^{142}Cs + ^{142}Xe

REFERENCES

1. L. V. East and R. B. Walton, Nucl. Instrum. Methods 72, 161 (1969).

2. P. L. Reeder, J. F. Wright and L. J. Alquist, Phys. Rev. C 15, 2098 (1977).

3. S. Shalev and G. Rudstam, Nucl. Phys. A230, 153 (1974); G. Rudstam and S. Shalev, Nucl. Phys. A235, 397 (1974); and S. Shalev and G. Rudstam, Nucl. Phys. A275, 76 (1977).

4. K. L. Kratz, Proceedings of Second Advisory Group Meeting on FPND, Petten, Sept. 1977. K. L. Kratz, H. Ohm, M. Zendel, J. Crancon, C. Ristori, K. D. Wünsch, G. Jung, and M. Asghar, Jahresbericht 1976, Institute für Kernchemie der Universität Mainz, June 1977. H. Ohm, K. L. Kratz, C. Ristori, J. Crancon, K. D. Wünsch, and G. Jung, Jahresbericht 1977, Institute fur Kernchemie der Universität Mainz, May 1978.

5. J. J. Stoffels, Nucl. Instrum. Methods 119, 251 (1974).

6. J. DePangher and L. L. Nichols, Battelle, Pacific Northwest Laboratories, Report No. BNWL-260, 1966 (unpublished).

7. P. L. Reeder, Proceedings of Ames-BNL Workshop on ISOL Systems, BNL-50847, July 1978.

8. G. Rudstam, Proceedings of Second Advisory Group Meeting on FPND, Petten, September 1977.

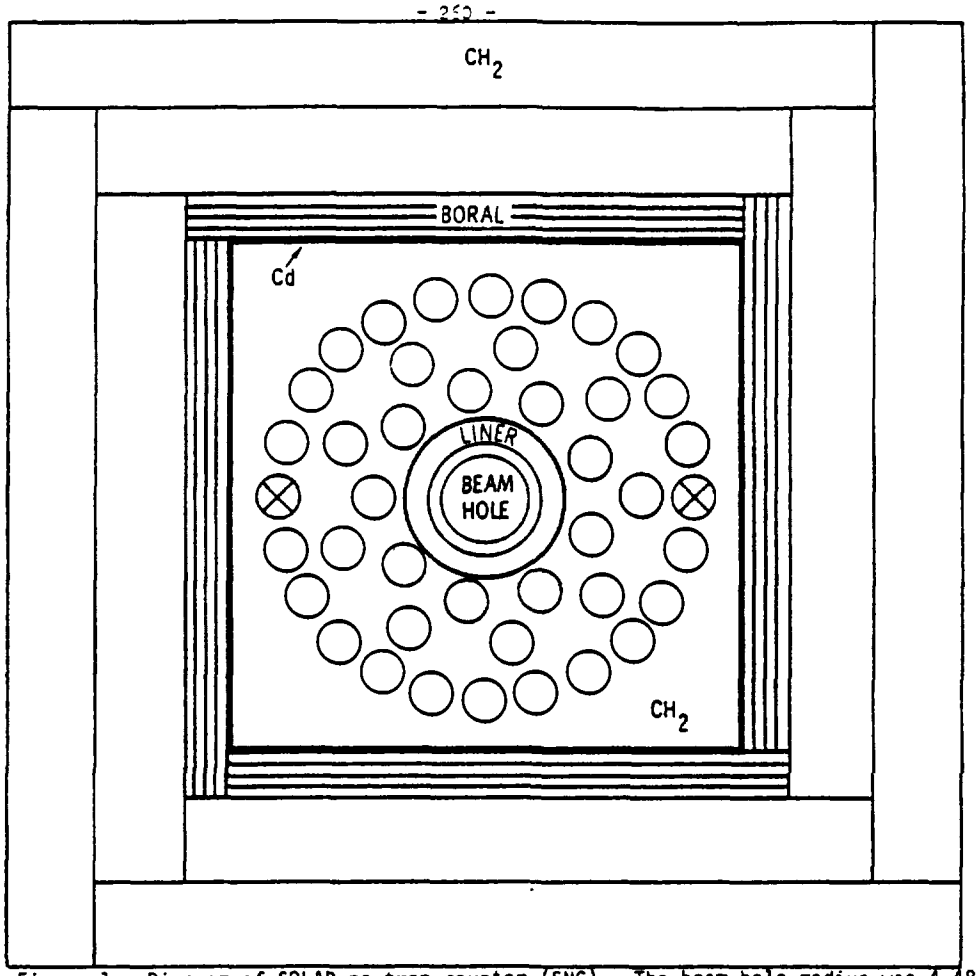

Figure 1. Diagram of SOLAR neutron counter (SNC). The beam hole radius was 4.48 cm before the addition of the polyethylene liners. The radii of the inner, middle and outer counter rings were 6.35, 8.89 and 12.07 cm, respectively. ⊗ Counter hole filled with polyethylene.

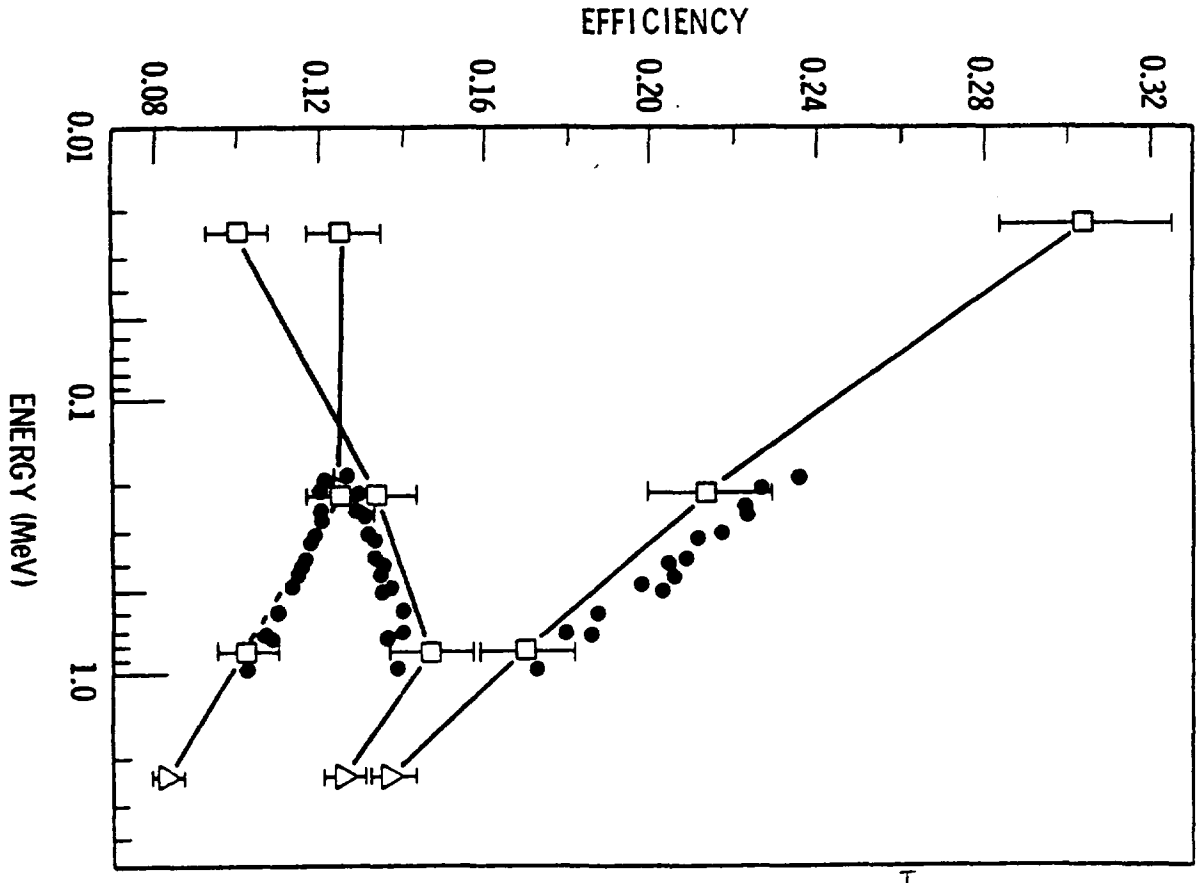

Figure 2. Absolute efficiency of the SNC versus neutron energy. ⊟ Photoneutron sources, ⊥ ^{252}Cf, ○ Effective efficiencies calculated for delayed neutron sources.

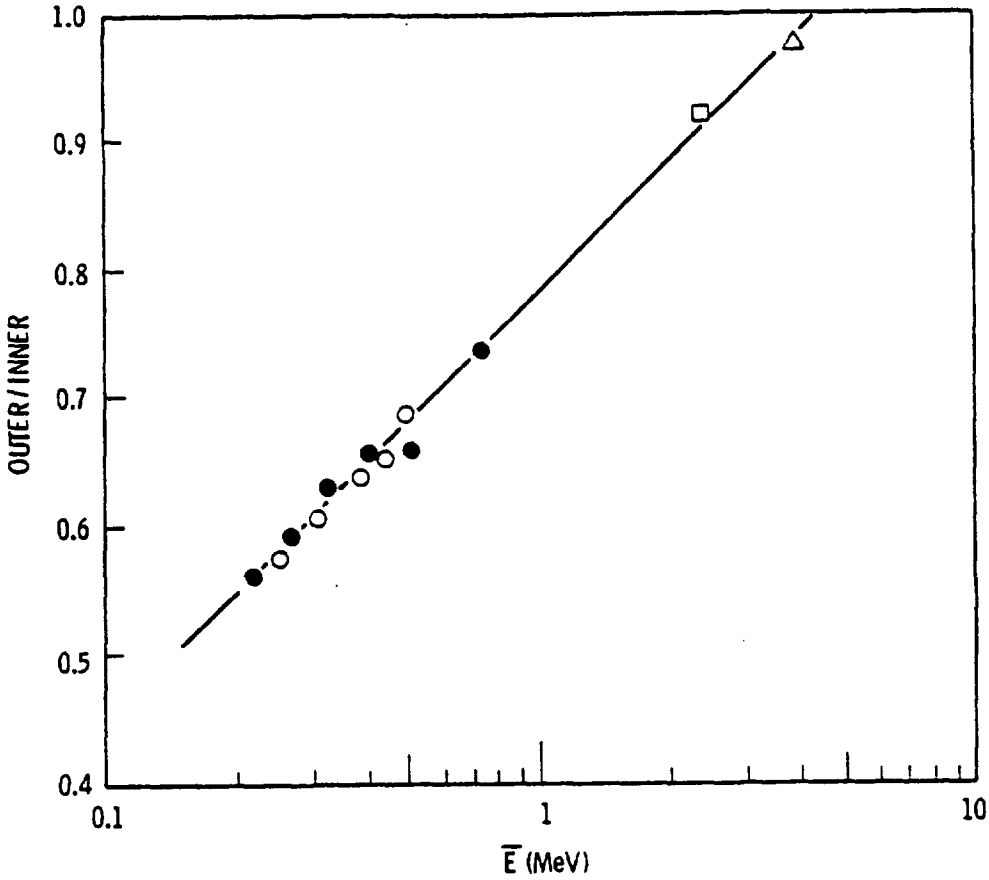

Figure 3. Outer to inner ring ratio corrected for spectral sources versus calculated average energy.

● Odd-mass Rb, Cs delayed neutron precursors

○ Even-mass Rb, Cs delayed neutron precursors

□ ^{252}Cf

△ $^{226}RaBe$

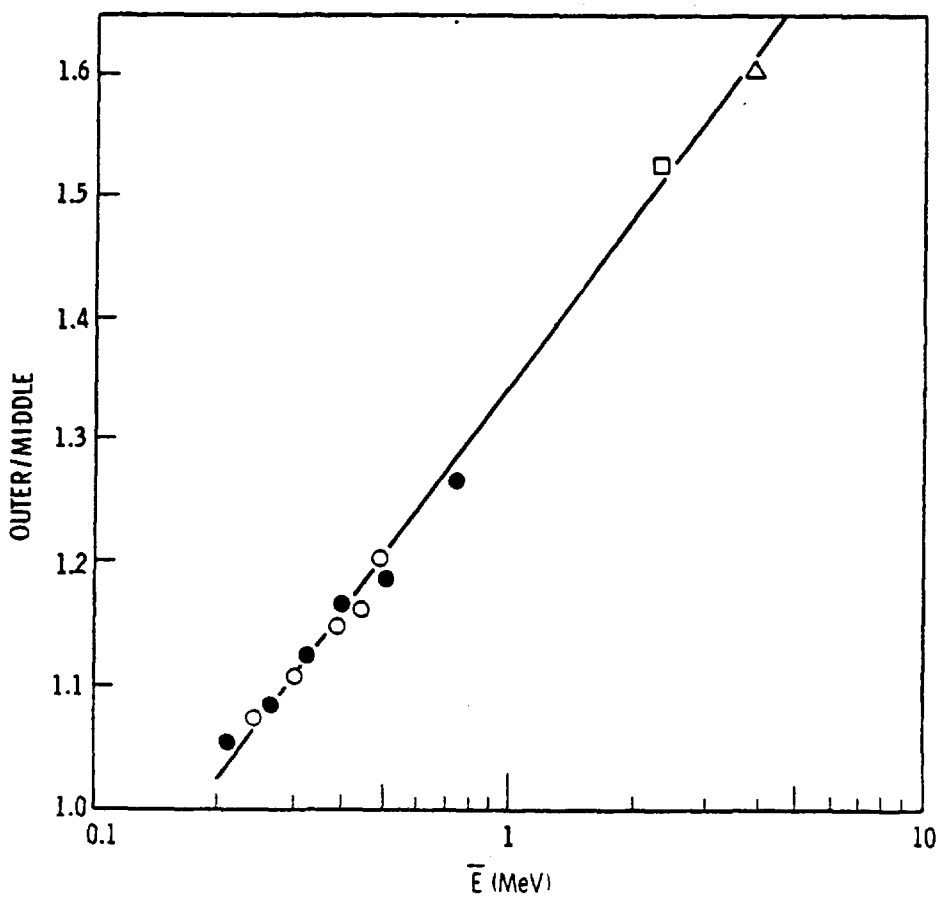

Figure 4. Outer to middle ring ratio corrected for spectral sources versus calculated average energy.

● Odd-mass Rb, Cs delayed neutron precursors

○ Even-mass Rb, Cs delayed neutron precursors

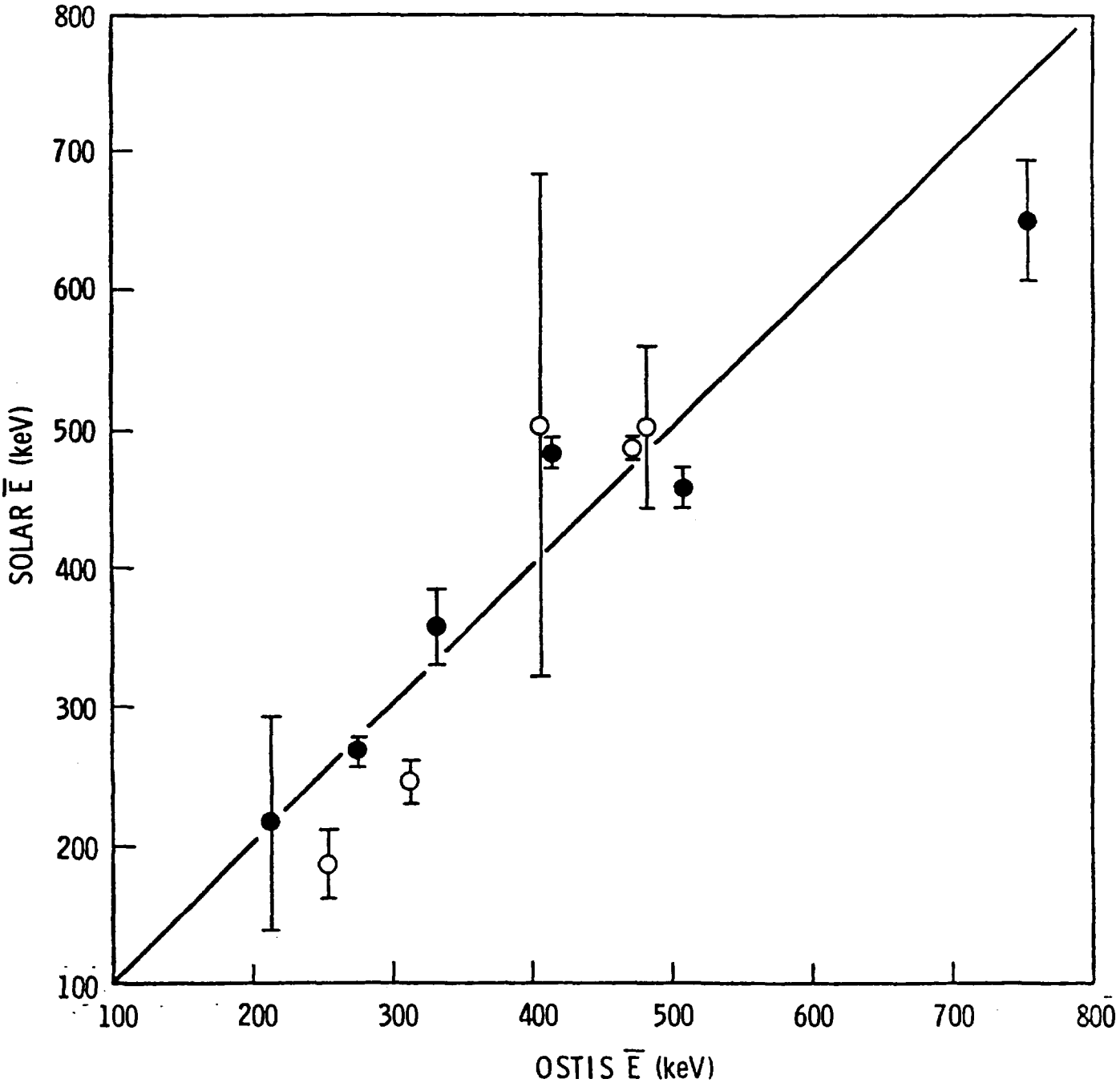

Figure 5. Average energy of delayed neutrons measured by the SOLAR ring ratio technique versus average energies calculated from delayed neutron spectra from OSTIS facility.

● Odd-mass precursors

○ Even-mass precursors

DELAYED NEUTRON EMISSION PROBABILITIES - SOLAR 1978

P. L. Reeder

We repeated the measurements which we did in 1976 [Phys. Rev. C 15, 2108 (1977)] using the same neutron counter and ion counting techniques. The neutron counter was modified slightly to increase the efficiency of the inner ring and make the ring ratio more sensitive to the average energy of the delayed neutron spectra. The total efficiency of the neutron counter was about 47% at 200 keV and decreased to 42% at 800 keV. We now get good agreement between average energies based on our ring ratio technique and average energies taken from the spectra of Kratz, et al. You will note that our new values for P_n by the ion counting technique generally agree well with our previous measurements except for ^{144}Cs and ^{145}Cs.

In addition to the ion counting measurements, we also measured P_n by the beta counting technique using a thin Si detector for counting betas. Decay curves were measured simultaneously for neutrons and betas and P_n values were obtained from initial counting rates determined by decay curve analysis. The absolute efficiency of the beta detector was measured by counting a source of ^{93}Y on both the Si detector and a Ge(Li) detector. Other experiments verified that the Si beta detector efficiency was constant for ^{93}Y, $^{93,94,95}Rb$, and ^{143}Cs. The P_n results from the beta counting method are in good agreement with the ion counting data. It should be noted that the ion counting data and beta counting data are not quite independent measurements since the same neutron counter and efficiencies were used for both measurements. However, these results show that there is no systematic difference between the ion counting technique and the beta counting technique.

DELAYED NEUTRON EMISSION PROBABILITIES - SOLAR 1978

Element	Mass	Ion Counting	Beta Counting
RB	92	.0118 ± .0004 (3)	
	93	1.66 ± .06 (4)	1.87 ± .02 (1)
	94	12.4 ± .2 (8)	12.3 ± .2 (1)
	95	10.8 ± .1 (12)	10.3 ± .1 (2)
	96	17.7 ± .4 (8)	17.2 ±1.0 (1)
	97	32.5 ±1.4 (3)	
	98	16.5 ±1.9 (1)	
Cs	141	.034 ± .001 (1)	
	142	.094 ± .004 (1)	.097 ±.006(1)
	143	1.79 ± .04 (2)	1.70 ±.02 (1)
	144	2.89 ± .21 (4)	2.92 ±.13 (1)
	145	13.0 ± .3 (3)	
	146	11.3 ±2.5 (1)	

Note: Errors given above are random errors. Ion counting data have a systematic error of 7% due primarily to uncertainty in neutron counting efficiency. Beta counting data have a systematic uncertainty of 10.1% due to the 7% uncertainty in neutron counting efficiency and 7.3% uncertainty in beta counting efficiency.

The numbers in parentheses give the number of measurements.

ERROR ANALYSIS OF THE DELAYED NEUTRON SPECTRUM FROM ^{87}BR MEASURED BY A PROTON RECOIL COUNTER

by

Pradosh K. Ray

January 1979

School of Engineering
Tuskegee Institute
Alabama - 36088, U.S.A.

ABSTRACT

The effects of possible errors on the delayed neutron spectrum from ^{87}Br measured by a proton recoil proportional counter were evaluated to determine if any of these might contribute to the softness observed in the measured energy distribution. Through a qualitative and semi-quantitative analysis, it is concluded that none of these is large enough to alter neutron energy distribution significantly.

1. INTRODUCTION

Delayed neutron spectra from a large number of mass separated and chemically separated precursors have been measured in the past few years[1-5]. Out of these, only one measurement [5, 6] (from chemically separated ^{87}Br) was performed by a proton recoil proportional counter; the others used ^{3}He filled counters. The neutron energy distribution from ^{87}Br measured by proton recoil counter was found to be significantly softer than those measured by ^{3}He filled counters[7], although the locations of the peaks agreed relatively well. To determine the reason for this discrepancy in the spectral distribution, a detailed analysis of the possible errors is made in this paper for the proton recoil counter measurement. A qualitative and semi-quantitative approach has been taken in this study. As will be shown, the errors, if properly accounted for will alter the neutron energy distribution slightly and cannot account for the large discrepancy.

The errors in a spectral measurement can be conveniently divided into two groups;

1. Those arising from the operation of the spectrometer
2. Those arising from the physical set-up of the experiment.

2. ERRORS DUE TO THE SPECTROMETER OPERATION

In a proton recoil counter, the energy spectrum of protons from neutron collisions is not directly measured. Rather, one measures the electrons collected at the anode from ionizations produced by the recoil proton track. The output pulse height distribution deviates from the spectrum of proton recoil energies by a number of distorting effects, among which the most important is due to the termination of the longer

proton recoil tracks in the walls and end regions of the counter (wall and end effect).

These effects can be taken care of by the use of a counter response matrix, $\bar{K}_{\nu\mu}$, where each row $\bar{K}_{\nu}$ represents a response vector for monoenergetic neutrons having an energy E_{μ}. Matrix representation of the detection system takes the form,

$$\underline{y} = \underline{\underline{K}}\,\underline{x} \quad .. \quad (1)$$

where, $\underline{y}$ is the observed distribution and $\underline{x}$ is the actual distribution. The input vector $\underline{x}$ can be obtained through a number of methods available for spectral unfolding.

In the case of our measurement, it was planned to measure the counter response functions to monoenergetic neutrons and then use them in obtaining the corrected proton recoil spectrum. But, this part of the project could not be completed due to the closure of the accelerator facility. However, Bennett[8] has found that in the region where neutron distribution decreases rapidly with energy, neutron spectra tend to be only moderately influenced by the response function, even though there were rather large changes in recoil proton spectra before and after unfolding. This is presumably due to the fact that neutron energy distribution is a measure of the slope of the recoil proton spectrum rather than its actual value and in a proton recoil unfolding the slopes change only moderately.

Alternatively, the departures from the ionization spectrum due to the distorting effects could be calculated and the appropriate corrections applied. These corrections are built into the PSNS-N codes prepared by Bennett and Yule[9]. Verbinski [10] has compared neutron spectra

obtained with no corrections as well as with all the corrections in the PSNS-N codes for fast reactor neutron spectra in the energy range from 100 Kev to 1 Mev. Even when all the corrections were combined, there were only small changes in the corrected spectra.

In view of the preceding observations, it seems unlikely that the use of the response functions would alter the measured spectrum from ^{87}Br in such a way as to account for the large discrepancy.

During the early stages of the spectrometer operation and check-up, we have been able to measure a number of response functions from mono-energetic neutrons in few hundred Kev region using the $^{7}Li(p, n)^{7}Be$ reaction. In all cases, the response functions were similar to those obtained by other researchers. The flat portion of the proton recoil response had very little slope indicating that the electric field distortion and wall and end effects were small. The wall and end effects were minimized by the large size (1.5 inches diameter) and high pressure (5 atm. methane) of the counter. Besides, the counter behaved predictably when exposed to thermal neutrons (less than 10% resolution for the $^{3}He(n, p)^{3}H$ peak at 764 Kev) and also obeyed the Diethorn equation[11] relating gas multiplication to counter voltage. Thus, it appears highly unlikely that the counter was malfunctioning in any way.

The entire spectrum from ^{87}Br was measured at one voltage setting having a gas multiplication of 3.47. In the field tube region, the gas gain is near unity. The use of low gas multiplication might suggest that there were unity gain contaminations to the protron recoil data in the lower energy region due to the higher energy neutrons. But, all the measured neutron spectra from ^{87}Br are characterized by decreasing

neutron intensity with energy. Since, only a fraction of these high energy neutrons would undergo unity multiplication, it is doubtful that this could explain the discrepancies. Incidentally, for the methane filled counters, Verbinski found that the electric field distortion corrections were small when low gas gains were used.

During the early phases of our work, we operated the counter at many different voltages. On all occasions, the recoil proton spectra would sharply come down to very low values at about 275 Kev and then decrease at a much slower rate. This bothered us immensely, so much so, that we undertook to use a different approach (calculating γ-ray induced responses to the counter through the measurement of γ-ray spectrum and using monoenergetic γ-ray responses to the counter) to deduce the neutron induced recoil proton spectra[12]. The results were similar in both cases. It was reasoned that since, the major part of the spectrum is only up to 275 Kev, the data ranging from 275 to 275/3.47 i.e., 79 Kev should be relatively free from unity gain contamination.

3. ERRORS DUE TO EXPERIMENTAL SET-UP

The neutron spectrum from ^{87}Br was measured by using a neutron filter made of a mixture of boric acid and paraffin. When the neutron filter was positioned between the source and the counter, the output of the proton recoil counter represented events induced primarily by γ-rays. Data taken without the filter represented both γ-rays and neutron induced events. The difference between the two sets of data with proper corrections for neutron transmission through the filter and

γ-ray scattering by the filter represented events induced by neutrons alone.

In obtaining the neutron spectrum it was assumed that the neutron filter was 100% effective in removing the neutrons out of the range of the proton recoil counter. However, some neutrons after being scattered would in fact reach the counter and still have sufficient energy to register a count (the uncollided neutrons that reach the counter are 1.8% of the total neutrons at 150 Kev and 4.7% at 400 Kev). These scattered neutrons would be of a lower energy and hence would be able to produce counts only in the lower channels of the spectrometer. In correcting the γ-ray induced responses in the proton recoil counter with the filter in position, these neutron induced lower energy counts would have to be subtracted, thus lowering the supposed γ-ray induced response in the initial channels of the spectrometer. Therefore, if this set of data was subtracted from the total counts, there would be more events in the lower channels. This, in turn, would tend to make the neutron distribution fall even faster with increasing energy. Therefore, this interference clearly can not explain the appearance of more neutrons at low energies.

It could also be argued that the percentage of neutron induced events was more or less than the computed 13.82% due to errors that had not been accounted for. To check this possibility, neutron spectra were calculated using assumed values for the percentage of neutron induced events. At a lower percentage of neutrons, the two sets of

data with and without the filter become so close together that large quantities of negative numbers were obtained in the subtracted data, making the slope negative and physically meaningless. For larger percentages of neutrons, the peaks become gradually smaller, indicating the presence of additional smooth background counts, a characteristic of γ-ray induced events. Besides, in calculating neutron energy distribution through the measurement of γ-ray spectrum (our second approach), neutron percentage had to be the same as computed in the part of the experiment using neutron filter. It was invariably found that only for neutron counts of approximately 14% would the neutron spectra in the second set of experiments maintain reproducibility from one run to another.

4. CONCLUSION

From a physical point of view, the existence of the two prominent peaks with good resolution below 200 Kev indicates that the contamination of the proton recoil data in this region must be relatively small; because, any contamination tends to reduce and/or distort the peaks. Indeed, it has been our experience that γ-ray contaminations in the proton recoil spectrum do just that. It is thus concluded that the possible errors are not large enough to alter neutron energy distribution significantly and cannot account for the large discrepancy between the present measurement and those made by the other researchers.

REFERENCES

1. Shalev, S. and Rudstam, G., Nucl. Phys. A230, 153 (1974).
2. Shalev, S. and Rudstam, G., Nucl. Phys. A235, 397 (1974).
3. Franz, H. et. al., Phys, Rev. Lett. 33, 859 (1974).
4. Rudstam, G. and E. Lund, Nucl. Sci. Eng., 64, 749 (1977).
5. Ray, P. K. and E. S. Kenney, Nucl. Inst. Meth., 134, 559 (1976).
6. Ray, P. K. and E. S. Kenney, J. Radioana. Chemistry, 42, 367 (1978).
7. Rudstam, G., Personal Communication (1978).
8. Benett, E. F., Gold, R. and Olson, I. K., ANL-7394 (1968).
9. Benett, E. F. and Yule, T. J., ANL-7763 (1971).
10. Verbinski, V. V., GULF-RT-B-12155 (1972).
11. Diethorn, W. S., NYO-6628 (1956).
12. Ray, P. K. and E. S. Kenney, Nucl. Inst. Meth. 144, 579 (1977).

ABSTRACT

Spectroscopy of Delayed Neutrons from Continuously Separated Precursors in ^{235}U fission, E. S. Kenney and P. K. Ray.

Reactor design and safety are extremely dependent upon accurate measurement of neutron spectral distributions and quantitites. The problems surrounding the implementation of research in a university laboratory with chemical solutions of continuously fissioning ^{235}U are considerable. The apparatus must be designed to minimize any form of failure which could relesse activity to the laboratory and yet allow unobstructed access to precursor accumulation vessels for neutron and gamma ray spectral studies.

The longest lived delayed neutron precursor in ^{235}fission is ^{87}Br. Because it is a gas, it is relatively easy to separate in a fission system and to transport continuously. Carrier bromine gas has been used by the authors to efficiently carry active bromine from the reaction vessel to a chemical accumulator. The accumulator is constructed to surround a methane filled proportional counter. This counter responds to neutrons and gamma rays. The gamma rays constitute an interference, a problem which is well known.

Simultaneous recording of neutron (proton recoil) spectral data and gamma ray spectral data provided the computer input to determine the uncontaminated (free from γ-ray effects) neutron spectrum from ^{87}Br; only one of many delayed neutron precursors. To substantiate the data, neutron spectra were determined two ways; by the gamma substraction menthod noted and by a selective boron-paraffin shield. Both methods eliminated gamma contribution. The two methods yielded the same general results. The existance of difinite peaks in the spectrum is confirmed (large peaks at 131 and 192 kev and smaller peaks at 337, 420 and 520 kev). The end point energy appears to be 750 kev, a value smaller than previously believed.

It is the considered opinion of the authors that research on delayed neutrons has not been carried out with an expenditure of time and funds equivalent to the value of the data in reactor safety and design. Further, the work can be done in many national labs or at universities. The equipment to perform this work exists at many locations with the exception of some special electronic units. Chemical separation systems can be constructed to handle precursors down to the range of 1 second decay half lives. Transport delays will inhibit work in the range of 1 second and lower if chemical separators are used.

The time interval discussed here is particularly important in light of the uncertainty of energy released after emergency shutdown of a reactor.

DELAYED NEUTRONS AND SYMMETRIC FISSION

B.P. Maksyutenko, A.A. Shimanskij
Institue of Physics and Energetics, Obninsk

(not presented)

ABSTRACT

It is shown that at $E_n = 15$ MeV, a significant contribution to the delayed neutron yields is made by fragments from the symmetric fission region, and in particular by ^{128}In. The distribution parameters of the fragment isotopes at this energy are calculated and the value of P_n for ^{128}In is determined from the decay of the delayed neutron activity. The ratios of the cumulative yields of seven pure precursors at this energy are calculated.

The full paper has been distributed as report INDC (CCP)-126 and is available on request from the IAEA Nuclear Data Section.

CONCLUSIONS AND RECOMMENDATIONS

I. Requirements for Delayed Neutron Data

Chairman: Ph. Hammer
Secretary: R.J. Tuttle

For nuclear reactors, delayed neutron data are primarily used for measurement and interpretation of reactivity effects. An additional use is in the detection of fuel cladding failure.

1. Experimental reactivity (ρ) is measured by analyzing the time behaviour of the reactor flux using fractional group yields (a_i) and decay constants (λ_i).

2. Theoretical reactivity ($\frac{\Delta k}{k}$) is calculated as the difference of two eigenvalues.

These two measures of reactivity are related by the effective delayed neutron fraction ($\tilde{\beta}$):

$$\rho = \frac{1}{\tilde{\beta}} \left(\frac{\Delta k}{k}\right)$$

$\tilde{\beta}$ is calculated as the sum of individual effective group fractions, given by:

$$\tilde{\beta}_i = \frac{1}{INF} \sum_k N(e,k) \int_{v_k} d\bar{r} \int_0^\infty dE' \, \Phi^*(E',r) \, \chi_i^d(E') \int_0^\infty dE \; a_i \; \nu^d \sigma_f(e,E,k) \Phi(E,r)$$

where $$INF = \sum_k \int_{v_k} d\bar{r} \int_0^\infty dE' \Phi^*(E',r) \; \bar{\chi}(E') \int_0^\infty dE \bar{\nu} \, \Sigma_f(E,r) \Phi(E,r)$$

for each reactor region k (core, blanket etc) and each fissioning isotope e.

$$a_i = \nu_i^d / \nu^d, \quad \sum a_i = 1$$

The data required for this calculation are:

$\nu_i^d(e)$ = the absolute delayed neutron yields

Φ, Φ^* = the real and adjoint neutron fluxes

χ_i^d, χ = the delayed and total fission neutron energy distributions

$\sigma_f, \bar{\nu}\sigma_f$ = fission and neutron production cross sections

Sensitivity studies show the accuracy achievable in $\tilde{\beta}$ with current and desired uncertainties in these data. The major source of uncertainty is in the absolute delayed neutron yields.

The different applications require data of different accuracies to be of use; for these purposes, $\tilde{\beta}$ must be known to:

Design	± 10%
Power reactor operation	± 5%
Critical experiment operation and interpretation	± 3%
Dynamics	± 10%
Safety	± 10%

Table I

The accuracy in the total delayed neutron yields in the more significant fissionable isotopes required to achieve these uncertainties in $\tilde{\beta}$ is estimated to be ± 9% for a 10% uncertainty in β, 4% for a 5% uncertainty, and 1.5 to 2% for a 3% uncertainty.

On the basis of Dr. Hammer's sensitivity studies this represents a more stringent requirement for accuracy than the 3% requested at the Petten meeting (Report IAEA-213), and data users are requested to confirm the need for data of this accuracy. Reducing the uncertainty in the delayed neutron yields to 1.5 to 2% will require additional measurements.

To achieve commensurate accuracy in the experimental determination of reactivity, the decay curve as represented by the a_i and λ_i values must be known to better accuracy than at present. Differences between measured sets of these parameters produce differences in reactivity values of about 2%. At present a 6-group representation is still considered adequate and preferable to alternative group structures in reactor physics analysis for the sake of simplicity. The possibility of deriving group parameters from precursor data (P_n, $t_{1/2}$) and fission yields should be looked into with the view of finding a method to determine those parameters for unmeasured fissionable nuclides.

For most reactor systems, $\tilde{\beta}$ is relatively insensitive to changes in the delayed neutron spectrum. However, current versions of these spectra show very large differences. The primary need is for group spectra, which were so far assumed in reactor physics calculations to be independent of the fissioning nuclide and the incident neutron energy, in a form suitable for use in multigroup calculations with various energy group structures. The spectra should be known with sufficient accuracy that the mean energy is known to better than ± 20%. This appears to be met by a spectrum description using energy bins about 20 keV wide, with 15-25% uncertainties on the intensities. Efforts should be made to generate covariance matrices in order to define unambiguously the accuracy of the measured spectra.

Integral measurements of $\tilde{\beta}$ may be used to provide values of this parameter for use at individual laboratories and may indicate the existence of biases in the basic data, but should not be expected to provide a basis for the adjustment of these data.

For fuel failure detection systems, the fission yields and neutron emission probabilities of important precursors should be known to ± 10 to 20%.

Based on significance in power reactor development, the most important fissionable nuclides can be identified. The most stringent requirements for accuracy in the delayed-neutron data of these isotopes are for the interpretation of fast-spectrum critical experiments. The desired percentage accuracies are shown for the various parameters in the following table.

Table II

Nuclide	^{232}Th	^{233}U	^{235}U	^{238}U	^{239}Pu	^{240}Pu	^{241}Pu
Yield, ν^d	3	1.5	1.5	3	1.5	5	5
Group parameters a_i, λ_i, to achieve the following accuracy in relative reactivity for periods ⟨3, 3000s⟩	3	1	1	3–	1	3	3
Spectrum, χ^d	25	15	15	25	15	25	25
Individual precursor yields and emission probabilities, $Y_f P_n$, combined	20	10	10	20	10	20	20

The inhour equation is suggested as a means for evaluating the practical accuracy of a group parameter set. The product of the precursor fission yields and neutron emission probabilities is the significant parameter for estimating yields and for designing fuel failure detection systems. Achievement of the requested accuracy will require improvement in fission yield information.

The accuracies given in Table II appear to be attainable in the near future through the use of some additional measurements, the resolution of discrepancies, and more detailed intercomparisons and evaluations.

If the desired accuracy is not achieved for the absolute yields, improvement in the accuracy of the other parameters (such as the delayed neutron spectra) is not of significant benefit.

II. Delayed Neutron Yields

Chairman: R.J. Tuttle
Secretary: E.S. Kenney

Requirements for improved data on delayed neutron yields exist for several significant fissionable nuclides. The quantity of data available and the accuracy with which it is known reflects the long-standing interest in ^{235}U, ^{238}U and ^{239}Pu. With a view towards breeding cycles, data must be developed and verified for delayed neutron yields as a function of neutron energy for the fuels expected in these systems. Whereas ^{232}Th, ^{233}U, ^{235}U, ^{238}U and ^{239}Pu have received considerable attention in the laboratory, the data available are not totally adequate. Certainly at higher energies, the information on yields must be considered somewhat speculative. Except in the 14 MeV energy region, the yield values for all interesting materials are non-existant above 7 MeV. For the important cases of ^{232}Th and ^{239}Pu, measurements do not appear to exist above 4 and 6 MeV respectively.

The delayed neutron fraction may be expressed as:

$$\beta = \frac{\nu_d}{\nu} .$$

For β, the determination of the fission rate is not necessary. Only relative neutron counting is required, thus improving resultant accuracies. For thermal fission, the accurately known value of $\bar{\nu}$ is used to derive $\bar{\nu}_d$. It is therefore recommended to measure β at thermal energy.

Table III (page 5) summarizes the extent of the reported research on delayed neutron yields at this time. The entries indicate the number of measurements in each case. Hyphens indicate that measurements are not possible or, as in the case of spontaneous fission, impractical. Zeroes indicate a lack of experiments in areas which can be studied. It is clear that there is considerable room for new research as well as reinforcement in "older" areas of interest.

Table IV summarizes the present state of accuracy for recommended values of the delayed neutron yield for the commonly used fissionable nuclides:

Table IV

Isotope	Present Accuracy
^{232}Th	4 %
^{233}U	4 - 5 %
^{235}U	2 - 4 %
^{238}U	2 %
^{239}Pu	3 - 6 %

Reactor physicists' most demanding requirements are for interpretation of critical experiments, where $\tilde{\beta}$ must be known to $\pm$ 3%. This may be translated into a requirement for $\pm$ 1.5% to $\pm$ 2% on the accuracy of ν_d.

Delayed Neutron Yield Measurements *

Source \ Nuclide	^{231}Pa	^{232}Th	^{233}U	^{234}U	^{235}U	^{236}U	^{237}Np	^{238}U	^{239}Pu	^{240}Pu	^{241}Pu	^{242}Pu	^{243}Am	^{252}Cf
thermal (0 MeV)	0	-	4	-	7	-	-	-	6	-	1	-	-	-
fast reactor	0	3	3	0	5	0	0	5	4	1	0	0	0	-
mono-energetic														
0-7 MeV	0	3	1	0	5	0	0	5	3	0	0	1	0	-
14 MeV	1	10	3	0	4	0	0	9	3	1	1	0	0	-
photo-fission	0	3	1	1	2	1	1	3	2	0	0	0	0	-
spontaneous	-	-	-	-	-	-	-	-	-	0	-	0	-	1
β(thermal)**	-	-	1	-	3	-	-	-	2	-	0	-	-	-

* Including measurements omitted from evaluation

** Also included in thermal yield measurements

Table III

R.J. Tuttle

Depending upon how one chooses to view the data of Table IV, it is probably prudent to draw attention to the need for some additional work on these important materials.

If one looks at the data for ^{233}U and ^{232}Th, the situation does not appear to meet the reactor design needs already expressed, particularly in light of the present emphasis directed towards the ^{233}U fuel breeding cycle. ^{235}U and ^{239}Pu data are probably within the design accuracies needed for reactors involving these fuels. However, for extended fuel cycles, the build-up of other plutonium isotopes forces attention towards their delayed neutron yields. A check of Table III shows a very poor state of affairs here.

It would appear reasonable to continue to examine the progress towards unifying the data available for such quantities as fission yields and P_n (branching ratios) values. In certain cases (^{235}U, ^{239}Pu) values of the expected delayed neutron yields can be derived with an error of 4-5% which in principle should agree with the experimental value of the delayed neutron yield for ^{235}U. Residual errors here are small enough to warrant consideration of such values in the evaluation of delayed neutron yields. As more information is accumulated, the many weak areas in Table III may be at least partially satisfied with fission product yield data and existing (possibly improved) P_n values. As an example the measured yield for ^{242}Pu has an uncertainty of 33%. This instance is probably one which can be improved directly using known P_n values.

The method of maximum likelihood should be used in a future evaluation of existing data to extract as much information as possible. More measurements are recommended to cover the energy dependence up to ~7 MeV for the important nuclides.

In order to insure a degree of independence in work, more than one laboratory should be involved. At present, a great deal of statistical weight rests upon the results of the U.K. Imperial College - AWRE collaboration. It is recommended that similar measurements are made by other groups and that Imperial College-AWRE extend their measurements to other important nuclides.

III. Delayed Neutron Branching Ratios (P_n- values)

Chairman: G. Rudstam
Secretary: K.L. Kratz

1) The request from the Petten meeting that P_n be measured to $\pm$ 10% has now been achieved for all the high yield precursors except ^{94}Rb and ^{138}I.

2) For all those precursors where only one P_n determination exists, further measurements are requested. However, for most of these cases this should have only minor priority because of their small contribution to the total delayed neutron yield.

3) All P_n-values deduced from measured neutron abundances and estimated fission yields should be recalculated using updated yields.

4) P_n-values based on a determination of the sample strength by counting γ-rays of daughter products should be checked according to the absolute γ-branching ratios used.

5) For those precursors where systematic deviations exist between different techniques/laboratories, like for the Rb and Cs isotopes, a re-evaluation seems to be necessary. In the meantime averages with larger uncertainties (according to the χ^2-method) should be used. If the re-evaluation will not solve the discrepancies, new precision measurements for specific precursors should be requested.

6) Because delayed neutrons are emitted with a spectrum of energies, all users of delayed neutron counters are advised to determine the energy dependence of the efficiency of their counters, rather than relying on an efficiency measurement from a single source.

Table V

INDIVIDUAL PRECURSOR DATA

Nuclide	P_n-values			D.N. Spectra			Directly measured E_n available	$T_{1/2}$-Group	Contribution **)
	P_n-value, % Petten 77	P_n-value, % Vienna 79	Comment *)	Detect. technique	No. of meas.	Energy Range (keV)			
^{79}Ga	-	0.102±0.015	Possible contribution from ^{79}Zn	^{3}He	1	100 - 1000 keV	no	4	1.1×10^{-3}
^{80}Ga	-	0.87±0.05	Only one determination	^{3}He	1	100 - 800	no	4	5.7×10^{-3}
^{81}Ga	-	12.2±0.9	" " "	^{3}He	1	80 - 1350	no	4,5	5.7×10^{-2}
^{82}Ga	-	21.0±1.4	" " "				no	5	3.2×10^{-2}
^{84}As	0.13±0.06	0.13±0.06	Only one determination; reevaluate P_n from Ref.[8]	"			no	3	1.9×10^{-2}
^{85}As	23±3	22±8	Reevaluate P_n from Ref.[8]	^{3}He	3	50 - 3500	no	4	2.0
^{86}As	10.5±2.2	10.5±2.2	"				no	5	0.51
^{87}As	44±14	44±14	Only one determination				no	5	1.8
^{87}Se	0.21±0.03	0.19±0.03					no	3	0.10
^{88}Se	0.15±0.09	0.5±0.3	Large discrepancy between experiments; reevaluate P_n from Refs. [12,14]				no	4	0.068
^{89}Se	5.0±1.5	5.0±1.5	Only one determination; reevaluate P_n from Ref.[14]				no	5,6	0.34
^{91}Se	21±8	21±8	Only one determination				no	6	0.020
^{87}Br	2.37±0.14	2.54±0.10	Reevaluate P_n from Ref.[18]	^{3}He	4	10 - 1300	yes	1	2.9
				p-recoil	1	100 - 550			
^{88}Br	6.9±0.3	6.9±0.3	Reevaluate P_n from Ref.[18]	^{3}He	1	100 - 1600	yes	2	7.7
^{89}Br	13.5±2.3	13.9±1.0	Reevaluate P_n from Ref.[18]	^{3}He	1	100 - 1600	yes	3	10.4
^{90}Br	21.2±2.4	21.2±2.4	Reevaluate P_n from Ref.[18]	^{3}He	1	100 - 1600	no	4	7.8
				TOF	1	150 - 2000			
^{91}Br	10.8±1.7	10.9±1.8		^{3}He	1	100 - 1600	no	5	1.6
^{92}Br	22±6	22±6					no	6	0.45

*) The References are given in the Review Paper on Delayed Neutron Branching Ratios by G. Rudstam

**) Contribution = % of total delayed neutron yield for ^{235}U using Rider-Week (1977) fission yields

Table V: Individual Precursor Data (continued)

Nuclide	P_n-values			D.N. Spectra			Directly measured E_n available	$T_{1/2}$-Group	Contribution
	P_n-value, % Petten 77	P_n-value, % Vienna 79	Comment	Detect. technique	No. of meas.	Energy Range (keV)			
^{92}Kr	0.033±0.003	0.033±0.003	Check on γ-abundance [4]				no	4	0.033
^{93}Kr	2.0±0.3	1.95±0.11	"				yes	4,5	0.58
^{94}Kr	2.2±1.4	5.7±2.2	Only one determination				no	6	0.76
^{92}Rb	0.012±0.001	0.0119±0.0006		^{3}He	1	10 - 800	yes	3	0.033
^{93}Rb	1.38±0.11	1.37±0.08	Reevaluate P_n from Ref.[18]	^{3}He	3	10 - $(Q_\beta - B_n)$	yes	3	2.9
^{94}Rb	10.6±0.7	10.3±0.5	Spread outside 10%	^{3}He	3	10 - $(Q_\beta - B_n)$	yes	4	10.6
				TOF	1	100 - $(Q_\beta - B_n)$			
^{95}Rb	8.9±0.5	8.8±0.4		^{3}He	3	10 - $(Q_\beta - B_n)$	yes	5,6	4.2
				TOF	1	10 - $(Q_\beta - B_n)$			
^{96}Rb	14.2±1.0	13.9±0.7		^{3}He	1	10 - $(Q_\beta - B_n)$	yes	6	1.7
^{97}Rb	30±3	27.8±2.5		^{3}He	2	10 - $(Q_\beta - B_n)$	yes	6	1.2
^{98}Rb	15.0±2.4	16.0±1.0		^{3}He	1	10 - $(Q_\beta - B_n)$	no	6	0.028
^{99}Rb	-	15±3	Only one determination				no	6	2.2×10^{-3}
^{97}Sr	-	0.27±0.09	" " "				no	5,6	0.31
^{98}Sr	-	0.36±0.11	" " "				no	5	0.18
^{99}Sr	3.4±2.4	3.4±2.4	" " "				no	5	0.68
^{97}Y	1.6±0.3	0.06±0.02	" " "				no	4,5	0.23
^{98}Y	-	3.44±0.95	" " "				no	4,5	6.0
^{99}Y	1.2±0.8	1.2±0.8	" " "				no	4	1.6
^{127}In	-	0.72±0.04 (1/2⁻) <0.03 (9/2⁺)	Two sets of data for indium isotopes, at variance with each other, have been reported (Refs.[7] and [25]). In this table ^{129}In is taken from Ref.[25] and the others from Ref.[7].				no	3,4	0.012
^{128}In	-	0.063±0.008 (3⁺ + 8⁻)					no	5	3.2×10^{-3}
^{129}In	-	3.5±0.5		^{3}He	1	100 - 1500	no	4	0.026
^{130}In	-	1.39±0.08 (3⁺ + 8⁻)	Discrepancies should be resolved	^{3}He	1	150 - 1300	no	5	0.080
^{131}In	-	1.66±0.19	"				no	6	0.027
^{132}In	-	4.1±0.8	Only one determination				no	6	0.016
^{134}Sn	17±7	17±7	" " "	^{3}He	1	100 - 1350	no	5	1.1

Table V: Individual Precursor Data (continued)

Nuclide	P_n-values			D.N. Spectra			Directly measured E_n available	$T_{1/2}$-Group	Contribution
	P_n-value, % Petten 77	P_n-value, % Vienna 79	Comment	Detect. technique	No. of meas.	Energy Range (keV)			
^{134}Sb (10 s)	0.086±0.012	0.122±0.013					no	2,3	0.028
^{135}Sb	13.9±2.4	14.9±1.1		^{3}He	2	50 - (Q_β-B_n)	no	4	1.3
^{136}Sb	23±8	23±8					no	5	0.21
^{136}Te	0.9±0.4	0.9±0.4	Error > 10%	^{3}He	2	10 - (Q_β-B_n)	no	2	0.78
^{137}Te	2.2±0.5	2.5±0.5	Only one determination				no	3	0.62
^{138}Te	5.6±1.6	6.3±2.1	" " "				no	4	0.32
^{137}I	6.7±0.5	6.4±0.4	Reevaluate P_n from Ref.[18]	^{3}He	2	10 - 1500	no	2	11.8
				TOF	1	200 - 2000			
^{138}I	2.6±0.3	5.4±0.3	The value decreases to 3.6±0.8 if a value from Ref. [15] is included. Reevaluate P_n from Ref.[18]	^{3}He	2	10 - 1600	no	3	4.9
^{139}I	10.2±0.9	9.5±0.5	Reevaluate P_n from Ref. [18]	^{3}He	1	50 - 1600	no	4	5.3
^{140}I	22±6	22±6	" "	^{3}He	1	100 - 1500	no	5	2.7
^{141}I	39±13	39±13	Only one determination				no	5,6	0.44
^{141}Xe	0.043±0.003	0.043±0.003	Check on γ-abundance [4]				no	4	0.032
^{142}Xe	0.41±0.03	0.41±0.03	" "				no	4,5	0.10
^{141}Cs	0.053±0.004	0.037±0.004	" "	^{3}He	1	10 - (Q_β-B_n)	yes	2	0.091
^{142}Cs	~0.18	0.095±0.004		^{3}He	2	10 - (Q_β-B_n)	yes	4	0.14
^{143}Cs	1.82±0.12	1.74±0.07		^{3}He	3	10 - (Q_β-B_n)	yes	4	1.47
^{144}Cs	3.0±0.7	3.07±0.25		^{3}He	2	10 - (Q_β-B_n)	yes	4,5	0.63
^{145}Cs	14.3±1.9	12.9±0.5	The value increases to 13.4±0.9 if a value from Ref. [25] is included.	^{3}He	1	10 - (Q_β-B_n)	yes	5	0.43
^{146}Cs	13.4±0.7	13.2±0.6		^{3}He	1	10 - (Q_β-B_n)	yes	6	0.13
^{147}Cs	25±3	25.4±3.2	Only one determination	^{3}He	1	10 - (Q_β-B_n)	no	6	1.4×10^{-3}
^{147}Ba	-	5.2±0.5	" " "				no		0.28
^{148}Ba	-	23.9±2.1	" " "				no		0.15
^{147}La	-	0.50±0.17	" " "				no		0.26

IV. Delayed Neutron Spectra

Chairman: J.G. Williams
Secretary: D.R. Weaver

During the last few years there has been a great increase in the available information on delayed neutron spectra. These new data have not always been taken into account in reactor analysis. Two reasons for this are that the reliability of the measurements has sometimes been questioned and that the information is often not in a form which can be readily used. On the other hand the requirements for spectrum data have seldom been clearly stated.

As was requested at the Petten meeting, further work on assessment of the properties of different neutron spectrometer types has been done, especially concerning response function and detector efficiency of the ^{3}He-spectrometers and on error analysis of the spectra measured with proton-recoil and ^{3}He(n,p) techniques. These analyses have not succeeded in clarifying the apparent differences in neutron intensities, so further efforts are needed.

It has become clear that a significant fraction of delayed neutrons are emitted with energies less than 100 keV (approximately 20%) or more than 1.2 MeV (approximately 10%). The effect that these might have on calculations of reactivity has not been adequately studied. Such studies should be made so that the accuracy demanded of spectrum measurements at the extremes of the energy range can be stated.

The current needs of reactor physicists are for equilibrium spectra and spectra for each of the six decay groups.

Individual precursor spectra are being measured primarily because of the fundamental interest of these for nuclear physics; it is however concluded that this type of information can make a contribution to reactor applications.

The following conclusions and recommendations were agreed for equilibrium, group and precursor spectra and for theoretical predictions of delayed neutron spectra.

A. Equilibrium and near-equilibrium spectra

1. Because of the recent increase in experimental information, a new evaluation of the equilibrium spectra should be performed. Special attention should be paid in this to those parts of the energy range, below 100 keV and above 1.2 MeV, not covered in earlier measurements. Dr. Weaver has agreed to undertake this.

2. The practice of reporting measured or evaluated spectra without clear information on the uncertainties present should be discontinued. Systematic errors and the extent to which they are common to different parts of the energy range or between different spectra must be quantified in addition to the presentation of random error information.

3. More spectrum measurements will be needed to resolve existing conflicts in the published data, particularly at the extremes of the energy range. A variety of experimental techniques should be used.

4. Good integral information, for instance average delayed neutron energies, can contribute valuable consistency checks on the spectrum data.

5. It has been observed that in reported spectra the unit or dimension of the data has not always been clearly specified. Relative intensity per unit energy or per unit lethargy are acceptable. The latter is often of more direct use in reactor physics.

6. Americium-lithium sources are in common use for calibration of delayed neutron yield detectors. It is recommended that new spectrum measurements of these sources should be made, particularly by groups involved in delayed neutron spectrometry. Details of the source construction should be specified when measurements are reported.

B. Decay-group spectra

1. Data on the time dependence of spectra from unseparated precursors remain very sparse. New measurements with the more recent spectrometry techniques capable of covering the complete energy range should have a high priority.

2. The groups at Mainz, Birmingham and Pacific Northwest Laboratory have indicated an interest in performing new measurements and they and others are encouraged to fulfil this requirement.

3. Group spectra constructed from individual precursor data can provide valuable information provided the full energy range is covered in the precursor spectra, if necessary by including semi-empirical extrapolations as exemplified by Dr. Rudstam's paper to the Petten meeting (IAEA-213). It is expected that almost complete experimental coverage of the important precursors will be available within about one year.

C. Separated precursor spectra

1. Many individual precursor spectra have now been measured in different laboratories, mostly using ^{3}He spectrometers, but also proton recoil and time-of-flight data are available in some cases.

2. Given the precursor spectra and P_n values it will be possible to construct group spectra for any desired set of decay-groups and any fissioning isotope for which the yields are available. In many cases these data will be more reliable than any foreseeable data from direct measurements.

3. Partly because most of these data are so recent no systematic intercomparison has been done. In particular the spectra from five isotopes have been measured in a number of laboratories and should be intercompared. These are ^{87}Br, ^{93}Rb, ^{94}Rb, ^{95}Rb, and ^{143}Cs. Dr. Reeder has agreed to undertake this intercomparison, at least for the last

four isotopes. When new data are published authors should compare their results with previous measurements. In order to make these comparisons meaningful experimenters must provide uncertainty information.

4. It will be useful also to communicate pulse height spectra and response functions to theoreticians, so that they can compare their predictions folded by the response function with the raw measurements.

5. A compilation of peaks and intensities for measured spectra should be made where the data are good enough to warrant it.

6. A new compilation of mean energies of neutrons from individual precursors including an intercomparison of data from different sources should be made.

7. A list of precursors of which measured spectra or mean energies are available is contained in Table V (p. 8-10).

8. New measurements are required for some precursors spectra because of the lack of data below 100 keV and above 1600 keV. Among these the isotopes most important for reactors are ^{88}Br, ^{89}Br, ^{90}Br, ^{91}Br, ^{134}Sn, ^{139}I, ^{140}I. Further precursors still requiring a measurement of neutron spectra are ^{92}Br, ^{93}Kr, ^{94}Kr, ^{98}Sr, ^{99}Sr, ^{100}Sr, ^{97}Y, ^{98}Y, ^{99}Y, ^{100}Y, ^{101}Y, ^{137}Te, ^{138}Te, ^{139}Te and ^{141}I (for the relative importance see Table V). Among these ^{98}Y and ^{99}Y are the most important for reactor technology.

D. Theoretical spectra

In order for theoretical predictions of delayed neutron spectra to become more quantitative and reliable, nuclear physicists require the following data to be experimentally determined:

1. The masses of the precursor and the final nucleus. So far we have to a great extent to rely on mass formulae for determination of $(Q_\beta - B_n)$.

2. The neutron branching ratio P_n^i to the i-th excited state of the final nucleus. At present the available data are very sparse and the few data existing should be confirmed.

3. The spins and parities of the relevant excited states in the final nucleus. In many cases there are great ambiguities in the data available.

4. The spin and parity of the precursor. So far we have in most cases to make guided guesses (shell model systematics).

Appendix A

Consultants' Meeting on Delayed Neutron Properties

IAEA, Vienna, 26-30 March 1979

Meeting Room Wasagasse

ADOPTED MEETING AGENDA

Monday, 26 March

9:30 a.m. Opening, Adoption of the Agenda

Review Paper 1: Requirements of delayed neutron data for the design, operation, dynamics and safety of fast breeder and thermal power reactors (Ph. Hammer)

Review Paper 2: Delayed Neutron Yields in Nuclear Fission (R.T. Tuttle)

Afternoon: Contributed Paper: Delayed neutron yield and decay constants for thermal neutron induced fission of U-235 (S. Synetos, J.G. Williams)

Review Paper 3: Delayed Neutron Branching Ratios (G. Rudstam)

Review Paper 4: Delayed Neutron Energy Spectra (K.L. Kratz)

Tuesday, 27 March

Morning: Contributed papers and notes

Delayed Neutron Spectrum Measurements using a ^{3}He Spectrometer (D.R. Weaver, J.G. Owen and J. Walker)

Spectroscopy of Delayed Neutrons from Continuously Separated Precursors in ^{235}U Fission (E.S. Kenney, P.K. Ray)

Error Analysis of the Delayed Neutron Spectrum from ^{87}Br Measured by a Proton Recoil Counter (P.K. Ray)

Note on the uncertainty of delayed neutron energy spectra (G. Rudstam)

Measurement of average neutron energies by a counting rate ratio technique (P.L. Reeder, R.A. Warner)

Note: A correction to the delayed neutron yields of Besant et al., 1977 (J.G. Williams)

Delayed neutrons and symmetric fission [not presented] (B.P. Maksyntenko, A.A. Shimanskij)

Afternoon: Discussion of requirements

Wednesday, 28 March

Morning: Discussion of branching ratios

Afternoon: Discussion of delayed neutron yields

Thursday, 29 March

All day: Discussion of delayed neutron spectra

Friday, 30 March

Morning: Closing session: Summary of conclusions and recommendations

Appendix B

LIST OF PARTICIPANTS

Consultants' Meeting on Delayed Neutron Properties
Vienna, 26-30 March 1979

Crawford, G.J.	Kelvin Laboratory, University of Glasgow Glasgow, Scotland, United Kingdom
Gjøtterud, O.K.	Fysisk Institut, Universitetet i Oslo, Blindern, Oslo 3, Norway
Hammer, Ph. (part-time)	DRNR/SEDE, B.P. No. 1 F-13115 St. Paul-les-Durances, France
Kamelander, G. (part-time)	Inst. fuer Reaktorsicherheit, Oesterr. Studiengesellschaft fuer Atomenergie, Wien, Austria
Kenney, Edward S.	The Pennsylvania State University University Park, Penn. 16802, USA
Kratz, K.L.	Institut fuer Kernchemie, Universitaet Mainz, Friedrich V. Pfefferweg 14, D-6500 Mainz, Fed. Rep. of Germany
Reeder, P.	Battelle-Northwest, P.O. Box 999 Richland, Washington 99352, USA
Rudstam, G.	The Swedish Research Council's Laboratory, Studsvik, Fack, S-611 01 Nykoeping, Sweden
Sdouz, G. (part-time)	Inst. fuer Raktorsicherheit, Oesterr. Studiengesellschaft fuer Atomenergie, Wien, Austria
Takahashi, K.	Technische Hochschule Darmstadt, Institut fuer Kernphysik, D-6100 Darmstadt Red. Rep. of Germany
Tuttle, R.J.	Rockwell International, 8900 De Soto Avenue Canoga Park, Calif. 91304, USA
Weaver, D.R.	Birmingham Radiation Centre, University of Birmingham, Birmingham B15 2TT, United Kingdom
Williams, J.G.	University of London, Reactor Centre, Silwood Park, Sunninghil, Ascot, Berkshire SL5 7PY United Kingdom

J.J. Schmidt
K. Okamoto } Scientific Secretaries
O. Schwerer }
G. Lammer

H.D. Lemmel }
N. DayDay } part-time
N. Kocherov }

} IAEA Nuclear Data Section